

BORENIUM IONIC LIQUIDS

By

Sesime Coffie, MPharmSci

Being a thesis submitted for the degree of

Doctor of Philosophy

To the

School of Chemistry and Chemical Engineering

Of

Queen's University of Belfast



February 2018

-

DEDICATED
TO MY FAMILY
FOR THEIR PRAYERS AND CONTINOUS SUPPORT
TO GOD BE THE GLORY

ABSTRACT

Over the years, ionic liquids (ILs) with halometallate Lewis acidic anions have received a lot of attention because of their high Lewis acidity and tuneability of properties. Numerous industrial reaction have been carried out using Lewis acidic ionic liquids as co-catalysts in transition metal catalysis and as catalysts for Friedel-Crafts chemistry and other carbocationic processes.^{1,2} Until recently, Lewis acidity in ILs arise almost exclusively from a halometallate anion.³ There were exceptions in Al(III)-based systems, where halides were partially replaced with alkyl, alkoxy, or perfluoroalkoxy groups – but also here the Lewis acidic component was the anion.

The aim of this research was to study, develop and investigate a new class of Lewis acidic ionic liquids, based on Lewis acidic borenium cations. The aim was to create highly Lewis acidic ionic liquids, with electrophilicity of the empty *p* orbital increased by the positive charge. The focus was on two aspects: syntheses of these borenium ionic liquids and throughout spectroscopic characterisation, and the applications of these liquids in catalysis, namely for Diels-Alder reaction and aldol condensation.

The first generation of borenium ionic liquids reported was based on borenium cation and halometallate: formed by reacting a tetracoordinate boron complex, $[BCl_3L]$, with a metal chloride as a halide-abstracting agent.⁴ They were accessed by the solvent free reaction of 1 or 2 equivalents of MCl_3 ($M = Al$ or Ga) to $[BCl_3L]$, resulting in the formation of ionic liquids of a general formula $[BCl_2L][M_xCl_y]$.⁴ These were the first ILs to have dual Lewis acidity, arising from both cation and anion - and the first ionic liquids with Lewis acidic cations in general. Lewis acidity was quantified through Gutmann acceptor number (AN). The extremely high acidity ($AN > 160$) of cationic boron centres has been confirmed, placing borenium ILs amongst the strongest Lewis acid reported (by AN measurements).

The second generation of borenium ionic liquids was envisaged to contain a non-coordinating, non-chlorometallate anion. A range of liquids with triflate were developed, but these were found to form tetracoordinate adducts, the triflate acting as a ligand to the boron centre. AN values for these liquids were still high, about *ca.*143.

The first generation of borenium ionic liquids was used as catalysts in a model Diels-Alder reaction, to examine the influence of different borenium ILs on the rate and selectivity.⁵ The investigations showed that excellent stereoselectivity and superior reaction rates can be achieved with borenium ionic liquids compared to other benchmark Lewis acid

-
catalysts. A sigmoidal correlation between conversion and AN values recorded for borenium cations was found. Furthermore, self-condensation of acetophenone to dyprone was successfully achieved using borenium ionic liquids as a catalyst.

Results of this work have contributed to a patent application, two published papers with two more papers are in preparation.

ACKNOWLEDGEMENTS

First and foremost, I will like to thank the almighty God for my wellbeing and health during the three years of my PhD. Couldn't have made it this far without God's grace and favour.

I would like to express my heartfelt appreciation to my supervisor Dr. Malgorzata Swadzba-Kwasny for her motivation, constructive criticism, patience and considerable depth of knowledge. Her supervision fine-tuned my research and lighted the path for a smooth thesis write-up. Her guidance helped me in my research and writing of this thesis. Also, I express my warm thanks to Dr. John Holbrey for his insightful comments and encouragement, hard questions which incited me to widen my research from various perspectives. I could not have imagine better supervisors for my PhD study.

Going further, I would like to thank Professor Ken Seddon and the whole team that ensured I left no Is un-dotted and Ts uncrossed by subjecting my work to thorough and constructive scrutiny and in the process, providing me with invaluable guidance undoubtedly gained from years and years of experience: May his soul rest in peace.

My sincere thanks goes to my department who have supported me in every possible way even with tasks I felt were over-burdening. I could not have reached this stage without their administrative support or otherwise of my grant applications and conference attendances as well as my general quest to achieve doctoral status.

How could I forget my colleagues who stood hand-in-hand with me through this journey? The sleepless nights, the pats on the back, the hurried hellos in the morning followed immediately by changing into the white coats ready for the next challenge of the day, the social events and the overarching urge to see each other succeed.

Last but not the least, I would like to thank my family and loved ones who built an invisible protective cloak around me, ensuring that I get through this course successfully. My sincere gratitude to my mum, brother and sister for their continuous support and prayers throughout writing this thesis and my life in general.

PUBLICATIONS ARISING FROM THIS WORK

Published papers:

S. Coffie, J.M. Hogg, L. Cailler, A. Ferrer-Ugalde, R.W. Murphy, J.D. Holbrey, F. Coleman and M. Swadźba-Kwaśny, *Lewis superacidic ionic liquids with tricoordinate borenium cations*, *Angew. Chem. Int. Ed. Engl.*, 2015, **54**, 14970–14973.

K. Matuszek, S. Coffie, A. Chrobok and M. Swadźba-Kwaśny, *Borenium ionic liquids as catalysts for Diels–Alder reaction: tuneable Lewis superacids for catalytic applications*, *Catal. Sci. Technol.*, 2017, **7**, 1045–1049.

Filed patent applications:

F. Coleman, S. Coffie, M.P. Atkins, J. Hogg, A. Ugalde, M. Swadzba-Kwasny and G. Fedor, *Oligomerisation Process* WO2016/005769 A1, 2016

Papers in preparation:

S. Coffie, L.C. Brown and M. Swadźba-Kwaśny, *Borenium ionic liquids as catalysts for dypnone synthesis via aldol condensation*, in preparation for *Catal. Sci. Technol.*

L.C. Brown, S. Coffie, J. D. Holbrey and M. Swadźba-Kwaśny, *Ionic liquids with borenium cations and fluorinated anions: acces to ‘naked’ borenium ion*, in preparation for *Inorg. Chem.*

TABLE OF CONTENTS

LIST OF FIGURES	x
LIST OF TABLES	xiv
LIST OF ABBREVIATIONS	xvii
1 Introduction	20
1.1 Chemistry of Group 13 elements	20
1.1.1 Electron structure and periodicity of Group 13 elements	20
1.1.2 Reactivity of halides of the Group 13 elements	21
1.2 Borocations	23
1.2.1 Borinium cations	23
1.2.2 Boronium cations	24
1.2.3 Borenium cations	24
1.3 Acidity	27
1.3.1 Historical understanding and definitions of acidity	27
1.3.2 Brønsted-Lowry definition	29
1.3.3 Lewis definition	29
1.4 Lewis acidity measurements	32
1.4.1 Gutmann acceptor number (AN)	32
1.4.2 Childs method	33
1.4.3 Fluoride Ion Affinity (FIA) scale	34
1.4.4 Superacids	35
1.5 Ionic liquids	36
1.5.1 History	36
1.5.2 General characteristics and state-of-the-art	37
1.6 Lewis acidic ionic liquids	39
1.6.1 Halometallate ionic liquids	39
1.6.2 Ionic liquids with Lewis acidic cations	41
1.6.3 Quantifying Lewis acidity of ionic liquids	42
1.7 Rationale for this work	44
2 Synthesis and Characterisation of Boron Complexes	46
2.1 Experimental	46
2.1.1 Synthesis of boron complexes	46
2.1.2 Characterisation of boron complexes	47
2.2 Results and discussion	50

2.2.1	Selection of reactants	50
2.2.2	Synthetic procedure	52
2.2.3	NMR spectroscopic characterisation of adducts	53
2.2.4	FT-IR spectroscopy	63
2.2.5	Elemental analysis	63
2.2.6	Differential scanning calorimetry measurements and thermogravimetric analysis	64
2.2.7	Crystallographic analysis	71
2.3	Conclusions	72
3	Synthesis and characterisation of borenium ionic liquids	74
3.1	Experimental	74
3.1.1	Synthesis	74
3.1.2	Characterisation of borenium ionic liquids	75
3.2	Results and discussions	78
3.2.1	General synthetic considerations	78
3.2.2	Chlorometallate counterions to borenium ionic liquids	79
3.2.3	<i>Viscosity measurements</i>	100
3.2.4	Borenium triflate ionic liquids	106
3.2.5	Lewis acidity of chlorometallate and triflate systems	118
3.3	Conclusions	126
4	Diels-Alder cycloaddition	129
4.1	Introduction	129
4.1.1	General remarks on Diels-Alder reaction	129
4.1.2	Boron Lewis acids in Diels-Alder reaction	131
4.1.3	Ionic liquids in Diels-Alder reaction	132
4.3	Experimental	134
4.3.1	Syntheses	134
4.4	Results and Discussion	137
4.4.1	General remarks	137
4.4.2	Borenium chlorometallate ionic liquids as catalysts for Diels-Alder reaction	137
4.4.3	Triflate boron complexes as catalysts for Diels-Alder reaction	154
4.5	Conclusions	154
5	Aldol Condensation	156
5.1	Introduction	156
5.1.1	Aldol condensation	156
5.1.2	Synthesis of dyppone	160
5.2	Experimental	164

-	
5.2.1	Aldol condensation of acetophenone 164
5.2.2	Large-scale reaction to isolate the product 165
5.3	Results and Discussion 166
5.3.1	Reaction conditions 166
5.3.2	Screening of borenium chlorometallate ionic liquids 167
5.3.3	<i>Isolated dyprnone</i> 173
5.4	Conclusions 176
6	Summary and future work 177
7	References 178

LIST OF FIGURES

Figure 1-1: Lewis acidity of boron trihalides. ¹⁰	22
Figure 1-2: Structure of borinium ion, where R is formally a monoanionic substituent. ⁸	24
Figure 1-3: Structure of boronium ion, where L is formally a neutral two-electron donor and R is formally a monoanionic substituent. ⁸	24
Figure 1-4: Structure of borenium ion, where L is formally a neutral two-electron donor and R is formally a monoanionic substituent. ⁸	25
Figure 1-5: Structure of bis(dimethyl amino)(dimethylamine) borenium ion. ³¹	25
Figure 1-6: The formation and structure of a borenium cation in solution with $[Al_2Cl_7]^-$ anion. ²¹	26
Figure 1-7: Complexation of triethylphosphine oxide (tepotepo) with a Lewis acid (LA) for Gutmann Lewis acidity test.	33
Figure 1-8: Complexation of Lewis acid (LA) to the oxygen on crotonaldehyde in Childs Lewis acidity test. ^{59,60}	34
Figure 1-9: Some cations and anions commonly used in the design of ionic liquids (where R_x are alkyl groups). ¹	38
Figure 1-10: The structure of components of two solvate ionic liquids: $[Li(G3)][NTf_2]$ and $[Li(G4)][NTf_2]$. ^{88,109}	41
Figure 1-11: Ionic liquid with Lewis acidic boron centre in the cation. ¹¹⁵	42
Figure 1-12: Guttmann acceptor number scale of various halometallate systems, Brønsted acids and solvents. ^{118,119}	43
Figure 2-1. Synthesis of a tetracoordinate boron fluoride complex: $[BF_3(4-pic)]$.	52
Figure 2-2. Synthesis of a tetracoordinate boron chloride complex: $[BCl_3(4-pic)]$.	52
Figure 2-3: ^{11}B NMR spectra (128 MHz, 27 °C, $CDCl_3$) of tetracoordinate boron complexes, $[BCl_3L]$.	56
Figure 2-4: ^{11}B NMR spectra (128 MHz, 27 °C, $CDCl_3$) of tetracoordinate boron complexes, $[BF_3L]$.	58
Figure 2-5: ^{31}P NMR spectra (162 MHz, $CDCl_3$) of tetracoordinate boron trifluoride complexes	59
Figure 2-6: ^{31}P NMR spectra (162 MHz, $CDCl_3$) of tetracoordinate boron chloride complexes.	60
Figure 2-7: ^{19}F NMR (376 MHz, $CDCl_3$) spectra of tetracoordinate boron trifluoride complexes $[BF_3L]$ with N-donors.	61
Figure 2-8: ^{19}F NMR (376 MHz, $CDCl_3$) spectra of tetracoordinate boron trifluoride complexes $[BF_3L]$ with O-donors.	62
Figure 2-9: ^{19}F NMR (376 MHz, $CDCl_3$) spectra of tetracoordinate boron trifluoride complexes $[BF_3L]$ with P-donor.	62
Figure 2-10: TGA themograms of $[BCl_3L]$ adducts.	66

Figure 2-11: TGA themograms of [BF ₃ L] adducts.	67
Figure 2-12: DSC graph showing melting points (exo, down) of [BCl ₃ L] adducts.	68
Figure 2-13: DSC graph showing melting points (exo, down) of [[BF ₃ L] adducts.	69
Figure 2-14: Crystal structure of [BF ₃ (mim)]: molecular structure (left), and packing (right)	71
Figure 2-15: Crystal structure of [BCl ₃ (4pic)]: molecular structure (top), and packing (bottom).	72
Figure 3-1: The formation and structure of a borenium cation with [Al ₂ Cl ₇] ⁻ anion.	79
Figure 3-2: ¹ H NMR (400 MHz, neat liquid with DMSO-d ₆ lock) of dma-BCl ₃ -2MCl ₃ borenium ionic liquids.	83
Figure 3-3: ¹¹ B NMR spectra (128.37 MHz, 27 °C, neat liquid with DMSO-d ₆ lock) of borenium ionic liquids of a general formula L-BCl ₃ -2AlCl ₃ .	86
Figure 3-4: ¹¹ B NMR spectra (128.37 MHz, 27 °C, neat liquid with DMSO-d ₆ lock) of borenium ionic liquids of a general formula L-BCl ₃ -2GaCl ₃ .	87
Figure 3-5: ¹¹ B NMR spectra (128.37 MHz, 27 °C, neat liquid with DMSO-d ₆ lock) of borenium ionic liquids of a general formula L-BCl ₃ -AlCl ₃ .	87
Figure 3-6: ¹¹ B NMR spectra (128.37 MHz, 27 °C, neat liquid with DMSO-d ₆ lock) of borenium ionic liquids of a general formula L-BCl ₃ -GaCl ₃ .	88
Figure 3-7: ¹¹ B NMR spectra (128.37 MHz, 27 °C, neat liquid with DMSO-d ₆ lock) of borenium ionic liquids of a general formula 4pic-BCl ₃ -nMCl ₃ , where M = Al or Ga and n = 1, 2 or 3.	89
Figure 3-8: ²⁷ Al NMR spectra (104.28 MHz, 25 °C, neat liquid with DMSO-d ₆ lock) of borenium ionic liquids of a general formula L-BCl ₃ -2AlCl ₃ .	91
Figure 3-9: ²⁷ Al NMR spectra (104.28 MHz, 25 °C, neat liquid with DMSO-d ₆ lock) of borenium ionic liquids of a general formula L-BCl ₃ -AlCl ₃ .	92
Figure 3-10: Corrected fitted densities, ρ, of the studied borenium ionic liquids.	98
Figure 3-11: Corrected fitted densities, ρ, of the studied borenium ionic liquids.	99
Figure 3-12: Experimental values for viscosities, η, of borenium ionic liquids of a general formula L-BCl ₃ -2AlCl ₃ , plotted as a function of temperature, fitted to a Vogel-Fulcher-Tammann (VFT) equation.	103
Figure 3-13: Experimental values for viscosities, η, of borenium ionic liquids of a general formula L-BCl ₃ -2GaCl ₃ , plotted as a function of temperature, fitted to a Vogel-Fulcher-Tammann (VFT) equation for.	104
Figure 3-14: ¹ H NMR (400 MHz, DMSO) spectrum of 4-pic-BCl ₂ -OTf.	108
Figure 3-15: ¹ H NMR (400 MHz, DMSO) spectrum of 4-pic-BF ₂ -OTf.	109
Figure 3-16: ¹³ C NMR (101 MHz, DMSO) spectrum of 4-pic-BCl ₂ -OTf.	110
Figure 3-17: ¹³ C NMR (101 MHz, DMSO) spectrum of 4-pic-BF ₂ -OTf.	111

Figure 3-18: ^{11}B NMR (160 MHz, DMSO, 27 °C, neat liquid with DMSO- d_6 lock) of triflate systems of a general formula with $[\text{L}-\text{BCl}_2-\text{OTf}]$.	112
Figure 3-19: ^{11}B NMR (160 MHz, DMSO, 27 °C, neat liquid with DMSO- d_6 lock) of triflate systems of a general formula with $[\text{L}-\text{BF}_2-\text{OTf-L}]$	112
Figure 3-20: ^{19}F NMR (376 MHz, DMSO) spectra of triflate systems of a general formula: $[\text{L}-\text{BF}_2-\text{OTf}]$.	114
Figure 3-21: ^{19}F NMR (376 MHz, DMSO) spectra of triflate systems of a general formula: $[\text{L}-\text{BCl}_2-\text{OTf}]$.	115
Figure 3-22: Example of a “masked” borenium cation.	118
Figure 3-23: Possible main coordination modes for tepo in a borenium ionic liquid, 4-pic- $\text{BCl}_3-2\text{AlCl}_3$.	119
Figure 3-24: ^{31}P NMR spectra (161.96 MHz, 27 °C, neat liquid with DMSO- d_6 lock) of 1 % tepo solution in borenium ionic liquids.	121
Figure 4-1: Simple $[4 + 2]$ cycloaddition reaction.	129
Figure 4-2: Stereoselectivity (endo: exo) in Diels–Alder reaction.	130
Figure 4-3: Lewis acid catalysis in Diels-Alder reaction. ²⁰³	131
Figure 4-4: 1-Boron-substituted 1,3-diene in a tandem cycloaddition $[4 + 2]/\text{allylboration}$. ²¹²	132
Figure 4-5: Diels-Alder reaction between ethyl acrylate (EA) and cyclopentadiene (CPD), catalyzed with borenium ILs.	137
Figure 4-6: Boltzmann fit of experimental data showing conversions in Diels-Alder cycloaddition of cyclopentadiene to ethyl acrylate, catalysed with 0.10 mol% of Lewis acidic ionic liquids vs. AN values of the catalysts.	139
Figure 4-7: Conversion of ethyl acrylate in Diels-Alder reaction, plotted as the function of catalyst loading (mol%, per dienophile).	140
Figure 4-8: ^{11}B NMR spectra of a) neat $[\text{BCl}_2(4\text{pic})][\text{AlCl}_4]$, and b) solution of $[\text{BCl}_2(4\text{pic})][\text{AlCl}_4]$ in ethyl acrylate (EA). Both recorded with external $\text{d}_6\text{-DMSO}$ lock.	142
Figure 4-9: ^{27}Al NMR spectra of a) neat $[\text{BCl}_2(4\text{pic})][\text{AlCl}_4]$, and b) solution of $[\text{BCl}_2(4\text{pic})][\text{AlCl}_4]$ in ethyl acrylate (EA). Both recorded with external $\text{d}_6\text{-DMSO}$ lock.	143
Figure 4-10: ^{11}B NMR (128 MHz, external $\text{d}_6\text{-DMSO}$ lock) spectrum of solution $[\text{BCl}_2(\text{mim})][\text{Al}_2\text{Cl}_7]$ in ethyl acrylate(EA).	144
Figure 4-11: ^{27}Al NMR (104 MHz, external $\text{d}_6\text{-DMSO}$ lock) spectrum of solution $[\text{BCl}_2(\text{mim})][\text{Al}_2\text{Cl}_7]$ in ethyl acrylate (EA).	145
Figure 4-12: ^{11}B NMR (128 MHz, external $\text{d}_6\text{-DMSO}$ lock) spectrum of solution $[\text{BCl}_2(\text{mim})][\text{Ga}_2\text{Cl}_7]$ in ethyl acrylate (EA).	146

Figure 4-13: ^{91}Ga NMR (122 MHz, external $\text{d}_6\text{-DMSO}$ lock) spectrum of solution [$\text{BCl}_2(\text{mim})$][Ga_2Cl_7] in dienophile ethyl acrylate (EA).	146
Figure 4-14: Conversion of EA in reactions with CPD with different catalyst amounts in toluene (10 cm^3) at 23 $^\circ\text{C}$.	148
Figure 4-15: Conversion of EA in reactions with CPD with different catalyst amounts in toluene (10 cm^3) at 23 $^\circ\text{C}$.	149
Figure 4-16: Conversion of EA in reactions with CPD in different catalyst amounts in toluene (10 cm^3) at 23 $^\circ\text{C}$.	150
Figure 4-17: Conversion of EA in varying volumes of DCM and temperature with 2 mol% [$\text{BCl}_2(\text{mim})$][Ga_2Cl_7].	151
Figure 5-1: Formation of boron enolate in aldol condensation. ²⁵⁰	159
Figure 5-2: Boron enolates in aldol condensation. ^{252,250}	160
Figure 5-3: Structure of dypnone. ²³³	160
Figure 5-4: Mechanism for the synthesis of dypnone via self-condensation of acetophenone over an acidic catalyst. ²³⁰	161
Figure 5-5: Typical products of the self-condensation of acetophenone: a) trans-dypnone, b) cis- dypnone, and c) 1-phenyl-2-(2-vinylphenyl) ethanone	162
Figure 5-6: Synthesis of dypnone catalysed with borenium ionic liquids.	166
Figure 5-7: Left: GC calibration curve of dypnone with n-decane as internal standard (AcP - acetophenone, Dec - n-decane); right: GC calibration curve of acetophenone with n-decane as internal standard (DP - dypnone, Dec - n-decane)	168
Figure 5-8: Experimental data showing conversions in aldol condensation of acetophenone to dypnone catalysed with 2.8 mol% of Lewis acidic ionic liquids vs. AN values of the catalysts.	171
Figure 5-9: Experimental data showing selectivity in Aldol condensation of acetophenone to dypnone catalysed with 2.8 mol% of Lewis acidic ionic liquids vs. AN values of the catalysts.	171
Figure 5-10: Aldol-type self-condensation of dypnone to 1,3,5-triarylbenzene.	173
Figure 5-11: IR spectrum of isolated pure dypnone.	174
Figure 5-12: ^1H NMR (400 MHz, DMSO) NMR spectrum of reaction product in dypnone synthesis.	175
Figure 5-13: Enlarge area of integration of dypnone between 6 to 7 ppm showing individual peak splitting.	175

LIST OF TABLES

Table 1-1: Some properties of the Group 13 elements: boron, aluminium, gallium, indium and thallium. ⁶	21
Table 1-2: Examples of the various routes for borenium cation formation. ²⁷	26
Table 1-3: Synthetic route in the formation borocations.	27
Table 2-1. A list of ligands used in this work, their abbreviations, structures and pK _a values of conjugate acids.	51
Table 2-2: Yield and appearance of boron halide adducts, [BX ₃ L]; S = solid, L = liquid	53
Table 2-3: ¹ H NMR (400 MHz, CDCl ₃) chemical shifts recorded for boron complexes and corresponding free ligands.	54
Table 2-4: ¹³ C NMR (101 MHz, CDCl ₃) chemical shifts recorded for boron complexes and corresponding free ligands.	55
Table 2-5: ¹¹ B NMR (128 MHz, 27 °C, CDCl ₃) spectra of tetracoordinate boron complexes, [BCl ₃ L].	58
Table 2-6: CHN, metal and halogen analysis of the boron complexes, by % mass	64
Table 2-7: The melting decomposition points of the synthesised boron complexes.	65
Table 2-8: The melting onsets (T _m), melting maxima and enthalpies of boron complexes.	70
Table 3-1: Physical state at ambient conditions of products of reaction between [BCl ₃ L] complexes and nMCl ₃ (n = 1, 2 or 3, M = Al or Ga); L - liquid, W - waxy solid and L+P = liquid + precipitation	80
Table 3-2: ¹ H NMR (400 MHz, DMSO) chemical shifts recorded for borenium chlorometallate ionic liquids complexes.	82
Table 3-3: ¹³ C NMR (101 MHz, DMSO) chemical shifts recorded for borenium chlorometallate ionic liquids complexes.	84
Table 3-4: ¹¹ B NMR spectra (128.37 MHz, 27 °C, neat liquid with DMSO-d ₆ lock) parameters for borenium ionic liquids of a general formula L-BCl ₃ -nMCl ₃ , where M = Al or Ga.	85
Table 3-5: Chemical shifts of ²⁷ Al NMR signals (104.28 MHz, 25 °C, neat liquid with DMSO-d ₆ lock) recorded for ionic liquids of a general formula L-BCl ₃ -nAlCl ₃ (n = 1 or 2)	90
Table 3-6: FT-IR frequencies (cm ⁻¹) for ligands (L), corresponding tetracoordinate boron complexes, [BCl ₃ L], and corresponding borenium ionic liquids of a general formula L-BCl ₃ -nMCl ₃ , where M = Al or Ga.	94

Table 3-7: FT-IR frequencies (cm^{-1}) corresponding to the synthesised borenium chloroaluminate systems with O-, and P donors: $\text{L-BCl}_3\text{-nMCl}_3$, where $\text{M} = \text{Al}$ or Ga .	95
Table 3-8: Experimental values for viscosity-corrected densities, ρ , of the studied borenium ionic liquids for temperatures between 293 to 343 K and at atmospheric pressure.	97
Table 3-9: Parameters a and b of the fitting of corrected experimental densities of borenium ionic liquids, along with the standard deviation of each fit between the temperatures of 293 K and 343 K at atmospheric pressure.	99
Table 3-10: Experimental values for viscosities, η , of the studied borenium ionic liquids, for temperatures from 293 to 343 K.	102
Table 3-11: Vogel-Fulcher-Tammann equation parameters obtained for the measurements of viscosity, η , of borenium ionic liquids for temperatures between 293 K and 343 K.	105
Table 3-12: Appearances of the borenium triflate ionic liquids, $\text{L-BX}_3\text{-OTf}$ and % yields	106
Table 3-13: The main ^1H NMR (400 MHz) chemical shifts for the triflate systems.	108
Table 3-14: ^{13}C NMR (101 MHz, DMSO) chemical shifts recorded for the triflate systems.	110
Table 3-15: ^{11}B NMR (160 MHz, DMSO, 27 °C, neat liquid with DMSO- d_6 lock) parameters for the triflate liquids	113
Table 3-16: ^{19}F NMR (376 MHz, DMSO) chemical shift recorded for the triflate liquids	115
Table 3-17: FT-IR frequencies (cm^{-1}) for the triflate systems: $[\text{L-BCl}_2\text{-OTf}]$ and $[\text{L-BF}_2\text{-OTf}]$.	117
Table 3-18: AN values for $\text{L-BCl}_3\text{-nMCl}_3$ systems, along with the $\delta_{31\text{P}}$ resonances (in ppm) measured for solutions of 1 mol% tepo in these liquids, referenced to $\delta_{31\text{P}}$, H_3PO_4 (85%) = 0.0 ppm.	122
Table 3-19: AN values for all $\text{L-BCl}_3\text{-nMCl}_3$ systems, neat and in DCM solution, along with the $\delta_{31\text{P}}$ resonances (in ppm) measured for 1 mol% tepo content, and referenced to $\delta_{31\text{P}}$, H_3PO_4 (85%) = 0.0 ppm.	123
Table 3-20: AN values for all $\text{L-BX}_2\text{-nOTf}$ systems based on the different donors that were homogenous liquids along with the $\delta_{31\text{P}}$ resonances (in ppm) measured for solutions of these liquids containing 1 mol% tepo (referenced to $\delta_{31\text{P}}$, H_3PO_4 85% = 0.0 ppm).	125
Table 4-1: Diels-Alder reaction between cyclopentadiene and ethyl acrylate in the presence borenium ionic liquids, AlCl_3 and chloroaluminate ionic liquids, along with the corresponding AN values, conversions and endo: exo selectivity.	138
Table 4-2: A list of dienes and dienophiles used in this work and their abbreviations.	152

Table 4-3: Conversions and selectivities in Diels-Alder reactions of cyclopentadiene with different dienophiles, catalyzed by borenium chlorogallate ionic liquids.	153
Table 5-1: Typical literature examples of various dynone synthesis.	163
Table 5-2: Condensation of acetophenone over borenium halometallate ionic liquids as catalyst and benchmark acids.	169
Table 5-4: Condensation of acetophenone over borenium halometallate ionic liquids as catalyst, in chloroform.	172

LIST OF ABBREVIATIONS

Item	Name
<i>ACN</i>	Acrylonitrile
<i>AN</i>	Acceptor number
<i>bp</i>	Boiling point
<i>C₆H₅CF₃</i>	trifluoro-toluene
<i>CPD</i>	Cyclopentadiene
<i>DA</i>	Diels-Alder
<i>DCM</i>	Dichloromethane
<i>DEM</i>	Diethyl maleate
<i>DES</i>	Deep Eutectic Solvents
<i>dma</i>	Dimethylacetamide
<i>DSC</i>	Differential scanning calorimetry
<i>EA</i>	Ethyl acrylate
<i>FIA</i>	Fluoride ion affinity
<i>FLP</i>	Frustrated Lewis Pairs
<i>FMO</i>	Frontier molecular orbital
<i>HIA</i>	Hydride ion affinity
<i>HOMO</i>	Highest occupied molecular orbital
<i>HSAB</i>	Hard and soft acids and bases
<i>IL</i>	Ionic liquid
<i>IR</i>	Infrared
<i>IPN</i>	Isoprene
<i>L</i>	Ligand
<i>LCC</i>	Liquid coordination complexes
<i>LPDE</i>	Lithium perchlorate-diethyl ether
<i>LUMO</i>	Lowest unoccupied molecular orbital
<i>MA</i>	Methyl acrylate
<i>MAC</i>	Methacrolein
<i>MeOTf</i>	methyl trifluoromethanesulfonate
<i>MMA</i>	Methyl methacrylate

<i>mim</i>	1- methyl imidazole
<i>MO</i>	Molecular orbital
<i>mp</i>	Melting point
<i>MVK</i>	Methyl vinyl ketone
<i>MW</i>	Molecular weight
<i>4-pic</i>	4-methylpyridine/ 4-picoline
<i>NMR</i>	Nuclear magnetic resonance
<i>[NTf₂]⁻</i>	Bis(trifluoromethanesulfonyl)amide, bistriflamide
<i>[OTf]⁻</i>	Trifluoromethanesulfonate, triflate
<i>P₈₈₈</i>	Trioctylphosphine
<i>P₈₈₈O</i>	Trioctylphosphine oxide
<i>PILs</i>	Protic ionic liquids
<i>TGA</i>	Thermogravimetric analysis
<i>TMSOTf</i>	Trimethylsilyl trifluoromethanesulfonate
<i>tepo</i>	Triethylphosphine oxide
<i>RTILs</i>	Room temperature ionic liquids
<i>X</i>	Halide
<i>SILs</i>	Solvate ionic liquids



CHAPTER ONE

“Honesty is the first chapter in the book of wisdom”.
-Thomas Jefferson



1 INTRODUCTION

This chapter covers a very short introduction to Group 13, followed by a more subject-specific introduction to borocations. Subsequently, a discussion on acidity is provided, including its definitions and approaches to quantifying Lewis acidity. Finally, a short introduction to ionic liquids is followed by a more detailed description of state-of-the-art in Lewis acidic ionic liquids.

1.1 CHEMISTRY OF GROUP 13 ELEMENTS

1.1.1 Electron structure and periodicity of Group 13 elements

Group 13 consist of the elements, boron, aluminium, gallium, indium and thallium. Elements in this group show similar patterns; however, each element does have its own characteristic with boron being the most different from the others. Metallic character increases with increasing atomic number of Group 13 elements. Boron is a non-metal and a semiconductor, whereas all the other elements are metals and good conductors under normal conditions.⁶ Aluminium is the most abundant and naturally occurring metal (see Table 1-1). The other elements of Group 13 are rare and occur in smaller amounts.

The elements in Group 13 belong to the *p*-block. They have 3 electrons in their outermost energy shell and a general electron configuration of $ns^2 p^1$.^{6,7,8} The atomic radius increases down the group, making boron the smallest element of the group as its electrons are close to the nucleus hence more closely held together. Furthermore, the ionization energy decreases down the group, since the electrons are farther away from the nucleus making them easier to remove compare to boron. Electronegativity also decreases in the same order.

Table 1-1: Some properties of the Group 13 elements: boron, aluminium, gallium, indium and thallium.⁶

	B	Al	Ga	In	Tl
1) Properties of isolated atom					
Atomic number	5	13	31	49	81
Naturally occurring isotopes	¹⁰ B (19.9%) ¹¹ B (80.1%)	²⁷ Al (100%)	⁶⁹ Ga (60.108%) ⁷¹ Ga (39.892%)	¹¹³ In (4.29%) ¹¹⁵ In (95.71%)	²⁰³ Tl (29.524%) ²⁰⁵ Tl (70.47%)
Relative atomic mass (¹² C=12.0000)	10.811(7)	26.9815386(8)	69.723(1)	114.818(3)	204.3833(2)
Ground state electron configuration	[He]2s ² 2p ¹	[Ne]3s ² 3p ¹	[Ar]3d ¹⁰ 4s ² 4p ¹	[Kr]4d ¹⁰ 5s ² 5p ¹	[Xe]4f ¹⁴ 5d ¹⁰ 6s ² 6p ¹
Ionisation energies(KJ mol ⁻¹)					
M→M ⁺	800.637	577.539	578.844	558.299	589.351
M ⁺ →M ²⁺	2427.07	1816.68	1979.41	1820.71	1971.03
M ²⁺ →M ³⁺	3659.75	2744.78	2963	2704	2878
M ³⁺ →M ⁴⁺	25025.9	11577.46	6175	5210	4900
2) Properties of the bound atom					
Electronegativity, x					
Pauling Scale	2.04	1.61	1.81	1.78	1.62(Tl ^I),2.04(Tl ^{III})
Atomic radius(Å)	0.80-0.90	1.431	1.22-1.40	1.62-1.68	1.701(α-form)

The formal oxidation state of Group 13 is +3, but the heavier metals tends to favour an oxidation state of +1 due. Crucially for this work, the partially filled *p*-orbitals of Group 13 members make them Lewis acidic, as they are able to receive electron pairs from available electron pair donors (Lewis bases).^{9,10}

1.1.2 Reactivity of halides of the Group 13 elements

The elements in the boron group form stable compounds with halogens (Group 17 elements) of a general formula of MX₃ (M - boron group element, X - halogen element).^{11,6} The most significant chemical property that Group 13 elements impart to neutral M(III) compounds is the innate electrophilicity or acidity of the M(III) center.^{6,8} Consequently, all Group 13 halides based on the +3 oxidation state of the boron element are Lewis acids and form addition products with neutral or anionic electron-rich species (halides, organic donor molecules).⁶ The strength of

Lewis acidity of chlorides decreases with increasing atomic number of Group 13 elements: boron(III) chloride > aluminium(III) chloride > gallium(III) chloride > indium (III) chloride.¹²

Aluminium, gallium and indium all form trifluorides, MF₃ which are naturally ionic with high melting points (~1000 °C).^{11,6} The chlorides, bromides and iodides of these metals are covalent, much more volatile, having much lower melting points.⁶ They exist as dimeric molecules with the formula M₂X₆, which have the form of edge-sharing tetrahedral, with two halides bridging the metals. They are soluble in nonpolar organic solvents. The trihalides of thallium are much less stable than those of the rest of the group.

Just like the rest of the Group 13 elements, boron reacts with halides to form Lewis acidic trihalides, BX₃, that form adducts with electron donor molecules and halide ions.¹³ However, boron trihalides are monomeric, with trigonal planar geometry, bond angle of 120°, and sp² hybridised boron.¹⁰ Lewis acidity increases with increasing ionic radius of the halide, from fluoride to iodide: BF₃ < BCl₃ < BBr₃ < BI₃, which is quite opposite to what might be expected considering the decrease in electronegativity and increase in atomic radius of the halogen atoms (Figure 1-1)^{10,7} This apparent anomaly can be explained by the strength of boron-halogen π -bonding, which decreases from BF₃ to BI₃.^{10,8} Since the *p*-orbitals of boron and fluorine are similar in size, the electron pair donation from fluorine 2*p* π orbital into the formally empty boron 2*p* π atomic orbital is more efficient and leads to stronger B-X π -bonding than the (increasingly weaker) electron pair donation of chlorine, bromine and iodine.^{8,10} As a result of the very strong B-F π -bonding, BF₃ exhibits the lowest Lewis acidic character in the series.^{10,8}

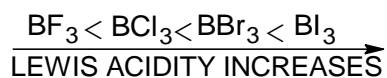


Figure 1-1: Lewis acidity of boron trihalides.¹⁰

The Lewis acidity of boron trihalides strongly influences their chemistry.^{10,14} They react with O, S, N and P-donors (Lewis bases) to form donor-acceptor complexes.^{10,15} Boron trifluoride may be the least Lewis acid in the boron trihalides series but is the key halide in Lewis acid catalysis. It is slightly soluble in many organic solvents, including saturated hydrocarbons.⁶ Due to the strength of B-F bonds, there is no or little undesirable by-products in BF₃-catalysed reactions. Being a gas, it is easily recovered from the reaction products. In consequence, BF₃ is widely used for numerous organic reactions: including polymerisation, isomerisation, acylation, alkylation,¹⁶

esterification, condensation and Mukaiyama aldol addition.^{17,7,10,11} Although less popular, boron trichloride and boron tribromide are also used as Lewis acid catalysts, predominantly in various polymerisation, alkylation, and acylation reactions.⁸ For example, copolymerisation of butadiene with olefins is a typical example of a BBr₃-catalysed process.^{7,18}

1.2 BOROCATIONS

Borocations are cationic species of boron, characterised by electron deficiency bonding, with varying numbers of coordinate covalent bonds at the boron centre.¹⁹ The inception of the borocation chemistry is dated for 1906, when Dilthey obtained the first boronium cations by the reaction of beta-diketones with boron trichloride.²⁰ Early publications on borocations included the works of Ryschkewittsch and Wiggins²¹ and Shitov *et al.*²⁰ in 1970, and in 1980s by Kolle and Noth.²² More recently, several excellent reviews on the topic have been published, including Piers *et al.*²³ who discussed the synthesis, reactivity and applications of boron cations in more detail, whereas a comprehensive review by Ingleson²⁴ covers fundamentals and applications.²³

The electrophilic nature of borocations qualified them as Lewis acids; yet, until the early 90s, this fact received little attention. Over two decades ago, high Lewis acidity and reactivity of borocations began to be harnessed in useful ways, such as hydroboration chemistry,²⁵ Lewis acidic boron-mediated chemistry, boron-enolate chemistry,²⁴ C-H borylation²⁶ and as Lewis acidic components in frustrated Lewis pairs.^{27,28} They have also been used as alternatives to other expensive, potentially toxic, high-molecular-weight metal-based Lewis acids.²⁷

Borocations can be classified under three groups based on their coordination number, namely, borinium (dicoordinate), boronium (tetracoordinate) and borenium (tricoordinate).

1.2.1 Borinium cations

Borinium cations (Figure 1-2) are strongly coordinationally unsaturated, with two substituents that relieve the electron deficiency on boron through π -donation from their lone pairs.²³ Borinium compounds are very reactive and difficult to handle or use in solution studies, as they readily react with solvents and counterions, owing to the highly unsaturated coordination sphere. Borinium cations are *sp*-hybridised, with a linear structure.²³

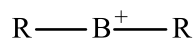


Figure 1-2: Structure of borinium ion, where R is formally a monoanionic substituent.⁸

1.2.2 Boronium cations

Boronium cations (Figure 1-3) are the most common borocations, with all four coordination sites filled: with two sigma bound substituents and two dative bound neutral ligands.²³ This group is very stable owing to the saturation of the coordination sphere of boron, and by the same trait - the least reactive. The electron density provided by the donor ligands aids to partially quench the positive charge on boron.^{23,24} Boronium cations are sp^3 -hybridised, with tetrahedral geometry around the boron centre.

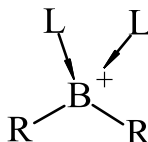


Figure 1-3: Structure of boronium ion, where L is formally a neutral two-electron donor and R is formally a monoanionic substituent.⁸

1.2.3 Borenium cations

Three coordinate borocations with the boron atom surrounded by two sigma bound substituents and one dative ligand, borenium cations (Figure 1-4) were the focus of research in this thesis.^{29,23} Borenium cations are very strong Lewis acids, owing to the electron deficiency of the vacant boron p -orbital, which is also enhanced by the positive charge. Borenium cations are sp^2 -hybridised, with a trigonal planar geometry.^{27,21} Although the coordination sphere of borenium cations is not saturated, the three ligands provide enough stabilisation to facilitate their handling, rendering them useful as intermediates in many reactions and suitable for studies in solution.^{8,24} Additionally, π -back-bonding stabilisation of the boron atom plays an important role in the overall stability of these tricoordinate species.³⁰ Despite the attractive characteristics of borenium cations, until recently they have been the least studied among the three classes of the borocations.^{20,22,8}

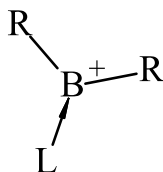


Figure 1-4: Structure of borenium ion, where *L* is formally a neutral two-electron donor and *R* is formally a monoanionic substituent.⁸

The chemistry of the cationic, trivalent boron complexes (borenium ions) was founded by Noth and Fritz²² in 1963, where they described the formation of a bis(dimethyl amino)(dimethylamine) borenium ion (Figure 1-5).³¹ Until then, the literature contained only a little information on these cations: they were only known as intermediates in reactions, leaving their reactivity and applications unexplored.

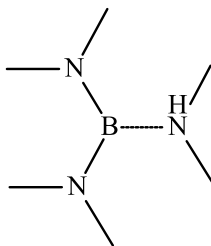


Figure 1-5: Structure of bis(dimethyl amino)(dimethylamine) borenium ion.³¹

Subsequently, publications by Ryschkewitsch,²¹ Noth and Kolle²² and others gave early insight into the chemistry and applications of borocations,^{21,22,32} but this field of research only began popular in the last couple of years, these recent discoveries covered by the comprehensive reviews by Piers *et al.*,²³ De Vries *et al.*,⁸ and Ingleson.²⁴ Borenium cations are now gaining increasing interest as Lewis acidic catalysts for various reactions, such as hydrogenations and hydroborations, as well as stoichiometric reagents in aromatic or aliphatic C–H borylation.^{25,29}

There are numerous routes to generate borenium cations, including electrophilic attack at B–N bond, nucleophilic displacement, base addition to borinium ions, metathesis and halide/hydride abstraction (see Table 1-2).²³

Table 1-2: Examples of the various routes for borenium cation formation.²⁷

Entry	Synthetic route	Equation
1	BX bond heterolysis	$\begin{array}{c} \text{L} \\ \downarrow \\ \text{X}-\text{B}-\text{X} \\ \uparrow \\ \text{X} \end{array} + \text{MX}_n \longrightarrow \left[\begin{array}{c} \text{L} \\ \downarrow \\ \text{X}-\text{B}^+-\text{X} \\ \uparrow \\ \text{X} \end{array} \right]^- \text{MX}_{n+1}^-$
2	Protic attack of BN bond	$\begin{array}{c} \text{NR}'_2 \\ \\ \text{R}-\text{N}-\text{B}-\text{N}-\text{R} \\ \quad \\ \text{H} \quad \text{H} \end{array} + \text{HX} \longrightarrow \left[\begin{array}{c} \text{NR}'_2 \\ \\ \text{R}-\text{N}-\text{B}^+-\text{N}-\text{R} \\ \quad \\ \text{H} \quad \text{H} \end{array} \right]^- \text{X}^-$
3	Electrophilic attack at BN bond	$\text{R}_2\text{N}-\text{B}=\text{N}-\text{R}' + \text{Me}_3\text{SiX} \longrightarrow \left[\begin{array}{c} + \text{SiMe}_3 \\ \\ \text{R}_2\text{N}-\text{B}-\text{N}-\text{R}' \\ \\ \text{R}' \end{array} \right]^- \text{X}^-$
4	Nucleophilic displacement	$\begin{array}{c} \text{X} \\ \\ \text{R}-\text{B}-\text{R}' \end{array} + \text{L} \longrightarrow \left[\begin{array}{c} \text{L} \\ \downarrow \\ \text{R}-\text{B}^+-\text{R}' \end{array} \right]^- \text{X}^-$
5	Base addition to borinium ions	$\left[\begin{array}{c} + \\ \text{R}_2\text{N}-\text{B}-\text{NR}'_2 \end{array} \right]^- \text{X}^- + \text{L} \longrightarrow \left[\begin{array}{c} \text{L} \\ \downarrow \\ \text{R}_2\text{N}-\text{B}^+-\text{NR}'_2 \end{array} \right]^- \text{X}^-$
6	Metathesis	$\begin{array}{c} \text{L} \\ \downarrow \\ \text{R}-\text{B}-\text{X} \\ \uparrow \\ \text{R}' \end{array} + \text{AgY} \xrightarrow{-\text{AgX}} \left[\begin{array}{c} \text{L} \\ \downarrow \\ \text{R}-\text{B}^+-\text{R}' \end{array} \right]^- \text{Y}^-$

The most common amongst these synthetic strategies is hydride/halide abstraction from a tetracoordinate boron adduct, $[\text{BX}_3\text{L}]$, using an excess of abstracting agent.²⁷ By 1970, Ryschkewitsch and Wiggins²¹ observed the formation of this tricoordinate borenium ion when the tetracoordinate $[\text{BCl}_3(4\text{-picoline})]$ adduct was combined with AlCl_3 , in dichloromethane (DCM) solution (Figure 1-6).²¹ This was reported as the first observable borenium salt,²¹ and the evidence for the formation of this borenium cation was deshielded ^{11}B NMR signal, at $\delta = 47.3$ ppm.²¹

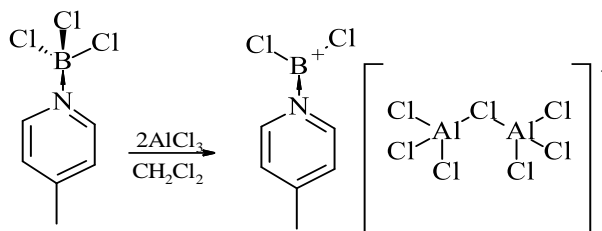


Figure 1-6: The formation and structure of a borenium cation in solution with $[\text{Al}_2\text{Cl}_7]^-$ anion.²¹

All standard synthetic routes towards borocations are listed in Table 1-3.

Table 1-3: Synthetic route in the formation of borocations.

Entry	Synthetic route	Equation
1	BX bond heterolysis	$\begin{array}{c} \text{X} \\ \\ \text{R}-\text{B}-\text{R}' \end{array} + \text{MX}_n \longrightarrow \left[\text{R}-\text{B}-\text{R}' \right]^+ \text{MX}_{n+1}^-$ $\begin{array}{c} \text{L} \\ \\ \text{X}-\text{B}-\text{X} \end{array} + \text{MX}_n \longrightarrow \left[\text{X}-\text{B}-\text{X} \right]^+ \text{MX}_{n+1}^-$
2	Protic attack of BN bond	$\begin{array}{c} \text{NR}'_2 \\ \\ \text{R}-\text{N}-\text{B}-\text{N}-\text{R} \\ \quad \\ \text{H} \quad \text{H} \end{array} + \text{HX} \longrightarrow \left[\begin{array}{c} \text{NR}'_2 \\ \\ \text{R}-\text{N}-\text{B}-\text{N}-\text{R} \\ \quad \\ \text{H} \quad \text{H} \end{array} \right]^+ \text{X}^-$
3	Electrophilic attack at BN bond	$\text{R}_2\text{N}-\text{B}=\text{N}-\text{R}' + \text{Me}_3\text{SiX} \longrightarrow \left[\begin{array}{c} + \quad \text{SiMe}_3 \\ \\ \text{R}_2\text{N}-\text{B}-\text{N}-\text{R}' \end{array} \right]^+ \text{X}^-$
4	Nucleophilic displacement	$\begin{array}{c} \text{X} \\ \\ \text{R}-\text{B}-\text{R}' \end{array} + \text{L} \longrightarrow \left[\begin{array}{c} \text{L} \\ \\ \text{R}-\text{B}-\text{R}' \end{array} \right]^+ \text{X}^-$
5	Base addition to borinium ions	$\left[\text{R}_2\text{N}-\text{B}-\text{NR}'_2 \right]^+ \text{X}^- + \text{L} \longrightarrow \left[\begin{array}{c} \text{L} \\ \\ \text{R}_2\text{N}-\text{B}-\text{NR}'_2 \end{array} \right]^+ \text{X}^-$
6	Metathesis	$\begin{array}{c} \text{L} \\ \\ \text{R}-\text{B}-\text{X} \\ \\ \text{R}' \end{array} + \text{AgY} \xrightarrow{-\text{AgX}} \left[\begin{array}{c} \text{L} \\ \\ \text{R}-\text{B}-\text{R}' \end{array} \right]^+ \text{Y}^-$

The stabilisation of these compounds or coordination generated from all these routes can be associated to the σ -accepting factors of a electronegative atoms such as nitrogen or oxygen and the π -bonding lone pairs of the heteroatom.²⁴

1.3 ACIDITY

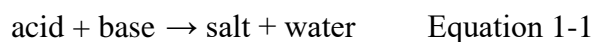
1.3.1 Historical understanding and definitions of acidity

The term acid is derived from the Latin word *acidus/acēre* meaning sour³³ and alkali is from an Arabic *al-qaliy* meaning “ashes of the saltwort or the calcined ashes.”^{34,35} Historically, acids were referred to as substances with a sour taste but this definition is rarely of scientific significance. Many commonly used household items like vinegar, citrus fruits can be characterised as acids based on their distinct sour taste.³³ Alkalis were identified with things having bitter-soapy taste or solutions that are slippery or soapy to touch.^{34,35} Acidity is amongst the most important concepts in chemistry.³⁶ French chemist Antione Lavoisier provided the first generalised

scientific concept of acids in 1776.³⁷ Based on his knowledge of oxoacids such as HNO_3 , H_2SO_4 , Lavoisier defined acid as compound containing oxygen also known as “acid former”. Berzelius defined acids as oxides of non-metals, and bases as oxides of metals.³⁷ In 1810, Sir Humphry Davy proved the lack of oxygen in hydrohalic acids (HF , HCl , HBr and HI) and other acids, like H_2S . This recognition led to the modification of the oxygen theory. In 1838,³⁷ Justus von Liebig defined acid as a hydrogen-containing compound, where the hydrogen can be replaced by a metal.^{37,38} The hydrogen theory of acids by Liebig³⁷ was then improved upon by Arrhenius in 1884.^{33,38}

Svante Arrhenius was a Swedish chemist, whose work on acid-base reactions contributed greatly to the understanding of acid-base equilibria, and brought him the Nobel Prize in Chemistry in 1903. Arrhenius defined an acid as a substance that can donate, or add, hydrogen ions, H^+ , in solution. In the context of aqueous solutions, for example, an acid is a substance containing hydrogen which forms hydrogen ions, or that otherwise increases the concentration of hydroxonium ion, $[\text{H}_3\text{O}]^+$ when added to water.^{33,39} An Arrhenius base is a compound that results in the increase of a hydroxide ion, OH^- , in solution.^{35,37}

The general relationship between acid and bases, as defined by Arrhenius, is that they undergo a neutralisation reaction, where a salt and water are formed (Equation 1-1)³⁷



A major limitation to Arrhenius concept of acids and bases was that, although acidic and basic properties may appear in any solvent, Arrhenius concept could only identify acids and bases in aqueous environments.^{35,40} Additionally, this definition limits acids and bases to compounds generating H^+ or OH^- ions, respectively.³⁷ Acids and bases in non-aqueous solvents were studied in the beginning of 20th century by Edward C. Franklin; his work on acid-base interactions in liquid ammonia highlighted similarities to Arrhenius aqueous solution theory. Then, in 1925, Albert F. O. German⁴¹ who worked with liquid phosgene (COCl_2) introduced the solvent system theory - a more general alternative definition to Arrhenius’ definition, including also aprotic solvents.⁴¹ However, a few years before German’s solvents theory, another

definition - now known as Brønsted-Lowry - was published and gained far more prominence.^{38,35,40}

Currently, there are two universally accepted definitions of acidity and basicity, one formulated simultaneously by Brønsted and Lowry, and another more general - by Lewis.

1.3.2 Brønsted-Lowry definition

One of the most used definitions of acidity was proposed in 1923 by both J. N. Brønsted and T. M. Lowry, almost simultaneously.³⁸ The Brønsted-Lowry concept acids and bases is focused on compounds donating and receiving protons, as opposed to the formation of salts and solvent as in the case of Arrhenius theory.⁴² Brønsted-Lowry theory is independent of the solvent (Equation 1-2): the symbol H^+ in this definition represents the bare proton, and not the "hydrogen ion" of variable nature, which is formed in solution by the addition of a proton to the solvent.^{37,35}



Unlike Arrhenius theory, neutralisation reaction is not present in Brønsted-Lowry acid and bases reaction but rather new acid and new base forms when a Brønsted Lowry acid and base react.³⁷ In Equation 1-3, the acid (A) and the base (B) are termed a conjugate acid/base pair. Acid is defined as a substance that can lose a proton, or can otherwise be defined as a proton donor, whereas a base is a proton acceptor.³⁸ In essence, by Brønsted-Lowry definition any compound that can be deprotonated is an acid, and any compound that can accept a proton is a base.⁴³

Although Brønsted and Lowry's concepts did much by complimenting and including most of the compounds excluded by Arrhenius theory, it still left behind some compounds which are electrophilic, but lack hydrogen, such as SO_3 , $SnCl_4$, BF_3 or BCl_3 .⁴⁴ This major limitation was addressed in the Lewis theory of acids and bases.

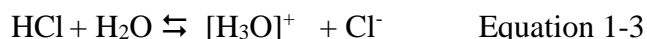
1.3.3 Lewis definition

As chance would have it, Lewis theory of acids and bases, which removed the hydrogen requirement present in both the Arrhenius and the Brønsted-Lowry definitions, was published in 1923, the same year as papers by Brønsted and Lowry.^{38,45} However, the concept of Lewis acidity has not been fully expanded upon until 1938,⁴⁵ when it has proved undoubtedly to be a

very useful generalisation of the Brønsted-Lowry definition, including non-hydrogen bearing compounds with acidic properties (electrophilic character), and thus linking nucleophilic behaviour with basicity.

The Lewis definition of acids states that an acid is a substance that accepts an electron pair, whereas a Lewis base is an electron-pair donor.^{43,45} This definition is more general theory which works outside of the protons and the bonding of substances definition as given by Brønsted according to which an acid is a molecule that is able to give protons. Elaborating on his theory, Lewis made this profound statement: “To restrict the group of acids to those substances which contain hydrogen interferes as seriously with systematic understanding of chemistry, as would restriction of the term ‘oxidising agent’ to substances containing oxygen”.⁴⁵

Lewis acids and base formulations differ from the preceding ones, *i.e.* Arrhenius and Brønsted definitions, in a fundamental manner: by Lewis definition, proton is indeed a particular case of an electron pair acceptor (Lewis acid). However, in aqueous solution, protons exist as $[\text{H}_3\text{O}]^+$ and related hydrated species. In the light of the above definition, $[\text{H}_3\text{O}]^+$ and other Brønsted acids are not Lewis acids, but Lewis adducts of a Lewis acid (proton) and a Lewis base (Equation 1-3).



Lewis theory of acids and bases was further advanced by Ralph G. Pearson, by introducing a qualitative concept in 1963,⁴⁶ explaining the behaviour of Lewis acids and bases in reaction. Several years later, with the help of Robert Parr,⁴⁷ Pearson proposed more a quantitative concept in 1983.⁴⁷ This concept was known as Hard Soft Acids Bases (HSAB).⁴⁶ By experimental reactions, Pearson observed that certain substrates acids tend to bind or coordinate strongly to bases that are highly polarisable whilst others tend to coordinate with bases that are non-polarisable to form stable complexes.^{46,48} Pearson divided Lewis acids and bases into hard and soft,^{2,3} founding hard and soft acids and bases (HSAB) theory, according to which hard acids have affinity towards hard bases, and soft acids - towards soft bases. Soft bases are large donors or nucleophiles with high charge states or valence electrons that are easily polarised, whilst hard bases are the ones with low charge states or valence electrons that are non-polarisable.^{49,48} In the same vein, soft acids are large acceptors or electrophiles with low positive charge that are

polarisable, and hard acids are small sized, highly positive and non-polarisable.^{49,46} The electrostatic interaction is thought to be the dominant source of stabilisation in a complex between a hard acid and a hard base, while electron delocalization between the frontier orbitals plays a key role in the interaction between a soft acid and a soft base.^{46,49}

Within the HSAB definition, the level of hardness/softness of acids and bases would be explained in terms of the attraction of hard acids to hard bases, and soft acids to soft bases, but not hard to soft components - which reactions tend to be produce polar covalent complexes that are more reactive (less stable).⁴⁶ The major criticism was originating from the HSAB inability to rank and quantify acids and bases in terms hardness.⁵⁰

Before Parr and Pearson⁴⁷ quantification of hardness, Klopman in 1968⁵⁰ proposed an equation based on the frontier molecular orbital (FMO) analysis. The concept of Lewis acid/base reaction can be described in terms of molecular orbital theory; the molecule with the highest occupied molecular orbital (HOMO) with lone pairs (the base) donates its electron to the molecule with the lowest unoccupied molecular orbital (LUMO) - *i.e.* the acid, to form an adduct through coordinate covalent bond.^{37,42} Such adducts containing metals ions are called coordination compounds.⁴² By Klopman's FMO analysis, hard Lewis acids have high energy LUMOs and soft Lewis acids - low energy LUMOs. Furthermore, hard Lewis bases have high energy HOMOs and soft Lewis bases - low high energy HOMOs. Klopman's equation has two different parts: one addressed the charge/charge interactions and the other described the FMO/FMO interaction.⁵⁰ Building on this, Parr and Pearson⁴⁷ proposed a quantitative operational definition of hardness (see Equation 1-4) based on Mulliken and Pauling electronegativity scales.^{51,47}

$$\eta_s = 1/2 (I_s + A_s) \quad \text{Equation 1-4}$$

where I is the ionization potential and A the electron affinity.⁴⁷

1.4 LEWIS ACIDITY MEASUREMENTS

Depending on the field of research, a range of scales to describe Lewis acidity and basicity have been developed over time. Lewis acidity could be for example measured in terms of the acid-base reactions, by using the equilibrium constant equation (Equation 1-5) as a universal method to determine the relative strengths of acids.⁵² However, this equation was found inadequate in determining the relative acid strength due to solvent effects, steric effects and other factors found in real-life acid-base reactions.⁵²

$$\log K = [S_A][S_B] \quad \text{Equation 1-5}$$

where S is the relative strength

Several other methods, both computational and experimental, have been established as convenient means of measuring Lewis acidity of various acidic compounds.⁵³ Methods using basic spectroscopic probes (typically in IR or NMR spectroscopy)⁵³ have been found to be reliable at estimating Lewis acidity. In IR spectroscopy, *N*-donors such as pyridine (py) or acetonitrile (AcCN)⁵³ are used, and the vibrational frequency of the adducts formed upon the coordination of the ligand to the Lewis acid is compared to a free probe molecule. This difference is then used as a measurement of Lewis acidity of the acid in question. Additional advantage is that the methodology allows for distinguishing between Lewis and Brønsted acidic sites, if both are present. NMR approaches include Gutmann acceptor number (AN), with trioctylphosphine as the ³¹P NMR probe, and Childs method, using crotonaldehyde as the ¹H/¹³C NMR probe.⁵³ Finally, computational methods tend to be based around the modelling of interactions of a Lewis acid with a very small anion: Fluoride Ion Affinity (FIA) scale is the most commonly used, but hydride ion affinity and chloride ion affinity are also studied.^{36,53} Due to difference in softness of these basic anions, differences in the ordering of Lewis acidity strengths were found for each probe. Methods most commonly used for ionic liquids are discussed in detail.

1.4.1 Gutmann acceptor number (AN)

Gutmann introduced his acceptor number (AN) approach in 1975,⁵⁴ as an experimental method for measuring solvent effects (namely donor and acceptor properties of solvents and molecular

species). The Gutmann experiment involved complexation of triethylphosphine oxide (tepo) with a Lewis acid (Figure 1-7), where tepo is used as a probe molecule to study the electrophilic properties of a solvent through ^{31}P NMR spectroscopy.⁵⁵

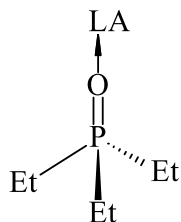


Figure 1-7: Complexation of triethylphosphine oxide (tepo) with a Lewis acid (LA) for Gutmann Lewis acidity test.

The Lewis acidity scale was set arbitrary, based on the measurement performed for a range of solvents. The ^{31}P NMR chemical shift of tepo in hexane was assigned $\text{AN} = 0$, and for tepo in SbCl_5 (2 M dichloromethane solution) at $\text{AN} = 100$. To eliminate the influence of concentration, ^{31}P NMR chemical shifts were extrapolated to infinite dilution and corrected for the differences in volume of each solvent.⁵³ The interaction between tepo and hexane gave ^{31}P NMR chemical shift of $\delta = 41.0$ ppm,^{55,56,57} whilst that of tepo in the strongly Lewis acidic SbCl_5 solution resulted in the ^{31}P NMR chemical shift at $\delta = 86.1$ ppm.^{54,55} Using H_3PO_4 (85%) as a reference ($\delta = 0.0$ ppm), the AN value can be calculated using Equation 1-6.

$$\text{AN} = 2.21 (\delta_{\text{sample inf dilution}} - 41.0) \quad \text{Equation 1-6}$$

Boron-containing Lewis acids have been commonly ranked *via* this method.⁵³ It is also the most common method to quantify Lewis acidity of Lewis acidic ionic liquids.⁵⁷ It was therefore natural that in this work the acceptor number (AN) scale was employed to measure the Lewis acidity of the borenium ionic liquids.

1.4.2 Childs method

Childs approach was introduced in 1982,^{58,59} and it explores the use of crotonaldehyde complexed with a Lewis acid (Figure 1-8) for determining the acid strength.^{58,59} When a Lewis acid reacts with crotonaldehyde in a 1:1 ratio, a complex is formed, which can be studied by ^1H NMR spectroscopy. Although chemical shifts of all the protons were found to have shifted

downfield upon complexation with a Lewis acid, the magnitude of chemical shift difference was largest for the hydrogen in position three (H3).^{59,60} Consequently, the change in chemical shift of the H3 hydrogen of crotonaldehyde is typically used to quantify the acid.^{59,60} BF₃, BC1₃, BBr₃, SbCl₅, TiCl₄, SnCl₄ and AlCl₃, are examples of some of the common acids explored in Childs' early studies of Lewis acidity measurement with ¹H NMR spectroscopy. Ionic liquids have never been studied by the method, and strong acids were reported to react with the probe, therefore this approach has not been explored here.⁶⁰

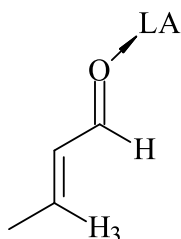


Figure 1-8: Complexation of Lewis acid (LA) to the oxygen on crotonaldehyde in Childs' Lewis acidity test.^{59,60}

1.4.3 Fluoride Ion Affinity (FIA) scale

This quantitative scale for Lewis acidity is based on the affinity of the Lewis acid to a hard base: the fluoride ion, and is more often computed rather than measured.⁶¹ The fluoride ion was selected for its high basicity and small size; it can readily react with nearly all Lewis acids, without steric hindrance issues. The enthalpy of reaction between the fluoride ion and a Lewis acid is used to quantify the strength of the acid. This method, however, has suffered from inconsistent results, and various researchers have used different forms of calculations to generate self-consistent fluoride affinity scales.

Christe *et al.*, for example, proposed pF^- values, which represent the fluoride ion affinity in kcal/mol, divided by 10 (Equation 1-7).⁶¹

$$\text{pF} = \text{F} \frac{\text{affinity} \left(\frac{\text{Kcal}}{\text{mol}} \right)}{10} \quad \text{Equation 1-7}$$

Krossing and co-workers have used a range of affinity scales including the fluoride affinity scale and ligand affinity in the computational study of the relative stabilities and coordinating abilities of various coordinating compounds.⁶² Ingleson and co-workers, studying frustrated Lewis pairs (FLPs) for H₂ activation, used a range of borenium cations and measured their hydride ion affinity (HIA) as well as fluoride ion affinity (FIA).^{63,64} One type of such borenium cations was

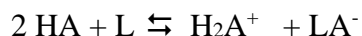
[CatB(amine)]⁺, where amine = Et₃N or 4,N,N-trimethylaniline.⁶³ Dichloro-ligated borenium cations were reported to have considerably greater high hydride ion affinity than that of conventional, charge-neutral boron compounds, such as B(C₆F₅)₃, which were typically used in FLPs. Furthermore, the high hydride ion affinity of the borenium ions were reported to be highly dependent on both the degree of steric crowding in the four-coordinate neutral borane (HBX₂L) and the electrophilicity of the borenium cation. Lewis acidity of borenium cations on the basis of Gutmann AN were also found to be correlated with the ability of borenium ion to abstract fluoride from [SbF₆]⁻, which indicated that the borenium cations have extremely high Lewis acidity, as measured by both AN and FIA methodology.^{64,65}

1.4.4 Superacids

Superacidity was firstly described in 1927 by James Bryant Conant and Norris F. Hall.⁴⁰ Connant and Norris studied the hydrogen ion activity of non-aqueous solutions where they observed salt formation with perchloric or sulfuric acid in glacial acetic acid with weak bases like unsaturated ketones and other carbonyl compounds.^{40,66} However in water, these weak bases did not form salts with the same acids but rather the acids were completely hydrolysed in water forming solutions with no basic properties and with very high hydrogen-ion activity. They described such solutions as “superacid solutions”.^{40,33} Although the definition of superacids is not included inherently in any major acidity theory, they are very important in describing some aspects of acidity above certain threshold of acidity strength.

Most work on superacidity was limited to Brønsted acids. Brønsted superacids are most often described as substances whose acidity is greater than 100% sulphuric acid.⁴⁰ Brønsted superacidity (and acidity in general) is commonly measured by Hammett acidity function, *H*₀, which is correlated to the equilibrium proton transfer between the superacids and its conjugate base. Pure H₂SO₄ has a *H*₀ value of -12, so superacids can be said to be acids with *H*₀ ≤ -12.⁶⁵ For example, pyrosulfuric acid has *H*₀ ~ -15, whereas trifluoromethanesulfonic acid (CF₃SO₃H) and fluorosulfuric acid (HSO₃F) have *H*₀ values about -14.1 and -15.1, respectively.^{33,65}

A common route to generate Brønsted superacids is the reaction of Lewis acids, such as BF₃ or AlCl₃, with Brønsted acids. Conjugate acid is formed, and auto protonation equilibrium is shifted to form counterion with a more delocalised charge, which in turn results in less bound proton - and therefore a stronger acid (Equation 1-8).^{65,66}



Equation 1-8

The term ‘Lewis superacids’ covers a wide range of compounds whose Lewis acidity is higher than conventional Lewis acids - but it is less frequently used than Brønsted superacid, and lacks unambiguous definition. This is of course related to the absence of a universal Lewis acidity scale, which makes it very difficult to determine a universally agreed upon threshold for Lewis superacidity.

Olah’s definition of Lewis superacids states that acids stronger than anhydrous aluminium chloride can be classified as superacids.^{65,66} This strength was manifested through catalytic activity in Friedel-Crafts reactions. By quantitative definition using Gutmann acceptor number scaling, acids with AN greater than 100 (*i.e.* acids greater than antimony pentachloride, SbCl₅) are classified as Lewis superacids. Some commonly known Lewis superacids include metal triflates and metal bistriflimides, arsenic pentafluoride and tris(pentafluorophenyl)borane, B(C₆F₅)₃. As already described, the coordinating strength of Lewis acids can vary widely with different Lewis bases and it is the strength of coordinating with tepo that determines the Lewis superacidity by Gutmann AN scale. An alternate quantitative definition of Lewis superacidity is based on the FIA scale, where Lewis acids with higher FIA than monomeric SbF₅ (489 kJ/mol) are termed Lewis superacids.⁶⁷

1.5 IONIC LIQUIDS

1.5.1 History

The concept on ionic liquids (ILs) is not new but has long existed scientifically before the introduction of the term ‘ionic liquids’. The history of ionic liquids goes back to the 19th century where Gabriel and Weiner⁶⁸ reported on the synthesis ethanol ammonium nitrate (m.p. 52-55 °C), which is an ionic liquid. In 1914, Walden⁶⁹ described ethylammonium nitrate, [C₂H₅NH₃][NO₃], as a molten salt with melting temperature of 12 °C,^{70,7} prepared by the neutralisation of ethylamine with concentrated nitric acid.^{70,69} However, following these early reports, the interest in ionic liquids remained dormant over a long period of time. Over 30 years later, Hurley and Weir⁷¹ reported on the first low melting aluminium chloride salts with organic cations,

synthesised by the combination of AlCl_3 and ethylpyridinium bromide, $[\text{C}_2\text{py}]\text{Br}-\text{AlCl}_3$, and their use in electroplating.⁷¹ This drew a lot of attention to the use of ionic liquids in electrodeposition, which remains among their prominent applications to date.⁷² Several more decades down the line, in 1975 Jones and Osteryoung⁷³ published a review on the use of chloroaluminate molten salts in organic reactions, which catapulted interest in ionic liquids and their applications beyond the field of electrochemistry.⁷³ The next milestone was the introduction of 1-ethyl-3-methylimidazolium-based chloroaluminate ionic liquids in 1982 by Wilkes *et al.*⁷⁴ These were among the first reported room temperature ionic liquids, that were noticed by the wider scientific community.⁷⁴ Still, hydrolytic instability of chloroaluminate ionic liquids limited their widespread applications.

In 1992, Wilkes and Zaworotko⁷⁵ reported the synthesis of the first air- and water-stable IL. The 1-ethyl-3-methylimidazolium cation, $[\text{C}_2\text{mim}]^+$, could be combined with hydrolytically stable anions, such as tetrafluoroborate or ethanoate.^{75,76} The discovery of less corrosive, air- and water-stable ILs led to the tremendous advancement in the field, supported by many publications reporting their applications as solvents and/or in catalysis.⁷⁷

1.5.2 General characteristics and state-of-the-art

According to the ‘traditional’ definition, ionic liquids are defined as molten salts with low melting points⁷⁸ ($<100\text{ }^\circ\text{C}$), that consist exclusively of ions.⁷⁹ However, many ionic liquids are liquid at ambient temperature (room-temperature ionic liquids),⁸⁰ and molten salts with higher melting temperatures are sometimes described as ionic liquids, too.^{70,7} The most commonly used are heterocyclic cations such as imidazolium, pyrrolidinium, or pyridinium, in addition to tetraalkylphosphonium salts (that melt at lower temperatures than their tetraalkylammonium analogues).⁷ The anions can either be organic: alkylsulfates, $[\text{RSO}_4]^-$ or alkylcarboxylates, $[\text{RCO}_2]^-$, or more commonly inorganic, such as already mentioned chloroaluminates, $[\text{AlCl}_4]^-$ and $[\text{Al}_2\text{Cl}_7]^-$, hexafluorophosphate, $[\text{PF}_6]^-$, tetrafluoroborate, $[\text{BF}_4]^-$ and triflate, $[\text{CF}_3\text{SO}_3]^-$.^{81,7}

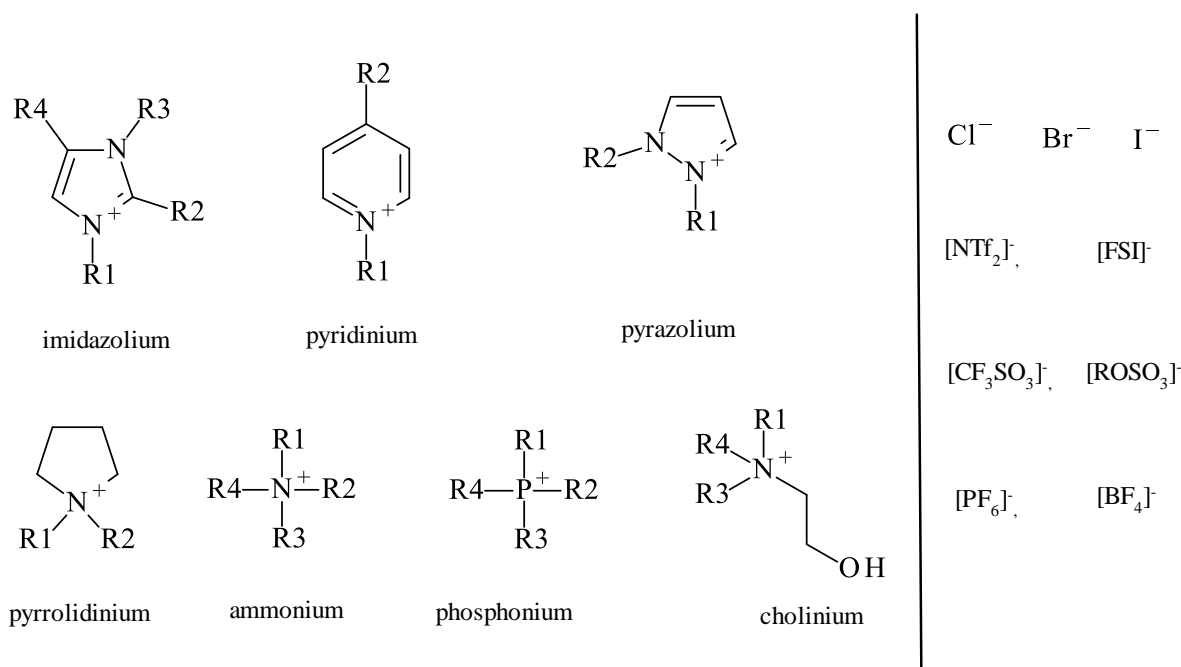


Figure 1-9: Some cations and anions commonly used in the design of ionic liquids (where R_x are alkyl groups).¹

The interest in ionic liquids has stemmed from their unique physical and chemical properties. Ionic liquids have very low to negligible vapour pressure at ambient temperature, which renders them inflammable under most conditions - this property gave them early on a badge of greener alternative to most organic solvents. Later it was recognised that these properties are dependent on the type of cation and anion used: in the simplest terms, the change in the cation affects the physical properties of an ionic liquid (viscosity, density, melting point), whereas a change in the anion affects its chemical properties and stability.⁷⁸ The structural differences in the cations and anions make ionic liquids synthetically flexible, which creates the possibility of developing ionic liquid with specific, tailored properties.¹

Research on ionic liquids developed over decades from manipulating their physical properties, through to their chemical properties to biological properties. Owing to their non-flammability and high thermal stability, ionic liquids have been used to replace volatile organic solvent the performance of battery cells.^{82,83} The incorporation of biological components/ions in ILs led to their application in biological membranes.^{84,85} Hydrated ionic liquids have been used to dissolve and stabilise proteins by providing these bio-macromolecules with hydration needed for structural stability.^{86,87} Current trends rely often on taking functional materials with desired

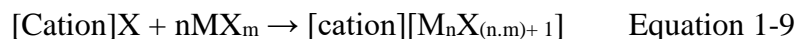
properties, and turning them to ionic liquids, rather than using generic ILs to address scientific challenges - this strategy is also the theme of this work.

1.6 LEWIS ACIDIC IONIC LIQUIDS

1.6.1 Halometallate ionic liquids

Until recently, Lewis acidic ionic liquids have been synonymous with halometallate ionic liquids - the oldest family of ILs (see Section 1.7.1).⁸⁸ Several reviews have covered various aspects of the preparation and properties of halometallate ionic liquids: Welton⁸⁹ in 1999 published a review entitled “*Room-Temperature Ionic Liquids: Solvents for Synthesis and Catalysis*” which discussed the synthesis, handling and properties of chloroaluminate(III) ionic liquids.⁸⁹ Estager *et al.*³ in 2014 covered various aspects of halometallate ionic liquids in general, especially the anionic speciation in chlorometallate systems and innovative applications of these compounds.³ Finally, a very recent review chapter by Swadzba-Kwasny and co-workers^{88,90,91} in 2017 gave a comprehensive overview of Lewis acidic ionic liquids and their developments, synthesis and structural diversity.⁹³

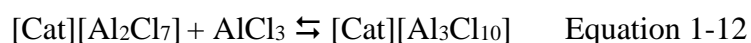
Halometallate ionic liquids are synthesised by reacting organic halide salt with Lewis acidic metal halide under anhydrous (see Equation 1-9)^{3,88} The resulting ionic liquid contains a well-defined cation, but the anionic component is often comprised of several halometallate species in a dynamic equilibrium.



Vast majority of research into halometallate ionic liquids, carried out over the past 60 years, focused on group 13 chlorides, in particular on a chloroaluminate(III) ionic liquids. An interesting exception is Parshall’s paper from 1974, which reported the use of organic ‘molten salts’ containing coordinating chlorostannate(II) or germanate(II) anions as solvents and co-catalysts for platinum-catalysed hydrogenation of olefins.⁸⁸ Otherwise, U.S. Air Force in the quest for lower temperature electrolytes for batteries engaged the use of room temperature chloroaluminate(III) ionic.^{92,93} Shortly after, chloroaluminate(III) ionic liquids have been reported as Lewis acid catalysts in Friedel–Crafts chemistry.^{3,94} In the following decades, various

other metal halides have been used in the synthesis of halometallate ionic liquids, for example chlorogallate, chlorozincate and chlorostannate(II) ionic liquids.

As stated earlier, the speciation of chloroaluminate(III) ionic liquids is characterised by complex anionic equilibria, which depend on the molar ratio of aluminium chloride to organic chloride salt.³ Depending of the molar ratios, $[\text{AlCl}_4]^-$, $[\text{Al}_2\text{Cl}_7]^-$, and potentially even $[\text{Al}_3\text{Cl}_{10}]^-$ may be formed, as shown in Equation 1-10 to Equation 1-12, where $[\text{Cat}]\text{Cl}$ is the organic chloride salt.



By changing the speciation, the high Lewis acidity of chloroaluminate(III) ionic liquids can be tuned to a certain extent. High Lewis acidity, combined with a degree of tuneability, resulted in numerous applications of chloroaluminates as catalyst and co-catalysts.⁹¹ However, very high Lewis acidity means also that chloroaluminates react vigorously with water, which acts as the base, and decompose releasing HCl.⁹⁵ Therefore, synthesis and handling of chloroaluminates are typically carried out in a glovebox using very dry equipment.

Aluminium halides are the most water sensitive and the most Lewis acidic from Group 13 metal halides (gallium and indium). From these three metals, indium halides are the least Lewis acidic but the most water stable. In the search for optimum catalytic systems, haloindate(III) ionic liquids have been used in reactions where mild Lewis acidity is required, and where reduced oxophilicity and moisture stability is the key, such as refinery alkylation⁹⁶, decreased isomerization in oligomerization of 1-decene⁹⁷ and Bayer–Villiger oxidation^{98,12}. Chlorogallate ionic liquids, highly acidic but slightly less moisture sensitive than chloroaluminates, were used in acetalization of aldehydes⁹⁹ and oligomerization of 1-decene⁹⁷. Looking outside Group 13, Sun and coworkers^{100,101,102} developed Lewis acidic ionic liquids based on zinc chloride combined with pyridinium, imidazolium or ethylphenylammonium salts.^{100,101,102} Although moisture stable and moderately acidic, these chlorozincate ILs had higher melting points compared to chloroaluminate(III) analogues.^{100,103} Research into finding moisture- and air-stable Lewis acidic ionic liquids with low melting point brought further development of

chlorostannate(II) and chlorozincate ionic liquids with quaternary ammonium cations, in particular choline.^{76,104} Such systems were used in many applications, from zinc alloy deposition¹⁰⁵ to Lewis acid catalysis in Diels-Alder cycloaddition¹⁰⁶ and Fisher indole synthesis.¹⁰⁷ Sitze *et al.*¹⁰³ also reported the use of FeCl₂ and FeCl₃ to synthesise chloroferrate ionic liquids,¹⁰⁸ which could be used in catalysis, and benefited from easy phase-separation when magnetic field was applied.⁹⁰ Ultimately, most metals in the periodic table have been used to access novel Lewis acidic anions in the synthesis of Lewis acidic ionic liquids.³

1.6.2 Ionic liquids with Lewis acidic cations

Prior to work described in this thesis, Lewis acidic cations have not been explored in the ionic liquids context. In the recent years, in parallel to studies on borenium ionic liquids described here, another family has emerged: solvate ionic liquids.

Several years ago, Watanabe and co-workers reported on the formation of solvate ionic liquids¹⁰⁹ from equimolar mixtures of a glyme (typically triglyme, G3, or tetraglyme, G4) and a lithium salt - typically lithium bis(trifluoromethylsulfonyl)imide, Li[NTf₂], lithium bis(pentafluoroethanesulfonyl)amide, Li[BETI],¹¹⁰ or lithium trifluoromethanesulfonate, Li[OTf] – see Figure 1-10.^{111,88}

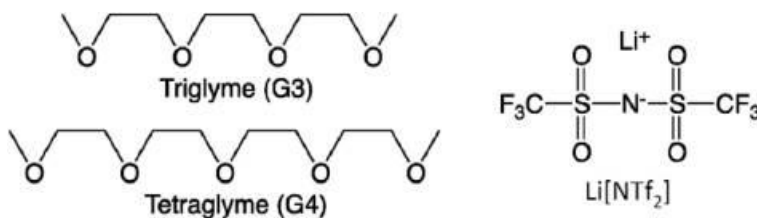


Figure 1-10: The structure of components of two solvate ionic liquids: [Li(G3)][NTf₂] and [Li(G4)][NTf₂].^{88,109}

Designed originally for electrochemical applications, these systems had quite high thermal stability, high conductivity (0.6–1.6 mS cm⁻¹ at 30 °C) and low viscosity (68.0–156.0 mPa s). Recently, also Lewis acidity of the solvate [Li(Gn)]⁺ cation was noted. In 2017, Henderson *et al.*¹¹² reported the use of such lithium-based solvate ionic liquids as catalysts in electrocyclic transformations (*i.e.* Diels-Alder reaction), in which it performed better than the traditional lithium-based catalyst like lithium perchlorate-diethyl ether (LPDE).^{113,114} ANs for two such solvate ionic liquids were measured, but the values reported were surprisingly low: AN = 26.5 and 26.5, [Li(G3)][NTf₂] and [Li(G4)][NTf₂] respectively.

Furthermore, an isolated example of IL with a Lewis acidic boron centre on the cation was reported by Mutelet *et al.* (Figure 1-11).¹¹⁵ However, in this case the positive charge is isolated from the boron centre.

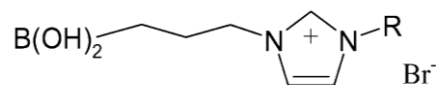


Figure 1-11: Ionic liquid with Lewis acidic boron centre in the cation.¹¹⁵

1.6.3 Quantifying Lewis acidity of ionic liquids

The most common approach to quantifying Lewis acidity of ionic liquids is Gutmann AN approach. Advantages of this method compared to the others was described in Section 1.4.2 and 1.4.3. In short, tepo is a nearly-ideal spectroscopy probe: stable towards most strong acids, with good sensitivity of the ³¹P nucleus to its electronic environment, posing low steric hindrance and having good solubility in a wide variety of solvents.^{116,88}

The AN approach has been used to quantify Lewis acidity of a number of chlorometallate ionic liquids, and it was found to correlate with their complex anionic speciation. Osteryoung *et al.*^{117,57} determined the AN values of many chloroaluminate ionic liquids based on either *N*-(1-butyl)pyridinium or 1-ethyl-3-methylimidazolium cations. Acceptor numbers were reported for different molar ratios of AlCl₃. Estager *et al.*¹¹⁸ expanded this approach to study acceptor properties of other chlorometallate(III) systems and compared them with a range of standard molecular solvents and acids, to produce an entire toolbox of Lewis acidic ionic liquids, from very weak to very strong (Figure 1-12).

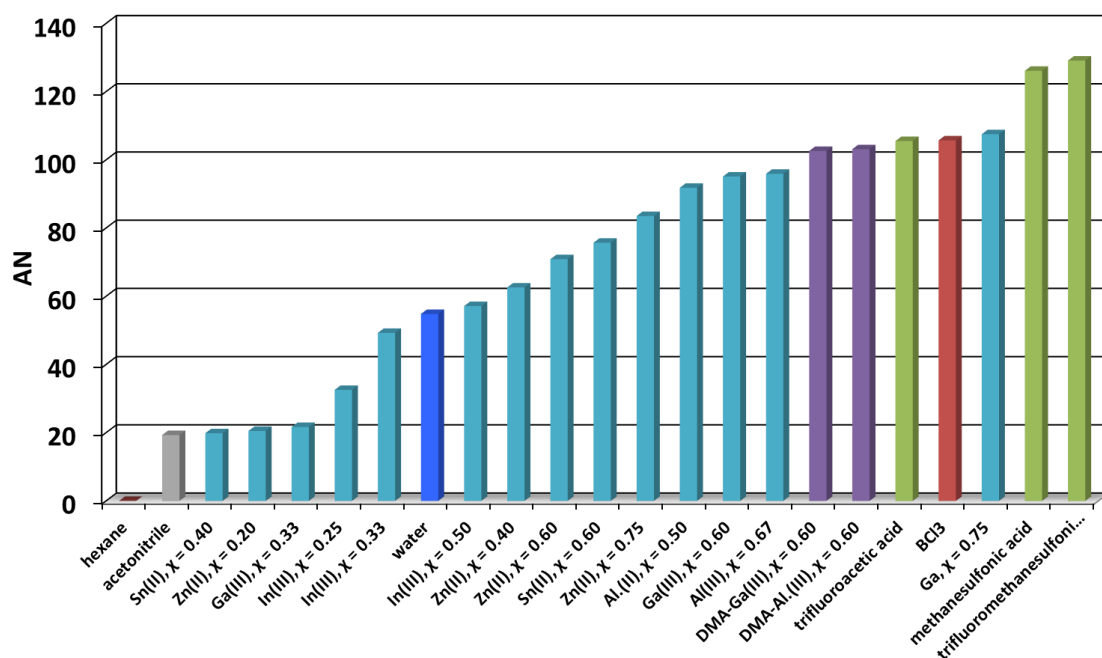


Figure 1-12: Guttmann acceptor number scale of various halometallate systems, Brønsted acids and solvents.^{118,119}

For individual families, such as chlorozincates¹²⁰ or chlorostannates(II),¹²¹ they found a very good correlation between AN values and anionic speciation of the given system.¹¹⁸

Whilst Gutmann's method is used for liquid Lewis acids, solid-state Lewis acids have most commonly been quantified using vibrational spectroscopy with *N*-donor probes (pyridine, acetonitrile).¹²² Using near-stoichiometric amounts, *N*-donor probes were condensed into the surface of the solid Lewis, which were then studied by vibrational spectroscopy.^{122,123} This methodology has also been adapted to Lewis acidic ILs, which were studied by IR spectroscopy of both pyridine and acetonitrile.^{123,118} This approach was not sensitive to speciation and had less resolution compared to the Gutmann method, but benefited from distinguishing between Brønsted and Lewis acidic species.

1.7 RATIONALE FOR THIS WORK

Lewis acidity, as discussed in Section 1.3.3, is related to electron deficiency in a molecule, and its ability to accept an electron pair. It is therefore surprising that most Lewis acidic ionic liquids contain their Lewis acidic function in the anion, which is electron-rich, and is typically associated with being a Lewis base, rather than an acid. As shown in Section 1.6.1, the reason for this was historical: chloroaluminate(III) ionic liquids, developed for electrochemical applications, were found to catalyse Friedel-Crafts chemistry. At the same time, in main group chemistry, there are multiple examples of strongly Lewis acidic cations (borenium, fluorophosphonium), awaiting to be explored as components of ionic liquids (Section 1.2.3).

This work represents a new approach in ionic liquids research, where a molecule of a certain functionality is converted to ionic liquid, rather than generic ionic liquids are modified to attain certain properties. In this case, a group of Lewis acidic borenium cations was explored as highly Lewis acidic cations. Synthesis, characterisation and some applications of these new ionic liquids were studied, aiming to open up a new chapter of Lewis acid chemistry in ionic liquids.



CHAPTER TWO

“The idea is to write something worth reading or to do something worth writing.”
— Benjamin Franklin



2 SYNTHESIS AND CHARACTERISATION OF BORON COMPLEXES

This chapter describes synthesis and characterisation of tetracoordinate boron complexes, which were used as precursors for the synthesis of new families of Lewis acidic borenium ionic liquids (Chapter 3).

2.1 EXPERIMENTAL

2.1.1 Synthesis of boron complexes

Unless stated otherwise, all moisture-sensitive procedures/experiments were carried out under an argon atmosphere, by using Schlenk techniques or in a nitrogen-filled glove box (O_2 and $\text{H}_2\text{O} < 0.1\text{ppm}$). Unless stated otherwise, all materials were purchased from Sigma-Aldrich and used as received. All solvents were dried over molecular sieves (3 \AA) and stored under argon. All glassware was dried in an oven (*ca.* 140°C , for at least 24 h) overnight prior to use.

2.1.1.1 Boron trichloride complexes

In a typical experiment, a 250 cm^3 two-necked round bottom flask equipped with a magnetic stirring bar, a gas tap and a septum was connected to Schlenk line. The flask was opened to vacuum and refilled with argon - this was repeated twice to ensure an inert atmosphere of argon. Then the flask was immersed in -78°C acetone/dry ice bath. Boron trichloride (20 g, 1 mol eq.) was subsequently transferred into the flask *via* a cannula. Appropriate amount of dichloromethane (1.5% v/v of boron trichloride) was added, and the solution was stirred vigorously (1000 rpm, 20-30 min). The required amount of base (0.9 mol eq.) was placed in a gas-tight syringe and added drop-wise using a syringe pump to a vigorously stirred (1000 rpm) mixture. After the addition was complete, the reaction mixture was left to react (1000 rpm, 30-60 min); the ice bath was removed, letting the mixture to slowly reach ambient temperature. Subsequently, the gas tap was opened to the vacuum (10^{-2} bar), and all volatiles (excess reactant and the solvent) were removed from the reaction flask and collected in a liquid nitrogen trap. The remaining traces of volatile materials were removed from the boron trichloride complex by heating under reduced pressure (60°C , 10^{-2} bar, overnight). The product was characterised using ^1H , ^{13}C and ^{11}B NMR spectroscopy, FT-IR spectroscopy, DSC and TGA.

2.1.1.2 Boron trifluoride complexes

In a typical experiment, a 250 cm³ two-necked round bottom flask equipped with a magnetic stirring bar, a tap and septum was connected to Schlenk line. The flask was opened to vacuum and refilled with argon - this was repeated twice to ensure an inert atmosphere of argon. Then the flask was immersed in 0 °C ice bath. Boron trifluoride etherate (30 g, 1 mol eq.) was transferred *via* a cannula into the flask, followed by the addition of dichloromethane (1.5 %v/v of boron trifluoride). The mixture was stirred vigorously (1000 rpm, 20-30 min). Then, using a gas-tight syringe, the base (0.9 mol eq.) was added drop-wise using a syringe pump and the mixture was left to react (1000 rpm, 30-60 min); the ice bath was removed, letting the mixture to slowly reach ambient temperature. Subsequently, the gas tap was opened to the vacuum (10⁻² bar), and all volatiles (excess reactant and the solvent) were removed from the reaction flask and collected in a liquid nitrogen trap. The remaining traces of volatile materials were removed from the boron trichloride complex by heating under reduced pressure (60 °C, 10⁻² bar, overnight). Adducts of O and P- ligands were used as received, in contrast to adducts of 4-pic and mim, which were purified by recrystallization (Section 2.1.1.3). The product obtained was characterised using ¹H, ¹³C, ¹⁹F and ¹¹B NMR spectroscopy, FT-IR spectroscopy, DSC and TGA.

2.1.1.3 Recrystallization of boron complexes

A small portion of hot chloroform solution at (10 cm³, 60 °C) was added to a beaker containing 0.5-1.0 g boron complex. The beaker was then transferred onto a hotplate (70 °C) with continuous addition of the hot solvent incrementally until all of the solute had dissolved. The solution was taken off heat and allowed to cool in the open air for a few minutes, following which it was cooled in an ice bath. Where suitable single crystals were obtained, their structure was analysed by single-crystal X-ray crystallography.

2.1.2 Characterisation of boron complexes

2.1.2.1 NMR spectroscopy

¹H, ¹³C, ¹⁹F, and ¹¹B NMR spectra were recorded using a Bruker AvanceIII 400 MHz spectrometer at frequencies of 400 MHz, 101 MHz, 376 MHz and 128 MHz respectively. Chemical shift values were reported in parts per million (ppm).

Sample preparation was carried out in a glove box, where dry boron complexes were stored. Each sample (*ca.* 0.025 g) was loaded into NMR tube (5 mm, borosilicate glass). The tube was closed with a standard cap and removed from the glove box; outside, dry deuterated solvent (*d*₆-dimethyl sulfoxide, *d*₃-acetonitrile or *d*₆-chloroform) was quickly added prior to the measurement. ¹H NMR spectra were referenced to solvent signals: (CD₃)₂SO at 2.54 ppm, CD₃CN at 1.96 ppm or CDCl₃ at 7.26 ppm. ¹³C NMR spectra were referenced to (CD₃)₂SO at 40.45 ppm, CD₃CN at 118.26 ppm or CDCl₃ at 77.36 ppm. For other NMR spectroscopies, external references were used: BF₃·OEt₂ for ¹¹B{¹H} NMR spectroscopy, C₆H₅CF₃ for ¹⁹F{¹H} spectroscopy and H₃PO₄ (85% water solution) for ³¹P{¹H} spectroscopy.

2.1.2.2 FT-IR spectroscopy

FT-IR spectra were recorded using the Perkin Elmer Spectrum 100 Series FT-IR spectrometer with an ATR attachment. Eight scans were acquired for each sample.

In a glove box, small amounts (<0.5 g) of samples were placed in GC sample vials and sealed with a GC cap. The vials were removed from the glovebox, transferred to the FT-IR instrument, opened immediately prior to the measurement, and tipped onto the ATR crystal. The vial was left over the sample, offering provisional protection of inert gas for the sample for the duration of the measurement (*ca.* 10 s).

2.1.2.3 Raman spectroscopy

Raman spectra were recorded using the PerkinElmer® Raman 400F series spectrometer with 750 nm laser. Eighty scans were acquired for each sample.

In a glove box, small amounts (<0.5 g) of samples were placed in quartz cuvettes and sealed with parafilm. The cuvettes were removed from the glove box immediately prior to the measurement and placed directly in the Raman spectrometer.

2.1.2.4 Thermogravimetric analysis (TGA)

Decomposition temperatures were obtained using a TA TGA Q5000 analyser, operating under the flow of dry nitrogen gas (50 ml min⁻¹), with a heating rate of 5 °C min⁻¹ and the temperature ramp from ambient to 600 °C. Sample pans (Tzero alodined hermetic pans and Tzero alodined hermetic lids) were tared on the TGA microbalance prior to sample preparation.

In the glove box, small amounts (*ca.* 0.005 g) of samples were loaded in a Tzero alodined hermetic pans and sealed with Tzero alodined hermetic lids, using a dedicated sealing press. The samples were taken out of the glovebox and placed in the TGA autosampler.

2.1.2.5 Differential scanning calorimetry (DSC)

DSC scans were recorded using TA DSC Q2000 with a TA 90 refrigerated cooling system and an autosampler under dry nitrogen furnace purge (50 ml min⁻¹). Sample temperature was ramped between -90 °C and 200 °C at 5 °C min⁻¹; three cycles were recorded.

The samples were accurately weighed (0.0005 g) into medium pressure Tzero alodined hermetic pans, ensuring that the samples were evenly distributed and had good contact with the base of the pan. The pan was then sealed using the sealing press. The weighed samples were taken out of the glovebox and placed in the autosampler carousel of the DSC instrument. An empty sealed pan of the same type was used as a reference sample.

2.1.2.6 Elemental analysis

Elemental analysis (percentage content of carbon, hydrogen, nitrogen and chlorine) were quantified using PerkinElmer 2400 II CHN/O and Cl analyser. In a glovebox, small amounts of samples (<0.5 g) were weighed out into a sample vial and tightly sealed. The samples were then removed from the glovebox and opened immediately prior to the measurement. They were placed in tin capsules of pre-recorded mass, and loaded into the combustion tube for analysis.

2.2 RESULTS AND DISCUSSION

The first step towards the preparation of borenium ionic liquids was the synthesis of a tetracoordinate boron compound using boron halides and monodentate ligands, L (Equation 2-1)



The formation of the tetracoordinate boron adducts is an equilibrium process, involving a nucleophilic addition of a Lewis base to a boron trihalide.^{23,124} It relies on the strength of the Lewis acid,²³ and on the ligand: its Lewis basicity, electronegativity (σ -donor capability) and π -bonding ability.^{20,125}

2.2.1 Selection of reactants

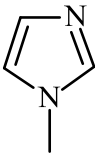
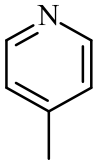
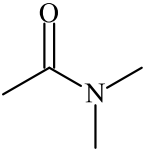
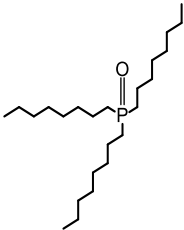
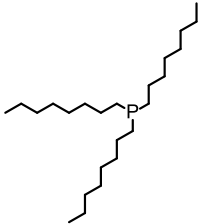
Acidity (and therefore the reactivity) of boron halides increases with increasing halide size ($\text{BF}_3 < \text{BCl}_3 < \text{BBr}_3$),¹²⁶ due to increasing disparity between B and X orbital sizes, and consequently decreasing π -back bonding to empty boron orbital.^{10,127,128} Therefore, for the highest acidity in borenium cation, BBr_3 would be recommended over BCl_3 and BF_3 . At the same time, stability of the B-X bond decreases with increasing halide mass.^{20,129,130} Although halide abstraction from $[\text{BBr}_3\text{L}]$ complexes is very easy, these compounds are light-sensitive and very prone to decomposition through bromine release which when used as catalysts, they are likely to yield brominated side-products.^{20,129,130} In consequence, BF_3 and BCl_3 were chosen as the starting materials (Equation 2-1), offering the correct balance between activity and stability, and BBr_3 complexes were excluded from the study.

It is known that the first-row donors, such as amines and ethers, exhibit greater Lewis basicity towards BF_3 or BCl_3 than the second-row donors, such as phosphines and sulphides; in other words $\text{N} > \text{P}$, $\text{O} > \text{S}$.¹³¹ Amongst the first row donors, *N*-donors are preferred over *O*-donors. In solution, aromatic *N*-donors, such as 4-picoline and 1-methylimidazole, were reported to form quantitatively the corresponding boron complexes, whilst the *O*-donors (acetamide, dimethyl acetamide) resulted in equilibrium between free ligand and BCl_3 , and the $[\text{BCl}_3\text{L}]$ adduct (Equation 2-1).^{131,132} Brinck *et al.* carried out computational analysis of the bonding between boron trifluoride or boron trichloride and *N*-donors: aliphatic (ammonia) or aromatic (pyridine).¹²⁶ Irrespective of the presence of the aromatic ring (π -back bonding), more stable complexes were formed with BCl_3 than with BF_3 , due to the major role of *N*-donor $\rightarrow\text{BX}_3$ charge transfer (σ -

donation) in these complexes, and due to the fact that the ability to accept the charge increases in the order $\text{BF}_3 < \text{BCl}_3 < \text{BBr}_3$.^{126,18} Additionally, the calculated force constant showed stronger Cl-B bond in the BCl_3 complex compared to F-B bond in the BF_3 complex (2.5 and 1.8 mdyn/Å, respectively).^{126,133}

With regards to the ligand selection in this work, they were chosen so that products of halide abstraction would yield stable borenium cations, structurally likely to form ionic liquids. Monodentate neutral ligands were selected, to form singly-charged borocations. The initial selection included *N*-, *O*- and *P*-donors (Table 2-1).

Table 2-1: A list of ligands used in this work, their abbreviations, structures and pK_a values of conjugate acids.

1- methylimidazole	4-methylpyridine (4-picoline)	dimethylacetamide	trioctylphosphine oxide	trioctylphosphine
mim $\text{pK}_a = 6.95$	4-pic $\text{pK}_a = 5.85$	dma $\text{pK}_a = -0.19$	P_{888}O $\text{pK}_a = -7.50$	P_{888} $\text{pK}_a = 9.58$
				

Aromatic *N*-donors were selected as ligands due to their ability to stabilise the positive charge on the borocation centre *via* π -back donation.²³ This also contributes to lowering of the melting point by charge dispersion, thus promoting the formation of ionic liquids, rather than crystals.¹³⁴ Two different ligands were selected, to study the influence of the σ -donation (*viz.* pK_a in Table 2-1) on both charge stabilisation and Lewis acidity. Another strategy to access room temperature ionic liquids is to introduce long alkyl chains, preferably 6-8 carbon atoms.¹³⁵ Following this reasoning, complexes with trioctylphosphine and trioctylphosphine oxide were synthesised. The strength of σ -donation is very different for phosphine and phosphine oxide, with phosphine being a much stronger base, which was expected to give differing results in terms of Lewis acidity of the resulting ionic liquids. Also, phosphine ligands in their boron complexes may be considered as pure σ -donors, in contrast to aromatic amines, so it was interesting to compare a strong σ -donor with weaker ones, but capable of significant π -back donation.¹³⁶

Finally, dimethylacetamide was used as strongly asymmetric *O*-donor (asymmetry was preferred for melting point depression) with some π -back donation capability.

2.2.2 Synthetic procedure

As previously stated, all boron trichloride and boron trifluoride adducts were prepared using Schlenk techniques due to the sensitivity of boron halides to moisture. The $[\text{BF}_3\text{L}]$ adducts were synthesised by drop-wise addition of a ligand to boron halides, in DCM. Both reactions were exothermic, and required cooling upon the addition: $[\text{BF}_3\text{L}]$ adducts were synthesised from $\text{BF}_3\cdot\text{OEt}_2$ at $0\text{ }^\circ\text{C}$ (see example reaction Figure 2-1) and $[\text{BCl}_3\text{L}]$ adducts were prepared from BCl_3 in heptane at $-78\text{ }^\circ\text{C}$ (see example in Figure 2-2).

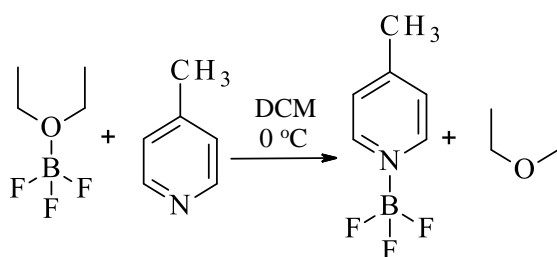


Figure 2-1: Synthesis of a tetracoordinate boron fluoride complex: $[\text{BF}_3(4\text{-pic})]$.

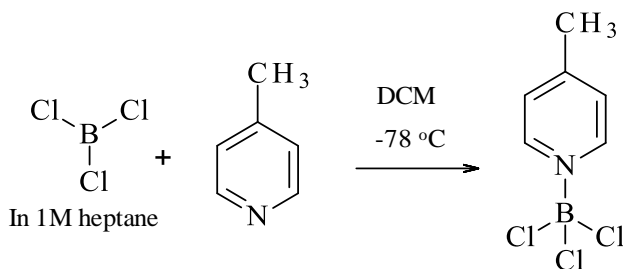


Figure 2-2: Synthesis of a tetracoordinate boron chloride complex: $[\text{BCl}_3(4\text{-pic})]$.

Heat of reaction of the boron halides is known to increase as atomic weight of the halogens increases, so although both additions were exothermic, the one involving BCl_3 produced more heat than that with $\text{BF}_3\cdot\text{OEt}_2$.^{8,12,137} Coordinating ability of boron trihalides increases with increasing atomic radius of the halogen due to the loss of π -bonding. This means that less energy is needed for BCl_3 , compared to BF_3 , to reorganise from trigonal planar to tetrahedral geometry of the adduct,^{10,127,128} and consequently the heat of reaction is higher for BCl_3 adducts. This

explains why reaction of BCl₃ required cooling to -78 °C, whilst that of BF₃·OEt₂ was carried out at 0 °C without thermal runaway.

All adducts were formed in high yields (Table 2-2) and were white solids, except for [BCl₃(P₈₈₈O)], [BF₃(P₈₈₈O)] and [BF₃(P₈₈₈)] complexes, which formed viscous oily liquids. All boron complexes were moderately moisture stable due to saturated coordination on boron, but upon prolonged exposure to the air some would hydrolyse slowly, for example [BCl₃(mim)]. They were stored in a glovebox, without decomposition for over six months.

Table 2-2: Yield and appearance of boron halide adducts, [BX₃L]; S = solid, L = liquid

Ligand	[BCl ₃ L]	Yield /%	[BF ₃ L]	Yield %
4-pic	S (ref. ¹³⁸)	99	S (ref. ¹³⁹)	86
mim	S (ref. ¹³⁸)	91	S	75
dma	S	70	S	97
P₈₈₈O	L	88	L	95
P₈₈₈	S	97	L	83

From the ten synthesised complexes, three were reported in the literature^{140,139} (Table 2-2) and partially characterised (NMR and IR spectroscopy).^{125,138} Seven new compounds are reported. All complexes were fully characterised using multinuclear NMR and IR spectroscopies, in addition to elemental analysis and thermal analysis (DSC and TGA). In some cases, single crystals were grown and their structures were recorded.

2.2.3 NMR spectroscopic characterisation of adducts

All complexes were studied by multinuclear NMR spectroscopy, in the form of solutions in aprotic deuterated solvents.

2.2.3.1 ¹H and ¹³C NMR spectroscopy

¹H and ¹³C NMR spectra were used as a simple way of monitoring and identifying the formation of the boron complexes through the alteration in the chemical shifts upon the synthesis of the tetracoordinate adduct. The ¹H and ¹³C NMR spectra (Table 2-3 and Table 2-4 respectively) were all supporting the presence of boron trichloride and boron trifluoride complexes, with no impurities such as unreacted ligands observed. The ¹H NMR chemical shift of complexed ligands

was found to be shifted downfield by 0.5-1.0 ppm with respect to the pure ligand, regardless of the boron trihalide used. For example, the ^1H NMR spectrum of $[\text{BCl}_3(4\text{-pic})]$ in CDCl_3 , recorded at room temperature, displayed pair of doublets due to the α , β -pyridinium protons at 7.67 and 9.10 ppm, which were shifted downfield from the analogous pair of doublets originating from the free ligand (6.51 and 8.03 ppm).¹⁴¹ Similar degree of change in chemical shifts was seen in the boron trifluoride complexes. The ^{13}C NMR spectra (Table 2-4) also supported the information about the complexes.

Table 2-3: ^1H NMR (400 MHz, CDCl_3) chemical shifts recorded for boron complexes and corresponding free ligands.

L	donor	$[\text{BCl}_3\text{L}]$	$[\text{BF}_3\text{L}]$	Assignment
4-pic	1.64(s)	2.60(s)	2.60(s)	Ar- CH ₃
	6.51(d)	7.67(d)	7.57(d)	- CH -C- CH -
	8.03(d)	9.10(d)	8.55(d)	- CH -N- CH -
mim	2.83(s)	3.92(s)	3.87(s)	Ar- CH ₃
	6.37(dd)	7.09(s)	7.02(s)	-CH= CH -N-
	6.37(dd)	7.62(s)	7.31(s)	- CH =CH-N
	6.93(s)	8.40(s)	8.05(s)	-N- CH -N-
DMA	1.93(s)	2.79 (s)		CH ₃ -CO-
	2.77(s)	3.32	2.49(s)	-N- CH ₃
	2.94(s)	3.41(s)	3.25(d)	CH ₃ -N-CO-
P₈₈₈O	0.88(m)	0.80(m)	0.88(m)	- CH ₃
	1.34(m)	1.21 (m)	1.28 (m)	-CH ₂ -
	1.61(m)	1.92(m)	2.0(m)	P-CH ₂ -
P₈₈₈	0.59(m)	0.89(m)	0.88(m)	- CH ₃
	1.04 (m)	1.30(m)	1.13(m)	-CH ₂ -
		1.62 (m)	1.70(m)	

Table 2-4: ^{13}C NMR (101 MHz, CDCl_3) chemical shifts recorded for boron complexes and corresponding free ligands.

L	donor	$[\text{BCl}_3\text{L}]$	$[\text{BF}_3\text{L}]$	Assignment
4-pic	149.15	157.55	156.66	-CH-N-CH-
	145.95	144.01	142.64	-CH-C-CH-
	123.98	126.70	126.78	-CH-C-CH-
	19.60	21.93	21.78	Ar-CH ₃
mim	137.45	136.39	135.30	-N-CH-N-
	128.16	124.82	123.27	-CH=CH-N-
	119.91	122.24	121.53	-CH=CH-N
	31.69	35.94	35.33	Ar-CH ₃
DMA	169.25	174.37	174.68	CH ₃ -CO-
	37.06	40.21	39.49	CH ₃ -N-CH ₃
	33.94	39.53	38.17	CH ₃ -N-CH ₃
	20.85	18.47	17.06	CH ₃ -CO-
P ₈₈₈ O	32.21	31.65	31.70	C ₂ H ₅ -CH ₂ -(CH ₂) ₅ -PO
	31.72	30.47	30.68	C ₅ H ₁₁ -CH ₂ -(CH ₂) ₂ -PO
	29.52	28.84	28.88	CH ₃ -CH ₂ -(CH ₂) ₃ -PO
	29.47	24.76	24.64	C ₇ H ₁₅ -CH ₂ -PO
	27.98	24.15	24.01	CH ₃ -CH ₂ -(CH ₂) ₄ -PO
	23.03	22.54	22.56	CH ₃ -CH ₂ -(CH ₂) ₆ -PO
	22.16	21.05	20.84	C ₆ H ₁₃ -CH ₂ -CH ₂ -PO
	14.48	14.00	14.01	CH ₃ -(CH ₂) ₇ -PO
P ₈₈₈	31.62	31.73	31.71	C ₂ H ₅ -CH ₂ -(CH ₂) ₅ -P
	31.23	31.30	31.17	C ₅ H ₁₁ -CH ₂ -(CH ₂) ₂ -P
	29.07	28.92	29.15	CH ₃ -CH ₂ -(CH ₂) ₃ -P
	27.49	22.60	22.58	CH ₃ -CH ₂ -(CH ₂) ₄ -P
	27.52	22.36	22.34	C ₆ H ₁₃ -CH ₂ -CH ₂ -P
	22.33	18.59	18.29	C ₇ H ₁₅ -CH ₂ -P
	13.61	18.22	17.99	CH ₃ -CH ₂ -(CH ₂) ₆ -P
		14.06	14.02	CH ₃ -(CH ₂) ₇ -P

2.2.3.2 ^{11}B NMR spectroscopy

^{11}B NMR spectroscopy proved invaluable for the identification of the boron complexes, being instrumental in confirming the geometry of the products. The ^{11}B chemical shift can be related to the strength of the interaction between boron trihalides and the ligands used.^{142,140} The electronic effect of the ligands on the boron centre are transmitted by sigma-bond mechanism, so for a series of complexes formed with the same boron trihalide and different ligands, it is possible to determine the donor strength of each ligand (relative basicity) towards the trihalide.^{142,143} The ^{11}B NMR chemical shift can be, by the same token, related to the stability of the boron complexes.¹⁴² Furthermore, the sp^3 -boron formed by the coordination of the ligands to the boron trihalides is asymmetrical; an increase in the quadrupolar coupling constant and asymmetry parameter

translates to signals being typically broader than those originating from symmetrical tetrahedral, such as $[\text{BF}_4]^-$.¹⁴⁴

In this work, ^{11}B NMR signals for the boron trichloride complexes, $[\text{BCl}_3\text{L}]$, were broad peaks between 0 to 10 ppm, downfield from the reference ($\text{F}_3\text{B}\cdot\text{OEt}_2$ at 0.00 ppm). This range of chemical shifts indicates tetrahedral environment of boron.¹⁴⁵ In agreement with the literature, ^{11}B chemical shift was dependant on the ligand used (Figure 2-4).¹²⁷

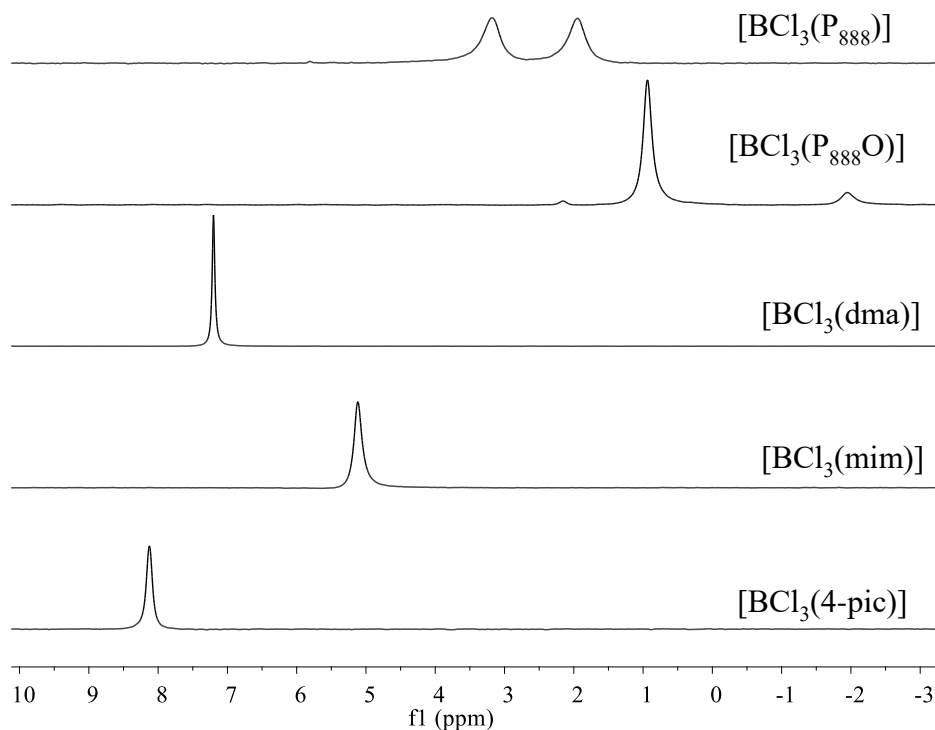


Figure 2-3: ^{11}B NMR spectra (128 MHz, 27 °C, CDCl_3) of tetracoordinate boron complexes, $[\text{BCl}_3\text{L}]$.

The *N*-donor complexes (mim and 4-pic) gave single ^{11}B NMR peaks at 5.12 and 8.13 ppm, respectively, corresponding to the $[\text{BCl}_3\text{L}]$ adducts. The $[(\text{BCl}_3(\text{dma}))]$ complex also showed a single peak at 7.20 ppm; it is uncertain whether it acts as *N*- or *O*-donor in this case, as both modes are plausible. $[\text{BCl}_3(\text{P}_{888})]$ complex showed a doublet at 2.51 ppm due to the ^{11}B - ^{31}P coupling, $^1J_{11\text{B}-31\text{P}} = 157.2$ Hz.^{127,145,146} Finally, the ^{11}B NMR spectrum of the $[(\text{BCl}_3(\text{P}_{888}\text{O}))]$ complex contained two low-intensity peaks at -1.95 and 2.16 ppm, in addition to the main signal at 0.94 ppm, due to disproportionation, as per Equation 2-2.



It is evident that there is no direct relationship between pK_a values of conjugate acids and ^{11}B NMR chemical shift of the tetracoordinate adducts (Table 2-5). These strongest complex appears to be that of $[\text{BCl}_3(4\text{-pic})]$, whereas the weakest one is $[\text{BCl}_3(\text{P}_{888}\text{O})]$. This finds confirmation in propensity of $[\text{BCl}_3(\text{P}_{888}\text{O})]$ to dissociate, as shown in Equation 2-2. Visually, signals originating from the $[\text{BCl}_3(\text{P}_{888})]$ adduct are broader than these from the other complexes; this is due to the bulky P_{888} ligand distorting symmetry around the ^{11}B centre.

The ^{11}B NMR spectra of the boron trifluoride complexes also featured peaks corresponding to the tetrahedral environment of boron. In most cases they were upfield from the reference ($\text{F}_3\text{B}\cdot\text{OEt}_2$ at 0.00 ppm), *i.e.* between 0 ppm and -2 ppm (Figure 2-4).

The N-donor complexes with mim and 4-pic featured poorly resolved quartets due to ^{11}B - ^{19}F coupling. The peaks for $[\text{BF}_3(\text{mim})]$ complex were at -0.27 ppm, $^1J_{11\text{B}-19\text{F}} = 10.4$ Hz, whilst that for the $[\text{BF}_3(4\text{-pic})]$ complex at 0.41 ppm, $^1J_{11\text{B}-19\text{F}} = 12.1$ Hz. Both complexes feature also a low intensity peak at -0.96 ppm for $[\text{BF}_3(\text{mim})]$ and -0.86 ppm for $[\text{BF}_3(4\text{-pic})]$, which may indicate traces of disproportionation, leading to the formation of $[\text{BF}_4]^-$ and $[\text{BF}_2\text{L}_2]^+$. The ^{11}B NMR signal for $[\text{BF}_3(\text{P}_{888})]$ complex was a doublet of quartets at 0.51 ppm, $^1J_{11\text{B}-31\text{P}} = 105.7$ Hz, $^1J_{11\text{B}-19\text{F}} = 53.6$ Hz.^{127,145,146} This splitting was due to the ^{31}P - ^{11}B and ^{11}B - ^{19}F coupling: boron peak was split into doublet 1:1 by ^{31}P - ^{11}B coupling followed by each component being further split into quartet 1:3:3:1 due to ^{11}B - ^{19}F coupling in the BF_3 complexes.^{142,147} For the $[(\text{BF}_3(\text{dma}))]$ and $[(\text{BF}_3(\text{P}_{888}\text{O}))]$ complexes, singlets at -0.32 and -1.08 ppm, respectively, were recorded at the corresponding ^{11}B NMR spectra. An additional low intensity peak at -1.12 ppm was detected for $[\text{BF}_3(\text{dma})]$.

The change in the chemical shifts of the complexes to the reference compound is best explained based on the change of boron hybridisation from sp^2 to sp^3 , which in effect reduced the paramagnetic shift of the spectra in the complex.^{145,148,22} The upfield shift in the boron trifluoride complexes, as opposed to the downfield shift observed in the boron trichloride complexes, was due to the fact that BF_3 is a weaker acceptor molecule (weaker Lewis acid) than BCl_3 , hence procuring less deshielding effect compared to BCl_3 .^{145,148,22} In contrast, the chlorine atoms in BF_3 are reducing the diamagnetic shielding at boron, giving rise to a low field shift.^{145,148,22}

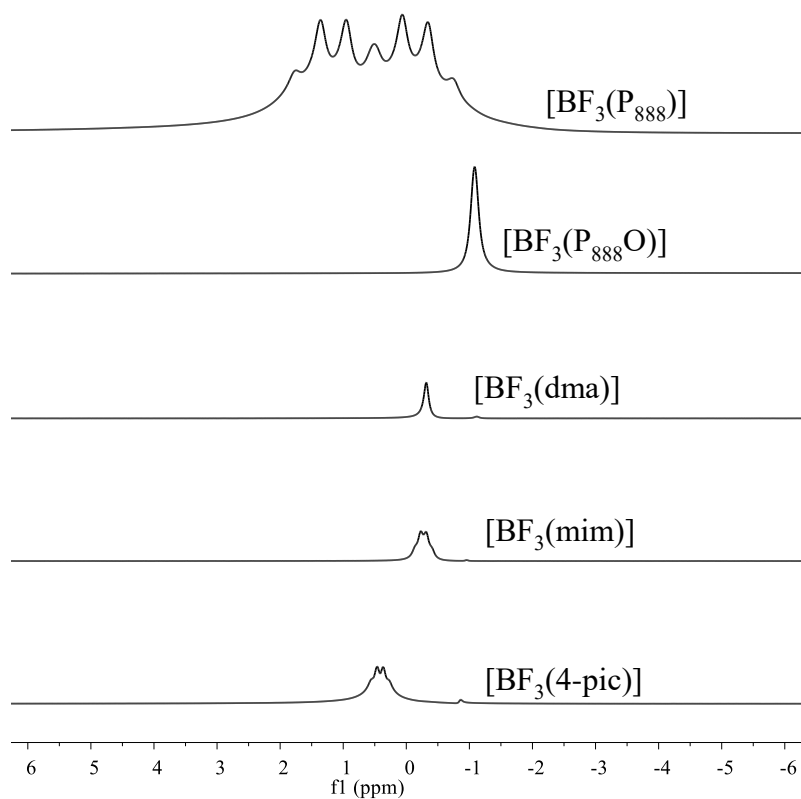


Figure 2-4: ^{11}B NMR spectra (128 MHz, 27 °C, CDCl_3) of tetracoordinate boron complexes, $[\text{BF}_3\text{L}]$.

In general, all ^{11}B NMR chemical shifts recorded for the synthesised adducts (Table 2-5) are consistent with tetrahedral sp^3 boron.^{138,140}

Table 2-5: ^{11}B NMR (128 MHz, 27 °C, CDCl_3) spectra of tetracoordinate boron complexes, $[\text{BCl}_3\text{L}]$.

L	$[\text{BCl}_3\text{L}]$	$[\text{BF}_3\text{L}]$
4-pic	8.13(s)	0.41(q)
		-0.86(s)
mim	5.12(s)	-0.27(q)
		-0.96 (s)
dma	7.20(s)	-0.32 (s)
		-1.12(s)
P₈₈₈O	2.51(d)	-1.08(s)
P₈₈₈	3.18(s)	
	0.94(s)	0.51(m)
	-1.95(s)	

2.2.3.3 ^{31}P NMR spectroscopy

The $^{31}\text{P}\{^1\text{H}\}$ NMR spectra of boron trifluoride complexes: $[\text{BF}_3(\text{P}_{888})]$ and $[\text{BF}_3(\text{P}_{888}\text{O})]$ exhibited a singlet at 74.0 ppm (Figure 2-5), but in the latter case the signal was irregular and could originate from a poorly-resolved multiplet. For boron trichloride complexes, $[\text{BCl}_3(\text{P}_{888})]$ gave signal at 80.49 ppm, whilst $[\text{BCl}_3(\text{P}_{888}\text{O})]$ exhibited a multiplet at 82.14 ppm (Figure 2-5). All the complexes were also accompanied by minor peaks, each of similar intensity.

Multiplets/broad peaks recorded for the $[\text{BX}_3(\text{P}_{888}\text{O})]$ complexes do not have a regular, symmetrical splitting pattern. They do not originate from splitting caused by coupled nuclei, but are most likely a group of signals of very similar chemical shift, indicating ligand exchange on the boron centre.

Zheng *et al*¹⁴⁹ in their theoretical study of ^{31}P chemical shifts of trialkylphosphine oxides adducts with Bronsted and Lewis acids saw chemical shifts at 85-94 ppm for various trialkylphosphine oxides including P_{888}O , which matches chemical shifts recorded in this work. for $[\text{BX}_3(\text{P}_{888}\text{O})]$ complexes (80-82 ppm).^{150,149} In agreement with well-established observations by Gutmann,^{54,56} Zheng *et al*¹⁵¹ reported correlations between the acidic strengths of Lewis acid sites and ^{31}P chemical shifts of trioctylphosphine oxide (P_{888}O) and trioctylphosphine (P_{888}).^{151,149} Though most of their work was on solid Lewis acid compounds, the NMR experimental data observed in this work showed good agreement with their work.

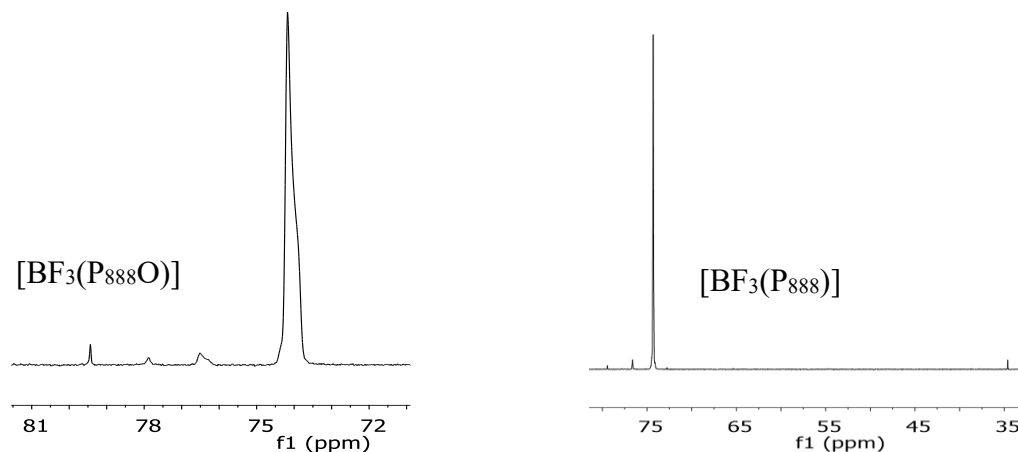


Figure 2-5: ^{31}P NMR spectra (162 MHz, CDCl_3) of tetracoordinate boron trifluoride complexes

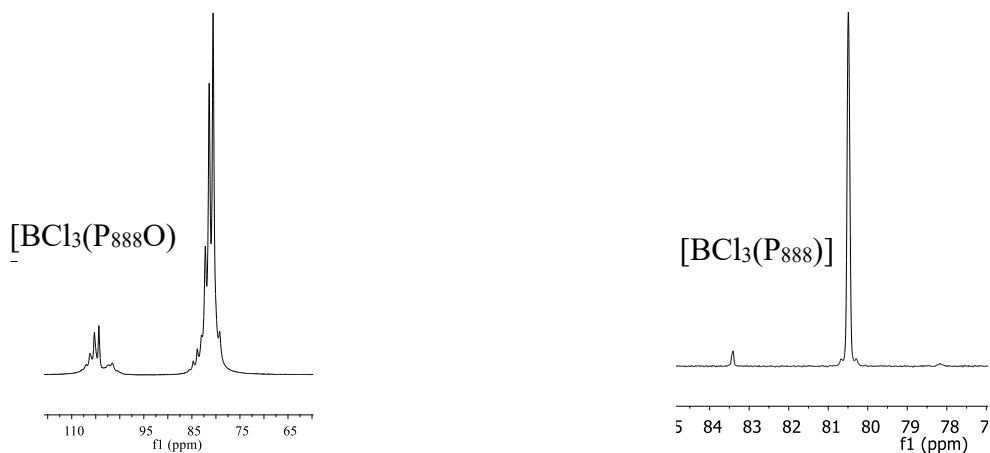


Figure 2-6: ^{31}P NMR spectra (162 MHz, CDCl_3) of tetracoordinate boron chloride complexes.

2.2.3.4 ^{19}F NMR spectroscopy

^{19}F NMR spectra of the BF_3 complexes all showed sharp signals upfield to the reference trifluorotoluene ($\text{C}_6\text{H}_5\text{CF}_3$ at -63.72 ppm). The ^{19}F NMR chemical shifts of each boron complex were indicative of the $\{\text{BF}_3\}$ unit (-153.0 ppm) in the complexes and peaks corresponded to a tetracoordinate BF_3 complex.^{142,152} Depending on the Lewis base, the ^{19}F NMR spectra featured chemical shifts between -130 to -150 ppm.

Since ^{11}B nucleus has spin $I = 3/2$, coupling with this nuclei do not follow Pascal triangle, but a more general formula for splitting pattern seen in Equation 2-3.¹⁵³

$$2nI + 1 \quad \text{Equation 2-3}$$

Where I is the nuclear spin value and n is number of neighbour nucleus.¹⁵³

In consequence, coupling of a ^{19}F nuclei with a single ^{11}B atom based on their nuclei spin of $1/2$ and $3/2$, respectively will give four lines of equal height. However, due to short relaxation times of ^{11}B , these multiplets are often merged into unshaped, broad signals with ragged tops (see Figure 2-7 and Figure 2-8).¹⁵³

The N -donor complexes, $[\text{BF}_3(\text{mim})]$ and $[\text{BF}_3(4\text{pic})]$ showed poorly resolved multiplet: at -149.2 ppm for $[\text{BF}_3(\text{mim})]$, and at -151.36 ppm $[\text{BF}_3(4\text{pic})]$ (see Figure 2-7). Four peaks of similar intensity (1 : 1 : 1 : 1) seen with $[\text{BF}_3(\text{mim})]$ could be explained by the coupling of one ^{11}B with the ^{19}F nucleus: $^1J_{^{19}\text{F}-^{11}\text{B}} = 11.28 \text{ Hz}$.¹⁵³ Additional complication might arise from

^{19}F - ^{14}N coupling; due to the spatial proximity between nitrogen and fluorine atoms with lone-pair orbitals, it was postulated that they may overlap.¹⁵⁴

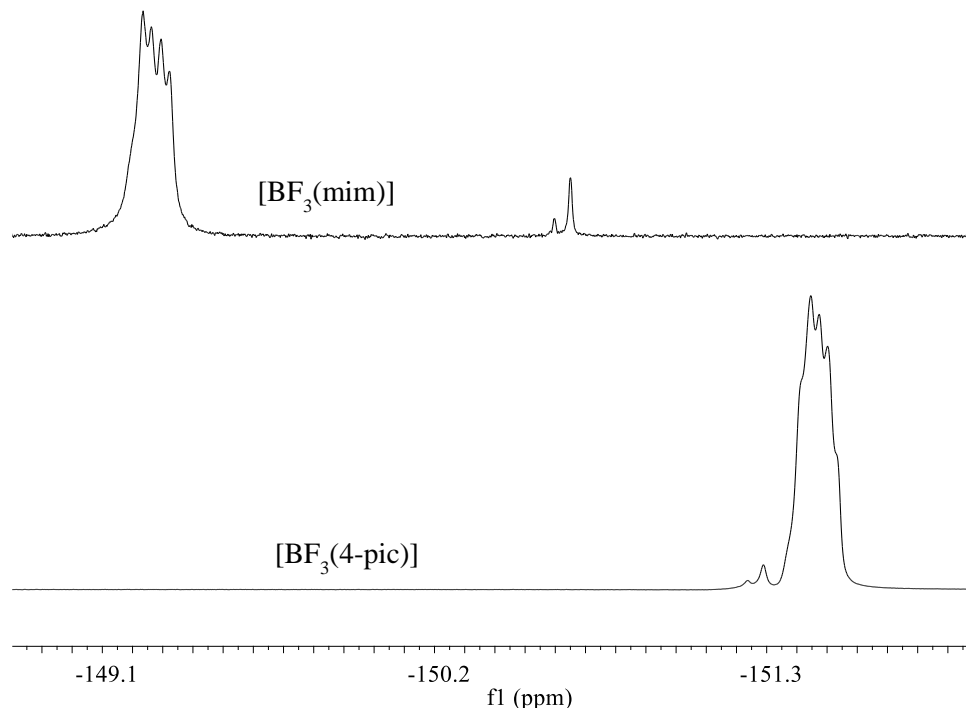


Figure 2-7: ^{19}F NMR (376 MHz, CDCl_3) spectra of tetracoordinate boron trifluoride complexes $[\text{BF}_3\text{L}]$ with N -donors.

For O -donors, $[\text{BF}_3(\text{P}_{888}\text{O})]$ $[\text{BF}_3(\text{dma})]$, a broad peak at -145.69 ppm was recorded for $[\text{BF}_3(\text{P}_{888}\text{O})]$. This peak broadening is due to short relaxation times of ^{11}B , leading to the splitting associated with the coupling of ^{19}F and ^{11}B being hindered, resulting in a poorly resolved broad signal instead of a multiplet which could have come from $^1J_{^{19}\text{F}-^{11}\text{B}}$.¹⁵³

The $[\text{BF}_3(\text{dma})]$ peak exhibited two singlets of unequal intensity at -148.86 ppm with a low intensity peak at -151.33 ppm (see Figure 2-8)) with no visible splitting observed.

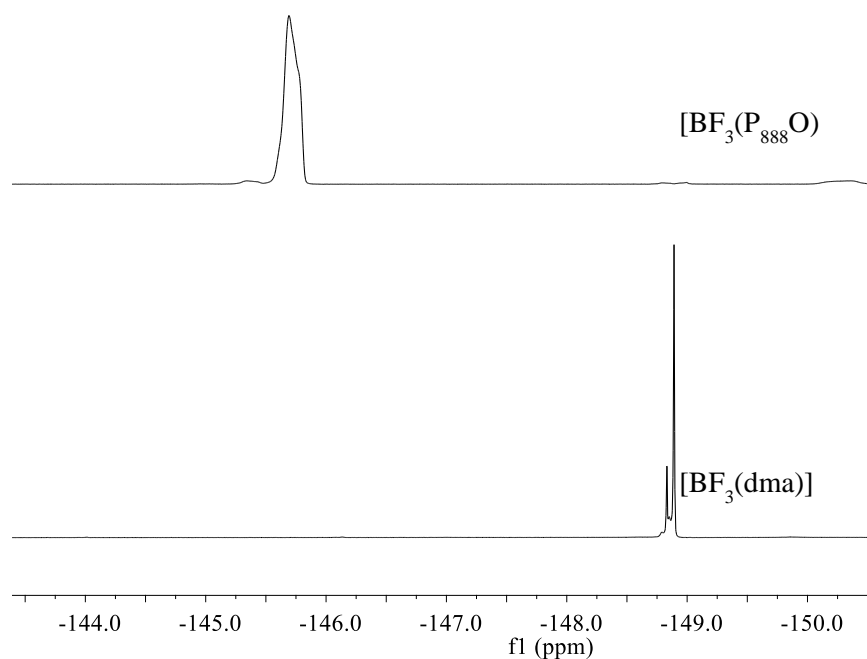


Figure 2-8: ^{19}F NMR (376 MHz, CDCl_3) spectra of tetracoordinate boron trifluoride complexes $[\text{BF}_3\text{L}]$ with O-donors.

Good resolution was obtained for the ^{19}F spectrum for $[\text{BF}_3(\text{P}_{888})]$ complex: exhibiting well resolved multiplets (doublet of quartet) at - 132.69 ppm (see Figure 2-9).

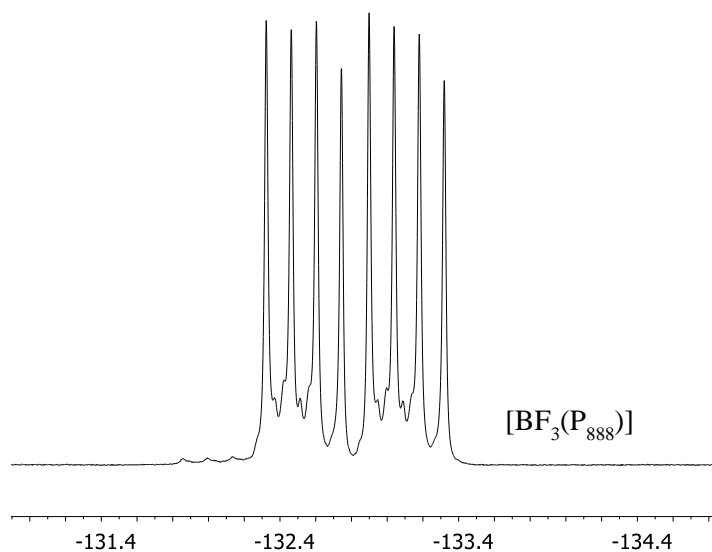


Figure 2-9: ^{19}F NMR (376 MHz, CDCl_3) spectra of tetracoordinate boron trifluoride complexes $[\text{BF}_3\text{L}]$ with P-donor.

This splitting was due the $^1J_{^{19}\text{F}-^{11}\text{B}} = 52.64 \text{ Hz}$ coupling with a quadrupolar ^{11}B given a quartet splitting of equal heights followed by second split by scalar $^2J_{^{19}\text{F}-^{31}\text{P}} = 218.08 \text{ Hz}$

coupling, resulting in doublet of quartet splitting.¹⁵³ Minor low intensity peaks were also observed due to the various possible coupling with either carbon or proton.^{142,152}

2.2.4 FT-IR spectroscopy

Infrared spectra were recorded for each tetracoordinate born complex. Neat complexes were studied using an ATR attachment. No traces of water (*i.e.* O-H bond or B-OH) were detected in the IR spectra, confirming that no hydrolysis has occurred (decomposition would manifest itself as a new band growing at round 1390 cm^{-1}).¹⁵⁵ Strong bands associated with an OH stretching vibrations of water and hydroxyl group would have also been detected in the IR spectra between 3200 and 3700 cm^{-1} in the case of water presence. Also, a band in the region $3650\text{-}3700\text{ cm}^{-1}$, indicative of an OH group, was never observed.

The N-donor complexes showed absorptions around $1275\text{-}1075\text{ cm}^{-1}$, indicative of a B-N stretch bond. Bands around $3070\text{-}3020\text{ cm}^{-1}$ were attributed to the aromatic C-H stretching (pyridines and amines) and -CH=CH- stretching in pyridines. Additionally, bands were observed for C=C, C=N, at around $1600\text{-}1440\text{ cm}^{-1}$, whereas those below 3000 cm^{-1} were attributed to diphasic C-H stretching and bands near $1220\text{-}1020\text{ cm}^{-1}$ for -C-N-stretch in amines.¹⁵⁶ Also bands near $1625\text{-}1580\text{ cm}^{-1}$ were indicative of aromatic -C=C- stretching, with absorptions near $1340\text{-}1250$ for C-N stretching.

The P-donor complexes showed C-H stretching vibrations for saturated aliphatic species between 3000 and 2800 cm^{-1} , bending C-H vibrations around 1400 cm^{-1} and also some C-H out-of-plane bending, overlapped by the $(\text{CH}_2)_n$ vibration of the long-chain aliphatic compounds between 900 and 600 cm^{-1} .¹⁵⁶

The main IR signals of each complex are listed, along with their corresponding ILs, in Table 3-6 (Chapter 3), where they are further discussed.

2.2.5 Elemental analysis

Elemental analysis is a quantitative method of determining the amount of CHN (and other elements) present in a sample under helium gas. By a combustion process, the sample to be analysed is oxidised and converted into simple combustion products. The combustion products are then swept through a chromatographic column by the carrier gas (helium), where they are separated. They are then pass through a thermal conductivity detector, where they are quantified according to the concertation of each component in the mixture.

Table 2-6: CHN, metal and halogen analysis of the boron complexes, by % mass

COMPLEX	% mass					
		C	H	N	B	Cl
[BCl ₃ (4-pic)]	real	34.35	3.63	6.43	-	49.00
	calc	34.24	3.33	6.66	5.2	50.57
[BCl ₃ (mim)]	real	24.21	3.13	14.00	-	54.50
	calc	24.09	3.01	14.05	-	53.37
[BCl ₃ (dma)]	real	23.96	5.17	6.76	-	53.19
	calc	23.50	4.41	6.85	-	52.06
[BCl ₃ (P ₈₈₈ O)]	real	57.76	10.83	-	-	18.4
	calc	57.16	10.58	-	-	21.80
[BCl ₃ (P ₈₈₈)]	real	59.74	10.62	-	-	21.25
	calc	59.1	10.00	-	-	21.80
[BF ₃ (4-pic)]	real	44.67	4.50	8.68	-	-
	calc	44.73	4.35	8.70	-	-
[BF ₃ (mim)]	real	32.34	4.02	18.87	-	-
	calc	32.02	4.67	18.68	-	-
[BF ₃ (dma)]	real	30.00	5.97	9.00	-	-
	calc	30.98	5.81	9.04	-	-
[BF ₃ (P ₈₈₈ O)]	real	63.35	11.67	-	-	-
	calc	63.43	11.22	-	-	-
[BF ₃ (P ₈₈₈)]	real	64.04	11.86	-	-	-
	calc	66.05	11.68	-	-	-

CHN, metal and halogen content analysis were carried out to additionally confirm the composition of the products, by confirming masses of boron, carbon, hydrogen, nitrogen and chlorine present in each complex. Complexes with significant amount of fluorine could not be analysed for halogen content due to instrumental reasons. The actual percentage masses were compared to the calculated percentage masses, which confirmed the correct composition of each complex (Table 2-6).

2.2.6 Differential scanning calorimetry measurements and thermogravimetric analysis

Thermal properties of the complexes were studied by thermogravimetric analysis (TGA) and differential scanning calorimetry (DSC). These data provided important information about the stability and thermal behaviour of these compounds. All TGA and DSC experiments were recorded twice, each time with a new batch of samples; in all reported cases the thermograms bore little or no variations. Decomposition temperatures were obtained from dynamic TGA scans, recorded at a heating rate of 5 °C min⁻¹ under dry nitrogen. From the thermogram, the onset of the first step of weight loss in each compound was reported as the decomposition temperature, T_d (Table 2-7). The thermal stability of the boron complexes were found to depend on both the

ligand (L) and the halide (X). It was observed that the [BF₃L] complexes (Figure 2-11) generally had higher thermal stability than the [BCl₃L] complexes (Figure 2-10). This can be attributed to the decreasing stability of the boron trichloride complexes with increasing halide mass. In other words, higher energy is required to break the stronger and shorter B-F bond (1.313 Å), compared to the longer and weaker B-Cl bond (1.75 Å).^{157,8,138,158} Furthermore, there several decomposition steps visible for [BCl₃L] adducts, with incomplete decomposition leaving behind *ca.* 10-30 % residue (Figure 2-10). In contrast, [BF₃L] adducts decomposed in a one-step process (Figure 2-11), leaving no residue behind. Small negative mass (-2%) was recorded in some cases, pointing to possible etching of the pan and/or wire of the TGA by fluorine compounds.

Table 2-7: The melting decomposition points of the synthesised boron complexes.

COMPLEX	<i>T_d</i> / °C	COMPLEX	<i>T_d</i> / °C
[BCl ₃ (4-pic)]	115.40	[BF ₃ (4-pic)]	140.56
[BCl ₃ (mim)]	101.25	[BF ₃ (mim)]	204.60
[BCl ₃ (dma)]	52.10	[BF ₃ (dma)]	95.96
[BCl ₃ (P ₈₈₈ O)]	122.44	[BF ₃ (P ₈₈₈ O)]	204.89
BCl ₃ (P ₈₈₈)	115.84	[BF ₃ (P ₈₈₈)	149.28

The stability of boron complexes was appreciably influenced also by the substituent at the boron atom. The stability decreased with decrease in the size of the substituent, in agreement with the literature.^{159,160}

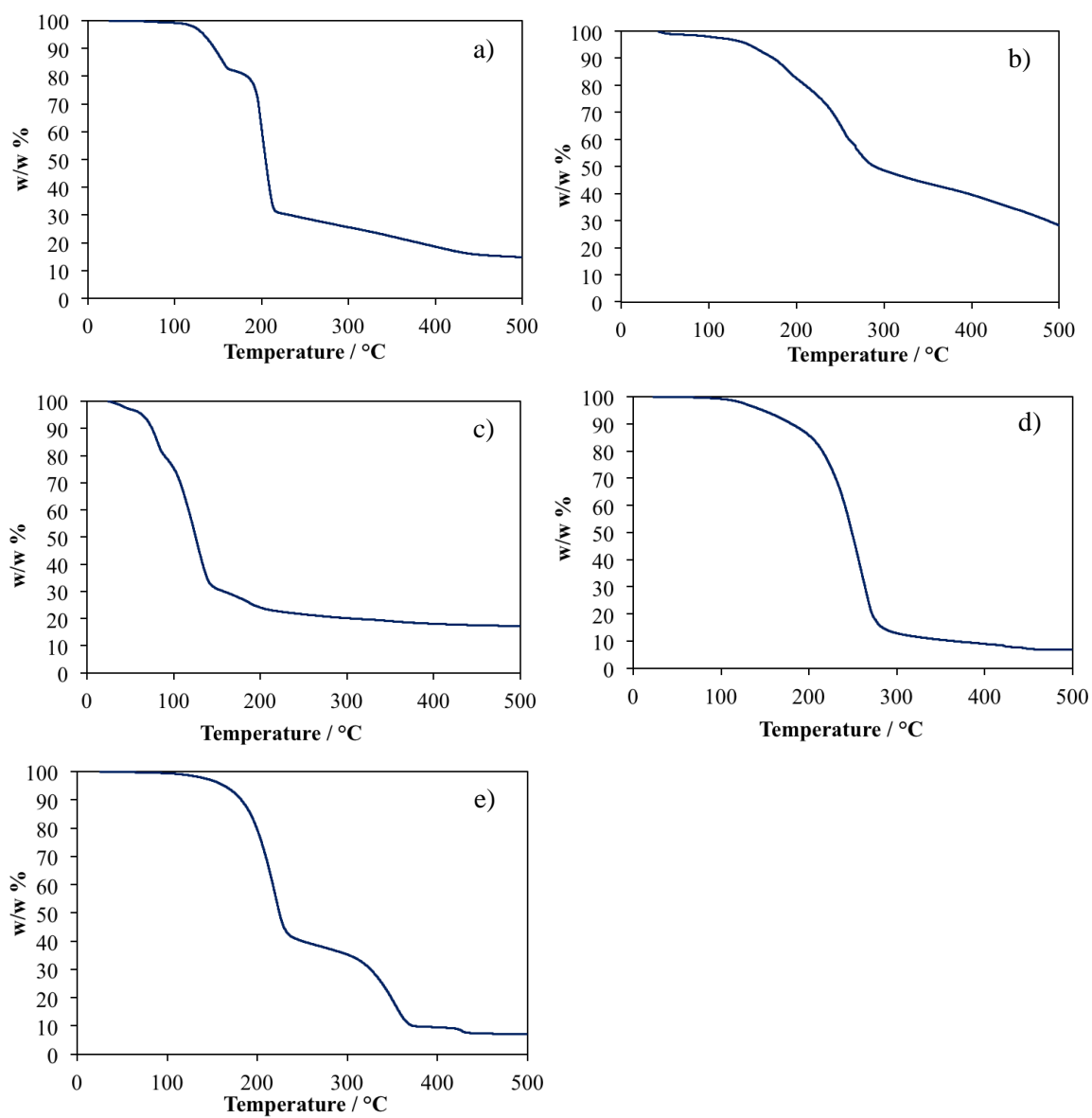


Figure 2-10: TGA thermograms of $[BCl_3L]$ adducts: a) $[BCl_3(4-pic)]$, b) $[BCl_3(mim)]$, c) $[BCl_3(dma)]$, d) $[BCl_3(P_{888}O)]$ and e) $[BCl_3(P_{888})]$.

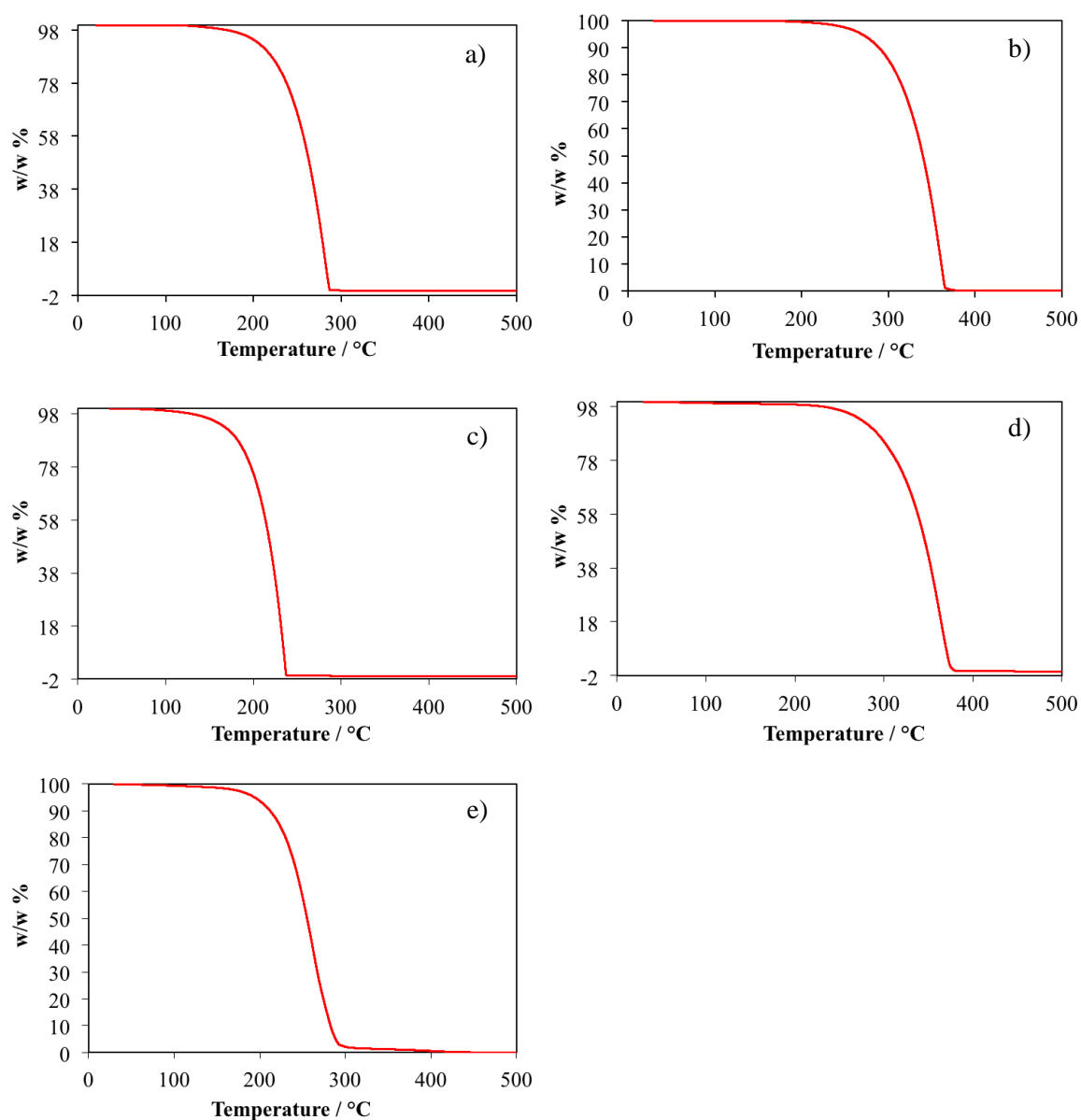


Figure 2-11: TGA thermograms of $[BF_3L]$ adducts: a) $[BF_3(4\text{-pic})]$, b) $[BF_3(mim)]$, c) $[BF_3(dma)]$, d) $[BF_3(P_{888}O)]$ and e) $[BF_3(P_{888})]$

DSC data were recorded over three full cycles at a scanning rate of $5\text{ }^{\circ}\text{C min}^{-1}$. Some of the $[BCl_3L]$ complexes decomposed with melting, whereas the $[BF_3L]$ complexes were all stable past their decomposition point. This is due to the weaker bonding between boron and chlorine compared to boron and fluorine.⁸ Some of the studied compounds simply form a crystals at low temperatures. The behaviour of the complexes during DSC measurements depended on their compositions.^{161,12} Most of the complexes showed one positive exothermic peak and one negative endothermic peaks (Figure 2-12(a, b and c) and Figure 2-13(a, b and c) however in some cases

two or three crystallisation events were present (Figure 2-12(e) and Figure 2-13(e) which suggest a polymorphic crystal structure or several compounds present.¹⁶² In subsequent cycles of heating and cooling, the ratio of both areas changed, indicating either different polymorphic structures, or different compounds in equilibrium and $[BX_3(P_{888})]$ compounds, this was an indication of crystallisation in two step with one presumably being crystallisation of the alkyl chain and the second being the rest of the compound.^{159,160}

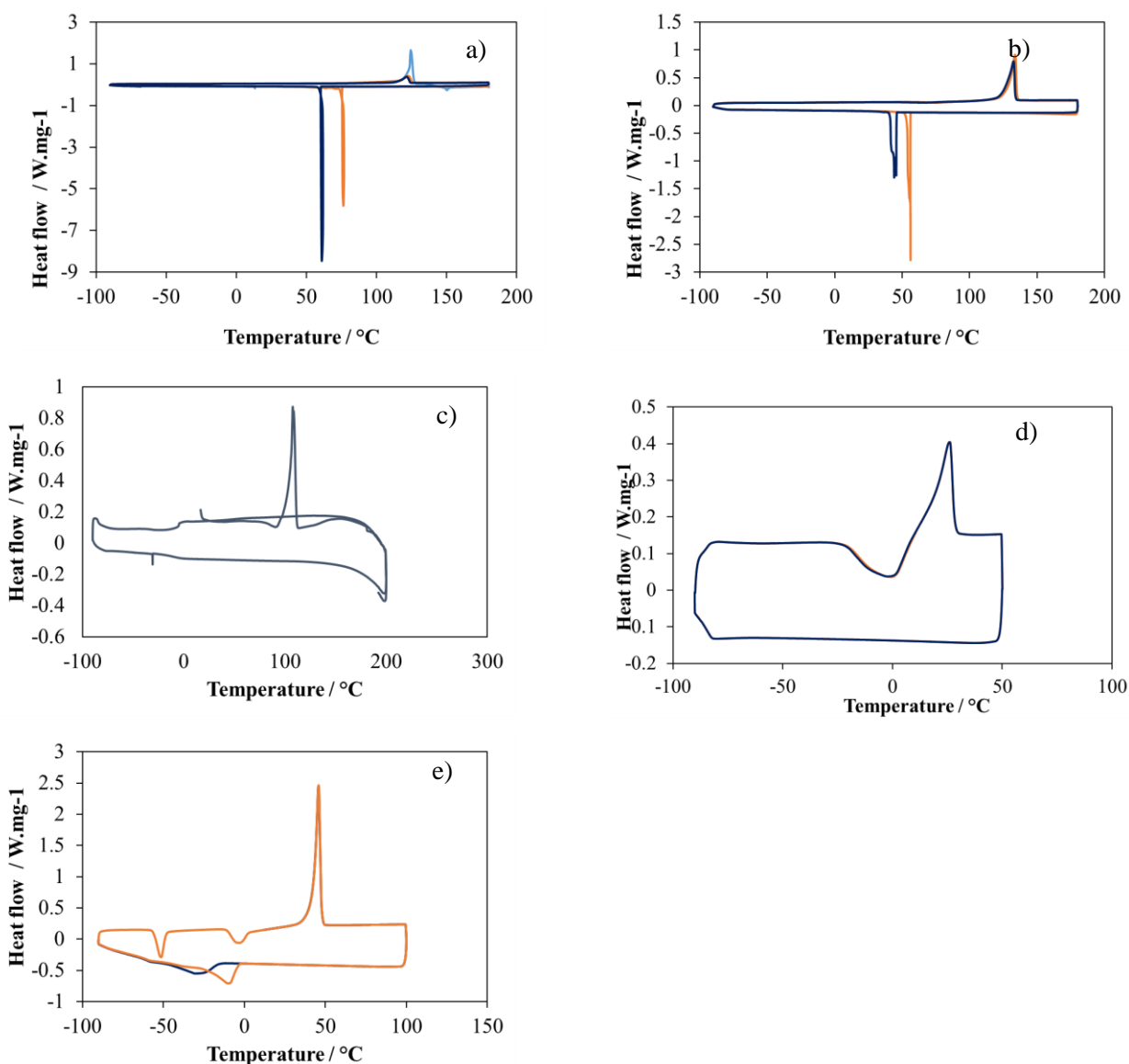


Figure 2-12: DSC graph showing melting points (exo, down) of $[BCl_3L]$ adducts a) $[BCl_3(4\text{-pic})]$, b) $[BCl_3(\text{mim})]$, c) $[BCl_3(\text{dma})]$, d) $[BCl_3(P_{888}O)]$ and e) $[BCl_3(P_{888})]$ recorded in a dynamic nitrogen atmosphere, at a heating rate of 5°C min^{-1} .

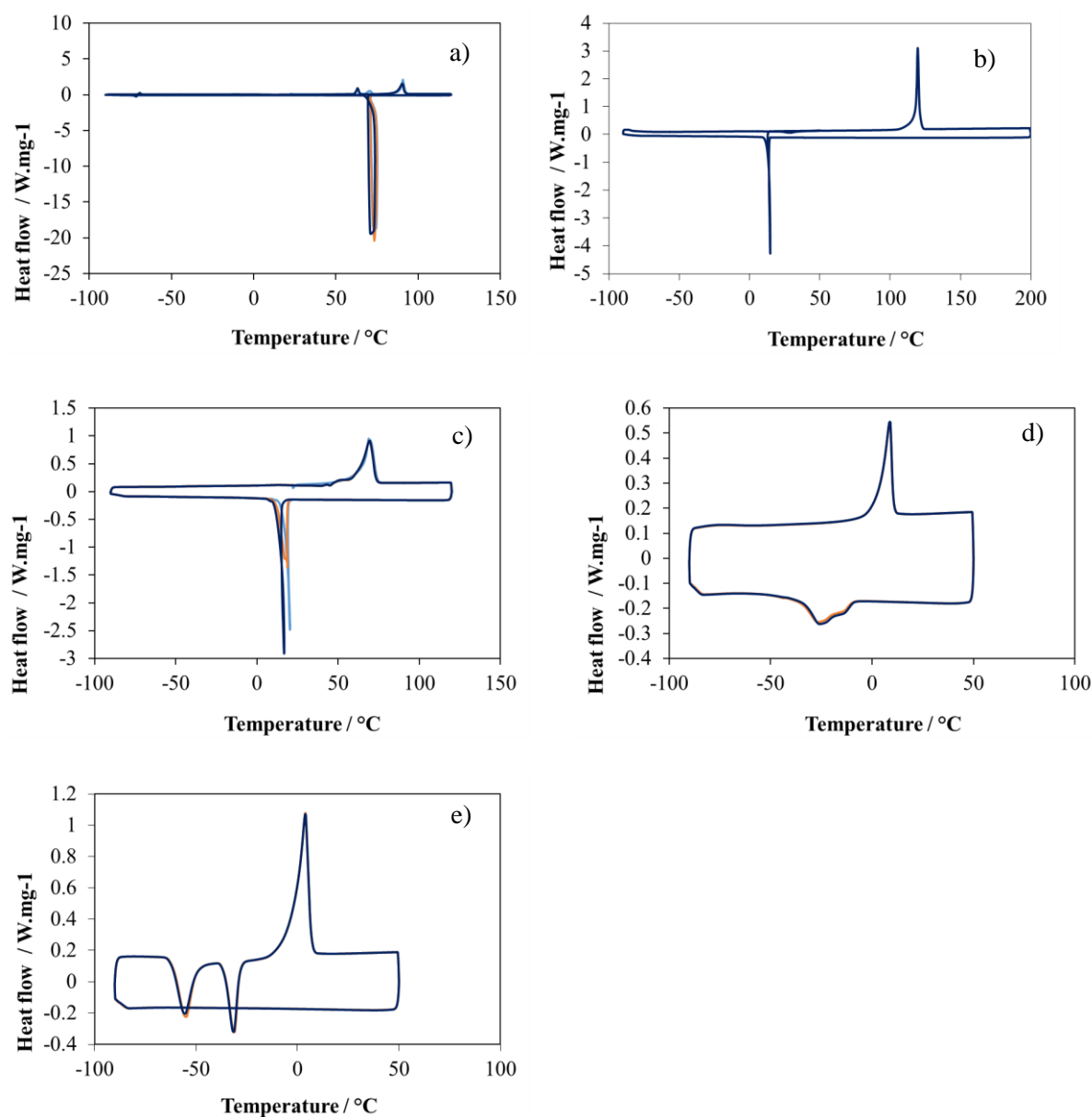


Figure 2-13: DSC graph showing melting points (exo, down) of $[\text{BF}_3\text{L}]$ adducts: a) $[\text{BF}_3(4\text{-pic})]$, b) $[\text{BF}_3(\text{mim})]$, c) $[\text{BF}_3(\text{dma})]$, d) $[\text{BF}_3(\text{P}_{888}\text{O})]$ and e) $[\text{BF}_3(\text{P}_{888})]$ recorded in a dynamic nitrogen atmosphere, at a heating rate of 5°C min^{-1} .

For the stable adducts that were thermally stable past their melting point, both the onset and the peak of melting event were recorded. The enthalpy of fusion was determined by integration of the experimental heat flow curves as functions of temperature. The melting point was taken as the onset of an endothermic peak on heating and the glass transition temperature is taken as the midpoint of a small heat flow change on heating from the amorphous glass state to a

liquid state. The values of the melting onset temperature (T_m), melting maxima and enthalpies of boron complexes are shown in Table 2-8 for all compounds investigated.

Table 2-8: The melting onsets (T_m), melting maxima and enthalpies of boron complexes.

COMPLEX	melting onset, $T_m/^\circ\text{C}$	peak maximum/ $^\circ\text{C}$	melting enthalpy/ kJ mol^{-1}
[$\text{BCl}_3(4\text{-pic})$]	123.26	124.44	15.73
[$\text{BF}_3(4\text{-pic})$]	86.60	90.41	11.94
[$\text{BCl}_3(\text{mim})$]	128.03	133.63	11.14
[$\text{BF}_3(\text{mim})$]	118.57	119.59	17.31
[$\text{BCl}_3(\text{dma})$]	104.89	107.81	12.29
[$\text{BF}_3(\text{dma})$]	62.47	69.42	9.81
[$\text{BCl}_3(\text{P}_{888}\text{O})$]	15.54	25.83	14.71
[$\text{BF}_3(\text{P}_{888}\text{O})$]	2.84	8.72	13.14
[$\text{BCl}_3(\text{P}_{888})$]	42.51	45.86	54.10
[$\text{BF}_3(\text{P}_{888})$]	-2.16	3.95	34.36

In general, [BCl_3L] complexes exhibited higher melting points than the corresponding [BF_3L] adducts. It is in agreement with literature reports that [BCl_3L] complexes tend to have more stable crystal structures, therefore more energy is required to transform them into disordered liquids, compared to the [BF_3L] complexes.¹⁶³ Size and symmetry of the complexes also made an impact on their melting points: the [$\text{BX}_3(\text{P}_{888})$] complexes with long alkyl chains and low symmetry had low melting points irrespective of the halide.^{70,163,156} In agreement with these general principles, [$\text{BF}_3(\text{P}_{888})$] had the lowest melting point; at $T_m = 3.95^\circ\text{C}$ it was a liquid at ambient conditions. In contrast, [$\text{BCl}_3(\text{mim})$] with small aromatic donor had the highest melting point of $T_m = 133.63^\circ\text{C}$. [$\text{BF}_3(4\text{-pic})$] showed an unusual repeated endothermic peak prior to the main melting point peak in both measurements and this was identified as an artefact possibly due to contamination of sample from residues of previous experiments.

2.2.7 Crystallographic analysis

In some cases, single crystals were obtained from slow recrystallization from a concentrated chloroform solution at 60 °C, by slow cooling it to ambient temperature. Two complexes have yielded crystals of quality sufficient for single-crystal X-ray analysis: $[\text{BF}_3(\text{mim})]$ and $[\text{BCl}_3(4\text{pic})]$.

$[\text{BF}_3(\text{mim})]$ crystallised in planes 3.3 Å apart, with parallel-offset π -stacking between imidazole rings (Figure 2-14).¹⁶⁴ Each plane is connected through a dense network of medium-strength hydrogen bonds. Geometry around the boron centre was distorted tetrahedron, consistent with literature.¹³⁸ This distortion was associated to the bond length difference between nitrogen and boron (~ 1.54 Å), and fluorine and boron (~ 1.34 Å).¹³³

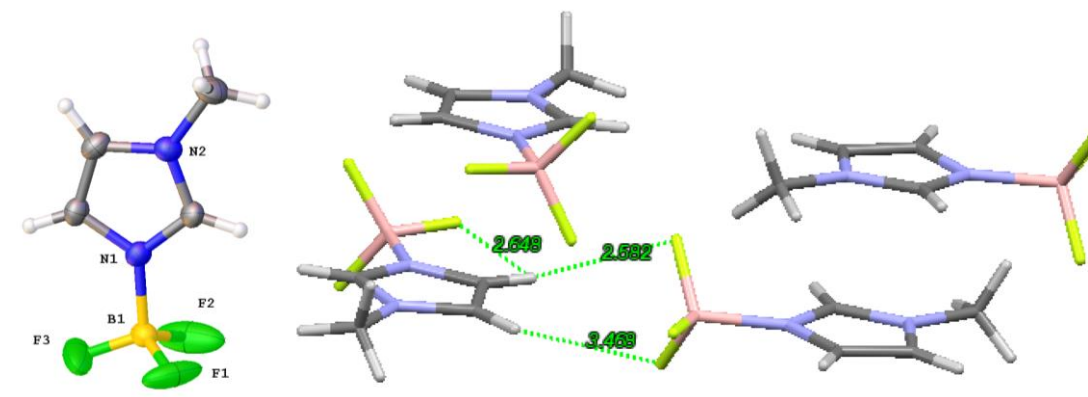


Figure 2-14: Crystal structure of $[\text{BF}_3(\text{mim})]$: molecular structure (left), and packing (right)

$[\text{BCl}_3(4\text{pic})]$ crystallised in planes *ca.* 3.5 Å apart; in contrast to $[\text{BF}_3(\text{mim})]$, no obvious evidence for π -stacking was detected (Figure 2-15).¹⁶⁴ Each plane was connected by hydrogen bonds, but many of these were intra-molecular rather than inter-molecular. Again, there was distorted tetrahedron geometry around the boron centre, the structure deriving from the contribution of the slightly shorter N-B bond (1.59 Å), when compared to the B-Cl bonds (1.72 Å).^{138,158,133}

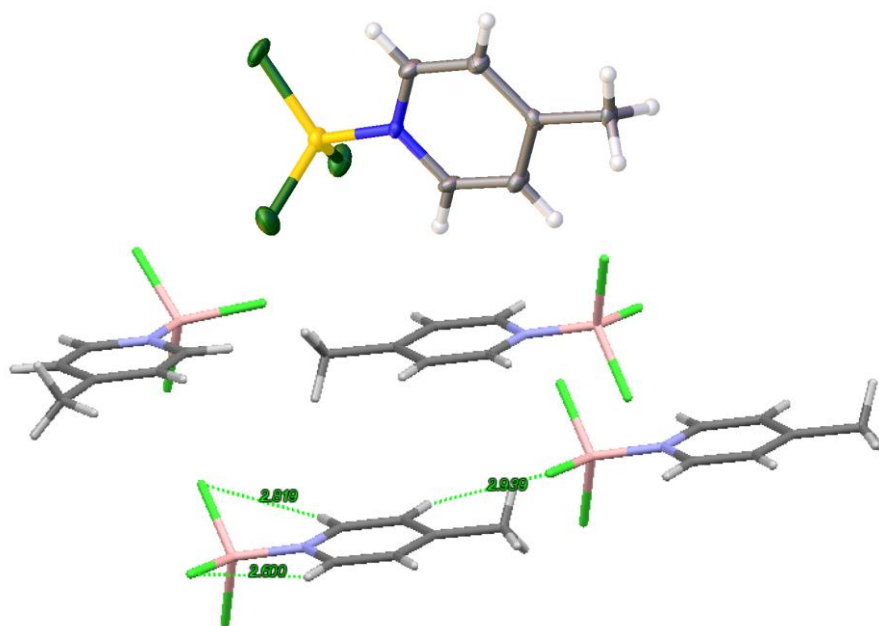


Figure 2-15: Crystal structure of $[BCl_3(4pic)]$: molecular structure (top), and packing (bottom).

2.3 CONCLUSIONS

In conclusion, two groups of boron trihalide complexes, $[BF_3L]$ and $[BCl_3L]$, were successfully synthesised using five different donor ligand (*i.e.* 4-methyl pyridine, 1-methylimidazole, dimethylacetamide, trioctylphosphine oxide and trioctylphosphine). The boron adducts were air-stable compounds and their characterisation (m.p, elemental analysis, IR, NMR) were described. Where possible, the crystal and molecular structure of the complexes were determined by a single-crystal X-ray diffraction study.

From the DSC results, the $[BCl_3L]$ complexes were seen to decompose with melting, whereas the $[BF_3L]$ complexes were all stable past their decomposition point. The 1H and ^{13}C NMR spectra of all the complexes were all supporting the presence of boron trichloride and boron trifluoride complexes, with no impurities such as unreacted ligands observed. ^{11}B NMR spectra were congruent to those of the tetracoordinate boron compounds with slight variations depending on the ligand present.

These complexes were subsequently used for the synthesis of a new class of Lewis acidic ionic liquids: borenium ionic liquids (Chapter 3).



CHAPTER THREE

“The idea is to write so that people hear it and it slides through the brain and goes straight to the heart.”

–Maya Angelou



3 SYNTHESIS AND CHARACTERISATION OF BORENIUM IONIC LIQUIDS

This chapter describes synthesis and characterisation of borenium ionic liquids from tetracoordinate $[BX_3L]$ adducts, by two synthetic routes: chloride abstraction by a Lewis acidic metal chloride or fluoride abstraction by a triflate ester. Physico-chemical characterisation of each synthesised family is presented. Finally, acidity measurements using Gutmann Acceptor Number approach are reported. Compounds described in this chapter were used as catalysts in two model reactions, described in Chapter 4 and Chapter 5.

3.1 EXPERIMENTAL

3.1.1 Synthesis

Unless stated otherwise, all moisture-sensitive procedures/experiments were carried out under an argon atmosphere, by using Schlenk techniques or in a nitrogen-filled glove box (O_2 and $H_2O < 0.1$ ppm); all materials were purchased from Sigma-Aldrich and used as received. Solvents were dried over molecular sieves (3 \AA) and stored under argon. Glassware was dried in the oven (*ca.* 140°C , for at least 24 h prior to use).

3.1.1.1 *Borenium chloroaluminate ionic liquids*

All syntheses were carried out in a glovebox. In a typical procedure, a boron trichloride complex (2 g, 1 mol eq.) was weighed out into sample vial (10 cm^3) equipped with PTFE-coated screw cap and a magnetic stirring bar. Then the required amount of aluminium(III) chloride (1 or 2 mol eq.) was slowly added and the mixture was stirred vigorously (800 rpm) for at least 1 h and left overnight. Heating (50°C) was employed when required to complete the reaction. Subsequently, the ionic liquid produced was stored in the glovebox.

3.1.1.2 *Borenium chlorogallate ionic liquids*

All syntheses were carried out in a glovebox. In a typical procedure, in a glove box a boron trichloride complex (2 g, 1 mol eq.) was weighed out into sample vial (10 cm^3) equipped with PTFE-coated screw cap and a magnetic stirring bar. Then the required amount gallium(III) chloride (1, 2 or 3 mol eq.) was slowly added and the mixture was stirred vigorously (800 rpm)

for at least 1 h and left overnight. Heating (50 °C) was employed when required to complete the reaction. Subsequently, the ionic liquid produced was stored in the glovebox.

3.1.1.3 Borenium triflate ionic liquids

In a typical procedure, a Schlenk flask (25 cm³) equipped with a gas tap, septum and a magnetic stirring bar was connected to the Schlenk line. The tap was opened to vacuum and then refilled with argon twice to ensure an inert atmosphere of argon. The flask was transferred into the glove box. In a glove box, a boron trifluoride/ boron trichloride complex (2 g, 0.9 mol eq.) was weighed out into the schlenk flask. Then the required amount trimethylsilyl trifluoromethanesulfonate/ methyl trifluoromethanesulfonate (1 mol eq.) was weighed out using a gas-tight syringe and added to the reaction flask. The reaction mixture was then moved to the fume hood and connected to the schlenk line and the mixture was left under inert gas stirring overnight (24 h) to ensure complete reaction. The reaction mixture was then heated (60 °C) for at least 1 h. All volatiles were removed under low vacuum (60 °C, 10⁻¹ bar and 1 h). Subsequently, the ionic liquid produced was transferred into the glovebox and stored in the sample vial (10 cm³) equipped with PTFE-coated screw cap.

3.1.2 Characterisation of borenium ionic liquids

3.1.2.1 NMR spectroscopy

In a glove box, dry, neat ionic liquids were loaded into NMR tubes (5 mm, borosilicate glass) containing sealed capillaries with d₆-dimethylsulfoxide (an external lock). The tubes were closed with a standard cap, sealed with parafilm, and removed from the glove box immediately prior to measurement. ¹H, ¹³C, ¹⁹F, ¹¹B and ²⁷Al NMR spectra was recorded using a Bruker AvanceIII 400 MHz spectrometer. The background signal from the borosilicate tube (a broad signal feature at 30 ppm) was removed from the ¹¹B NMR using iNMR (Mestrelab Research).

3.1.2.2 ATR FT-IR spectroscopy.

In a glove box, dry, neat ionic liquids (<0.5 g) were placed in vial and sealed with parafilm. Prior to scanning, the cuvettes were removed from the glove box immediately tip over onto the loading plate covering the ionic liquid and making sure that none of the ionic liquids were exposed to air. The Infrared spectra of the neat samples were recorded on a Perkin Elmer Spectrum 100 Series FT-IR with ATR attached spectrometer. Eight scans were acquired for each sample.

3.1.2.3 Acceptor number determination

Sample preparation was carried out in a dry, nitrogen-filled glove box. In a typical experiment, a sample (*ca.* 1 g) of each composition of ionic liquid was weighed into a sample vial (10 cm³) equipped with a PTFE-coated screw cap and a magnetic stirring bar. The vial was left on the balance and a small, accurately measured amount of triethylphosphine oxide (tepo) was added (1-3 mol % per mol of the [BX₂L]⁺ cation). The sample vial was then closed with a plastic cap and the mixture was stirred to ensure complete dissolution of tepo. After dissolution of tepo was ensured, the solutions were loaded into an NMR tube (5 mm, borosilicate glass), containing a sealed capillary with d₆-dimethylsulfoxide (as an external lock). The tube was closed with a standard cap, sealed with parafilm, and removed from the glove box immediately prior to measurement. ³¹P NMR spectra were recorded using a Bruker AvanceIII 400 MHz spectrometer. Phosphoric(V) acid, 85% solution in water, was used as an external reference.

Three solutions of tepo in hexane (*ca.* 5, 10 and 15 mol %) were prepared, and then measured at 27 °C. For each tepo ionic liquid system, the ³¹P NMR chemical shift for the infinite dilution of tepo, δ_{inf} , was determined by extrapolation from the ³¹P NMR chemical shifts measured at different tepo concentrations.¹⁶⁵ The chemical shift of tepo in hexane, extrapolated to infinite dilution, $\delta_{\text{inf hex}}$, was used as a reference ($\delta_{\text{inf hex}} = 0$ ppm). The AN values for all samples were calculated from the following formula: $\text{AN} = 2.348 \cdot \delta_{\text{inf}}$.^{165,53}

3.1.2.4 Density

In a glovebox, dry, neat ionic liquids (2 cm³) were weighed into a gas tight syringe. The gas tight syringe was then taken out and the liquid was transferred slowly into the vibrating-tube of the densimeter making sure to avoid the presence of bubbles. The density of the liquids were measured at a range of temperatures (20-70 °C) using a METTLER TOLEDO U-shape vibrating-tube densimeter, Benchtop model DM40. The temperature was regulated by circulating a fluid from an external temperature-controlled circulating bath (Polyscience PS 9110) through the heat exchanger of the vibrating tube cell. The temperature inside the cellblock was measured with Pt-100 platinum resistance thermometer connected to an Agilent 34970A data acquisition unit, with an uncertainty of ± 0.02 K.¹⁶⁰ The internal calibration of the instrument was confirmed by measuring the densities of atmospheric air, sodium chloride solution and distilled water as an appropriate reference fluids according to the recommendations of the manufacturer, at 293 and

343 K. The instruments have a built-in Peltier thermostat to accurately control the temperature was regulated by circulating a fluid from an external temperature-controlled circulating bath (Polyscience PS 9110) through the heat exchanger of the vibrating tube cell. The temperature inside the cellblock was measured with Pt-100 platinum resistance thermometer connected to an Agilent 34970. The precision of the density measurement is of the order 10^{-4} g/cm³, the results are expected to be accurate to 10^{-3} g/cm³. All data were recorded in g cm⁻³.

3.1.2.5 Viscosity

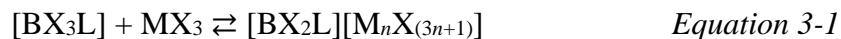
In a glovebox, dry, neat ionic liquid (2 cm³) were weighed using a syringe into the appropriate viscosity capillary tube equipped with a sphere falling ball. The capillary tube was sealed at both ends with an adapter and plug making sure to avoid the presence of bubbles. The sealed capillary tube was then moved out of the glovebox and transferred into the falling ball viscometer inclined at 60° angle to the vertical. The viscosity of the liquids were recorded at a range of temperatures (20-70 °C) as a function of their densities using an Anton Paar LOVIS 2000 M/ME Micro viscometer. The results were given as dynamic viscosity kg m⁻¹ s⁻¹.

3.2 RESULTS AND DISCUSSIONS

3.2.1 General synthetic considerations

Various synthetic routes to borenium cations have been explored in the past decades (See Table 1-2). However, typically the research effort was aimed at the synthesis of crystalline materials, ideally lending themselves to analysis *via* single crystal X-ray diffraction, or alternatively - borocations were used and studied in solution. This work covers the first attempt to generate ionic liquids with borenium cations, using design principles that lead to disruption of the crystal lattice. It was hoped that such materials would have high Lewis acidity, with electron deficiency on boron exacerbated by the positive charge. Furthermore, it was expected that using ionic liquids rather than solid catalysts will facilitate developing solvent-free catalytic reactions (see Chapter 4 and 5).

Precursors for the synthesis of the borenium ionic liquids were Lewis acid-base adducts of boron trichloride or boron trifluoride, described in Chapter 2.^{166,167} Selection of halides and L-donors used for the synthesis of tetracoordinate adducts was justified in Section 2.2.1. Borenium ions, $[BX_2L]^+$, were targeted by boron-halogen bond heterolysis. The halide-abstrating reagents used were halophilic Lewis acids, inducing halide abstraction from the boron adduct, forcing reaction equilibria in Equation 3-1 and Equation 3-2 to shift to the right, and forming borenium salt comprising a cationic tricoordinate boron and the anion.



The halide-abstrating agent had to fulfil two key requirements: (i) had to be strong enough to break the B-X bond, and (ii) in reacting with the tetracoordinate boron adduct, it had to produce an ionic-liquid generating anion - that is a non-coordinating, singly-charged anion, which is unlikely to promote crystallisation. For this reason, anions such as tetra(perfluorophenyl)borate or hexafluorophosphate were excluded for the investigation. Furthermore, a simple one-step technique without the need for complex purification procedure was preferred. Two groups of halide-abstrating agents were selected: Group 13 metal chlorides ($M = Al$ or Ga), which reacted following Equation 3-1, and triflate esters, which were expected

to generate ionic liquids following Equation 3-2. The former group is suitable for chloride abstraction, but not fluorine abstraction;²² the latter agents are capable of abstracting either fluoride or chloride,^{21,22} which determined which boron complexes were used in each case.

3.2.2 Chlorometallate counterions to borenium ionic liquids

Two Group 13 halide acceptors were used in this work: AlCl_3 and GaCl_3 , both in the form of strictly anhydrous solids. Due to water-sensitive nature of the reagents as well as the resulting ionic liquids, the preparation borenium ionic liquids was carried out in the glove box, under inert gas environment. To prevent large overheating of reaction mixtures, the reagents (*i.e.* AlCl_3 and GaCl_3) were added slowly and vigorous stirring was employed.^{168,169} Following this procedure, slightly exothermic effects occurred upon mixing both reactants, enhancing melting of the two solids into a mobile liquid. Solvent-free reaction of the boron complexes (Chapter 2) with either metal halide resulted in clear homogeneous liquids, or were stirred until the amount of unreacted solid did not change for several hours. Reactant ratios were varied, to generate borenium cations accompanied by different chlorometallate anions (see example in Figure 3-1).

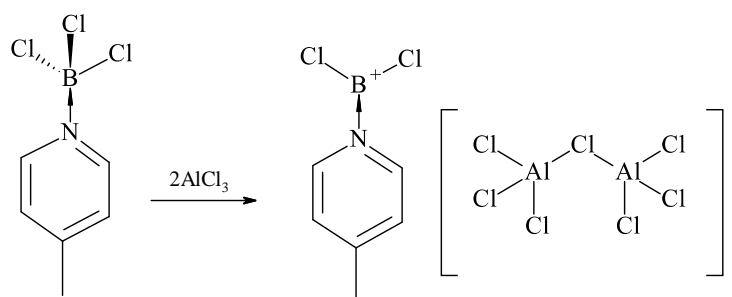


Figure 3-1: The formation and structure of a borenium cation with $[\text{Al}_2\text{Cl}_7]^-$ anion.

Boron trichloride complexes (1 mole) were reacted with 1 or 2 moles aluminium(III) chloride (here noted as $\text{L-BCl}_3\text{-AlCl}_3$ and $\text{L-BCl}_3\text{-2AlCl}_3$) and 1, 2 or 3 moles of gallium(III) chloride: $\text{L-BCl}_3\text{-GaCl}_3$, $\text{L-BCl}_3\text{-2GaCl}_3$ and $\text{L-BCl}_3\text{-3GaCl}_3$. The reaction with equimolar quantity of MCl_3 led to the formation of coordinationally saturated $[\text{MCl}_4]^-$ anions. Two equivalents of MCl_3 led to the formation of $[\text{M}_2\text{Cl}_7]^-$, which is considered Lewis acidic (1.6.1). Three equivalents of AlCl_3 did not react fully, because $[\text{Al}_3\text{Cl}_{10}]^-$ does not form in ionic liquids under ambient conditions, but AlCl_3 precipitates - therefore such samples have not been

tested.^{170,3} In contrast, three equivalents of GaCl₃ could be used, as [Ga₃Cl₁₀]⁻ is readily formed.^{3,12,171}

The reactions of two equivalents of metal halide (AlCl₃ or GaCl₃) with [BCl₃L] produced colourless, homogenous liquids in most cases (Table 3-1). Reactions of equimolar amounts of [BCl₃(mim)] and metal halides yielded soft, waxy solids, which were melting to form homogenous liquids below 60 °C. In contrast, mixtures of [BCl₃(dma)] and metal halides did not yield homogenous liquids. The dma-BCl₃-MCl₃ systems gave waxy solids, but upon overnight heating and stirring at 60 °C, the systems were biphasic, with liquid and significant amount of solid suspension. The dma-BCl₃-2MCl₃ systems initially formed homogenous liquids, but after several hours white solid precipitated from these liquids, and did not dissolve upon overnight heating and stirring at 60 °C.

Table 3-1: Physical state at ambient conditions of products of reaction between [BCl₃L] complexes and nMCl₃ (n = 1, 2 or 3, M = Al or Ga); L - liquid, W - waxy solid and L+P = liquid + precipitation

L	L-BCl ₃ -nMCl ₃				
	AlCl ₃	2AlCl ₃	GaCl ₃	2GaCl ₃	3GaCl ₃
4-pic	L	L	L	L	L
mim	W	L	W	L	L
dma	W	L+P	W	L+P	L+P
P ₈₈₈ O	L	L	L	L	L
P ₈₈₈	L	L	L	L	L

Although no further investigation into the matter were carried out, observations from taking small samples of ionic liquids out of the glovebox and to the open air suggest that borenium ionic liquids based on gallium(III) chloride were less water sensitive compared to the ionic liquids based on aluminium(III) chloride. The difference in hydrolytic stability of aluminium systems and gallium systems can be explained in terms of their bond energy. The bond energy D°₂₉₈ (Al-O) is 512(4) kJ mol⁻¹, only slightly higher to the bond energy of D°₂₉₈(Al-Cl) which is 494(13) kJ mol⁻¹.^{172,158} However, when tetracoordinate chloroaluminate anion with four Al-Cl bonds is exposed to water, it instantaneously losses its four Al-Cl bonds to form six bonds with water, which offers significant energy benefit due to increase in coordination number.²⁷ Although

the bond length between Al-Cl₃ and Ga-Cl₃ are similar, the bond dissociation energies at 298 K are different: $D^{\circ}_{298}(\text{Ga-O})$ is 285(63) kJ mol⁻¹, which is much smaller than $D^{\circ}_{298}(\text{Ga-Cl})$, which is 481(13) kJmol⁻¹.^{172,158} This higher bond energy of Ga-Cl helps it to remain quite stable compare to Al-Cl in water. This difference is key in enabling chlorogallate borenium ionic liquids to be less water sensitive than chloroaluminate borenium ionic liquids.

3.2.2.1 NMR spectroscopic characterisation

Multinuclear NMR spectroscopy was the main technique used to study all the ionic liquids. The NMR spectra were locked to (external) solvent signal (CD₃)₂SO: 2.54 ppm (¹H) and 40.45 ppm (¹³C). Heteronuclear chemical shift values were referenced to external F₃B·OEt₂ (¹¹B{¹H}), Al(NO₃)₃ in D₂O (²⁷Al{¹H}), and 85% H₃PO₄ in H₂O (³¹P{¹H}). All NMR spectra were recorded on a Bruker AvanceIII 400 MHz spectrometer at 27 °C.

3.2.2.1.1 ¹H and ¹³C NMR spectroscopy

The ¹H and ¹³C NMR spectra were useful to examine the L-type ligands in borenium cations. In particular, they confirmed that the ligands did not decompose, and that they were indeed coordinated to the boron centre. All systems that were homogenous liquids at ambient temperatures were studied; spectra of the dma-BCl₃-2MCl₃ systems were recorded for the liquids decanted from over the solid precipitation.

The ¹H NMR spectra of ionic liquids based on four cations: [BCl₂(4-pic)]⁺, [BCl₂(mim)]⁺, [BCl₂(P₈₈₈O)]⁺ and [BCl₂(P₈₈₈)]⁺, were similar to the spectra of corresponding [BCl₃L] adducts in terms of splitting patterns, but multiplets were less refined. Integrations matched assignments in Table 3-2. ¹H NMR spectra of the dma-BCl₃-2MCl₃ systems featured sharp signals, quite deshielded with respect to the ligand and difficult to assign (listed in Table 3-2), and some less shielded, very broad signal, indicative of residual solid suspension in the NMR tube (see Figure 3-2 for example).

Chemical shifts in ¹H NMR spectra of four cations: [BCl₂(4-pic)]⁺, [BCl₂(mim)]⁺, [BCl₂(P₈₈₈O)]⁺ and [BCl₂(P₈₈₈)]⁺ showed slight upfield shifts relative to the starting materials (tetracoordinate boron adducts) - as shown in Table 3-2. The shielding was a bit more pronounced for the chlorogallate anions, when compared to chloroaluminate ones, and more pronounced for L-BCl₃-2MCl₃ systems vs. L-BCl₃-MCl₃ systems. It was surprising that ligands associated with tricoordinate cations are more shielded than these associated with tetracoordinate

neutral adduct. However, these differences are not large, and can derive from the combination of many factors: electron-withdrawing effect of three chlorides compared to two chlorides, change in the molecule geometry from tetrahedral to trigonal planar, and finally solvent effect (adducts were measured as solutions in deuterated solvents, and ionic liquids - neat).

Table 3-2: ^1H NMR (400 MHz, DMSO) chemical shifts recorded for borenium chlorometallate ionic liquids complexes.

L	$[\text{BCl}_3\text{L}]$	L- $\text{BCl}_3\text{-AlCl}_3$	L- $\text{BCl}_3\text{-2AlCl}_3$	L- $\text{BCl}_3\text{-GaCl}_3$	L- $\text{BCl}_3\text{-2GaCl}_3$	Assignment
4-pic	2.60(s)	1.98(s)	2.00(s)	1.31(s)	1.55(s)	Ar- CH_3
	7.67(d)	7.17(d)	7.21(d)	6.50(s)	6.77(d)	-CH-C-CH-
	9.10(d)	8.33(d)	8.31(d)	7.64(s)	7.86(d)	-CH-N-CH-
mim	3.92(s)		2.97(s)		2.60(s)	Ar- CH_3
	7.09(s)		6.43(t)		6.06(s)	CH=CH-N
	7.62(s)	-	6.75(t)	-	6.37(s)	CH=CH-N
	8.40(s)		7.84(s)		7.47(s)	N-CH-N
dma	2.79 (s)		4.24(s)*			$\text{CH}_3\text{-CO}$
	3.32(s)	-	4.31(s)*	-	4.24(s)*	-N- CH_3
	3.41(s)					$\text{CH}_3\text{-N-CO}$
P₈₈₈O	0.80(m)					
	1.14 (m)	0.36(m)	0.22(m)	0.64(m)	0.56(m)	- CH_3
	1.70(m)	2.10(m)	1.67(m)	1.75(m)	1.67(m)	- CH_2 -
P₈₈₈	0.882(m)		0.20(m)	0.40(m)	0.05(m)	
	1.13(m)	0.85(m)	0.66(m)	0.75(m)	0.93(m)	- CH_3
	1.70(m)	2.10(m)	0.75(m)	1.18(m)	1.33(s)	- CH_2 -
			1.32 (m)			P- CH_2 -

Abbreviations: s = singlet, d = doublet, t = triplet, q = quartet, m = multiplet, * - no obvious assignment

^1H NMR spectra for the dma- $\text{BCl}_3\text{-2MCl}_3$ systems were very different, with sharp deshielded signals (Table 3-2), that were however difficult to assign, accompanied by broad upfield features which appear to originate from residual solids in the NMR tube (Figure 3-2). It could be speculated that the ligand has decomposed, but the corresponding ^{13}C NMR spectra (Table 3-3) featured signals that corresponded perfectly to dma ligands, therefore this hypothesis was not considered; rather three methyl groups must have very close chemical shifts in ^1H NMR spectroscopy. Nevertheless, it was evident that the speciation of liquids from the dma- $\text{BCl}_3\text{-2MCl}_3$ systems differed from the other samples.

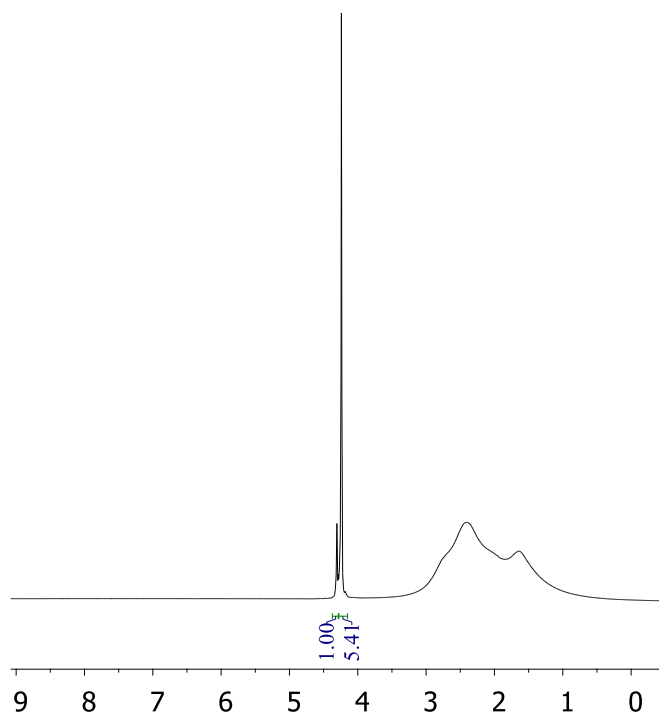


Figure 3-2: ^1H NMR (400 MHz, neat liquid with DMSO-d_6 lock) of $\text{dma-BCl}_3\text{-2MCl}_3$ borenium ionic liquids.

In general, ^{13}C NMR spectra contained in all cases the number of signals corresponding to the respective ligands, and at chemical shifts that were slightly shifted from the $[\text{BCl}_3\text{L}]$ adducts. Interestingly, irrespective of metal halide, ^{13}C NMR spectra of ionic liquids with *N*-donors have signals slightly deshielded with respect to the tetracoordinate adducts, and all other ionic liquids have slightly shielded signals. Furthermore, signals from $\text{dma-BCl}_3\text{-2MCl}_3$ systems had worse signal-to-noise ratio than those from other ionic liquids, which may indicate lower ligand concentration in the liquid.

There was no evidence for ligands remaining in two different environments.

Table 3-3: ^{13}C NMR (101 MHz, DMSO) chemical shifts recorded for borenium chlorometallate ionic liquids complexes.

L	[BCl ₃ L]	L-BCl ₃ -AlCl ₃	L-BCl ₃ -2AlCl ₃	L-BCl ₃ -GaCl ₃	L-BCl ₃ -2GaCl ₃	Assignment
4-pic	157.55	166.68	170.56	165.62	169.80	-CH-N-CH-
	144.01	143.98	144.63	143.57	144.17	-CH-C-CH-
	126.70	128.03	128.87	127.74	128.47	-CH-C-CH-
	21.93	22.65	23.42	22.48	23.17	Ar-CH ₃
mim	136.39		139.98		139.32	-N-CH-N-
	124.82	-	125.66	-	125.09	-CH=CH-N-
	122.24		124.22		123.63	-CH=CH-N
	35.94		37.07		36.61	Ar-CH ₃
dma	174.37		171.44		171.44	CH ₃ -CO-
	40.21	-	40.03	-	40.03	CH ₃ -N-CH ₃
	39.53		38.32		38.32	CH ₃ -N-CH ₃
	18.47		20.45		20.45	CH ₃ -CO-
P₈₈₈O	31.65	31.10	30.74	30.49	30.25	C ₂ H ₅ -CH ₂ -(CH ₂) ₅ -PO
	30.47	29.83	28.82	28.35	28.25	C ₅ H ₁₁ -CH ₂ -(CH ₂) ₂ -PO
	28.84	28.14	29.34	27.45	27.62	CH ₃ -CH ₂ -(CH ₂) ₃ -PO
	24.76	24.83	25.37	23.13	22.57	C ₇ H ₁₅ -CH ₂ -PO
	24.15	23.39	23.20	22.60	20.75	CH ₃ -CH ₂ -(CH ₂) ₄ -PO
	22.54	21.99	21.86	21.81	17.79	CH ₃ -CH ₂ -(CH ₂) ₆ -PO
	21.05	20.17	18.06	20.61	12.90	C ₆ H ₁₃ -CH ₂ -CH ₂ -PO
	14.00	13.40	13.34	12.94	10.14	CH ₃ -(CH ₂) ₇ -PO
P₈₈₈	31.73	30.96	30.96	30.53	30.35	C ₂ H ₅ -CH ₂ -(CH ₂) ₅ -P
	31.30	30.21	30.38	29.85	29.58	C ₅ H ₁₁ -CH ₂ -(CH ₂) ₂ -P
	28.92	28.06	28.13	27.64	27.57	CH ₃ -CH ₂ -(CH ₂) ₃ -P
	22.60	21.90	27.86	21.44	27.32	CH ₃ -CH ₂ -(CH ₂) ₄ -P
	22.36	21.57	21.74	21.07	26.50	C ₆ H ₁₃ -CH ₂ -CH ₂ -P
	18.59	17.58	18.45	17.88	21.29	C ₇ H ₁₅ -CH ₂ -P
	18.22	16.55	17.54	17.09	20.71	CH ₃ -CH ₂ -(CH ₂) ₆ -P
	14.06	13.41	13.42	12.97	12.95	CH ₃ -(CH ₂) ₇ -P

Abbreviations: s = singlet, d = doublet, t = triplet, q = quartet, m = multiplet

3.2.2.1.2 ^{11}B NMR spectroscopy

^{11}B NMR spectroscopy was used to probe the coordination number of boron, *i.e.* to confirm the presence of tricoordinate borenium cation. Generally, four-coordinate boron compounds of a general formula [BCl₃L] yield sharp ^{11}B NMR signals around 0-10 ppm, whereas tricoordinate cations, [BCl₂L]⁺, are reported to give signals at 30-50 ppm.^{23,8} The more complete the abstraction of the halide from [BCl₃L], the larger the upfield change in the chemical shift distinguishing these two coordinate sites. Results of the ^{11}B NMR spectroscopic study are summarised in Table 3-4.

Table 3-4: ^{11}B NMR spectra (128.37 MHz, 27 °C, neat liquid with DMSO- d_6 lock) parameters for borenium ionic liquids of a general formula $\text{L-BCl}_3\text{-}n\text{MCl}_3$, where $M = \text{Al}$ or Ga .

L	L-BCl ₃ -AlCl ₃	L-BCl ₃ -2AlCl ₃	L-BCl ₃ -GaCl ₃	L-BCl ₃ -2GaCl ₃
4-pic	45.23	45.66	45.56	43.82
	33.34	-3.48	32.06	-1.66
	5.03		7.41	
mim	-	46.76	-	40.87
		-0.95		2.13
dma	-	46.63	-	46.17
		34.32		34.09
		-0.36		2.28
				-0.36
P₈₈₈O	45.92	45.83	46.56	46.02
		31.09	32.06	30.08
				15.24
P₈₈₈	46.61	45.70	46.27	46.02
	20.09	37.69	14.14	30.08
	-5.70	-5.36	3.42	15.24
			2.01	

The ^{11}B NMR spectra indicated that the generation of the borenium cations, $[\text{BCl}_2\text{L}]^+$ occurred, but to various extent for different systems. ^{11}B NMR spectra for ionic liquids with N-donors (see Figure 3-3 for L-BCl₃-2AlCl₃ and Figure 3-4 for L-BCl₃-2GaCl₃) featured a broad main feature at 43 ± 3 ppm, corresponding to the $[\text{BCl}_2\text{L}]^+$ cation, and in some cases a shoulder at 45 ± 1 ppm, corresponding to BCl₃. Signals at tetracoordinate region were visible, but their integration was negligible compared to signals in tricoordinate region.

Systems based on trioctylphosphine featured signal at 36 ± 1 ppm, which is consistent with a tricoordinate cation with a P-donor (upfield shift with respect to N-donors), with a sharp peak *ca.* 45.5 ppm, originating from BCl₃. Spectra recorded for trioctylphosphine oxide systems, irrespectively of molar ratio of metal halide, were dominated by a sharp signal from BCl₃ around 45.5 ppm, with only a trace of a signal at 31 ppm for P₈₈₈O-BCl₃- n AlCl₃ (Figure 3-3 and Figure 3-5) and two low intensity signals (30 and 13 ppm) for P₈₈₈O-BCl₃- n GaCl₃ (Figure 3-4 and Figure 3-6). These likely correspond to $[\text{BCl}_2(\text{P}_{888}\text{O})]^+$ and $[\text{BCl}_3(\text{P}_{888}\text{O})]$ complexes. The presence of BCl₃ in the liquid, with no significant amount of tetracoordinate boron species, indicates that the ligand was abstracted from boron by the metal halide. This found confirmation in ^{27}Al NMR spectroscopy (see below: Section 3.2.2.1.3).

For both dma- BCl_3 - 2MCl_3 systems, the main feature was a sharp peak at -0.30 ppm corresponding to tetracoordinate boron species, but not to the original chemical shift of $[\text{BCl}_3(\text{dma})]$ at 7.20 ppm, therefore most likely $[\text{BCl}_4]^-$. Two broad, low intensity signals were also detected: at 34 ppm, presumably corresponding to the formation of tricoordinate $[\text{BCl}_2(\text{dma})]^+$, and at 46 ppm, which indicates the presence of BCl_3 . This speciation was different from that of other liquids; in addition to borocation and boron trichloride, a significant amount of boroanion was detected. It is important to note that whilst $[\text{BCl}_2(\text{dma})]^+$ signals were observed for dma- BCl_3 - 2MCl_3 systems these were with very low intensity compared to the other ionic liquids. Stoichiometry of the liquid appears to contain less organic ligand (judging by lower quality of ^1H and ^{13}C NMR spectra).

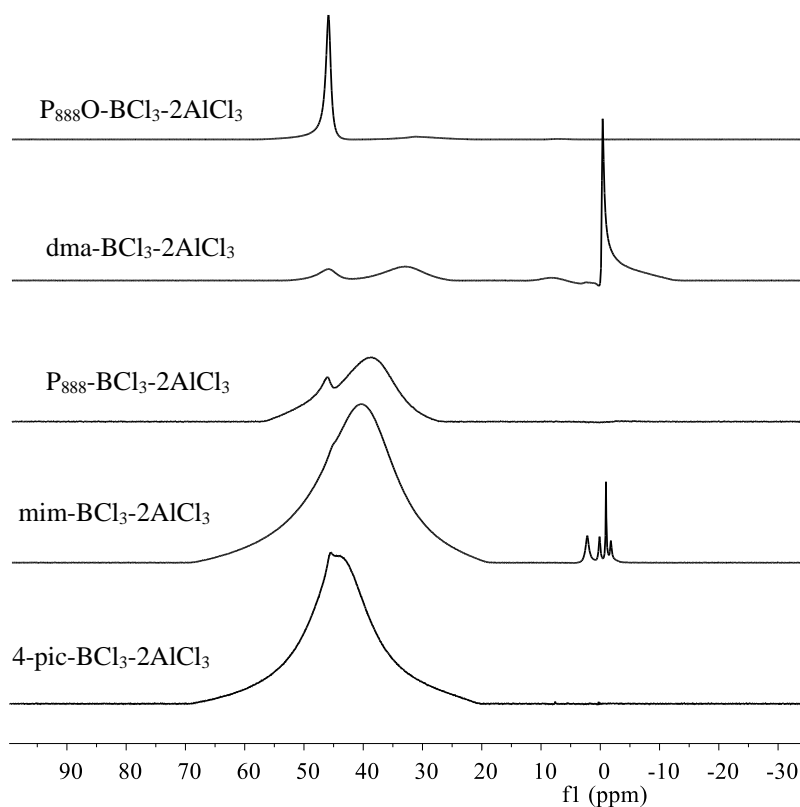


Figure 3-3: ^{11}B NMR spectra (128.37 MHz, 27°C , neat liquid with $\text{DMSO}-d_6$ lock) of borenium ionic liquids of a general formula $L\text{-BCl}_3\text{-}2\text{AlCl}_3$.

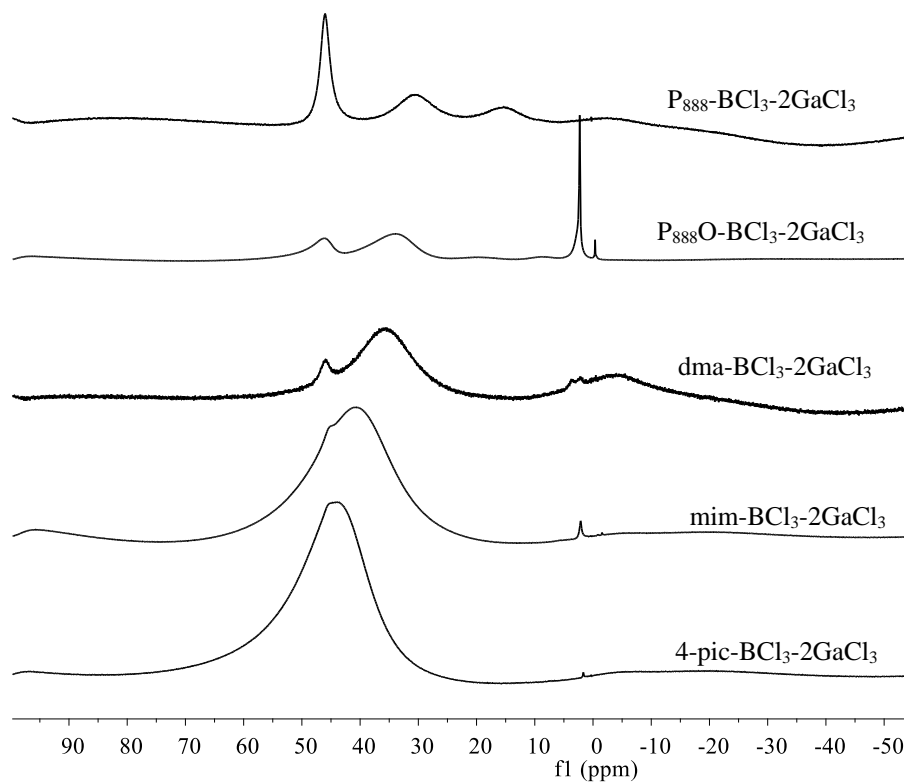


Figure 3-4: ^{11}B NMR spectra (128.37 MHz, 27 °C, neat liquid with DMSO- d_6 lock) of borenium ionic liquids of a general formula $L\text{-BCl}_3\text{-2GaCl}_3$.

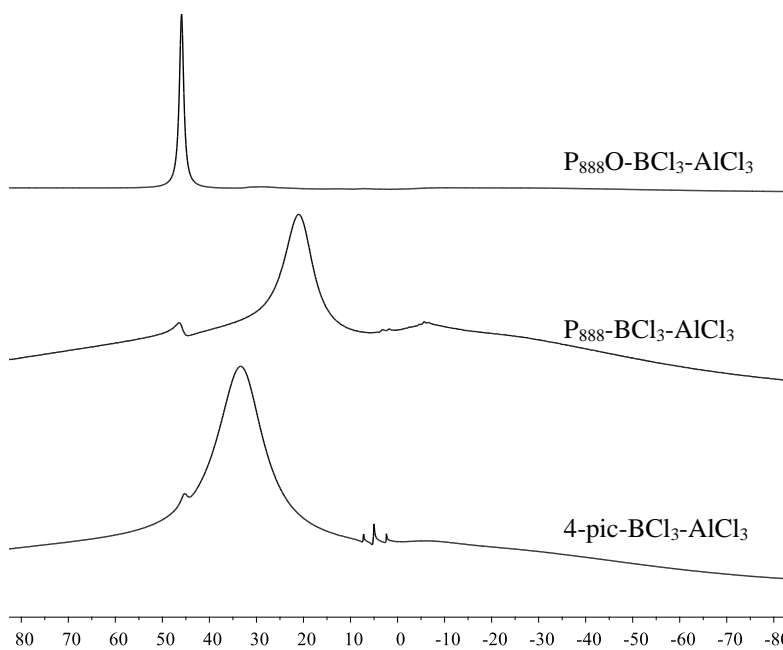


Figure 3-5: ^{11}B NMR spectra (128.37 MHz, 27 °C, neat liquid with DMSO- d_6 lock) of borenium ionic liquids of a general formula $L\text{-BCl}_3\text{-AlCl}_3$.

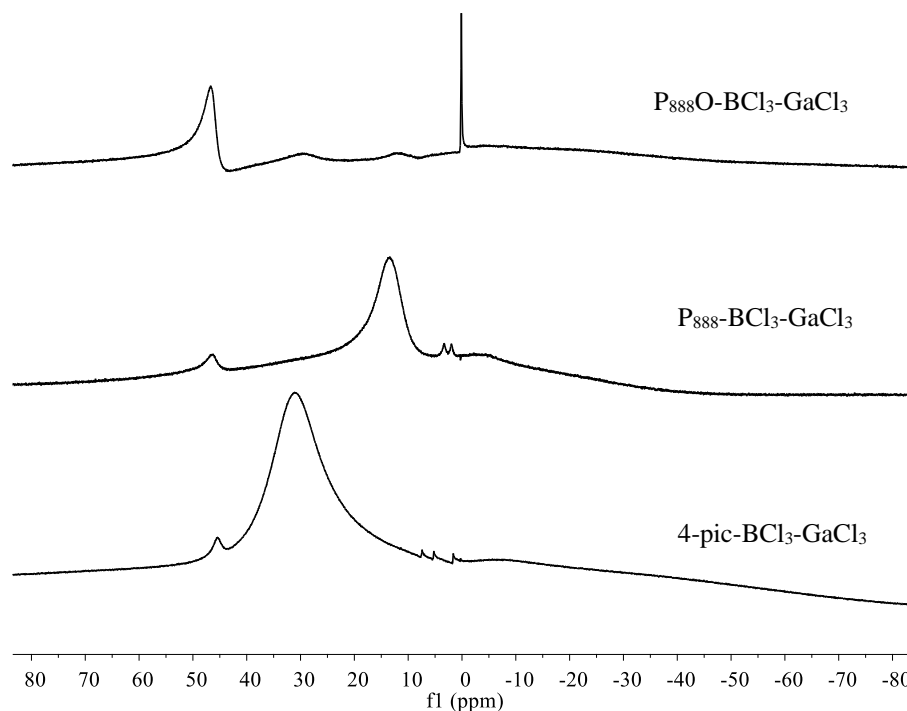
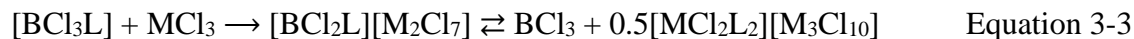


Figure 3-6: ^{11}B NMR spectra (128.37 MHz, 27 °C, neat liquid with $\text{DMSO-}d_6$ lock) of borenium ionic liquids of a general formula $\text{L-BCl}_3\text{-GaCl}_3$.

In conclusion, in reactions of $[\text{BCl}_3\text{L}]$ complexes - except for $[\text{BCl}_3(\text{dma})]$ - with MCl_3 ($\text{M} = \text{Al}$ or Ga) resulted in the formation of ionic liquids through halide abstraction, followed by (or paralleled by) ligand scrambling, leading to the generation of BCl_3 and liquid coordination complexes reported by our group,¹⁷³ of a general formula exemplified in Equation 3-3.



The extent of the ligand transfer depended on the affinity of the donor atom to both boron and metal; *N*-donors formed relatively stable ILs, similarly P_{888} , but with a bit more BCl_3 formation, whereas P_{888}O generated largely coordination complexes with Group 13 metals: particularly aluminium, which is easily explained considering its oxophilicity. This same phenomenon of ligand exchange between boron and chloroaluminate anions has been reported for solutions of such compounds in molecular solvents.¹⁷⁴

The $\text{dma-BCl}_3\text{-}n\text{MCl}_3$ systems do not yield homogenous ionic liquids, and the liquid part of the biphasic system contains $[\text{BCl}_4]^-$, and relatively little of dma. This points to the fact that

most dma transferred to aluminium and precipitated out as a coordination complex, leaving boron-rich liquid behind.

Considering borenium ionic liquids of a general formula 4pic-BCl₃-*n*MCl₃, the influence of metal (M) and stoichiometry of the metal chloride (*n*) can be derived by analysing Figure 3-7. For *n* = 1, irrespective of the metal used, signals are more shielded, suggesting less complete halide abstraction/strong interaction between [BCl₂L]⁺ and [MCl₄]⁻. For *n* = 2 or 3, all signals are strongly deshielded (*ca.* 46 ppm), again irrespective of the metal used, indicating relatively ‘free’ borenium cation; that is, weak interaction with chlorometallate anion. The same observation was made very early on by Ryschkiewicz and Wiggins,²¹ who studied aluminium chloride as halide abstracting agent for generating borenium cations in solution.

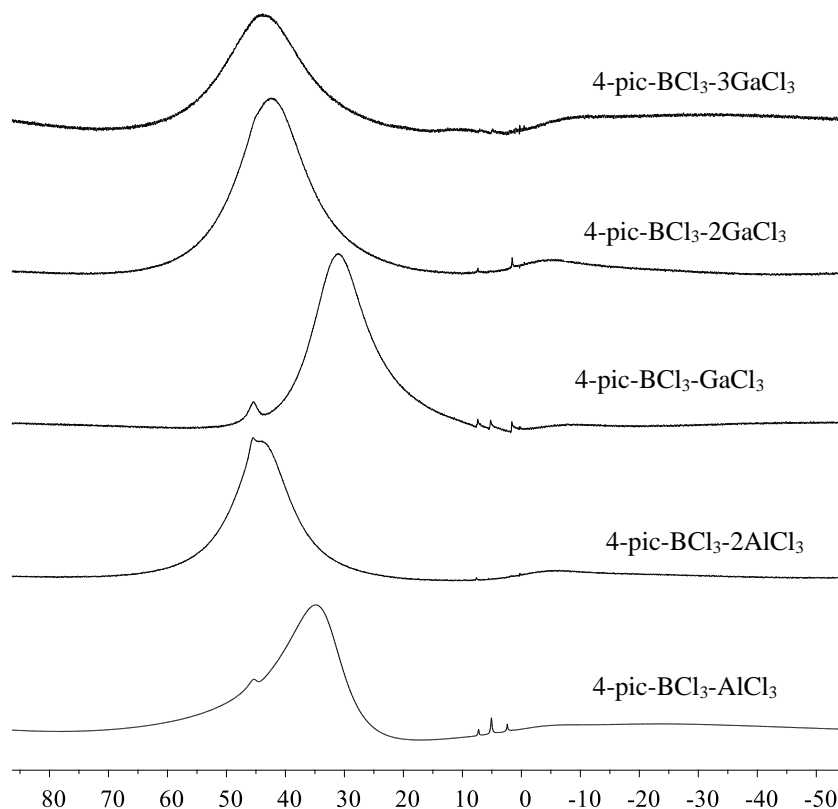


Figure 3-7: ¹¹B NMR spectra (128.37 MHz, 27 °C, neat liquid with DMSO-*d*₆ lock) of borenium ionic liquids of a general formula 4pic-BCl₃-*n*MCl₃, where M = Al or Ga and *n* = 1, 2 or 3.

3.2.2.1.3 ²⁷Al NMR spectroscopy

²⁷Al NMR spectra were recorded for all borenium chloroaluminate ionic liquids. ²⁷Al NMR studies of [AlCl₄]⁻ and [Al₂Cl₇]⁻ line widths in ionic liquids have revealed that the higher symmetry of the tetrahedral [AlCl₄]⁻ minimises the line broadening resulting from the quadrupole moment of the ²⁷Al nuclei,¹⁷⁵ while [Al₂Cl₇]⁻, being a larger anion of lower symmetry, gives signal broadened due to quadrupole relaxation.^{176,177} Chemical shift for both [AlCl₄]⁻ and [Al₂Cl₇]⁻ was expected around 103 ppm, with signal breadth dependent on the ratio of the two anions.

The actual ²⁷Al NMR spectra of borenium chloroaluminate ionic liquids showed broad signals between 65 and 115 ppm (Figure 3-8 and Figure 3-9). The ²⁷Al NMR for all L-BCl₃-2AlCl₃ systems based on *N*-donors featured the main signal at around *ca.* 106±1 ppm, corresponding to chloroaluminate complex (Table 3-5). This chemical shift is extraordinarily deshielded compared to the literature, either due to very strong interaction with the cation, or due to the contribution of [AlCl₃(*N*-donor)] coordination complex to this signal (or both). In all cases, a shoulder at 65±1 ppm was found, which is known to arise from the probe itself.

Table 3-5: Chemical shifts of ²⁷Al NMR signals (104.28 MHz, 25 °C, neat liquid with DMSO-*d*₆ lock) recorded for ionic liquids of a general formula L-BCl₃-*n*AlCl₃ (*n* = 1 or 2)

L	L-BCl ₃ -AlCl ₃	L-BCl ₃ -2AlCl ₃
4-pic	74.07(sh)	74.55(sh)
	104.58	107.49
mim	-	75.46(sh)
		106.6
dma	-	2.72
		112.48
		73.30
		59.32(sh)
P₈₈₈O	77.41	68.70
	92.30	
	105.04	
P₈₈₈	64.50	68.24
	114.45	114.06

²⁷Al NMR spectrum for P₈₈₈-BCl₃-2AlCl₃ contains a broad signal at 114 ppm (in addition to probe signal at 68 ppm), suggesting a large level of coordination of the ligand to the aluminium centre, which is in agreement with strong BCl₃ signal in the corresponding ¹¹B NMR spectrum. It is to be expected, since ‘softer’ *P*-donor will have higher affinity to the Al centre

than to B centre, compared to *N*-donors.^{173,4} Spectrum of $\text{P}_{888}\text{O-BCl}_3\text{-2AlCl}_3$ does not feature any signals corresponding to chloroaluminate anions, only a broad feature that coincides with the probe single at 68.7 ppm, suggesting the presence of $[\text{AlCl}_2(\text{P}_{888}\text{O})_2]^+$ (that appear at about the same chemical shift region) and possibly other coordination complexes of aluminium. Again, this is pointing to near-complete ligand transfer, in agreement with the corresponding ^{11}B NMR spectrum (Figure 3-7), where BCl_3 appears to be the only boron-containing species. Evidently, for this *O*-donor, a liquid coordination complex must have been formed, with BCl_3 dissolved in it. Finally, the dma-based system (neat liquid) gave a spectrum with three signals (excluding probe), but of very weak intensity (spectra were normalised for this Figure). It appeared as if most of aluminium reacted with the ligand and precipitated in a form of some coordination complex.

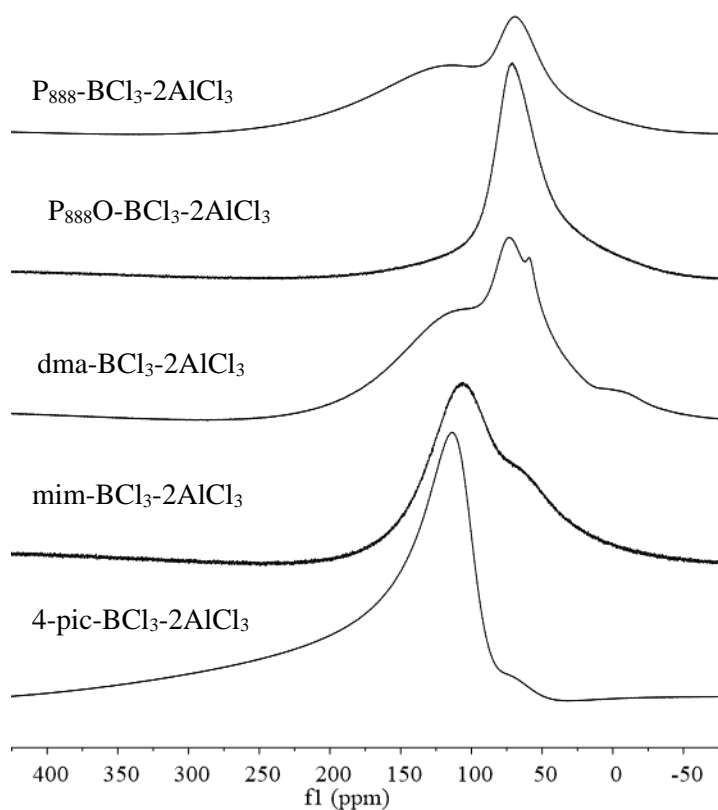


Figure 3-8: ^{27}Al NMR spectra (104.28 MHz, 25 °C, neat liquid with DMSO-d_6 lock) of borenium ionic liquids of a general formula $L\text{-BCl}_3\text{-2AlCl}_3$.

In $L\text{-BCl}_3\text{-AlCl}_3$ systems, no signals were sharp enough to indicate the presence of tetrahedral $[\text{AlCl}_4]^-$ as the only species. The 4-pic- $\text{BCl}_3\text{-AlCl}_3$ system was similar to 4-pic- $\text{BCl}_3\text{-2AlCl}_3$, with a chloroaluminate anion signal at 106 ppm and a shoulder at *ca.* 65 ppm. Again, broad signal is likely arising from partial contribution of $[\text{AlCl}_3(\text{N-donor})]$ and/or from cation-anion interactions that distort anion's symmetry.

The ^{27}Al NMR spectrum of $\text{P}_{888}\text{O-BCl}_3\text{-AlCl}_3$ sample had striking resemblance to analogous spectrum of liquid coordination complex based on trioctylphosphine oxide and aluminium(III) chloride, with three signals at 105.3, 92.3, 77.4 ppm, suggesting the presence of equilibrated cationic, neutral and anionic complexes of AlCl_3 and P_{888}O .¹⁷³ The complete transfer of *O*-donor to aluminium must have occurred, considering high oxophilicity of aluminium. Also the ^{27}Al NMR spectrum of the $\text{P}_{888}\text{-BCl}_3\text{-AlCl}_3$ system showed broad signals both at 64 and 114 ppm, consistent with observations made for the *N*-donors.^{173,178}

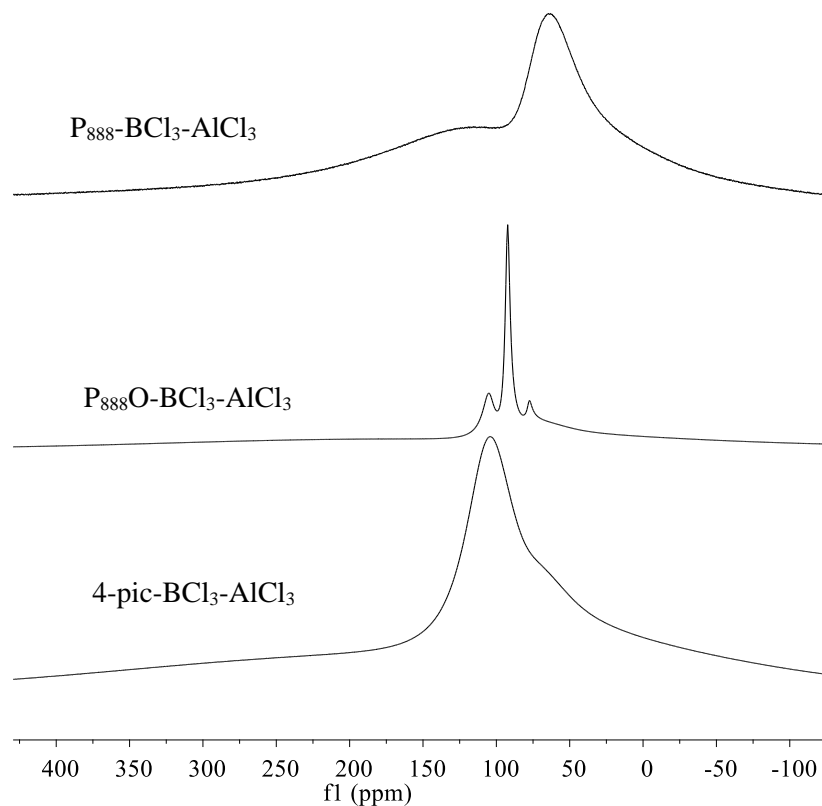


Figure 3-9: ^{27}Al NMR spectra (104.28 MHz, 25 °C, neat liquid with DMSO-d_6 lock) of borenium ionic liquids of a general formula $L\text{-BCl}_3\text{-AlCl}_3$.

3.2.2.1.4 ^{71}Ga NMR spectroscopy

Due to large quadrupole effect, ^{71}Ga NMR spectra were inconclusive, with signals typically indistinguishable from the baseline. Considering significant broadening observed even for expectedly sharp $[\text{AlCl}_4]^-$ anions, and reported broadness of signals in ^{71}Ga NMR spectra in ionic liquids, even for tetrahedral $[\text{GaCl}_4]^-$,⁴ this is unsurprising.

3.2.2.2 IR spectroscopy

Infrared spectra for neat ligands, complexes and their corresponding borenium ionic liquids were recorded (

Table 3-6 and Table 3-7). FT-IR spectrometer with ATR attachment was used, and samples needed to be momentarily exposed to atmospheric moisture. However, a simple but effective procedure developed procedure (see Experimental, 3.1.2.2 for detailed testing procedure) allowed to record spectra of ionic liquids without any traces of hydrolysis. Namely, there were no traces of O-H stretching frequency (see discussion in Section 2.2.4),^{155,179} in either of recorded spectra.

Again, all results point to ligands being coordinated to the boron/metal centre without decomposition. In general the *N*-donor aromatic compounds (Table 3-6) exhibited higher vibrational frequencies for C-H stretching frequencies than saturated hydrocarbon chains in P_{888} and P_{888}O , which is in agreement with the literature.^{155,179,180} All C-H stretching absorptions for the P_{888} and P_{888}O - donor compounds occurred below 3000 cm^{-1} whilst the aromatic *N*-donor complexes and ILs exhibited weak-to-moderate bands between 3150 and 3000 cm^{-1} which were indicative of unsaturated C=C-H of aromatic rings.^{180,181} It was also observed that the asymmetric =C-H stretch of the methylene groups in the complexes and ILs of 4-pic and mim at the overlapped region of the spectrum, mainly between 1050 and 908 cm^{-1} .^{180,181} With the *N*-donor aromatic compounds, C=C-C stretching and bending vibrations are highly characteristic and were pinpointed between 1638 - 1516 cm^{-1} with bands overlapped with C=N stretching and bending vibrations. Bands between 1350 - 1158 cm^{-1} were assigned to the C-N stretch in 4-pic and mim.^{180,181}

Comparing vibrations for uncoordinated ligands, and then ligands in tetracoordinate and tricoordinate boron compounds, there are no spectacular changes in vibrational frequencies. The

most affected is - expectedly - the C-N vibration, which is red-shifted for $[\text{BCl}_3(4\text{-pic})]$ compared to free 4-pic, and further red-shifted for borenium ionic liquids, which indicates bond elongation in coordinated forms. Interestingly, the trend is reversed for C-N vibrations in mim, but the situation is more complex due to two nitrogens present.

Table 3-6: FT-IR frequencies (cm^{-1}) for ligands (L), corresponding tetracoordinate boron complexes, $[\text{BCl}_3\text{L}]$, and corresponding borenium ionic liquids of a general formula $\text{L-BCl}_3\text{-nMCl}_3$, where $M = \text{Al}$ or Ga .

Compound	Stretching frequency / cm^{-1}					
	CH_3 , CH_2 , CH	$\text{C}=\text{C}$ $\text{C}=\text{N}$	CH_3 CH_2	$\text{C}-\text{N}$	$=\text{CH}_2$, $=\text{C}-\text{H}$	$\text{C}-\text{H}$
4-pic	2889(s) 3068(s)	1604(s)	1412(s)	1223(m)	995(s)	796(m)
$[\text{BCl}_3(4\text{-pic})]$	3095(s) 3120(s)	1634(s)	1445(s)	1237(m)	1090(s)	780(m)
4-pic- $\text{BCl}_3\text{-AlCl}_3$	3070(s) 3130(s)	1637(s)	1463	1162(m)	900(s) 1025(s)	738(m)
4-pic- $\text{BCl}_3\text{-2AlCl}_3$	3167(s)	1553(s)	1403	1181(m)	1004	636(m) 832(m)
4-pic- $\text{BCl}_3\text{-GaCl}_3$	3068(s) 3129(s)	1637(s)	1462	1160(m)	908(s) 1022(s)	738(m) 820(m)
4-pic- $\text{BCl}_3\text{-2GaCl}_3$	3071(s) 3129(s)	1637(s)	1463	1159(m)	908(s) 1024(s)	703(m) 1024(m)
mim	2953(s) 3106(s)	1516(s)	1420	1284(m) 1230(m)	907 1108	662(m) 907(m)
$[\text{BCl}_3(\text{mim})]$	3143(s) 3159(s)	1568(s) 1543(s)	1425	1251(m)	1132	727(m) 852(m)
mim- $\text{BCl}_3\text{-2AlCl}_3$	3147(s) 3168(s)	1597(s) 1534(s)	1404	1311(m)	1005	637(m) 833(m)
mim- $\text{BCl}_3\text{-2GaCl}_3$	3148(s) 3167(s)	1596(s) 1533(s)	1404	1310(m)	1008 1181	638(m) 832(m)

The C-N stretch in dma compounds, dma- $\text{BCl}_3\text{-2GaCl}_3$ and dma- $\text{BCl}_3\text{-2AlCl}_3$ was assigned to bands between $1360\text{-}1210\text{ cm}^{-1}$, whereas the strong feature at 1634 cm^{-1} is the C=O band.^{180,181} Upon coordination, the band was blue-shifted by 10 cm^{-1} .

The P=O asymmetric stretching band (Table 3-7) exhibited strong bands at $1015\text{-}1320\text{ cm}^{-1}$.¹⁸² Peak at 1154 cm^{-1} for neat P_{888}O was replaced by red-shifted 1067 cm^{-1} band for $[\text{BCl}_3(\text{P}_{888}\text{O})]$, suggesting bond elongation upon coordination to boron. Further shift to $1103\text{-}1109\text{ cm}^{-1}$ occurred in chloroaluminate liquids - this was likely related to P_{888}O coordination to aluminium. Likewise, very strong shift in opposite direction (Table 3-7), indicating P=O bond shortening, occurred in chlorogallate ionic liquids, suggesting that P_{888}O was bound to the

gallium centre. Seeing as gallium is far less oxophilic than aluminium, the P=O bond would be shorter and O→M bond would be longer for gallium, compared to aluminium.

Table 3-7: FT-IR frequencies (cm^{-1}) corresponding to the synthesised borenium chloroaluminate systems with O-, and P donors: $L\text{-BCl}_3\text{-}n\text{MCl}_3$, where $M = \text{Al}$ or Ga .

Compound	Stretching frequency / cm^{-1}				
	CH ₃ , CH ₂ , CH/(P)	CH ₂ CH/(P)	C-N	P=O(s)	C=O
dma	1498(s) 889(m)	-	1392(m)	-	1635(s)
[BCl₃(dma)]	1395(s) 998(m)	-	1355(m)	-	1646(s)
dma-BCl₃-2AlCl₃	1407(s) 658(m) 998(m)	-	1311(m) 1254(m)	-	1643(s)
dma-BCl₃-2GaCl₃	997(m)	-	1306(m)		1684(s)
P₈₈₈O	2951(s) 2918(s) 2850(s)	1465(s) 720(m)	-	1145(s)	
[BCl₃(P₈₈₈O)]	2957(s) 2929(s) 2856(s)	1464(s) 680(m)	-	1067(s)	
P₈₈₈O-BCl₃-AlCl₃	2956(s) 2928(s) 2856(s)	1461(s) 723(w)	-	1103(s)	
P₈₈₈O-BCl₃-2AlCl₃	2956(s) 2927(s) 2857(s)	1464(w) 940(s)		1109(s)	
P₈₈₈O-BCl₃-GaCl₃	2957(s) 2929(s) 285(s)7	1458(w) 971(s)		1255(s)	
P₈₈₈O-BCl₃-2GaCl₃	2940(s) 2030(s) 2860(s)	1458(s) 719(w)	-	1312(s)	-
P₈₈₈	2954(s) 2922(s) 2853(s)	1459(m) 720(s)	-	-	-
[BCl₃(P₈₈₈)]	2951(s) 2919(s) 2852(s)	1463(m) 694(s)	-	-	-
P₈₈₈-BCl₃-AlCl₃	2956(s) 2927(s) 2855(s)	1464(w) 708(s)	-	-	-
P₈₈₈-BCl₃-2AlCl₃	2955 2927 2857	1462(w) 707(s)	-	-	-
P₈₈₈-BCl₃-GaCl₃	2958 2928 2857	1458(w) 717(s)	-	-	-
P₈₈₈-BCl₃-2GaCl₃	2942 2925 2861	1456(s) 717(w)	-	-	-

3.2.2.3 Differential scanning calorimetry

It was attempted to record DSC scans for borenium ionic liquids. However, due to the corrosiveness of the synthesised ILs, no data could be recorded: aluminium pans and even aluminium pans with thin layer of aluminium oxide were corroded within minutes. The same has been found previously in our group for chloroaluminate ionic liquids. Stainless steel pans could have been used, but in the absence of equipment to seal stainless steel pans, this route had to be abandoned.

3.2.2.4 Density measurements

Density of borenium ionic liquids was measured using vibrating tube densimeter, which is the most common methodology for measuring viscosity of ionic liquids. It allows for measurement with very limited exposure to moisture, and does not require contact with metal elements (corrosion), therefore was ideal for this study. Densities were studied at atmospheric pressure, within the temperature range between 293 to 343 K. All ionic liquids used in the density determinations were prepared at least 24 h prior measurements and stored in sealed vials in the glovebox. Prior to measurement they were transferred to glass gas-tight syringes to prevent contact with moisture, and injected into the densimeter.

It is important to state that, due to the sensitive nature of the borenium ionic liquids, the water content of ionic liquids could not be measured by coulometric Karl Fischer titration. Furthermore, high acidity of these ionic liquids forbid them from being measured. It is well established in literature that the presence of impurities such as water can alter to a great extent the physico-chemical properties of ionic liquids (although it must be emphasised that viscosity is much more affected than density). However, it is safe to say that the borenium ionic liquids were very dried, as all syntheses and storage were under anhydrous conditions, and no signs of hydrolysis were detected through spectroscopic studies.

Density data, measured as a function of temperature, are listed in Table 3-8. During density measurements performed using vibrating tube approach, it is possible to produce forces that have a damping effect on the oscillation or rotation of the moving element.¹⁸³ Therefore, for accurate measurements of highly viscous fluids, it is advisable to calculate viscosity-corrected

densities.¹⁸³ This was taken into account with this work. Both density and viscosity measurements of each ionic liquid were collected within the same day.

N.B.: it was difficult to measure densities for $\text{P}_{888}\text{O-BCl}_3\text{-2AlCl}_3$ at the elevated temperatures: as the temperature increased, it was observed that bubbles began to form in the densimeter tube, which led to error in the reading. This was repeated several times with different batches, and always the same result, therefore only densities for 293 and 303 K are reported. The same reaction was seen for it with monomeric analogue: $\text{P}_{888}\text{O-BCl}_3\text{-AlCl}_3$. Other ILs with monomeric anions (*i.e.* $\text{L-BCl}_3\text{-MCl}_3$) were semi-solids at ambient temperature which made measurement impossible.

Table 3-8: Experimental values for viscosity-corrected densities, ρ , of the studied borenium ionic liquids for temperatures between 293 to 343 K and at atmospheric pressure.

L-BCl₃-2MCl₃	$\rho / \text{g}\cdot\text{cm}^3$						
	293.15	298.15	303.15	313.15	323.15	333.15	343.15
	/ K	/ K	/ K	/ K	/ K	/ K	/ K
4-pic-BCl₃-2AlCl₃	1.5081	1.5025	1.4976	1.4875	1.4776	1.4674	1.4558
mim-BCl₃-2AlCl₃	1.5315	1.5249	1.5178	1.5017	1.4856	1.4695	-
dma-BCl₃-2AlCl₃	1.4688	1.4625	1.456	1.4421	1.4321	1.4221	-
P₈₈₈O-BCl₃-2AlCl₃	1.1019	1.1009	1.0922	-	-	-	-
P₈₈₈-BCl₃-2AlCl₃	1.0927	1.0901	1.0848	1.0762	1.0706	1.065	1.0600
4-pic-BCl₃-2GaCl₃	1.7942	1.7883	1.7826	1.7709	1.7591	1.7477	1.7352
mim-BCl₃-2GaCl₃	1.8387	1.833	1.8265	1.8035	1.7795	1.7565	1.7335
dma-BCl₃-2GaCl₃	1.8183	1.8122	1.806	1.7926	1.7765	1.7527	1.736
P₈₈₈O-BCl₃-2GaCl₃	1.2862	1.2798	1.2727	1.2656	1.2586	1.2516	
P₈₈₈-BCl₃-2GaCl₃	1.2737	1.2693	1.2645	1.2548	1.2448	1.2348	1.2209

Ionic liquids have generally higher density values than water or typical organic solvents, with literature density values for ionic liquids at room temperature ranging from 1.0 to 1.6 g cm^{-3} at ambient conditions.^{70,160} Higher values are of course associated with metal-containing ionic liquids, whereas the increase of the alkyl chain lengths is associated with

decrease in density.^{184,183} In agreement with the literature, densities of borenium ionic liquids varied from 1.1 to 1.8 g cm⁻³ at 293 K.

As expected, densities of ionic liquids varied depending on the ligand; ionic liquids with P₈₈₈ and P₈₈₈O ligands (containing long alkyl chains) had lowest densities, whereas smaller ligands (*N*-donors) produced the dense ILs, due to high contribution of the chlorometallate anion. Furthermore, densities of ionic liquids were affected by the metal in the anion, with heavier gallium resulting in denser chlorogallate ionic liquids (up to 16 % when compared to chloroaluminate analogues with the same cation). The ionic liquid with the highest density, 1.84 g cm⁻³ at 293 K, was mim-BCl₃-2GaCl₃.

The experimental, viscosity-corrected density data reported in Table 3-8 were plotted as a function of the temperature, and fitted with linear Equation 3-4. Fitted data are shown in Figure 3-11 for L-BCl₃-2AlCl₃ and in Figure 3-11 for L-BCl₃-2GaCl₃.

$$\rho = a \cdot T + b$$

Equation 3-4

ρ - density (g·cm⁻³); T - temperature (K)

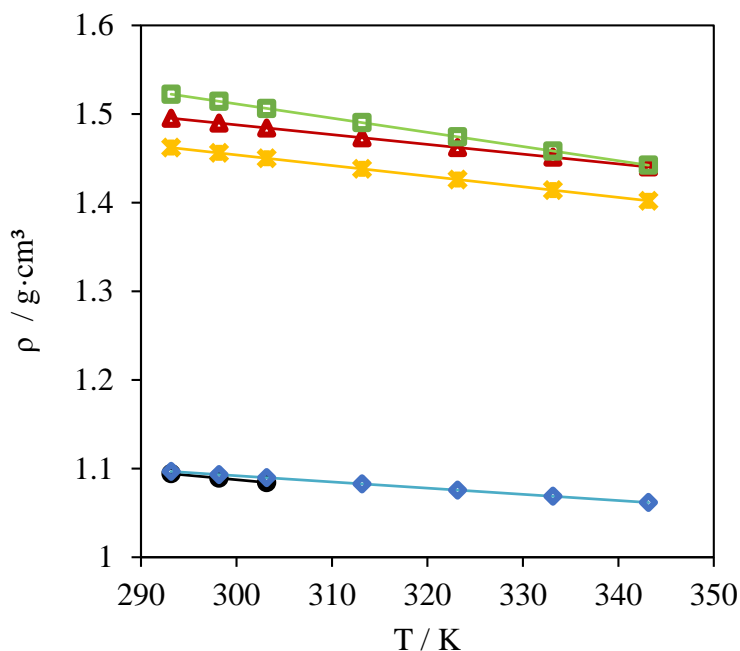


Figure 3-10: Corrected fitted densities, ρ , of the studied borenium ionic liquids, L-BCl₃-2AlCl₃ : \blacktriangledown BCl₃-4pic-2MCl₃, \square BCl₃-mim-2MCl₃, \ast BCl₃-dma-2MCl₃, \bullet BCl₃-P₈₈₈O-2MCl₃, \blacklozenge BCl₃-P₈₈₈-2MCl₃.

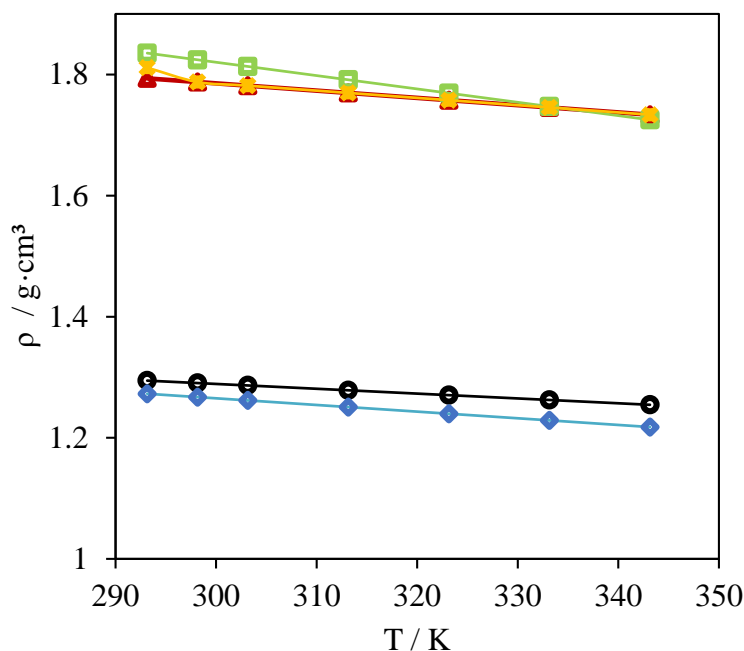


Figure 3-11: Corrected fitted densities, ρ , of the studied borenium ionic liquids: \blacktriangledown BCl_3 -4pic-2MCl₃, \square BCl_3 -mim-2MCl₃, \ast BCl_3 -dma-2MCl₃, \bullet BCl_3 -P₈₈₈O-2MCl₃, \blacklozenge BCl_3 -P₈₈₈-2MCl₃.

The fitting parameters a and b (Equation 3-4) and standard deviations for experimental data recorded for each ionic liquid, are reported in Table 3-9. The standard deviation was found to be below 0.05%, showing very good linear fit within the whole temperature range.

Table 3-9: Parameters a and b of the fitting of corrected experimental densities of borenium ionic liquids, along with the standard deviation of each fit between the temperatures of 293 K and 343 K at atmospheric pressure.

L-BCl ₃ -2MCl ₃	a	b	Dev (%)
4-pic-BCl ₃ -2AlCl ₃	-0.0011	1.8177	0.02
mim-BCl ₃ -2AlCl ₃	-0.0016	1.9913	0.03
dma-BCl ₃ -2AlCl ₃	-0.0012	1.8139	0.02
P ₈₈₈ O-BCl ₃ -2AlCl ₃	-0.0010	1.3874	0.02
P ₈₈₈ -BCl ₃ -2AlCl ₃	-0.0007	1.3020	0.01
4-pic-BCl ₃ -2GaCl ₃	-0.0012	2.1454	0.02
mim-BCl ₃ -2GaCl ₃	-0.0022	2.4802	0.04
dma-BCl ₃ -2GaCl ₃	-0.0017	2.3097	0.03
P ₈₈₈ O-BCl ₃ -2GaCl ₃	-0.0008	1.5291	0.01
P ₈₈₈ -BCl ₃ -2GaCl ₃	-0.0011	1.5052	0.02

3.2.3 Viscosity measurements

Viscosity is a measure of the internal friction of a moving fluid, *i.e.* the resistance of a liquid to flow and it is mostly associated with intermolecular force of attraction within the liquid.¹⁸³ Therefore, greater intermolecular force within a liquid results in high viscosity.^{185,160} Viscosity is crucial in chemical engineering operations, such as stirring, mixing and pumping and can affect transport properties such as diffusion, which affect for example catalytic applications of ILs, or their uses in gas absorption.^{185,160} Viscosity of ionic liquids is typically significantly higher (*i.e.* one to three orders of magnitude) than conventional solvents.⁷⁰ Viscosities of different ionic liquids vary within a very wide range, from 10-500 mPa·s at room temperature.^{80,185}

Since borenium ionic liquids are corrosive and moisture-sensitive, the falling ball viscometer was selected as the method of choice. Brizard *et al.*⁶ developed absolute falling ball viscometer and made it possible to cover a wide range of viscosities while minimising measurement uncertainty.^{185,160} This method is based on a spherical metal ball moving through a resistive component or fluid. The fluid to be measure is filled into a capillary tube equipped with a sphere ball. The capillary tube is then inserted into a chamber inclined at an angle and enclosed in a tubular jacket for thermal control.^{80,185,160} The sample viscosity correlates with the time required by the ball to drop a specific distance, and the test results are given as dynamic viscosity. The dynamic viscosity is a function of the time, D_t , required for the ball to roll from one end of a fluid-filled tube to the other at a fixed angle, the density difference between the ball and the fluid, and the apparatus parameter K . The measurement relies on determining the ball's rolling time in a diagonally mounted glass capillary filled with sample, which is related to the viscosity of the fluid. Because the tube is made of glass, and it can be sealed, this approach was superior to cone-and-plate viscometer, which is more often used to study ionic liquids.

To eliminate the problem of sample hydrolysis prior or during the measurements, the capillary, ball, adapter and cap were placed inside a glovebox and the ILs were transferred into the capillaries and sealed prior to measurement. Anton Paar AMVn rolling ball viscometer was used to measure viscosities of ionic liquids within temperature range between 293 and 343 K, in steps of 10 K. Densities for each temperature were provided for automated calculation of viscosities by the instrument. The viscometer was calibrated by the manufacturer, using several

density and viscosity standard reference fluids. The uncertainty of the temperature measurement is 0.02 K, the uncertainty of the dynamic viscosity is 1%. The tilt angle of the tube was chosen such that the speed of rolling ball did not drop below 10 s.^{80,185}

To minimise error, balls with the same batch number were used for each measurement. This enabled to keep the tolerance limit within the range of 0.3%. At each temperature, the dynamic viscosities were recorded at inclination angle of 60°, with four repetitions for each sample. The measurements were performed using a 1.8 mm diameter capillary and its respective calibrated ball as a function of temperature and angle of measurement.¹⁶⁰ Viscosity data for all studied ionic liquids are reported as a function of temperature in Table 3-10.

The viscosity of borenium ionic liquids varied between 35 to 303 mPa s at 293 K, which is at the lower end of viscosities recorded for ionic liquids, but higher than molecular solvents.⁷⁰ In general, viscosity of each IL decreased significantly as the temperature was increased; the lowest recorded value was 8.86 mPa s, determined for 4-pic-BCl₃-2AlCl₃ at 342 K.^{70,156} As expected, viscosities depended of the ligand and on the anion of ionic liquid (*viz.* Table 3-10 for comparison). Systems with long alkyl chains (*i.e.* containing P₈₈₈O or P₈₈₈ ligands) exhibited higher viscosities than ILs with other ligands (dma, mim and 4-pic) and the same anion. This can be explained in terms of van der Waals forces. The alkyl chains increase the overall contribution of van de Waal forces in the compound, which results in increased energy required for the molecular motion of the compound resulting in increased viscosity.^{70,156}

Furthermore, it was observed that viscosity depended on the metal in the anion. For *N*-donors, changing the metal from aluminium to gallium caused an increase in the viscosity of ILs up to 42 % at 293 K. In contrast, for ionic liquids with long alkyl chains, it was the chlorogallate ionic liquids that were slightly less viscous. However, this may derive from differing speciation depending on the donor. As shown through spectroscopic studies, *N*-donors were found to yield borenium ionic liquids with moderate ligand displacement, whereas the other systems were characterised by significant ligand scrambling and very complex speciation.

Table 3-10: Experimental values for viscosities, η , of the studied borenium ionic liquids, for temperatures from 293 to 343 K.

4-pic-BCl ₃ -2AlCl ₃		4-pic-BCl ₃ -2GaCl ₃	
T /K	η / mPa s	T /K	η / mPa s
293.15	35.21	293.15	50.01
298.15	29.13	298.15	39.83
303.15	24.67	303.15	32.73
313.15	18.26	313.15	23.33
323.15	14.01	323.15	17.56
333.15	11.09	333.15	13.67
343.15	8.86	343.15	10.90
mim-BCl ₃ -2AlCl ₃		mim-BCl ₃ -2GaCl ₃	
T /K	η / mPa s	T /K	η / mPa s
293.15	50.34	293.15	68.76
298.15	40.82	298.15	55.15
303.15	33.77	303.15	45.82
313.15	23.96	313.15	32.20
323.15	17.93	323.15	23.57
333.15	13.88	333.15	17.13
343.15		343.15	13.38
dma-BCl ₃ -2AlCl ₃		dma-BCl ₃ -2GaCl ₃	
T /K	η / mPa s	T /K	η / mPa s
293.15	137.86	293.15	-
298.15	100.12	298.15	-
303.15	73.11	303.15	-
313.15	43.09	313.15	-
323.15	25.87	323.15	-
333.15	17.63	333.15	-
343.15		343.15	-
P ₈₈₈ O-BCl ₃ -2AlCl ₃		P ₈₈₈ O-BCl ₃ -2GaCl ₃	
T /K	η / mPa s	T /K	η / mPa s
293.15	-	293.15	307.74
298.15	-	298.15	237.88
303.15	-	303.15	186.57
313.15	-	313.15	119.74
323.15	-	323.15	80.79
333.15	-	333.15	56.82
343.15	-	343.15	
P ₈₈₈ BCl ₃ -2AlCl ₃		P ₈₈₈ BCl ₃ -2GaCl ₃	
T /K	η / mPa s	T /K	η / mPa s
293.15	203.67	293.15	173.36
298.15	154.82	298.15	133.96
303.15	119.38	303.15	105.12
313.15	74.63	313.15	67.93
323.15	49.28	323.15	46.37
333.15	34.18	333.15	33.17
343.15		343.15	24.50

Data for two systems are missing from Table 3-10. It was technically impossible to record data for the highly viscous $P_{888}O\text{-}B\text{Cl}_3\text{-}2\text{AlCl}_3$ system, resulting in long relaxation time of the ball (practically getting stuck in practical terms) and reproducibly resulting in error reading.^{186,187} The $\text{dma-BCl}_3\text{-}2\text{GaCl}_3$ system, in turn, was corroding the ball, which obviously resulted in erroneous results.

Vogel-Fulcher-Tammann (VFT) equation was used to fit the experimental values of viscosity as a function of temperature (Equation 3-5).¹⁵⁹ The VFT equation is used for the description of temperature dependence of viscosity, accounting for the curvature typically observed in various glass-transition materials, such as ionic liquids.^{188,186} Fitted data are shown in Figure 3-12 for $L\text{-}B\text{Cl}_3\text{-}2\text{AlCl}_3$ and in Figure 3-13 for $L\text{-}B\text{Cl}_3\text{-}2\text{GaCl}_3$.

$$\eta = A \times T^{0.5} \exp\left(\frac{B}{T-T_0}\right) \quad \text{Equation 3-5}$$

A , B and T_0 - fitting parameters

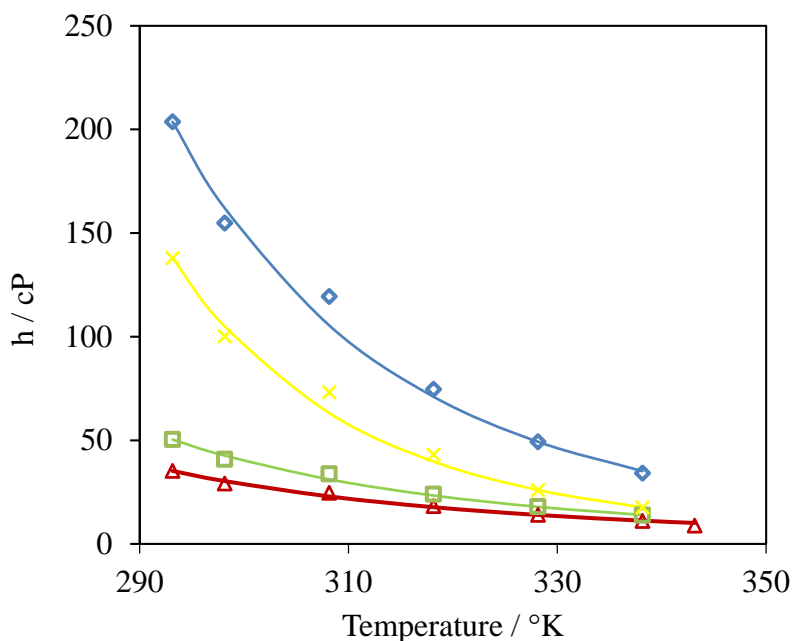


Figure 3-12: Experimental values for viscosities, η , of borenium ionic liquids of a general formula $L\text{-}B\text{Cl}_3\text{-}2\text{AlCl}_3$, plotted as a function of temperature, fitted to a Vogel-Fulcher-Tammann (VFT) equation, where $L = \blacktriangledown 4\text{pic}$, $\square \text{mim}$, $\ast \text{dma}$ and $\blacklozenge P_{888}$.

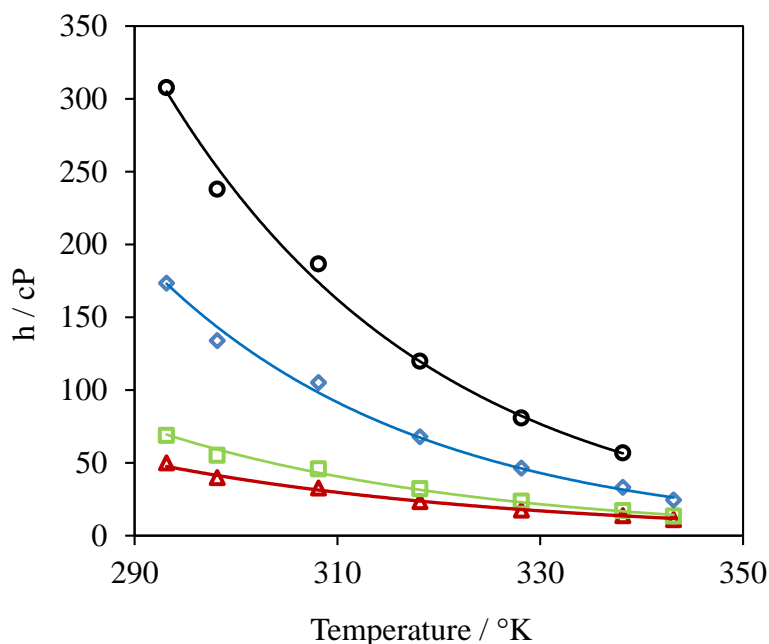


Figure 3-13: Experimental values for viscosities, η , of borenium ionic liquids of a general formula $L\text{-BCl}_3\text{-2GaCl}_3$, plotted as a function of temperature, fitted to a Vogel-Fulcher-Tammann (VFT) equation for: \blacktriangledown 4pic, \square mim, \bullet $P_{888}O$ and \blacklozenge P_{888} .

As shown in Figure 3-12 and Figure 3-13, the VFT equation gave good fit to all measured data, with the exception of inexplicable consistent deviation for 303.15 K, recorded for all borenium ILs, but not seen for other systems tested on the same machine by other users. The largest such deviation was found for $P_{888}O\text{-BCl}_3\text{-2GaCl}_3$, but it appears to be present in all tested samples to various extent. It is possible that a change in speciation occurred at this temperature, but elucidating this would require further speciation studies, for example variable temperature multinuclear NMR spectroscopy.

Table 3-11 lists fitting parameters for the VFT equations describing viscosity vs. temperature relationship for all tested borenium ionic liquids. The T_0 value has a physical meaning, and relates to theoretical glass transition temperature of the material.¹⁸⁹ And as a general rule, compounds with a more structured and higher molecular order tend to have higher glass transition temperatures.¹⁹⁰ From the studied ILs, $P_{888}O\text{-BCl}_3\text{-2GaCl}_3$ showed the highest $T_0 = 100$ K, second highest being $\text{dma-BCl}_3\text{-2AlCl}_3$ with $T_0 = 91.86$ K - both of these systems are actually far from ‘idealised’ speciation of borenium ionic liquid, with significant ligand scrambling. In contrast, the ‘near-ideal’ borenium ILs, with N -donor ligands and relatively small

degree of scrambling, had very low T_0 values, with the lowest value recorded for mim- BCl_3 - 2GaCl_3 ($T_0 = ca. 49$ K). This suggests that well-designed borenium ionic liquids, with charge dispersed anions and cations, can have very low theoretical glass transition temperatures.

Table 3-11: Vogel-Fulcher-Tammann equation parameters obtained for the measurements of viscosity, η , of borenium ionic liquids for temperatures between 293 K and 343 K.

L-BCl_3-2MCl_3	A	B	T_0/K
4-pic-BCl_3-2AlCl_3	-10.05	1470.74	73.70
mim-BCl_3-2AlCl_3	-10.67	1731.98	67.70
dma-BCl_3-2AlCl_3	-13.23	2265.65	91.86
P₈₈₈-BCl_3-2AlCl_3	-12.22	2414.37	65.98
4-pic-BCl_3-2GaCl_3	-10.87	1788.50	66.23
mim-BCl_3-2GaCl_3	-12.39	2376.89	48.55
P₈₈₈O-BCl_3-2GaCl_3	-11.89	2071.36	100.0
P₈₈₈-BCl_3-2GaCl_3	-11.35	2957.80	77.97

3.2.3.1 Conclusions from synthesis of borenium ILs with chlorometallate anions

Borenium chlorometallate ionic liquids were prepared by a solvent-free method reacting previously synthesised boron complexes with two metal chlorides acting as halide-abstracting agents: aluminium(III) chloride and gallium(III) chloride. Aluminium(III) chloride and the $[\text{BCl}_3\text{L}]$ adducts were reacted in 1:1 or 2:1 ratios, because only two chloroaluminate(III) anions - $[\text{AlCl}_4]^-$ and $[\text{Al}_2\text{Cl}_7]^-$ - are found in homogeneous chloroaluminate ionic liquids. In contrast, chlorogallate(III) anions form larger oligomeric species, hence GaCl_3 and $[\text{BCl}_3\text{L}]$ were used in ratios of 1:1 or 2:1 or 3:1.

From ^1H and ^{13}C NMR studies, supported by FT-IR spectroscopy, all ligands were stable in neat ionic liquids, and despite expected very high Lewis acidity did not decompose. However, there was significant ligand scrambling, with ligands from the boron centre migrating to the metal centre, releasing free BCl_3 . Extreme example was dma- BCl_3 - $n\text{MCl}_3$, where coordination complexes of metals precipitated from boron chloride-rich liquid. Also P₈₈₈O- BCl_3 - $n\text{MCl}_3$ had very significant ligand scrambling, which suggests that O-donors are not best candidates for generating ionic liquids *via* this methodology. In contrast, ligands based on N-donors resulted in

more stable borenium ILs, albeit some ligand scrambling has been observed, leading to a liquid with complicated speciation, which can be approximated as $(\text{BCl}_3)_a[\text{BCl}_2\text{L}]_b[\text{MCl}_2\text{L}_2]_c[\text{MCl}_4]_d[\text{M}_2\text{Cl}_7]_e$. This prompted the search for an alternative synthetic route, using non-metallic halide abstracting agent.

3.2.4 Borenium triflate ionic liquids

In addition to ligand scrambling considerations discussed above, chlorometallate anions are corrosive, and contain Lewis acidic centres that may compete with those from borenium cations in catalysis, impairing selectivity. In order to access borenium ionic liquids without chlorometallate anions, $[\text{BF}_3\text{L}]$ complexes were reacted with trimethylsilyl trifluoromethanesulfonate (Equation 3-2 in 3.2.1). Selected $[\text{BCl}_3\text{L}]$ complexes were used for comparison.

The advantage of using TMSOTf is that the only by-product generated from borenium ion generation is the volatile and easily remove trimethylsilyl halide (*i.e.* trimethylsilyl chloride or trimethylsilyl fluoride). However, care should be taken when preparing these ILs, because TMSOTf can hydrolyse in the presence of atmospheric moisture, and the hydrolysis of resulting ionic liquids generates corrosive HCl, or toxic HF, depending on the boron halide used.

All reaction products were clear, homogenous liquids (Table 3-12). It was also observed that colour of the all liquids changed; they darkened after 3-4 weeks. However, although the colour has changed, their chemical structure remained unaffected, as ^1H NMR recorded immediately after the synthesis and after a couple of weeks remained the same, regardless of the colour change.

Table 3-12. Appearances of the borenium triflate ionic liquids, $\text{L-BX}_3\text{-OTf}$ and % yields

L	L-BF ₃ -OTf		L-BCl ₃ -OTf	
	L-BF ₃ -OTf	Yield / %	L-BCl ₃ -OTf	Yield / %
4pic	liquid	65	liquid	66
mim	liquid	54	liquid	57
dma	liquid	34	-	-
P ₈₈₈ O	liquid	83	-	-
P ₈₈₈	liquid	90	liquid	87

3.2.4.1 NMR spectroscopic characterisation

Multinuclear NMR spectra were recorded for all the borenium triflate ILs. ^1H and ^{13}C NMR were referenced to external solvent signals (CD_3) $_2\text{SO}$ at 2.54 ppm and 40.45 ppm respectively. Heteronuclear chemical shift values were referenced to external $\text{F}_3\text{B}\cdot\text{OEt}_2$ for (^{11}B { ^1H }), and $\text{C}_6\text{H}_5\text{CF}_3$ for ^{19}F { ^1H } spectroscopy and H_3PO_4 (85% water solution) for ^{31}P { ^1H } spectroscopy.

3.2.4.1.1 ^1H and ^{13}C NMR spectroscopy

The ^1H and ^{13}C NMR evidence was useful for confirming that ligands have not been decomposed, and that the triflate ion was present in the product (^{13}C NMR spectra), but not conclusive in establishing the existence of the isolated borenium cations.

The general pattern of ^1H and ^{13}C NMR spectra of the triflate systems was different from the pattern that was noted for all chlorometallate systems. NMR chemical shifts recorded for borenium triflates were found to be slightly upfield, if not very similar, to that of the tetracoordinate boron adducts. This was the first indication that the liquids formed in the synthesis were probably not ionic liquids but mostly likely molecular species. In contrast, in chlorometallate systems downfield shifts were observed, which was consistent with the formation of electron-deficient borenium cation.

^1H NMR spectra of the triflate systems were more complicated: in all the systems, apart from the main signals (listed in bag Table 3-13), there were lower intensity peaks close to the main signals, with the same splitting patterns as the main signals. Groups of signals, when integrated, gave integrations consistent with the ligands. In conclusion, several different ligand environments were present and - in contrast to chlorometallate systems - these environments were distinguishable in the NMR timescale. Examples of such ^1H NMR spectra are shown in Figure 3-14 and Figure 3-15.

Table 3-13: The main ^1H NMR (400 MHz) chemical shifts for the triflate systems.

L	donor	$[\text{BF}_3(\text{L})]$	L- $\text{BF}_2\text{-OTf}$	L- $\text{BCl}_2\text{-OTf}$	Assignment
4pic	1.64(s)	2.60(s)	2.31(s)	1.92(s)	Ar- CH_3
	6.50(d)	7.57(d)	7.28(d)	7.11(m)	-CH-C-CH-
	8.09(d)	8.55(d)	8.35(d)	8.18(m)	-CH-N-CH-
mim	2.85(s)	3.87(s)	2.76(s)	3.04(m)	Ar- CH_3
	6.41(d)	7.02(s)	6.21(s)	6.42(d)	CH=CH-N
	6.93(s)	7.31(s)	6.53(s)	6.54(t)	CH=CH-N
		8.05(s)	7.63(s)	7.58(s)	N-CH-N
dma	2.46(s)	2.47(s)	2.42(s)	-	$\text{CH}_3\text{-CO}$
	3.30(s)	3.23(s)	2.72(s)		-N- CH_3
	3.48(s)	3.27(s)	3.15(s)		$\text{CH}_3\text{-N-CO}$
P₈₈₈O	0.86(m)	0.88(m)	0.48 (m)	-	-(CH_3)
	1.62(m)	1.56(m)	1.74(m)		-(CH_2) ₇ -
P₈₈₈	0.588(m)	0.88(m)	0.47(m)	0.84(m)	-(CH_3)
	1.08(m)	1.53(m)	1.76(m)	1.39(m)	-(CH_2) ₇ -

Abbreviations: s = singlet, d = doublet, t = triplet, q = quartet, m = multiplet

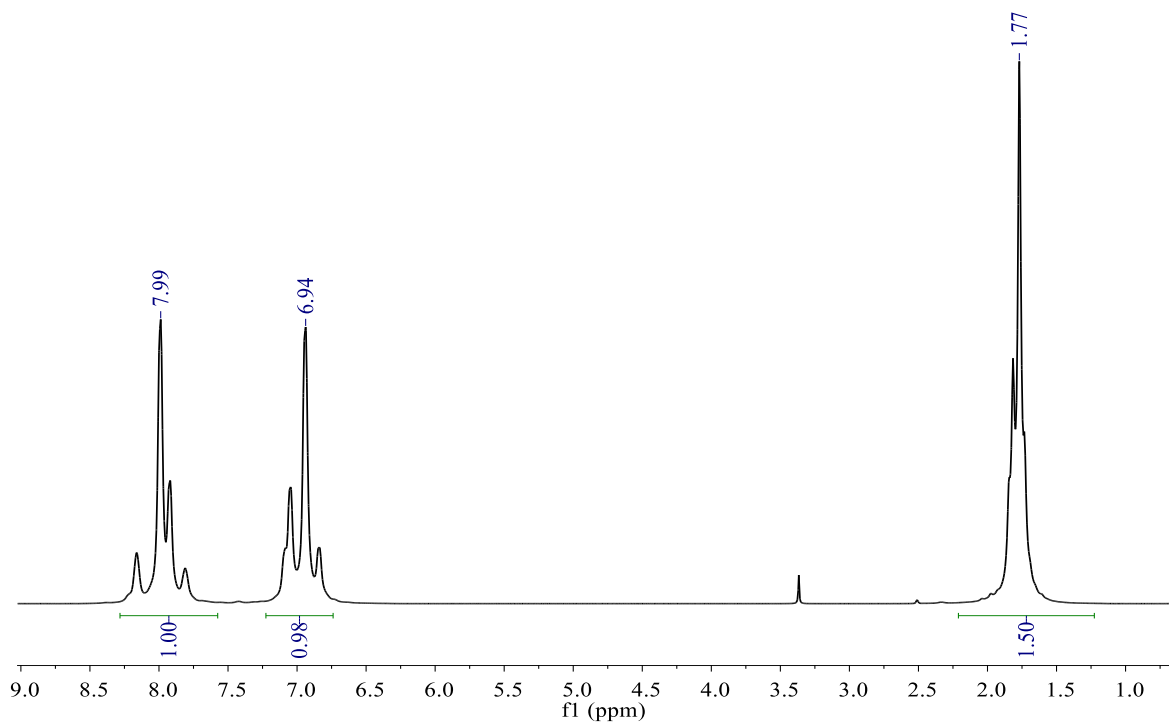


Figure 3-14. ^1H NMR (400 MHz, DMSO) spectrum of 4-pic- $\text{BCl}_2\text{-OTf}$.

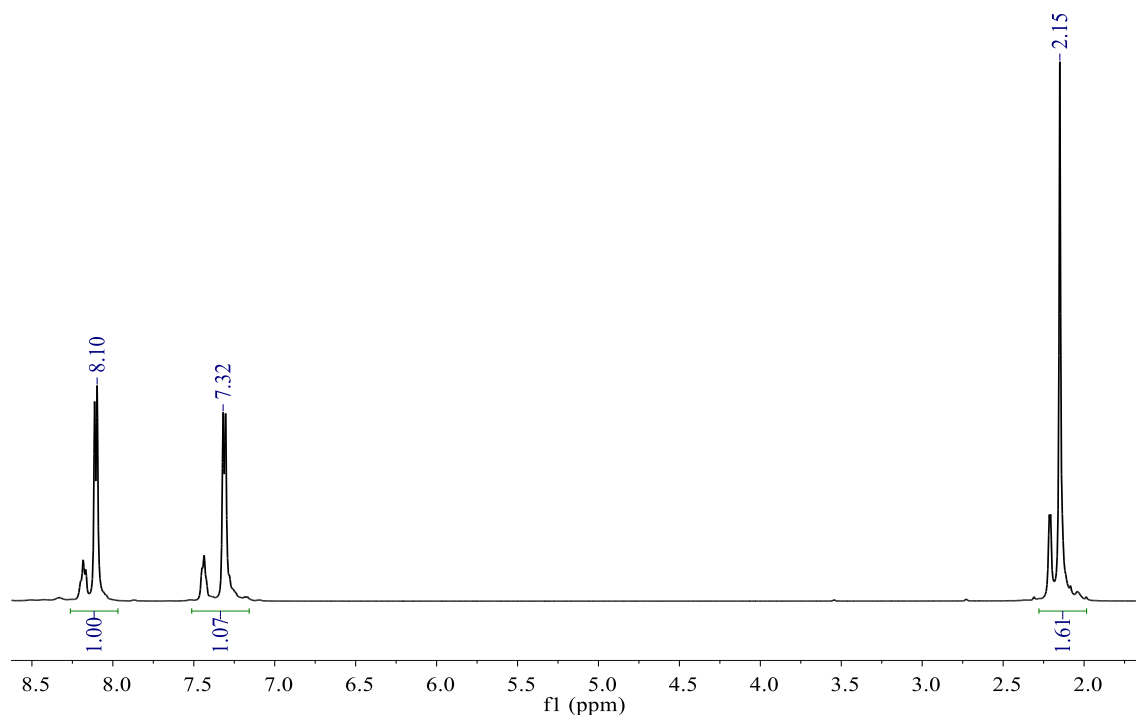


Figure 3-15: ^1H NMR (400 MHz, DMSO) spectrum of 4-pic- $\text{BF}_2\text{-OTf}$.

The fact that chemical shifts were not deshielded compared to the adducts suggested that the borenium cation was not generated, but rather the triflate was coordinating to the boron atom in a tetracoordinate compound. Furthermore, complicated ^1H NMR spectra suggested that there were several different coordination environments to the ligand; this suggests that ligand scrambling occurred between tetracoordinate boron compounds. In consequence, the reaction of $[\text{BF}_3\text{L}]$ and TMSOTf was envisaged to produce a mixture of different, equilibrated tetracoordinate compounds with varying number of L, X and $[\text{OTf}]^-$ ligands between them: $[\text{BF}_2(\text{OTf})\text{L}]$, $[\text{BF}_3\text{L}]$ and $[\text{BF}(\text{OTf})_2\text{L}]$, in addition to possible charged tetracoordinate species, for example $[\text{B}(\text{OTf})_2\text{L}_2]^+$ and $[\text{BF}_4]^-$. Additional spectroscopic studies were needed to shed more light on this speciation.

The ^{13}C NMR spectra (Table 3-14)) supported the conclusions drawn based on ^1H NMR spectra. Also here, the peaks were slightly upfield when compared to the boron complexes, consistent with the formation of tetracoordinate species. There were also lower intensity peaks close to the main signal for each ^{13}C NMR peak. In addition, all spectra exhibited $\{\text{CF}_3\}$ signal, which is a quartet around 116 ppm, splitting indicating the coupling of ^{13}C with three ^{19}F nuclei (see examples in Figure 3-16 and Figure 3-17).

Table 3-14: ^{13}C NMR (101 MHz, DMSO) chemical shifts recorded for the triflate systems.

L	[BF ₃ (L)]	L-BF ₂ -OTf	L-BCl ₂ -OTf	Assignment
4-pic	156.66	161.61	157.27	-CH-N-CH-
	142.64	139.52	140.41	-CH-C-CH-
	126.78	127.46	124.98	-CH-C-CH-
	21.78	20.79	19.00	Ar-CH ₃
mim	135.30	135.36	133.67	-N-CH-N-
	123.27	121.84	120.51	-CH=CH-N-
	121.53	118.52	114.55	-CH=CH-N
	35.33	34.27	32.93	Ar-CH ₃
dma	174.68	172.69		CH ₃ -CO-
	39.49	39.50	-	CH ₃ -N-CH ₃
	38.17	18.11		CH ₃ -N-CH ₃
	17.06			CH ₃ -CO-
P₈₈₈O	31.70	31.07		C ₂ H ₅ -CH ₂ -(CH ₂) ₅ -PO
	30.68	29.76		C ₅ H ₁₁ -CH ₂ -(CH ₂) ₂ -PO
	28.88	28.14		CH ₃ -CH ₂ -(CH ₂) ₃ -PO
	24.64	23.65		C ₇ H ₁₅ -CH ₂ -PO
	24.01	22.84	-	CH ₃ -CH ₂ -(CH ₂) ₄ -PO
	22.56	21.90		CH ₃ -CH ₂ -(CH ₂) ₆ -PO
	20.84	19.87		C ₆ H ₁₃ -CH ₂ -CH ₂ -PO
	14.01	13.01		CH ₃ -(CH ₂) ₇ -PO
P₈₈₈	31.71	31.11	31.98	C ₂ H ₅ -CH ₂ -(CH ₂) ₅ -P
	31.17	30.29	31.42	C ₅ H ₁₁ -CH ₂ -(CH ₂) ₂ -P
	29.15	29.61	29.08	CH ₃ -CH ₂ -(CH ₂) ₃ -P
	22.58	28.16	22.55	CH ₃ -CH ₂ -(CH ₂) ₄ -P
	22.34	21.94	22.43	C ₆ H ₁₃ -CH ₂ -CH ₂ -P
	18.29	21.32	18.59	C ₇ H ₁₅ -CH ₂ -P
	17.99	16.83	14.08	CH ₃ -CH ₂ -(CH ₂) ₆ -P
	14.02	13.06		CH ₃ -(CH ₂) ₇ -P

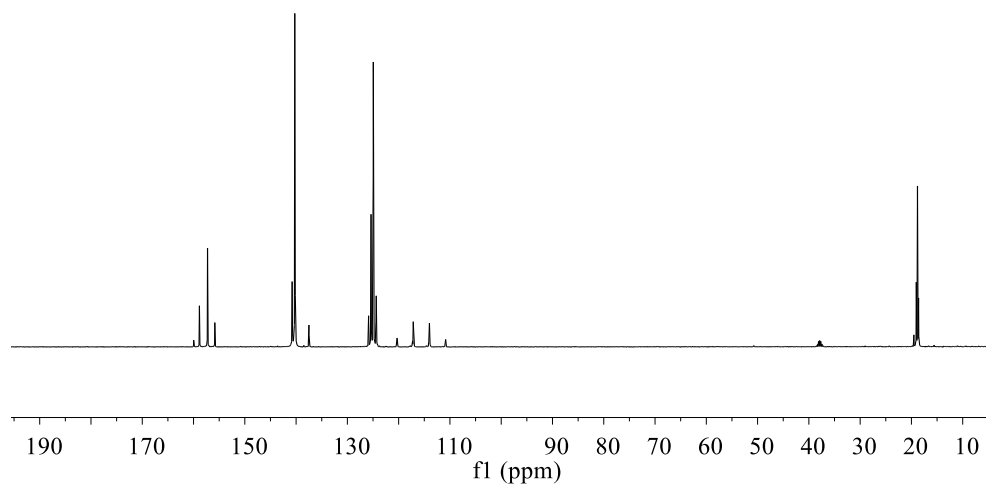


Figure 3-16: ^{13}C NMR (101 MHz, DMSO) spectrum of 4-pic-BCl₂-OTf.

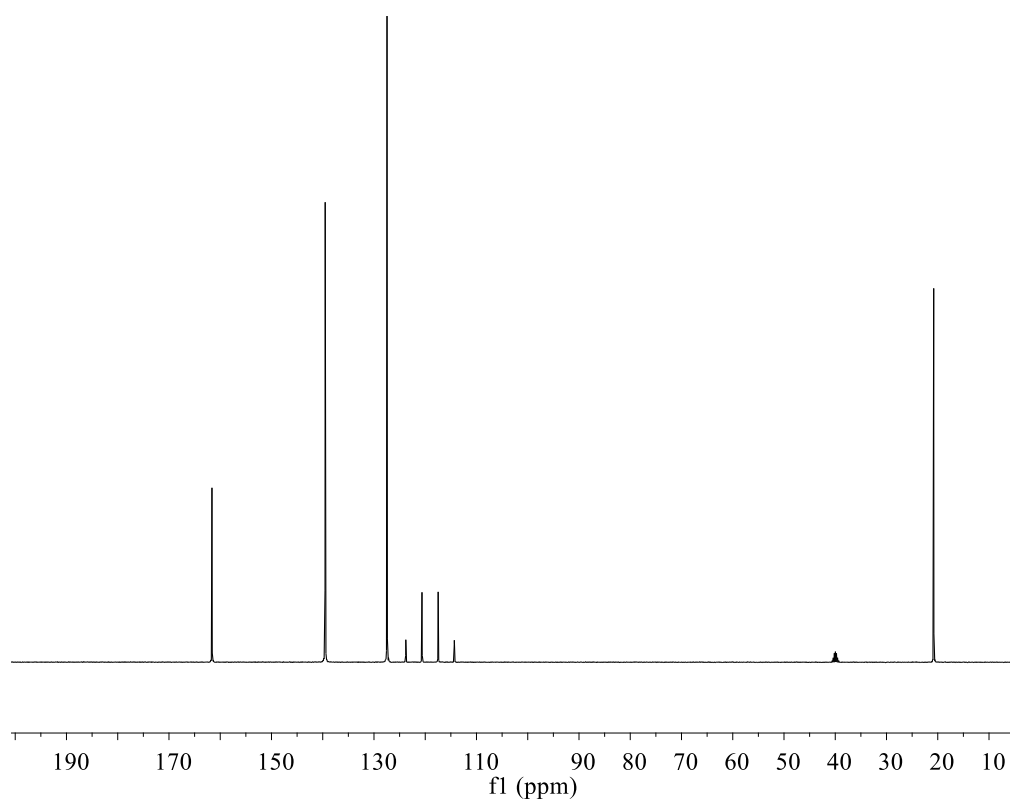


Figure 3-17: ^{13}C NMR (101 MHz, DMSO) spectrum of 4-pic-BF₂-OTf.

3.2.4.1.2 ^{11}B NMR spectroscopy

^{11}B NMR spectra were recorded for each triflate system. As expected from ^1H and ^{13}C NMR spectroscopy, the ^{11}B NMR spectra confirmed the presence of one or multiple tetracoordinate boron compounds in the triflate systems, with several overlapping signals below 10 ppm (see Figure 3-18 for L-BCl₂-OTf and Figure 3-17 for L-BF₂-OTf).

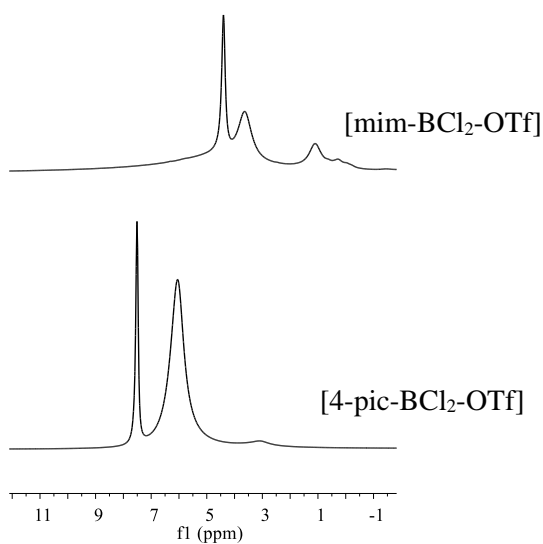


Figure 3-18: ^{11}B NMR (160 MHz, DMSO, 27 °C, neat liquid with DMSO-*d*₆ lock) of triflate systems of a general formula with [L-BCl₂-OTf].

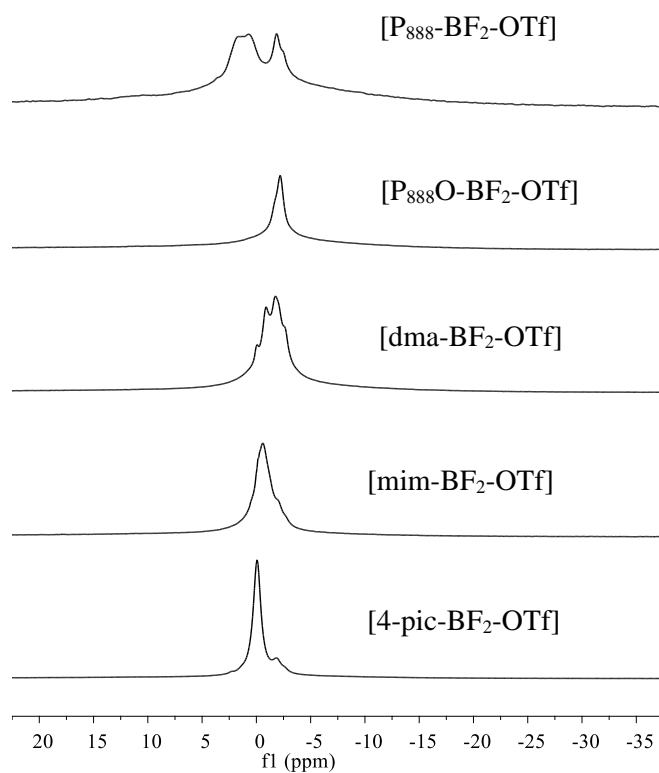


Figure 3-19: ^{11}B NMR (160 MHz, DMSO, 27 °C, neat liquid with DMSO-*d*₆ lock) of triflate systems of a general formula with [L-BF₂-OTf-L].

As listed in Table 3-15, ^{11}B NMR chemical shifts for L-BF₂-OTf were between -0.87 to 0.71 ppm and for L-BCl₂-OTf between 0.29 and 7.51 ppm, which is in agreement with literature

reports for tetracoordinate haloboron compounds.^{8,191} Multiple chemical shifts indicate ligand scrambling and different combinations of L, X⁻ (X = Cl or F) and [OTf]⁻ ligands around boron.

Table 3-15: ¹¹B NMR (160 MHz, DMSO, 27 °C, neat liquid with DMSO-d₆ lock) parameters for the triflate liquids

L	[BF ₃ L]	L-BF ₂ -OTf	[BCl ₃ L]	L-BCl ₂ -OTf
4-pic	0.41(q) -0.86(s)	-0.07, -1.84	8.13(s)	3.11, 6.05, 7.51
mim	-0.27(q) -0.96 (s)	-0.59	5.12(s)	0.29, 1.10, 3.64, 4.40
dma	-0.32 (s) -1.12(s)	-0.90, -1.75, 0.09		-
P₈₈₈O	-1.08(s)	-2.19		-
P₈₈₈	0.51(m)	0.71, -1.87	3.18(s) 0.94(s) -1.95(s)	3.53(d)

3.2.4.1.3 ¹⁹F NMR spectroscopy

¹⁹F NMR spectra of the L-BF₂-OTf systems (Figure 3-20) showed shifts upfield to the reference C₆H₅CF₃ but slightly downfield to the boron trifluoride complexes, *ca.* -140 ppm, in addition to the triflate signal appearing around -79 ppm.¹⁹² Seeing as multiple complexes were expected, it was not surprising that multiple peaks were recorded in both areas of chemical shift. However, it was expected that general integration of ¹⁹F NMR signals for the {CF₃} unit and the {BF₂} unit would be about 3:2. As clearly shown in Figure 3-20, this was not the case, and integration of these two regions against each other points to over substitution of the boron centre with triflate, and removal of most of the fluorides. This further helped to explain the extra peaks present in the corresponding ¹H and ¹³C NMR spectra. Each increased coordination of [OTf]⁻ created a different electronic environment, hence different chemical shifts for the ligand present.

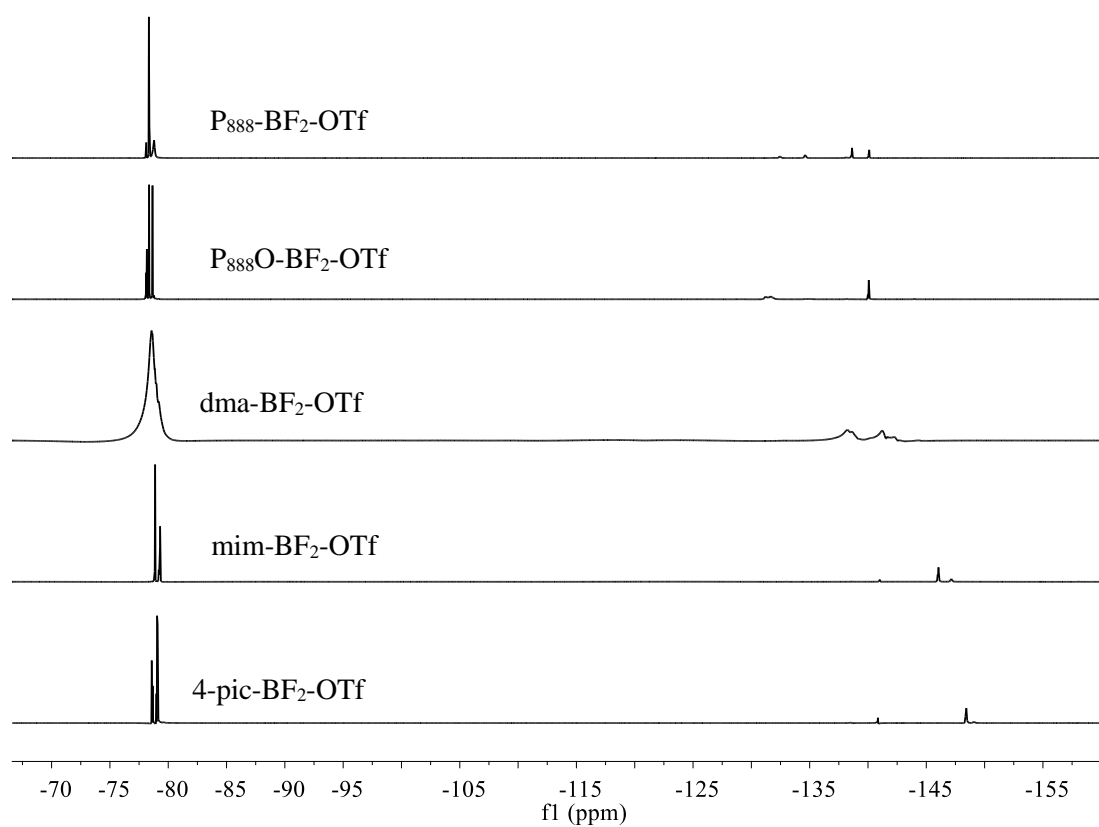


Figure 3-20: ^{19}F NMR (376 MHz, DMSO) spectra of triflate systems of a general formula: $[\text{L-BF}_2\text{-OTf}]$.

^{19}F NMR spectra of the $\text{L-BCl}_2\text{-OTf}$ systems (Figure 3-21) only showed ^{19}F NMR signals at *ca.* -79.11 ppm indicative of the $\{\text{CF}_3\}$ unit in $[\text{OTf}]^-$, therefore it was impossible to conclude about over substitution with triflate. However, since Cl-B bond is weaker than F-B bond¹⁵⁸ it can be assumed that this was the case also here.

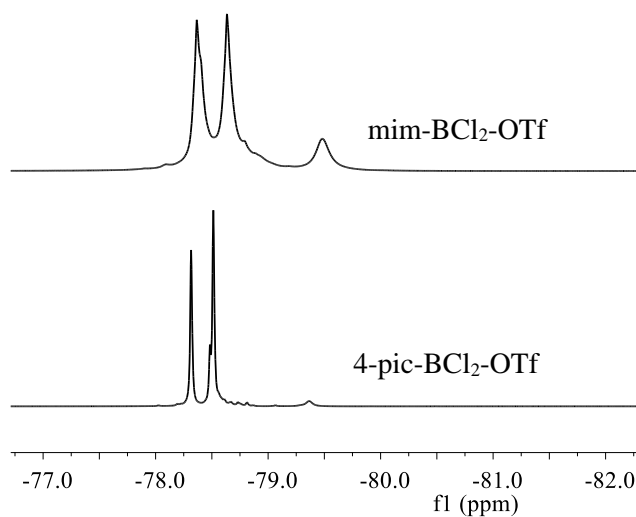


Figure 3-21: ^{19}F NMR (376 MHz, DMSO) spectra of triflate systems of a general formula: $[\text{L-BCl}_2\text{-OTf}]$.

Chemical shifts for both $\text{L-BF}_2\text{-OTf}$ and $\text{L-BCl}_2\text{-OTf}$ systems are listed in Table 3-16, along with overall integrations of $\{\text{CF}_3\} : \{\text{BF}_2\}$ units for the former group.

Table 3-16: ^{19}F NMR (376 MHz, DMSO) chemical shift recorded for the triflate liquids

L	$[\text{BF}_3\text{L}]$	L- $\text{BF}_2\text{-OTf}$	$\{\text{CF}_3\} : \{\text{BF}_2\}$	L- $\text{BCl}_2\text{-OTf}$
4-pic	-151.50(m)	-78.81 -148.63	4:1	-78.51
mim	-149.29(m)	-79.06 -146.57	3:1	-78.37
dma	-148.89(m)	-78.89 -141.69	5:1	-
P_{888}O	-145.69(m)	-78.41 -139.37	5:1	-
P_{888}	-132.82(m)	-78.40 -140.54	10:1	-78.35

3.2.4.2 IR spectroscopy

Like the borenium chlorometallate ILs, no O-H $3570\text{-}3200\text{ cm}^{-1}$ (broad), hydroxy group, H-bonded OH stretch were found in the triflate systems.

Like for borenium chlorometallate systems, the existence the aromatic ring in the structures of the *N*-donors compounds was reflected in the CH and C=CC ring-related vibrations.^{179,180} The strength of the bands was a distinguishing factor between the aromatic

N-donor compounds and the aliphatic *P*- and *O*-donor compounds. For the aromatic *N*-donors, C-H stretching occurred above 3000 cm⁻¹ and was typically exhibited as a multiplicity of weak-to-moderate bands, contrasting with the *O*-, *P*-donor aliphatic C-H stretch.^{179,180,181} Aromatic C-H out-of-plane bend vibrations occurring at 900-670 cm⁻¹ and bands around 770-730 or 710-690 cm⁻¹ were very indicative of the 4-pic and mim (monosubstituted *N*-donors). Absorbance of the P=O stretch around 1050–1000 cm⁻¹ for the P₈₈₈O-BX₂-OTf systems was relatively low.^{155,179} The 1200 to 1100 cm⁻¹ absorptions were assigned to S=O or C-S bonds in the triflate. In addition, strong absorption between 1250 and 1150 cm⁻¹ was assigned to numerous types of vibrations from the CF group.^{155,179}

The aromatic amino CN bands at 1300–1200 cm⁻¹ were assigned to the systems with amine ligands: 4-pic-BCl₂-OTf, 4-pic-BF₂-OTf, mim-BCl₂-OTf, mim-BF₂-OTf and dma-BF₂-OTf.^{179,181} The *N*-donor aromatic compounds with unsaturated hydrocarbons featuring C=C, with attached hydrogens, mostly occurred as either a single or a pair of absorptions. The position of the C=C stretching frequency with the BF₃ compounds compared to the BCl₃ compounds varied slightly as a function of orientation around the double bond in each environment and the ligand.^{180,181} The C=C stretching frequency were seen around 1640-1600 cm⁻¹ for the 4-pic compounds, *i.e.* [BCl₃(4pic)], [BF₃(4pic)], 4-pic-BCl₂-OTf and 4-pic-BF₂-OTf whereas the absorption of the mim compounds, *i.e.* [BCl₃(mim)], [BF₂(mim)], mim-BCl₂-OTf and mim-BF₂-OTf were around 1580-1520 cm⁻¹.

Table 3-17: FT-IR frequencies (cm^{-1}) for the triflate systems: $[L\text{-BCL}_2\text{-OTf}]$ and $[L\text{-BF}_2\text{-OTf}]$.

Compound	Assignment/ cm^{-1}							
	CH_3 , CH_2 , CH	$\text{C}=\text{C}$ $\text{C}=\text{N}$	CH_3 CH_2	$\text{C}-\text{N}$	$=\text{CH}_2$, $=\text{C}-\text{H}$	$\text{C}-\text{H}$	$\text{C}-\text{S}$	$\text{S}=\text{O}$
4pic	2889(s) 3068(s)	1604(s)	1412(s)	1223(m)	995(s)	796(m)	-	-
$[\text{BCL}_3(4\text{-pic})]$	3070(s) 3130(s)	1637(s)	1463	1162(m)	900(s) 1025(s)	738(m)		
4-pic-$\text{BCL}_2\text{-OTf}$		1640(s)	1393(s)	1199(m)	934(s)	624(m) 846(m)		1148
$[\text{BF}_3(4\text{pic})]$	3074(s)	1638(s)	1449(s)	1155(m)	1149(s) 1094(s)	750(m) 896(m)		
4-pic-$\text{BF}_2\text{-OTf}$	3123(s)	1643(s)	1381(s)	1194(m)	957(s)	766(m)	1251	1158
mim	2953(s) 310(s)	1516(s)	1420(s)	1284(m) 1230(m)	907(s) 1108(s)	662(m) 907(m)	-	-
mim-$\text{BCL}_2\text{-OTf}$	3158(s)	1546(s)	1387(s)	1200(m)	934(s) 1134(s)	618(m) 844(m)	-	-
$[\text{BF}_3(\text{mim})]$	3159(s) 3175(s)	1616(s) 1565(s)	1306	1258(m)	1032 1131	649(m) 889(m)	-	-
mim-$\text{BF}_2\text{-OTf}$	3159(s)	1575(s) 1547(s)		1251	1007 1136	616(m) 927(m)		- 1194
dma	1498(s) 889(m)	-	1392(m)	-	-	-	1635(s)	-
$[\text{BF}_2(\text{dma})]$	1407(s), 978(m) 1092(m)	-	1262(m)	-	-	-	1638(s)	-
dma-$\text{BF}_2\text{-OTf}$	1383(s), 615(m) 935(m)	-	1252(m)	-	1194(s) 1149(s)	-	1657(s)	-
P_{888}O	2951(s), 2918(s) 2850(s)	1465(s) 720(m)	-	-	-	1145(s)		
$[\text{BF}_3(\text{P}_{888}\text{O})]$	2957(s) 2925(s) 2856(s)	1465(s)	-	-	-	1055(s)	-	-
$\text{P}_{888}\text{O-}\text{BF}_2\text{-OTf}$	2944(s), 2928(s) 2858(s)	1469(s) 618(w)		1383(s)	1197(s)	-	-	1200
P_{888}	2954(s), 2922(s) 2853(s)	1459(s) 720(m)	-	-	-	-	-	-
$[\text{BCL}_3(\text{P}_{888})]$	2951(s), 2919(s) 2852(s)	1463(s) 694(m)	-	-	-	-	-	-
$\text{P}_{888}\text{-}\text{BCL}_2\text{-OTf}$	2951(s), 2919(s) 2852(s)	1469(s)	1463(m) 694(s)	-	-	-	-	1204
$[\text{BF}_3(\text{P}_{888})]$	2956(s) 2923(s) 2855(s)	1462(s) 878(s) 673(w)	-	-	-	-	-	-
$\text{P}_{888}\text{-}\text{BF}_2\text{-OTf}$	2954(s) 2928(s) 2858(s)	1468(s) 618(w)	-	1383(s)	1158(s)	-	-	1200

3.2.4.3 Conclusions and remarks on attempted synthesis of borenium ILs with triflate anions

Comparing electronic properties of the $[\text{OTf}]^-$ anion and chlorometallate anions, $[\text{MCl}_4]^-$ and $[\text{M}_2\text{Cl}_7]^-$, the triflate is most coordinating - clearly too much to sustain a free borenium cation. This was explicitly demonstrated through ^{11}B NMR spectra, where all signals from ^{11}B were in tetracoordinate region.¹⁹³ Furthermore, it appears that it is very easy to induce over triflation of the boron centre, irrespective of the halide, which leads to a complex mixture of tetracoordinate boron compounds. Surprisingly, these compounds remain liquids.

Since the triflate is an exceptionally good leaving group, it is assumed that there is only a very weak interaction of $[\text{OTf}]^-$ with the cationic boron, combined with the steric accessibility of the boron centre. In consequence, should a more coordinating group appear, triflate would be replaced leading to a more stable Lewis acid-base adduct formation.¹⁹⁴ This result echoes the masked borenium cation suggested by Ingleson (Figure 3-22).¹⁹⁴

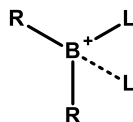


Figure 3-22: Example of a “masked” borenium cation.

Although coordinationally saturated, boron triflate systems may be catalytically active Lewis acids through generation of a transient ‘masked’ borenium cation. Therefore, these surprising liquids were considered worth further study for their Lewis acidity. At the same time, very corrosive nature of fluorides prevented physico-chemical characterisation characteristic of ionic liquids - TGA and viscosity/density measurements have not been recorded in fear of potential equipment damage.

3.2.5 Lewis acidity of chlorometallate and triflate systems

Lewis acidity of the chloroaluminate and triflate systems was measured *via* the acceptor number (AN) – discussed in introduction. Gutmann method which involved straightforward NMR-based approach,⁵³ which has already been used for Lewis acidic ionic liquids, over a wide compositional range, and gave good correlations for measurements performed independently by different groups.^{165,53} Furthermore, this method was considered an ideal analytical tool for measuring Lewis acidity in boron compounds.¹⁶⁵

3.2.5.1 Lewis acidity of borenium chlorometallate ionic liquids

3.2.5.1.1 Gutmann AN values for neat borenium chlorometallate ionic liquids

TEPO was added to ionic liquids in a glove box, and it dissolved readily in all chlorometallate samples within several minutes.

At a molecular level, it can be envisaged that the basic tepo coordinates to different Lewis acidic sites of borenium ionic liquid, acting as yet another donor ligand.^{192,195,165} In the first approximation, tepo was expected to react with two main Lewis acidic centres: the boron centre of the borenium cation and a Lewis acidic anion: $[\text{Al}_2\text{Cl}_7]^-$ or $[\text{Ga}_2\text{Cl}_7]^-$. Furthermore, considering the complicated speciation of borenium chlorometallate ionic liquids detected *via* NMR spectroscopy, and approximated as $(\text{BCl}_3)_a[\text{BCl}_2\text{L}]_b[\text{MCl}_2\text{L}_2]_c[\text{MCl}_4]_d[\text{M}_2\text{Cl}_7]_e$, the molecular BCl_3 could be targeted, in addition to $[\text{BCl}_2\text{L}]^+$ and $[\text{M}_2\text{Cl}_7]^-$. Some likely coordination modes of tepo in 4-pic- BCl_3 -2 AlCl_3 are exemplified in Figure 3-23.

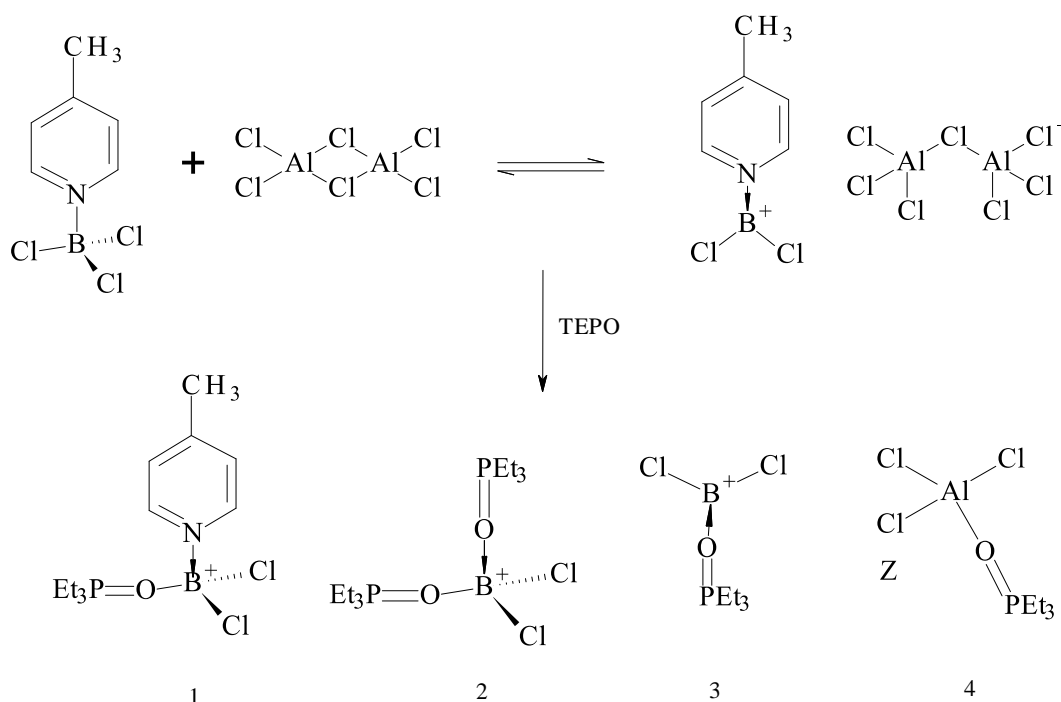
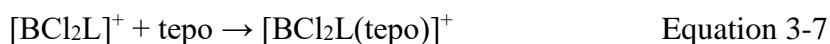


Figure 3-23: Possible main coordination modes for tepo in a borenium ionic liquid, 4-pic- BCl_3 -2 AlCl_3 .

In contrast to the expected complexity, the ^{31}P NMR spectra of tepo solutions in borenium chlorometallate ionic liquids were rather simple. ^{31}P NMR spectra obtained for the pure solutions of triethylphosphine oxide in the chloroaluminate systems showed consistently two peaks. In

addition, the ^{31}P NMR spectra for the $\text{P}_{888}\text{O-BCl}_3\text{-}n\text{MCl}_3$ and the $\text{P}_{888}\text{-BCl}_3\text{-}n\text{MCl}_3$ ionic liquids showed peaks originating from the ligands in these ionic liquids. Signals originating from the probe were much weaker than ligand signals, but could be identified by the comparison of ^{31}P NMR spectra of neat ionic liquids, and ILs with tepo in them. Finally, the ^{31}P NMR spectra for $\text{dma-BCl}_3\text{-2AlCl}_3$ also showed several weak peaks in the region associated with tepo-Al coordination, and this can be associated with complicated speciation of the aluminium species remaining in the liquid.

Where the two signals (or their groups) were identified, the more shielded one corresponded to chemical shifts recorded for tepo in chloroaluminate ionic liquids (Equation 3-6), and another was extremely deshielded - therefore assigned to the borenium cation (Equation 3-7).



The borenium chlorogallate ionic liquids, however, mostly showed a single ^{31}P NMR signal, corresponding to the borenium cation. The differences in ^{31}P NMR spectra of $\text{L-BCl}_3\text{-}n\text{AlCl}_3$ and $\text{L-BCl}_3\text{-}n\text{GaCl}_3$ systems can be derived from the differing affinity of boron, aluminium and gallium to *O*-donors, which holds true for any basic spectroscopic probe.^{14,53}

Examples of ^{31}P NMR spectra recorded for 1% of tepo in $\text{mim-BCl}_3\text{-2MCl}_3$ systems, along with assignments and resulting AN values, are shown in Figure 3-24.

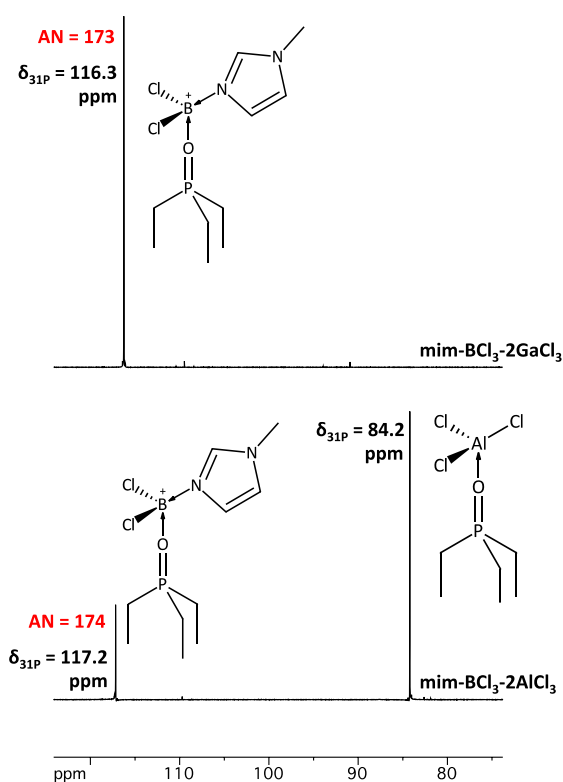


Figure 3-24. ^{31}P NMR spectra (161.96 MHz, 27 °C, neat liquid with DMSO-d_6 lock) of 1 % tepo solution in borenium ionic liquids of a general formula $\text{mim-BCl}_3\text{-2MCl}_3$; ^{31}P NMR chemical shifts and AN values marked for each signal

The ^{31}P NMR chemical shift recorded for tepo coordinating to chloroaluminate anion was pretty much independent of the ionic liquid measured. In contrast, in all measured borenium chlorometallate ionic liquids, chemical shift corresponding to the borenium cation varied through the range of compositions studied. Therefore, it was this signal that was the subject of further analysis in this work. The list of ^{31}P NMR chemical shifts associated with tepo coordinating to borenium cation is given in Table 3-18 *Table 3-18*.

Table 3-18: AN values for L-BCl₃-nMCl₃ systems, along with the δ_{31P} resonances (in ppm) measured for solutions of 1 mol% tepo in these liquids, referenced to δ_{31P} , H₃PO₄ (85%) = 0.0 ppm.

L	AlCl ₃		2AlCl ₃		GaCl ₃		2GaCl ₃		3GaCl ₃	
	δ_{31P}	AN	δ_{31P}	AN	δ_{31P}	AN	δ_{31P}	AN	δ_{31P}	AN
4-pic	96.2	124	105.6	170	96.5	121	100.6	140	119.5	180
mim	-	-	117.1	174	-	-	115.6	173	117.4	174
dma	-	-	112.4	163	-	-	112.2	163	112.2	163
P₈₈₈o	100.5	136	104.5	144	109.9	156	109.9	157	110.0	157
P₈₈₈	84.6	98	84.6	98	110.7	159	110.7	159	110.7	159

³¹P NMR chemical shifts for tepo in borenium chlorometallate ionic liquids with excess of MCl₃ showed larger deshielding, which indicated a higher functional Lewis acidity (Table 3-18). The trend was similar for both L-BCl₃-nAlCl₃ systems and L-BCl₃-nGaCl₃. This indicates that borenium cation is interacting strongly with the [MCl₄]⁻ anion, which lowers its acidity; in contrast, weak interaction with [M₂Cl₇]⁻ enhances the acidity by leaving ‘naked’ borocation exposed to the tepo probe.

Except for P₈₈₈-BCl₃-nAlCl₃, the borenium cations, [BCl₂L]⁺, were found to be the strongest Lewis acids in the system. Calculated AN values (AN = 120-181, Table 3-18) included the highest AN values reported in the literature to date. Reported values of AN >100 render borenium ionic liquids as Lewis superacids, according to Gutmann’s arbitrary scale, where hexane has AN = 0, and SbCl₅ in dichloroethane has AN =100, and any acid with AN > 100 is considered a Lewis superacid.^{4,53} Even for systems with equimolar amounts of metal chloride, where halide abstraction was not complete, the AN values were still superacidic in Gutmann’s arbitrary scale. These values are much higher than those determined for some borenium cations in solutions, for example, AN=80-85 for [B(C₆F₅)₂L]⁺ in CD₂Cl₂, and AN = 146 (δ_{31P} = 106.9 ppm) for the [(cat)B]⁺ cation (where cat is catecholato) in C₆D₆.^{196,197}

AN values of these ionic liquids varied in a wide range depending on the ligand used; higher values were recorded in systems with *N*-donor compared to *P*-donor. This is because first-row donors such as amines show greater Lewis basicity towards BCl₃ and BF₃ than second-row donors such as phosphines: *viz.*, N>P, O>S.¹⁹⁸ Interestingly, for the narrow selection of aromatic

N-donor ligands used in this work, AN values appear to correlate well with pK_a values reported in Table 2-1: the stronger the base, the higher the acceptor number.

Replacing $AlCl_3$ with $GaCl_3$ had no effect on the acidity of the mim- BCl_3 - $2MCl_3$ systems and dma- BCl_3 - $2MCl_3$ systems, which remained at $AN = 174 \pm 1$ and 163 ± 1 , respectively. In contrast, borenium cations with 4pic, P₈₈₈ and P₈₈₈O ligands still interacted to an extent with the anions, which resulted in anion-dependent AN values: the least coordinating anion, $[Ga_3Cl_{10}]^-$, afforded the highest acidity in these systems.⁴ This pattern was unforeseen, considering that a full halide abstraction by ^{11}B NMR spectroscopy was observed for all of the L- BCl_3 - $2MCl_3$ systems reported.

3.2.5.1.2 Influence of solvent on the Lewis acidity of borenium chlorometallate ionic liquids

In the section above, high values of AN for L- BCl_3 - $2MCl_3$ were explained based on the ionic environment - that is, a ‘free’ borenium cation, with very little interference from the anion. However, it was noted that borenium cations in solutions had lower AN values.^{196,197} In addition, previous studies showed that the solvent has an effect of the Lewis acidity of the solute.^{22,199}

To elucidate the influence of the organic solvent solution *vs.* the neat ionic liquid environment on Lewis acidity of borenium cations, the AN values of four neat borenium liquids: 4pic- BCl_3 - $2AlCl_3$, 4pic- BCl_3 - $2GaCl_3$, mim- BCl_3 - $2AlCl_3$ and mim- BCl_3 - $2GaCl_3$ were compared to AN values recorded for their solutions in dichloromethane (DCM). The DCM solutions were prepared by mixing of equal volumes of ionic liquids and dry DCM, and their AN values were measured using the same methodology as for neat ILs. The results of experiment are presented in the Table 3-19.

Table 3-19: AN values for all L- BCl_3 - $nMCl_3$ systems, neat and in DCM solution, along with the δ_{31P} resonances (in ppm) measured for 1 mol% *tepo* content, and referenced to δ_{31P} , H_3PO_4 (85%) = 0.0 ppm.

L	L- BCl_3 - $2AlCl_3$				L- BCl_3 - $2GaCl_3$			
	δ_{31P}		AN		δ_{31P}		AN	
	<i>solution</i>	<i>neat</i>	<i>solution</i>	<i>neat</i>	<i>solution</i>	<i>neat</i>	<i>solution</i>	<i>neat</i>
4-pic	98.4	105.6	140	170	95.5	100.6	124	140
mim	117.1	117.1	174	174	111.8	115.6	162	173

In the first instance, this huge change in acceptor number values of the ILs and the difference ^{31}P NMR chemical shift values was postulated to be due to (a very unexpected)

coordination of the solvent rather than just the introduction of a solvent. However, surprisingly, ^{11}B NMR spectra of the solutions revealed that the borenium cation retained its tricoordinate structure in DCM. This NMR data suggested that there was no strong solvent-IL interaction as first presumed. On the basis of this interpretation, the spectrum of the ILs in DCM represented the non-associated molecule, which suggested that the lower AN values seen was rather due to decrease in electrophilicity arises from solvation rather than coordination. This confirmed that ionic environment of the ILs were affected by the presence of a solvent in their Lewis acidity measurements. In consequence, turning borocations into ionic liquids has helped to harness the full Lewis acidity of the boron centre by access to the “naked” borenium cations.

3.2.5.2 *Lewis acidity of the triflate systems*

The Lewis acidity of borenium triflate systems was investigated to identify if these are stable molecular species (boranes), or masked borenium cations with a very weak $\text{B}\cdots\text{OTf}$ bond.²⁴ Ingleson explained that an “anion-coordinated species can exhibit borenium-type reactivity, provided the anion is sufficiently weakly coordinating and readily displaced by another nucleophile”.²⁴ On practical terms, this would be indicated by the ability of these systems to interact with the probe.

Since all triflate systems were liquids, tepo was dissolved in neat liquids (following the same procedure as for borenium chlorometallate ionic liquids) and ^{31}P NMR spectra were measured. Again, tepo dissolved readily in all tested samples.

The acceptor number measurements (Table 3-20) revealed that triflate liquids were indeed Lewis acidic, with acceptor numbers in the Lewis superacidic regions, albeit just about fitting within the threshold ($\text{AN} \leq 108$), which suggest that tetracoordinate boron complexes are indeed masked borenium cations, with transient $\text{B}\cdots\text{OTf}$ bond, readily displaced by another nucleophile (tepo).²⁴

Table 3-20: AN values for all L-BX₂-nOTf systems based on the different donors that were homogenous liquids along with the δ_{31P} resonances (in ppm) measured for solutions of these liquids containing 1 mol% tepo (referenced to δ_{31P} , H₃PO₄ 85%=0.0 ppm).

L	L-BF ₂ -OTf		L-BCL ₂ -OTf	
	δ_{31P}	AN	δ_{31P}	AN
4-pic	94.4	121	96.8	126
mim	92.5	116	103.9	143
dma	90.7	112	-	-
P₈₈₈O	89.2	108	-	-
P₈₈₈	88.8	108	-	-

A values recorded for the triflate systems were much lower for compared to the chlorometallate systems. This can be described in several ways. Either pyramidalisation to form [BX₂(OTf)L] adducts hindered tepo from accessing the “naked” borenium cations, in which the full Lewis acidity of the system could be explored,⁴ or tepo replaced [OTf]⁻, which acted as counteranion, more coordinating than [MCl₄]⁻, and consequently lowering the acidity of the boron centre. Finally, it must be realised that - as emphasised in the discussion on chlorometallate systems - tepo is partaking in complex equilibria. Therefore, its ³¹P NMR chemical shift value in its Lewis acid-base adduct is influenced by the position of the association/dissociation equilibrium.

Irrespective of the perspective we adopt, the practical conclusion that is bound to reflect in catalytic activity is as follows: acidity of a borenium cation decreases with increasing basicity of the accompanying anion.

With regards to the influence of a halide, it was observed that the triflate systems with chlorides on boron had higher acceptor numbers than those formed from boron trifluoride complexes (Table 3-20). This originates directly from Lewis acidities of boron trihalides towards nitrogen or oxygen bases, which increases down the halogen group BF₃< BCl₃< BI₃.¹⁸ Therefore, it could be expected that [BCL₂L]⁺ will have higher acidity compared to [BF₂L]⁺ - also in a masked version with coordinating triflate.

3.3 CONCLUSIONS

Work described in this chapter draws on development in borocation chemistry and in Lewis acidic ionic liquids. It was concluded with the first reported family of ionic liquids with Lewis acidic cations: borenium chlorometallate ionic liquids, L-BCl₃-MCl₃, which was reported in *Angewandte Chemie*.⁴ This work inspired an application of borenium ionic liquids as catalyst for oligomerisation of olefins (outside the scope of this thesis), which resulted in world patent application.²⁰⁰

These preliminary findings brought several conclusions:

1. The initial formation of a borenium ionic liquid by halide abstraction using MCl₃ (M = Al or Ga) depends on the propensity of [BX₃L] to undergo halide abstraction, and will work for L-BCl₃-MCl₃, but not for L-BF₃-MCl₃.
2. Successful formation of a borenium ionic liquid, [BCl₂L][M_xCl_y], depends on the nature of the donor, L, and its relative affinity to B and M. Aromatic *N*-donors tend to stabilise the borocation and only a small percentage of ligand undergoes scrambling, leading to ionic liquid of a general formula (BCl₃)_a[BCl₂L]_b[MCl₂L₂]_c[MCl₄]_d[M₂Cl₇]_e. The scrambling percentage was increased for aliphatic *P*-donor, and was very significant for the *O*-donors - to the extent that it formed liquid coordination complex of aluminium/gallium, with solubilised BCl₃.
3. Borenium chlorometallate ionic liquids were Lewis superacidic by Gutmann AN values, with [BCl₂(*N*-donor)]⁺ cations reaching acceptor numbers up to AN = 181 - the highest reported in the literature. It was explicitly demonstrated that this was achieved by the combination of two factors: (i) using non-coordinating anions [M₂Cl₇]⁻ and [Ga₃Cl₁₀]⁻, and (ii) the ionic environment, which removed solvating effect from molecular solvents, leaving in conclusion access to ‘naked’ borenium cation.
4. Metal chlorides as halide abstracting agents were not ideal, because they: (i) do not abstract fluoride readily, (ii) allow for ligand scrambling - thus decrease concentration of Lewis superacidic borenium cation, and (iii) introduce alternative Lewis acidic centres, that may have negative impact, *e.g.* on selectivity in a Lewis acid catalysed reaction.

Alternative systems with triflate anions, L-BX₂-OTf, were the first attempt to circumvent the problems outlined above. However, triflate - as more coordinating than chlorometallate anions -

coordinated to boron forming ‘masked’ borenium cations. Although they are molecular compounds, not ionic liquids, they remain highly Lewis acidic liquids - therefore potentially useful in Lewis acid catalysis.

Acceptor number measurements gave promising results, indicating the potential of high to extremely high catalytic activity of the synthesised liquids with electron-deficient boron centres. Naturally, a question remains as to whether the measurements with this particular probe - tepo - will correspond to catalytic activity. The next two chapters describe attempts to explore this question.



CHAPTER FOUR

“In three words, I can sum up everything I’ve learned about life: it goes on.”

—Robert Frost



4 DIELS-ALDER CYCLOADDITION

A large portion of this work was carried out on a placement in the Chrobok group, at Silesian University of Technology, Poland. This Short Term Scientific Mission (7 weeks) was funded by the EU programme, CMST COST EXIL 1206 - Exchange on Ionic Liquids.

4.1 INTRODUCTION

4.1.1 General remarks on Diels-Alder reaction

Diels–Alder reaction belongs to a class of reactions called cycloadditions, which are one of the most important tools for the carbon-carbon bond formation, particularly in the syntheses of polycyclic rings.¹⁷⁹ It is widely used in the chemical industry, as a powerful tool for one-step synthesis of six-membered carbocycles, which are found in compounds use for drug delivery, biochemical applications and material science.^{201,202,203}

Diels-Alder reaction was first discovered in 1928 by Otto Paul Hermann Diels and Kurt Alder.²⁰⁴ In 1950, Otto Paul Hermann Diels and Kurt Alder were jointly awarded the Nobel Prize in Chemistry for their discovery and development of the diene synthesis.^{204,203} It is a combined process, which involves the formation of bonds and the breaking of bonds at the same time.^{205,204} By definition, Diels-Alder reaction is the addition of a conjugated diene to dienophile, to form a cyclic olefin (Figure 4-1) - that is, a $[4 + 2]$ cycloaddition.^{201,204,205} In a typical Diels-Alder reaction, a conjugated diene reacts with a double-bonded dienophile through the interaction of a 4π electron system in the diene structure with a 2π electron system in the dienophile structure.^{206,207} The driving force is the conversion of two π -bonds into two σ -bonds.²⁰⁶

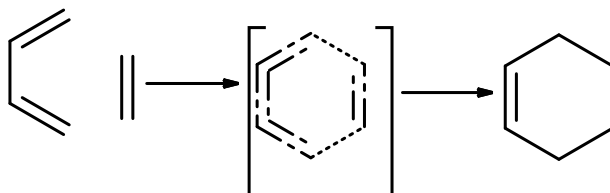


Figure 4-1: Simple $[4 + 2]$ cycloaddition reaction.

Considering a slightly more complicated case of Diels–Alder reaction involving a functionalised olefin, two different cycloadducts are formed, denoted as *endo* and *exo* (Figure 4-2)

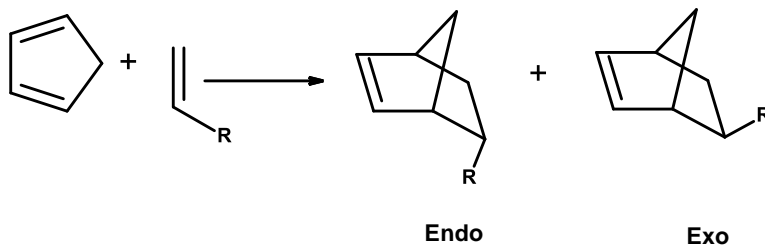


Figure 4-2: Stereoselectivity (*endo: exo*) in Diels–Alder reaction.

When the reaction is kinetically controlled, *endo* is often the major product.^{208,203} However, Diels-Alder reaction can also be thermodynamically controlled, and in such cases the *exo* cycloadduct is the major product formed.^{208,203}

Diels-Alder reaction can be carried out in the absence of catalysts in most cases.¹⁷⁹ However, when poor dienophiles such as cycloenones or methyl methacrylate (MMA) are used, the reaction proceeds extremely slowly.^{209,179} Increasing the temperature is naturally helpful in increasing the reaction rate, but often impairs the *endo:exo* selectivity. One key requirement for a green reactions/process is significant rate enhancement and high yield/selectivity^{114,43} Therefore, using homogeneous Lewis acid catalysts became the tool to retain good *endo:exo* selectivity whilst increasing the reaction rate. The complexation of the dienophile to the Lewis acid increases the reaction rate and improves the stereoselectivity, seeing that the *endo* orientation forms product faster, but *exo* orientation forms the more stable product.^{8203,8}

Lewis acidic catalysts tested in Diels-Alder include traditional Lewis acids such as BF_3 , ZnCl_4 , AlCl_3 and SnCl_4 ,²⁰⁹ and others including $\text{Sc}(\text{OTf})_3$.⁹⁰ Lithium perchlorate–diethyl ether compounds, also known as LPDE mixtures have received a lot of attention in this regards due to their ability to significantly accelerate the rate and improve selectivity obtained in Diels-Alder reaction.¹¹⁴ The improved reactivity in LPDE was thought to be due to high internal pressure and the Lewis acidic nature of the lithium ion.¹¹⁴

In a Diels-Alder reaction, Lewis acid acts through coordination to the dienophile, exerting a strong effect on the reaction rate and consequently on the selectivity (Figure 4-3).²⁰³ The Lewis acid-dienophile complex becomes highly electrophilic and more reactive towards the

diene. In addition to affecting the kinetics, the reaction is sensitive to the strength of Lewis acidity, which reflects mainly in changes in stereoselectivity of the *endo:exo* isomers.²⁰³

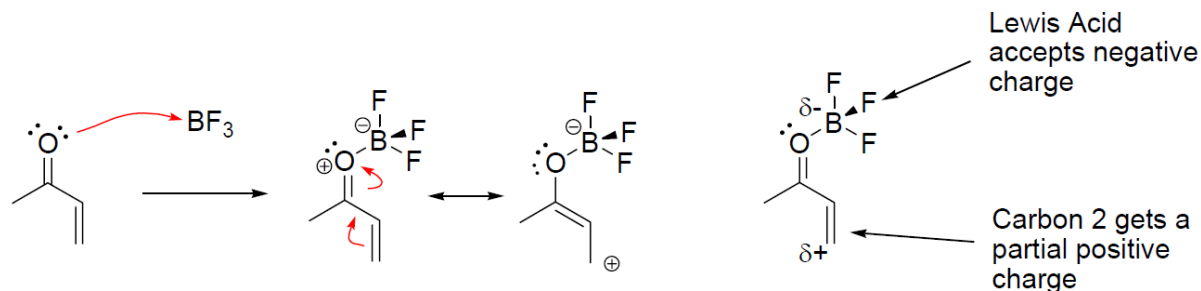


Figure 4-3: Lewis acid catalysis in Diels-Alder reaction.²⁰³

Main challenges in using conventional, homogenous Lewis acid catalysis for Diels-Alder reaction are: (i) large amounts of catalyst needed, and (ii) difficulties in recovery from the product mixtures and subsequent reuse.^{179,114,43} From these follow secondary problems with the production of environmentally hazardous waste, and the requirement for complex separation procedures.^{179,114} Solid-supported (heterogeneous) catalysts have been tested to overcome the problem of catalyst lost and separation difficulties.^{179,43} Examples of such catalysts include AlCl_3 immobilised on polymers (polystyrene) or inorganic oxides (silica). However, the immobilisation of the Lewis acid onto a support tends to be much more expensive than the catalyst itself, and often requires several steps.¹⁷⁹ Other approaches rely on the use of solvents altering the structure of transition states, such as water or surfactants.¹¹⁴ This category includes also ionic liquids, discussed at a greater length in section 1.5.^{23,95}

4.1.2 Boron Lewis acids in Diels-Alder reaction

In 2005, Piers *et al.*²³ published an extensive report on the use of borocations, more specifically borenium cations, as enantioselective Lewis acid catalysts in Diels-Alder reactions. Much of these were developed by Corey and co-workers.^{23,216} The topic was further covered in a 2012 review by DeVries,⁸ who outlined the uses of cationic tricoordinate boron compounds in two aspects: as Lewis acidic catalysts (especially chiral compounds used in asymmetric syntheses) and as reactants in hetero-Diels-Alder.

Hetero-Diels-Alder, where at least one heteroatom is involved in the cyclisation, and asymmetric Diels-Alder reactions, which are catalysed by chiral Lewis acids, are very broad

topics which were outside the scope of the screening study reported in this chapter - and consequently outside of the introduction scope. However, as an example, the first Diels-Alder reaction involving boron compounds (Mikhailov and co-workers, 1972),²¹² where 1-boron-substituted 1,3-diene is employed in a tandem [4+2] cycloaddition, is shown in Figure 4-4.^{212,213}

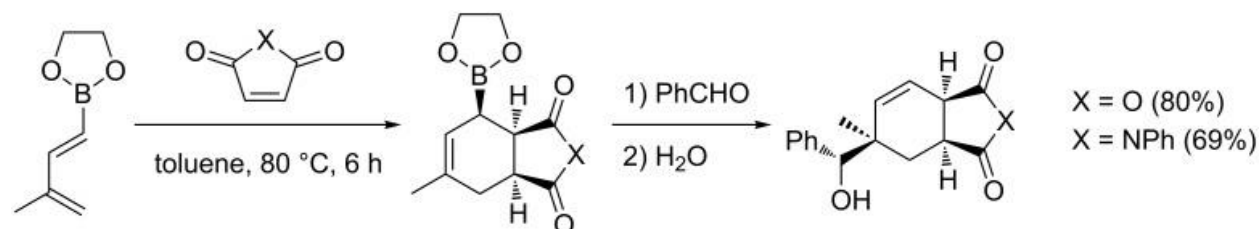


Figure 4-4: 1-Boron-substituted 1,3-diene in a tandem cycloaddition [4 + 2]/allylboration.²¹⁴

4.1.3 Ionic liquids in Diels-Alder reaction

Ionic liquids have been widely used in catalytic applications, as solvents, catalyst, catalyst activators - and often combining several of these functions.²¹⁵ This included their use as non-traditional solvents for Diels-Alder reactions.^{209,3,118} Their advantages in the Diels-Alder context were: the ease of products separation by extraction or under reduced pressure (ILs tend to have negligible vapour pressure), safety (non-flammable and non-explosive), and tuneability of structure, giving hope to tune catalytic activity.^{201,114}

The first application of ILs for Diels-Alder reactions was reported in 1989 by Tucker.²¹⁶ It involved the reaction between cyclopentadiene and an alkyl acrylate (*i.e.* methyl acrylate and methyl vinyl ketone) using ethylammonium nitrate, [EtNH₃][NO₃].^{216,202} The resulting ratio of *endo:exo* products was 6.7:1 (87% *endo* selectivity). A decade later, Lee reported the first study on chloroaluminate ionic liquids as solvent/catalyst for the Diels-Alder reaction, to improve the selectivity and reaction based on the polarity, high solubility towards organic and inorganic solutes and the variable Lewis acidity of these ILs. It was pointed out that they acted as Lewis acids as well as Bronsted superacids (due to the presence of adventitious protons).²¹⁷ Since then, Lewis acidic ionic liquids, most prominently chloroaluminate systems, have been reported to be highly active catalysts and exhibit high *endo:exo* stereoselectivity.^{218,216,202} Disadvantages of these chloroaluminate ILs include the fact that they are water-sensitive and sometimes soluble in the reactants.¹⁷⁹

Besides room temperature chloroaluminate ionic liquids, other types of ILs have consequently been used as solvent/catalyst for the Diels-Alder reaction. ‘Conventional’ room

temperature ionic liquids have been found to be excellent solvents for Diels-Alder reactions - examples include [bmim][OTf], [bmim][PF₆], [bmim][BF₄], and [bmim][lactate], where bmim = 1-butyl-3-methylimidazolium.²⁰¹ Solvate ionic liquids,¹¹² based on lithium salts solvated with glymes, were reported as greener and more efficient alternatives to lithium perchlorate in diethyl ether for Diels-Alder and [2+2] cycloaddition reactions.¹¹²

In this work, borenium ionic liquids were not intended to use as solvents, but as catalysts in solvent free mixture of liquid Diels-Alder reactants. Considering high acidity of borenium systems, it was anticipated that it would be feasible to use them at very low loadings and at low temperatures, to attain both high conversion rates and high *endo:exo* selectivities. This approach would deliver a greener alternative to the presently available Lewis acid catalysts for Diels-Alder reaction.²¹⁵ Before commencing this study, it was speculated that borenium ILs could be either separated (as immiscible with the products) or reused, or the amount would be so small that they would be neutralised and discarded - generating comparatively small waste stream.

4.3 EXPERIMENTAL

4.3.1 Syntheses

Unless otherwise mentioned, all chemicals were purchased from Sigma-Aldrich. Cyclopentadiene (CPD) was obtained by distilling of dicyclopentadiene (DCPD) prior to use and stored in the fridge. Starting materials used in Diels-Alder reaction were dried (for at least 24 h prior to use) over 3 Å molecular sieves. Borenium ionic liquids, synthesised as described in section 3.1.1, were stored and handled in the glovebox. All glassware, stirring bars, syringes *etc.* were oven-dried (*ca.* 140 °C, for at least 24 h prior to use). Cycloaddition reactions were carried out in a 50 cm³ flask under dry nitrogen atmosphere.

¹H, ¹³C and ¹¹B NMR spectra were recorded at ambient temperatures, using the Bruker Avance 400 (400 MHz) NMR spectrometer. Analytical thin layer chromatography (TLC) was performed on a 0.25 mm silica gel plates (*ex Merck*).

4.3.1.1 Diels-Alder reaction – solvent free

An internal standard, *n*-decane (0.2 g) was added into a 50 cm³ two-necked round-bottomed flask equipped with a stirring bar, thermometer and septum, followed by the dienophile (16 mmol) was dissolved in the solution. The reaction flask was purged with dry nitrogen and immersed in an ice bath (0 °C), with reaction mixture stirred to ensure equilibration at the temperature. In the glovebox, an appropriate amount of borenium ionic liquid (0.1-1.0 mol % per dienophile) was weighed into a gas-tight syringe. The tip of the syringe was protected until it reached the septum of the reaction flask. The catalyst was added to the solution containing the dienophile drop-wise and stirred vigorously (1500 rpm). The diene (24 mmol) was then added drop-wise to the solution, over 1 min. Reaction was allowed to carry on with stirring for 5 min, before it was stopped (quenched with deionised water). Progress of the reaction was followed using a Perkin Elmer Clarus 500 GC with FID detector, equipped with a SUPELCOWAXTM 10 column (30 m×0.2 mm×0.2 µm). As stated, *n*-decane was the internal standard.

4.3.1.2 Diels-Alder Reaction - in solvent

Dichloromethane (5 - 30 mL) was measured using a measuring cylinder, and transferred into a 50 cm³ two-necked round-bottomed flask equipped with a stirring bar, thermometer and septum. An internal standard, *n*-decane (0.2 g) was also added. Then the dienophile (16 mmol) was

dissolved into the solution. The reaction flask was purged with dry nitrogen and immersed in an ice bath (-10 °C, -5 °C, 0 °C, RT), with reaction mixture stirred to ensure equilibration at the temperature. In the glovebox, an appropriate amount of borenium ionic liquid (0.1 to 1.0 mol % per dienophile) was weighed into a gas-tight syringe. The tip of the syringe was protected until it reached the septum of the reaction flask. The catalyst was added to the solution containing the dienophile drop-wise and stirred vigorously (1500 rpm). The diene (24 mmol) was then added drop-wise to the solution, over 1 min. Reaction was allowed to carry on for 2 h before it was stopped (quenched with deionised water). Progress of the reaction was followed using a Perkin Elmer Clarus 500 GC with FID detector, equipped with a SUPELCOWAXTM 10 column (30 m×0.2 mm×0.2 µm). As stated, *n*-decane was the internal standard.

4.3.1.3 Analyses of Diels-Alder reaction products

The products solution, quenched with deionised water. The solution was then washed with dichloromethane (2 cm³) to extract organic layer from the reaction mixture. The bottom organic layer was then separated from the aqueous layer, dried over anhydrous magnesium sulphate and filtered. All the fractions were analysed by TLC (Merck pre-coated silica gel plates with F254 indicator using dichloromethane as solvent. The isolation of pure products was accomplished by silica gel (60-120 mesh) column chromatography with dichloromethane as eluting solvents. Fractions containing pure compounds were combined and the solvent was removed using a rotary evaporator (40-50 °C), and subsequently under high vacuum (temperature, pressure) to produce the crude cycloadducts. The products were analysed using Perkin Elmer Clarus 500 GC-MS with SUPELCOWAXTM 10 column (30 m×0.2 mm×0.2 µm), and Bruker AvanceIII 400 MHz spectrometer to confirm the structures (¹H and ¹³C NMR spectra were recorded). The yield of products and *endo:exo* ratios were calculated based on the GC with FID detector, equipped with a SUPELCOWAXTM 10 column (30 m×0.2 mm×0.2 µm), and *n*-decane as the internal standard.

4.3.1.4 NMR spectroscopy data of products

CPD + EA (Table 4-3) Analytical data of product **1**: **C₁₀H₁₄O₂**. ¹H NMR (400 MHz, CDCl₃) δ = 6.18(dd,1H), 5.92(dd,1H), 4.08(m,1H), 3.62(s,1H), 3.22(s,1H), 3.20(m,1H), 2.92(m,1H), 2.90(s,1H), 1.88(m,1H), 1.42(m,1H), 1.28(m,1H), 1.27(m,1H), 1.23(s,3H), ppm. ¹³C NMR

(CdCl₃, 151 MHz) δ = 177.36, 140.30, 134.96, 62.72, 52.24, 48.32, 45.98, 45.18, 31.85, 16.92 ppm.

CPD + MA (Table 4-3) Analytical data of product **2: C₉H₁₂O₂** ¹H NMR (400 MHz, CDCl₃) δ = 6.19(dd,1H), 5.93(dd,1H), 3.69(s,1H), 3.63(s,3H), 3.20(s,1H), 2.95(s,1H), 2.90(s,1H), 1.91(m,1H), 1.43(m,2H), 1.27(d,1H) ppm. ¹³C NMR (151 MHz, CdCl₃) δ = 177.89, 140.38, 135.01, 54.10, 52.26, 48.30, 45.82, 45.16, 31.91 ppm

CPD + MVK (Table 4-3) Analytical data of product **4: C₉H₁₂O**. ¹H NMR (400 MHz, CDCl₃): δ = 6.16(dd, 1H), 5.88 (dd, 1H), 3.26 (s, 1H), 3.03 (m, 1H), 2.87 (s, 1H), 2.15 (s, 3H), 1.67 (m, 1H), 1.48 (m, 1H), 1.33(m, 1H), 1.26(s, 1H) ppm. ¹³C NMR (CdCl₃, 151 MHz) δ = 211.61, 140.51, 133.86, 55.01, 52.59, 48.50, 45.32, 31.83, 30.08 ppm.

4.4 RESULTS AND DISCUSSION

4.4.1 General remarks

The main study on Diels-Alder cycloaddition was carried out in the presence of a borenium ionic liquid used in catalytic amounts, solvent free, with the combination of liquid starting materials used neat (diene in excess). This was to harvest all the benefits of using ‘naked’ borenium cation in catalysis.

The diene was added drop-wise to the solution to avoid dimerization/polymerisation. It is known that dienes especially cyclopentadiene tends to polymerise in the presence of Lewis acids which, in our case was most likely a major side reaction,²¹⁹ as proton-initiated side reactions such as polymerisation of the ene and isomerisation of double bonds in the ene or ene adduct can also occur with our Lewis acid catalyst.^{219,220} Furthermore, the products were isolated using column chromatography, which allowed for the separation of the desired products from any polymers. Using *n*-decane as an internal standard, a calibration curve was developed, based on which quantitative analysis by FID GC were carried out, to calculate the conversion and selectivity of the products. The conversion was defined as the percentage of the substrates consumed and transformed into the product. The *endo:exo* selectivity was expressed as the amount of the each product formed, divided by the amount of total products and multiplied by a factor of 100.

4.4.2 Borenium chlorometallate ionic liquids as catalysts for Diels-Alder reaction

In order to determine the activity of borenium ionic liquids in the Diels-Alder reaction, a model reaction between ethyl acrylate (EA) and cyclopentadiene (CPD) was selected (Figure 4-5)) - as often used and easily compared with other literature systems.

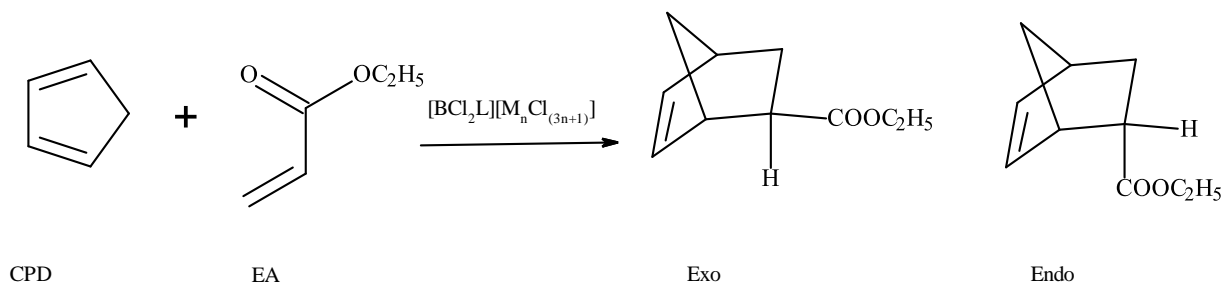


Figure 4-5: Diels-Alder reaction between ethyl acrylate (EA) and cyclopentadiene (CPD), catalyzed with borenium ILs of a general formula $L-BCl_3-2MCl_3$, where $L=mim$, $4-pic$, dma , $P_{888}O$ or P_{888} , $M = Al$ or Ga , $n = 1$ or 2 .

Expecting the high catalytic activity of the borenium ILs, they were firstly tested at 0 °C. Only 0.1 mol% of ionic liquid (per dienophile) was used, compared to mildly acidic chlorozincate ionic liquids being used at a 100-times higher loading of 10 mol% at ambient temperature, which gave *ca.* 90% conversion in 8 min.¹⁰⁶ Furthermore, even highly acidic chloroaluminate and chlorogallate ionic liquids were used at 50-times higher loading of 5 mol% at ambient temperature, which however gave 99% conversion in 5 min.^{3, 221,222}

All reactions carried out on the model reaction system, with a range of borenium ILs as catalysts, and some benchmark catalysts, are listed in Table 4-1. The influences of different variables, summarized in this table, will be discussed below.

Table 4-1: Diels-Alder reaction between cyclopentadiene and ethyl acrylate in the presence borenium ionic liquids, AlCl₃ and chloroaluminate ionic liquids, along with the corresponding AN values, conversions and endo: exo selectivity.

Entry	Catalyst	AN	Amount mol%	conversion α_{EA} , %	Product endo: exo
1	AlCl ₃	96	0.10 0.25	6 99	95:5
2	[C ₂ mim]Cl	-	0.10 0.50	0 3	- 94:6
3	[C ₂ mim][AlCl ₄]	-	0.10 0.50	0 3	- 94:6
4	[C ₂ mim][Al ₂ Cl ₇]	96	0.10 0.25	3 99	94:6
5	[BCl ₂ (4-pic)][GaCl ₄]	121	0.10 0.50	18 97	94:6
6	[BCl ₂ (4-pic)][AlCl ₄]	124	0.10 0.50	23 100	94:6
7	[BCl ₂ (P ₈₈₈)][Al ₂ Cl ₇]	98	0.10 0.50	21 100	94:6
8	[BCl ₂ (4-pic)][Ga ₂ Cl ₇]	140	0.10 0.25	90 100	93:7
10	[BCl ₂ (dma)][Ga ₂ Cl ₇]	163	0.10	97	94:6
11	[BCl ₂ (dma)][Al ₂ Cl ₇]	163	0.10	98	94:6
12	[BCl ₂ (4-pic)][Al ₂ Cl ₇]	170	0.10	100	94:6
12	[BCl ₂ (mim)][Ga ₂ Cl ₇]	172	0.10	100	93:7
13	[BCl ₂ (mim)][Al ₂ Cl ₇]	173	0.10	98	94:6

Reaction conditions: Unless otherwise stated, the reactions were performed with cyclopentadiene (1.586 g, 24 mmol), ethyl acrylate (1.602 g, 16 mmol), ice bath, time = 5 min., r = 1500 rpm; conversion and endo: exo ratio was determined by GC.

As presented in Table 4-1, in all borenium IL-catalysed reactions (entries 5 - 13) full conversion of ethyl acrylate was achieved just after 5 minutes of the reaction, with only 0.5 mol% of the catalyst, at *ca.* 0 °C. This is 10-times lower catalyst loading than that used for chloroaluminate ionic liquids in the literature,²²³ in combination with about 20 °C lower reaction temperature. The cycloadducts were obtained with high stereoselectivity, with ratio of *endo:exo* isomers in the range 93:7 - 94:6. *N.B.*: no traces of by-products were observed by GC.

4.4.2.1 Influence of Lewis acidity (AN) on the reaction products

Variations in *endo:exo* selectivities were minimal, and by and large were within the error bars of the measuring technique. In contrast, conversions at minimum catalyst loading (0.1 mol% per dienophile) varied significantly for different borenium ILs.

The conversion of the dienophile at 0.10% loading of borenium ionic liquid was plotted against AN values (Figure 4-6). For clarity, different borenium ionic liquids are marked on the graph by entry numbers in Table 4-1.

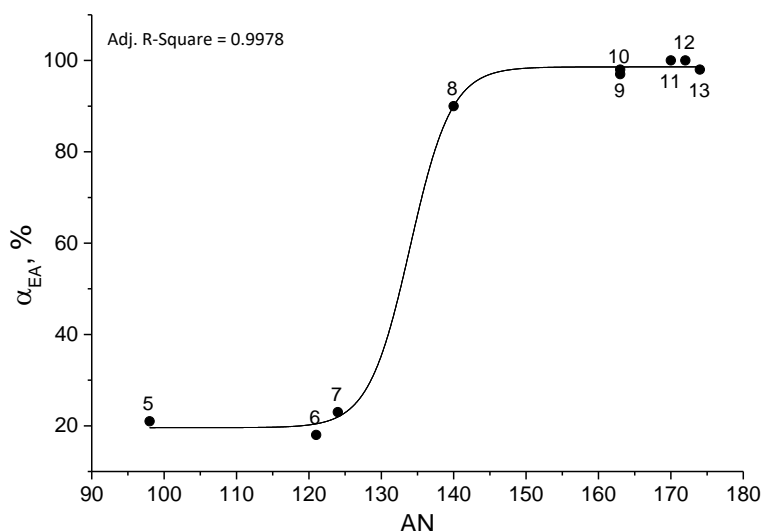


Figure 4-6: Boltzmann fit of experimental data showing conversions in Diels-Alder cycloaddition of cyclopentadiene to ethyl acrylate, catalysed with 0.10 mol% of Lewis acidic ionic liquids vs. AN values of the catalysts; numbers on the figure are identical as catalysts number in Table 4-1. Reaction conditions: cyclopentadiene (1.586 g, 24 mmol), ethyl acrylate (1.602 g, 16 mmol), ice bath, 5 min, 1500 rpm, conversion determined by GC.

Using such a small amount of catalyst was quite challenging, and required strict adherence to good laboratory practice, as the smallest amount of moisture as interfering with results. Nevertheless, despite using extremely small catalyst amount, a good correlation was

found with the experimental data, with Boltzmann sigmoidal correlation ($R^2 = 0.9978$) between the AN values and the dienophile conversion (Figure 4-6). This indicates that there is a certain threshold value in the AN values, for which reaction rate is significantly accelerated. The same was observed in another work of our group, on Diels-Alder reaction catalyzed with liquid coordination complexes.²²⁴

The first and foremost conclusion from this study was that borenium systems outperformed by far chloroaluminate ionic liquids, which are considered a very highly active Lewis acid, which is a promising result for further applications.

4.4.2.2 Influence of catalyst loading

The influence of catalyst loading (0.10 to 1.00 mol% per dienophile) on the conversion and selectivity was explored by testing a borenium ionic liquid of a relatively low AN value, $[\text{BCl}_2(4\text{-pic})][\text{GaCl}_4]$ (AN = 121). Again, the *endo:exo* ratio remained unaffected (94:6), but conversion varied with loading. The conversion of ethyl acrylate, as a function of the catalyst loading, was plotted in Figure 4-7.

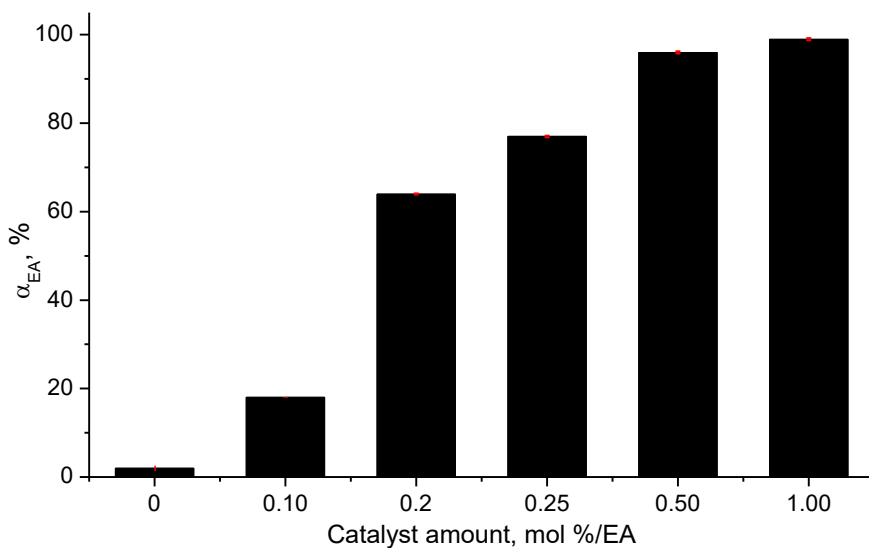


Figure 4-7: Conversion of ethyl acrylate in Diels-Alder reaction, plotted as the function of catalyst loading (mol%, per dienophile). Reaction conditions: cyclopentadiene (1.586 g, 24 mmol), ethyl acrylate (1.602 g, 16 mmol), catalyst $[\text{BCl}_2(4\text{pic})][\text{GaCl}_4]$.

As shown in Figure 4-7, the full conversion was achieved after 5 min, with the ionic liquid loading ≥ 0.50 mol% per dienophile, whereas catalyst loading below 0.50 mol% resulted in the lower conversion after the same reaction time. Still, even minimum loading of 0.1% gave

significantly higher conversion than the non-catalytic benchmark reaction. From previously demonstrated results (Table 4-1) and from this experiment, it was established that using 0.25 to 0.50 mol% of catalyst loading would generally produce 100% conversion of ethyl acrylate within 5-10 min, for any borenium chlorometallate ionic liquid.

4.4.2.3 The role of anionic metal centre in catalysis

Borenium chlorometallate ionic liquids of a general formula $L\text{-BCl}_2\text{-MCl}_3$ have two Lewis acidic centers, both in the cation and in the anion, therefore as experiments were performed, there was a question as to whether the catalytic activity originates from one or both of these centres.

The first indication that it is the borenium cation that catalyses the reaction almost exclusively (under these reaction conditions) was the fact that borenium ILs with $[\text{MCl}_4]^-$ anions, which are not considered catalytically active, retained high activity (entries 5 and 6 in Table 4-1). However, it was found beneficial to carry out experiments with a range of benchmark catalysts as well.

Entries 1 - 4 in Table 4-1 contain data recorded for the model reaction carried out in the presence of a range of known benchmark compounds: $[\text{C}_2\text{mim}]\text{Cl}$, $[\text{C}_2\text{mim}][\text{AlCl}_4]$ and $[\text{C}_2\text{mim}][\text{Al}_2\text{Cl}_7]$, where $[\text{C}_2\text{mim}]^+$ is the 1-ethyl-3-methylimidazolium cation and aluminium chloride, AlCl_3 . Among these systems, AlCl_3 and $[\text{C}_2\text{mim}][\text{Al}_2\text{Cl}_7]$ are both a strong Lewis acid (AN = 96). Lewis acidity of the $[\text{C}_2\text{mim}][\text{Al}_2\text{Cl}_7]$ ionic liquid comes solely from the dimeric $[\text{Al}_2\text{Cl}_7]^-$ anion. The $[\text{C}_2\text{mim}][\text{AlCl}_4]$ ionic liquid, in contrast, has monomeric anion that is considered neutral, and $[\text{C}_2\text{mim}]\text{Cl}$ is a basic salt (due to Cl^- basicity).

The same model reaction, under the same conditions, was carried out using these four compounds, at loadings ranging from 0.10 mol% to 0.50 mol% per dienophile. Both AlCl_3 and $[\text{C}_2\text{mim}][\text{Al}_2\text{Cl}_7]$, conventionally considered strong Lewis acids, showed negligible catalytic activity at 0.10 % in contrast to borenium systems. Yet, they were catalytically active at 0.25 mol% loading, giving 99 % conversion in 5 minutes. This proved the strength of the Lewis superacidity of the borenium ionic liquids, and that the catalytic activity at 0.10% loading arises solely from the borenium cation. As expected, the $[\text{C}_2\text{mim}][\text{AlCl}_4]$ ionic liquid had no activity (Table 4-1, entry 3), which contrasted with the borenium ILs of a general formula $[\text{BCl}_3(4\text{-pic})][\text{MCl}_4]$ (Table 4-1, entry 5 and 6), which had very high catalytic activity due to the cation. Finally, the basic halide salt, $[\text{C}_2\text{mim}]\text{Cl}$ had no activity irrespective of its concentrations.

4.4.2.4 NMR spectroscopic studies into catalytically active species

In order to gain further insight into the catalytic species, a spectroscopic study was carried out, where excess of dienophile (ethyl acrylate) was reacted with borenium ionic liquids comprising $[\text{MCl}_4]^-$ or $[\text{M}_2\text{Cl}_7]^-$ anion - without the subsequent addition of diene. The resulting reaction mixture was then investigated by ^{11}B , ^{27}Al and ^{71}Ga NMR spectroscopy to identify the coordination mode of the dienophile. The study was designed to ‘look’ at the ionic liquid, therefore ^1H and ^{13}C NMR studies were not carried out - dienophile was used in such an excess, that the coordinated part was below the detection limit of NMR spectroscopy.

A marked change in ^{11}B NMR chemical shift was expected upon coordination of the dienophile to the boron centre.^{202, 225} The adduct formation would alter the compound from a tri-coordinated compound to a tetra-coordinated compound, hence altering the ^{11}B NMR chemical shift from tricoordinated region (30-50 ppm) to a tetracoordinated region (0-10 ppm).²²⁶ Indeed, such change was detected for $[\text{BCl}_2(4\text{-pic})][\text{AlCl}_4]$ (Figure 4-10), confirming coordination of the dienophile to the borenium cation to form boronium cation, $[\text{BCl}_2(4\text{-pic})(\text{EA})]^+$.

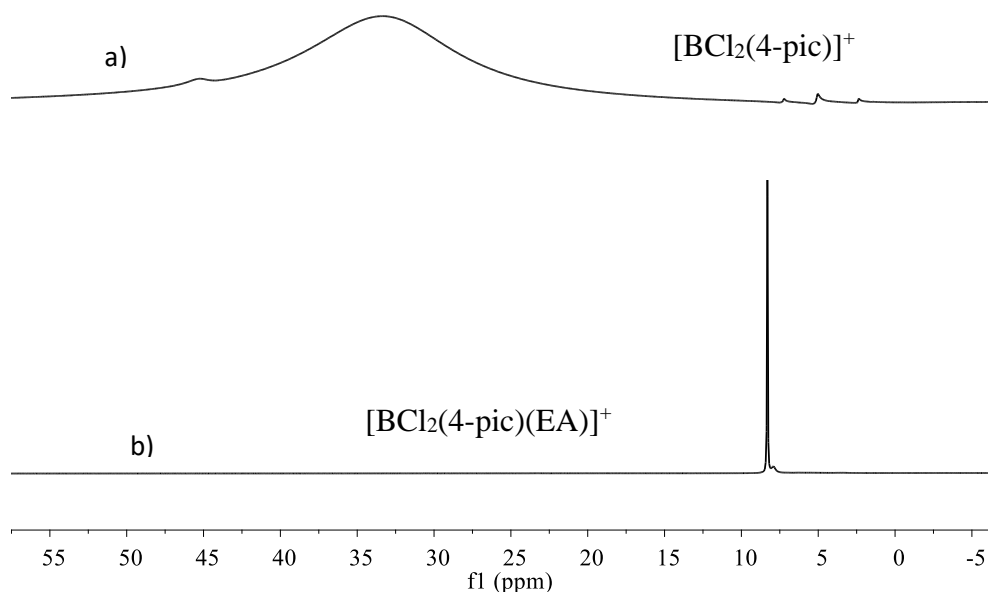


Figure 4-8: ^{11}B NMR spectra of a) neat $[\text{BCl}_2(4\text{pic})][\text{AlCl}_4]$, and b) solution of $[\text{BCl}_2(4\text{pic})][\text{AlCl}_4]$ in ethyl acrylate (EA). Both recorded with external $d_6\text{-DMSO}$ lock.

Studying the ^{27}Al NMR spectra of $[\text{BCl}_2(4\text{-pic})][\text{AlCl}_4]$, there was no change in the chemical shift of the neat borenium ionic liquid compared to the product of the reaction with the dienophile, ethyl acrylate. The chemical shift remained around 103 ± 1 ppm, indicative of four chlorides around the ^{27}Al centre; no oxygen substitution, no expansion of the coordination sphere above four, despite excess of the dienophile. Even more interestingly, however, the signal for the reaction product was dramatically narrower compared to the neat borenium ionic liquid (Figure 4-9). It appears that tetrahedral $[\text{AlCl}_4]^-$ was still present, and since coordinatively unsaturated $[\text{BCl}_2(4\text{-pic})]^+$ was replaced with boronium cation, $[\text{BCl}_2\text{L}(\text{EA})]^+$, the interaction between both ions decreased, restoring tetrahedral geometry around the ^{27}Al centre.

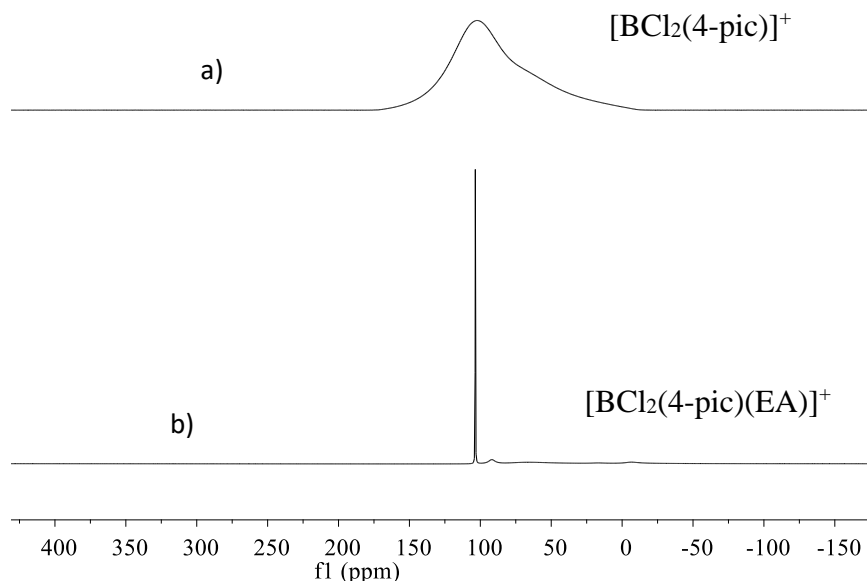


Figure 4-9: ^{27}Al NMR spectra of a) neat $[\text{BCl}_2(4\text{pic})][\text{AlCl}_4]$, and b) solution of $[\text{BCl}_2(4\text{pic})][\text{AlCl}_4]$ in ethyl acrylate (EA). Both recorded with external $d_6\text{-DMSO}$ lock.

^{11}B and ^{27}Al NMR spectra of $[\text{BCl}_2(\text{mim})][\text{Al}_2\text{Cl}_7]$ in excess of ethyl acrylate are shown in Figure 4-10 and Figure 4-11, respectively. Again, ^{11}B NMR spectrum shows the formation of several tetracoordinate boronium species (Figure 4-10). Very interestingly, the ^{27}Al NMR spectrum (Figure 4-11) features a sharp signal at 103 ppm, characteristic of $[\text{AlCl}_4]^-$, not of $[\text{Al}_2\text{Cl}_7]^-$. It appears that EA coordinates exclusively to the boron centre, and even partially replaces chloride, which interacts with $[\text{Al}_2\text{Cl}_7]^-$ to form a more symmetrical $[\text{AlCl}_4]^-$.

$([\text{BCl}_2(\text{mim})][\text{Al}_2\text{Cl}_7] + 2\text{EA} \rightarrow [\text{BCl}(\text{EA})_2(\text{mim})][\text{AlCl}_4]_2$ Equation 4-1). Considering the very large excess of EA, this reaction is practically irreversible, hence the sharp signal from the $[\text{AlCl}_4]^-$ anion.

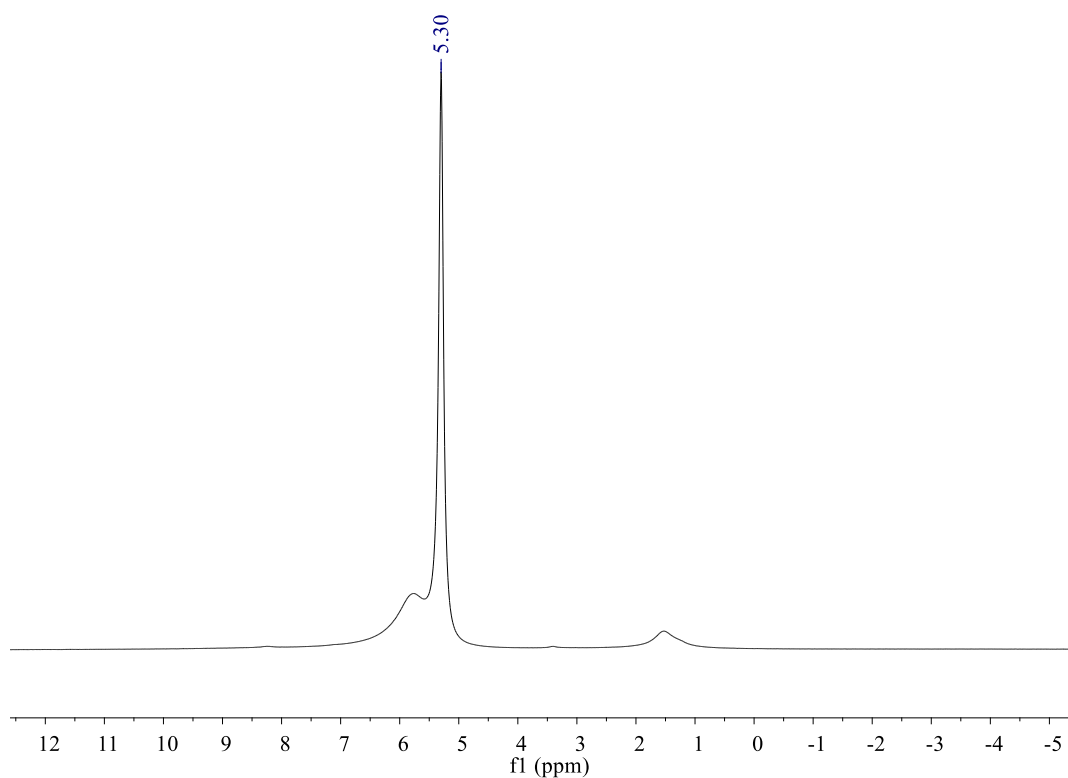


Figure 4-10: ^{11}B NMR (128 MHz, external d_6 -DMSO lock) spectrum of solution $[\text{BCl}_2(\text{mim})][\text{Al}_2\text{Cl}_7]$ in ethyl acrylate(EA).

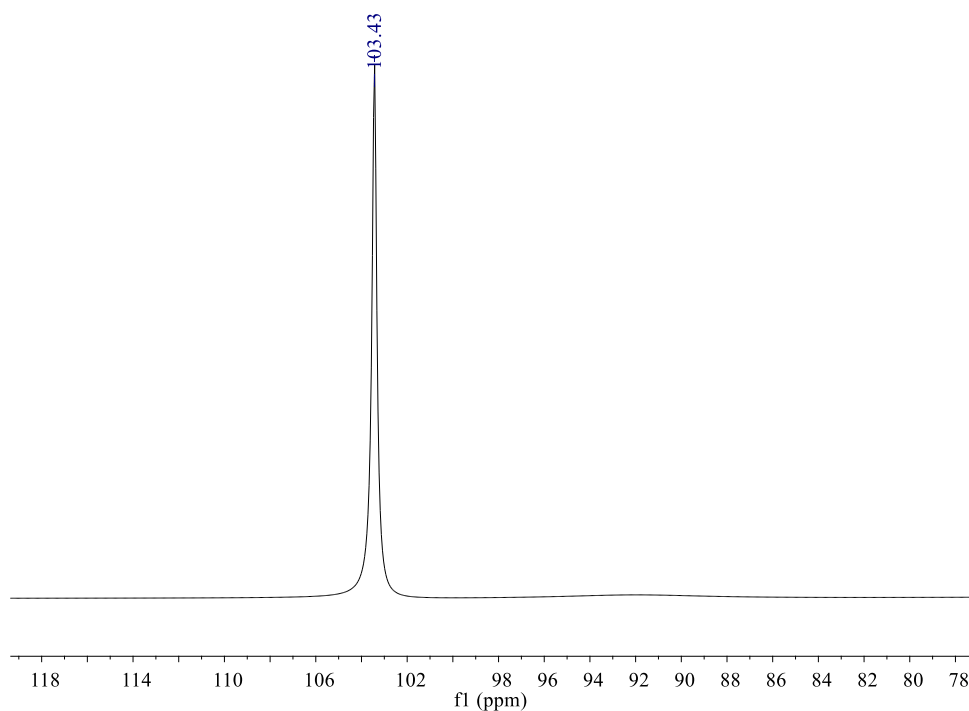


Figure 4-11: ^{27}Al NMR (104 MHz, external d_6 -DMSO lock) spectrum of solution $[\text{BCl}_2(\text{mim})][\text{Al}_2\text{Cl}_7]$ in ethyl acrylate (EA).

Finally, ^{11}B and ^{71}Ga NMR spectra were recorded for $[\text{BCl}_2(\text{mim})][\text{Ga}_2\text{Cl}_7]$ in large excess of ethyl acrylate (Figure 4-12 and Figure 4-13), respectively. The ^{11}B NMR spectrum shows the formation of several tetracoordinate boronium species (Figure 4-12), pretty much identical with these recorded for the analogues $[\text{BCl}_2(\text{mim})][\text{Al}_2\text{Cl}_7]$ - see Figure 4-10 - which points to the same speciation of boronium cations. Unexpectedly, it was possible to record the ^{71}Ga NMR spectrum (Figure 4-13), which featured a sharp and symmetrical signal at *ca.* 250 ppm. This signal indicates that a symmetrical $[\text{GaCl}_4]^-$ anion is present, and not exchanging 171 which leads to exactly the same conclusions as those made for the aluminium-containing analogue.

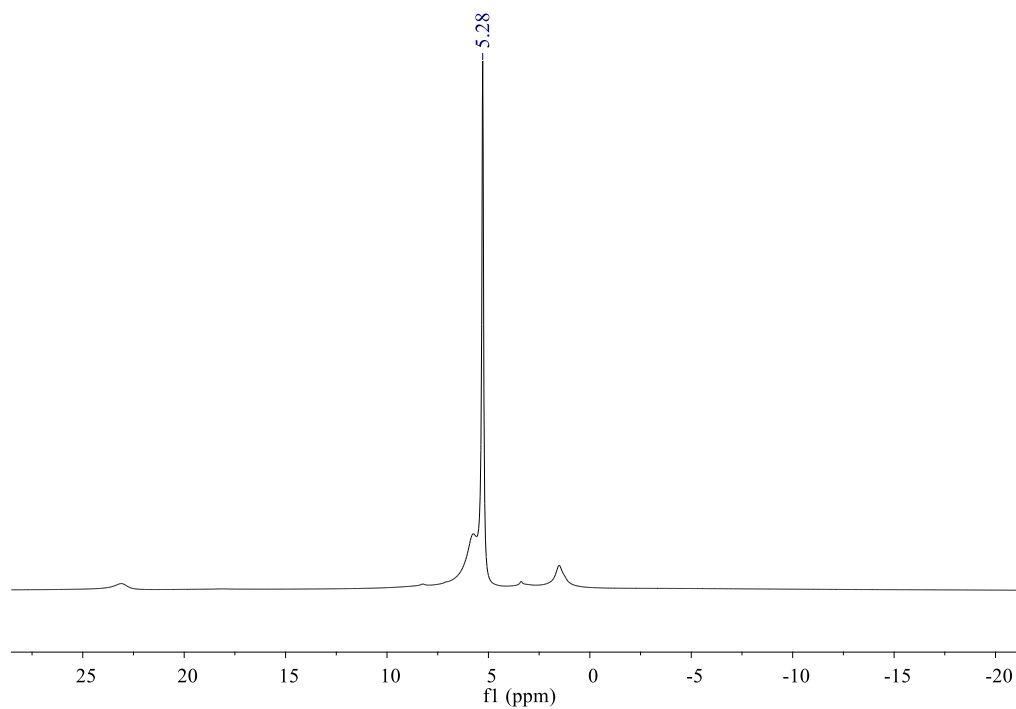


Figure 4-12: ^{11}B NMR (128 MHz, external d_6 -DMSO lock) spectrum of solution $[\text{BCl}_2(\text{mim})][\text{Ga}_2\text{Cl}_7]$ in ethyl acrylate (EA).

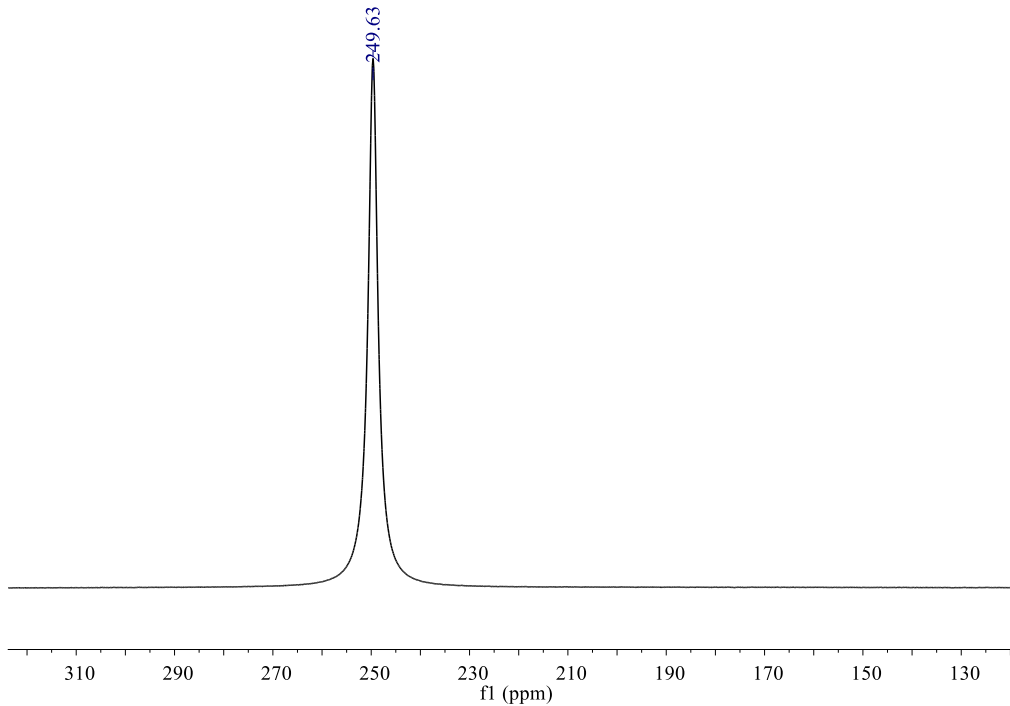


Figure 4-13: ^{91}Ga NMR (122 MHz, external d_6 -DMSO lock) spectrum of solution $[\text{BCl}_2(\text{mim})][\text{Ga}_2\text{Cl}_7]$ in dienophile ethyl acrylate (EA).

In concluding this multinuclear NMR spectroscopic study, it is rather clear that the borenium cation is the only species interacting with the dienophile, whereas the chlorometallate anion fully embraces its intended role of halide-abstracting agent.

4.4.2.5 Influence of molecular solvent

It has been demonstrated (section 3.2.5.1.2) that the presence of solvent can greatly influence the Lewis acidity (AN value) of borenium ionic liquids. Also, from the literature it is known that is crucial to avoid strongly coordinating solvents, and select solvents that are stable towards cationic boron compounds, when investigating borenium ion reactivity.^{24,203}

Reactions in molecular solvents were carried out to: (i) directly compare the performance of borenium ionic liquids in a Diels-Alder reaction with other catalysts in solvent, under the same conditions, and (ii) test whether catalytic activity of borenium ILs will be impaired by the presence of molecular solvent, as suggested by AN studies.

The reaction of ethyl acrylate with 4 mol eq. of cyclopentadiene in equal volume of various solvents, was used as the test study. Solvents selected: dichloromethane and toluene, were non-coordinating, aprotic and dissolved well reactants and products - all reaction mixtures were completely homogenous. Since the reactions were appreciably slower, it was possible to follow them with a GC - unlike the solvent free reactions.

The reactions in toluene were performed initially with 2 mol% of $[\text{BCl}_2(\text{mim})][\text{Ga}_2\text{Cl}_7]$, $[\text{BCl}_2(\text{P}_{888})][\text{Ga}_2\text{Cl}_7]$ and AlCl_3 , and then with decreasing amounts of the two ILs (0.5 % and 0.25 %), at ambient temperature. Conversion of EA was plotted as a function of reaction time, for IL-catalysed Diels-Alder reactions, at IL loading of 2 mol% per dienophile (Figure 4-14), 0.5 mol% per dienophile (Figure 4-15), and 0.25 mol% per dienophile (Figure 4-16). All results were plotted with a benchmark experiment, in which 2 mol% per dienophile of AlCl_3 was used as a catalyst. Reaction catalysed with AlCl_3 , carried out under solvent free conditions at 0 °C, gave 99% conversion after 5 min, with 0.25% catalyst loading. With negligible cyclopentadiene polymerisation. In contrast, using 2 mol% of AlCl_3 at room temperature, but in the presence of with 10 cm³ of toluene, gave 67 % conversion after 5 min. Of course, reactants concentration plays an important role in the reaction rate, but nevertheless - this example demonstrates the merit of using solvent-free system. Using 2 mol% of $[\text{BCl}_3(\text{mim})][\text{Ga}_2\text{Cl}_7]$, conversion reached *ca.* 96% after 5 min and reached a plateau - again demonstrating superior performance compared

to AlCl_3 . However, since the intention was to follow conversion over time, it was decided to lower the IL catalyst loading.

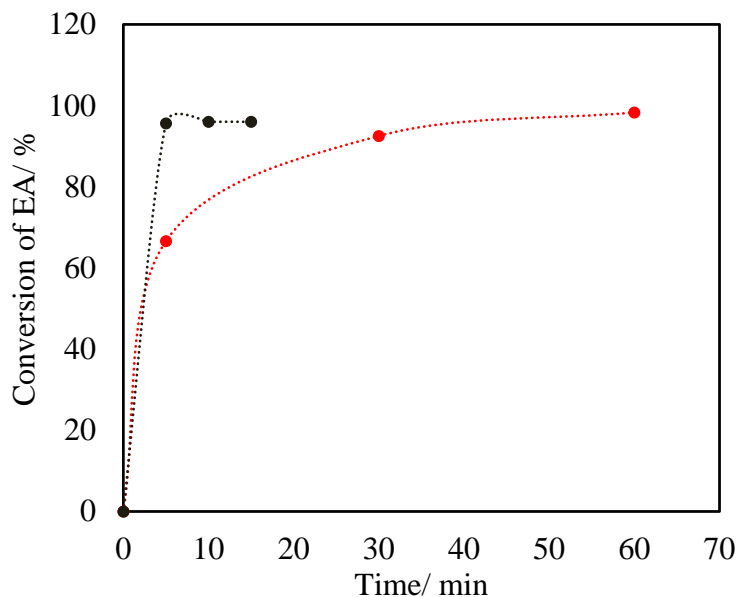


Figure 4-14: Conversion of EA in reactions with CPD with different catalyst amounts in toluene (10 cm^3) at 23°C . —●— 2 mol% AlCl_3 , —●— 2 mol% $[\text{BCl}_2(\text{mim})][\text{Ga}_2\text{Cl}_7]$. Dotted lines are just a guideline for the eye.

The loading of 0.5 mol% per dienophile was tested, using two borenium ILs with differing AN values: $[\text{BCl}_2(\text{mim})][\text{Ga}_2\text{Cl}_7]$ (AN = 173) and $[\text{BCl}_2(\text{P}_{888})][\text{Ga}_2\text{Cl}_7]$ (AN = 159). Although the kinetic curves have not been fitted, it is visible that the initial reaction rate is higher for: $[\text{BCl}_2(\text{mim})][\text{Ga}_2\text{Cl}_7]$ (AN = 173), followed by $[\text{BCl}_2(\text{P}_{888})][\text{Ga}_2\text{Cl}_7]$ (AN = 159), and then by AlCl_3 (AN = 96) - used at 2 mol% loading. In conclusion, certain correlation was found between acidities expressed through ANs and catalytic performance.

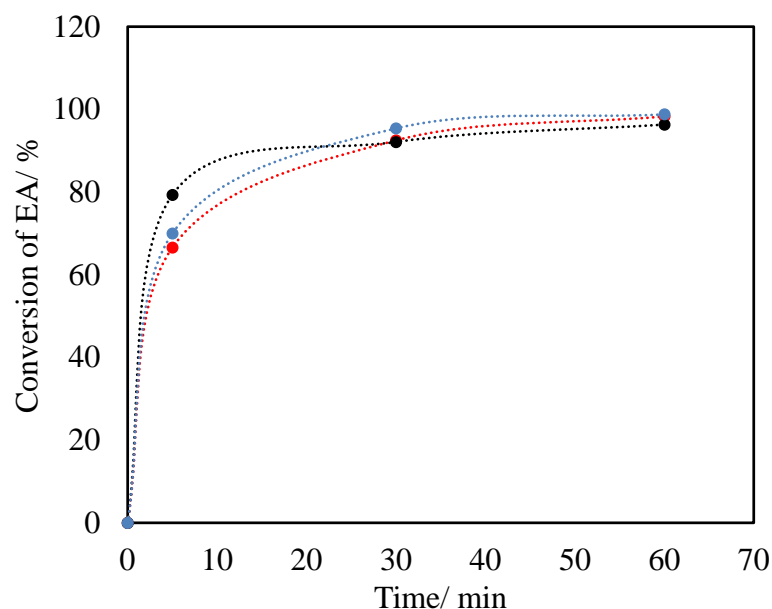


Figure 4-15: Conversion of EA in reactions with CPD with different catalyst amounts in toluene (10 cm³) at 23 °C. —●— 2 mol% AlCl₃, —●— 0.50 mol% [BCl₂(mim)][Ga₂Cl₇], —●— 0.50 mol% [BCl₂(P₈₈₈)] [Ga₂Cl₇]. Dotted lines are just a guideline for the eye.

At 0.25 mol% loading (Figure 4-16), both ILs performed significantly worse than the benchmark. [BCl₂(mim)][Ga₂Cl₇] had much higher initial reaction rate, but was then poisoned/deactivated, nearly reaching plateau at *ca.* 40% EA conversion. In contrast, [BCl₃(P₈₈₈)] [Ga₂Cl₇] gave much lower initial reaction rate, but steady conversion increase was observed up to 60 min, with a possibility of the two curves crossing for longer reaction time.

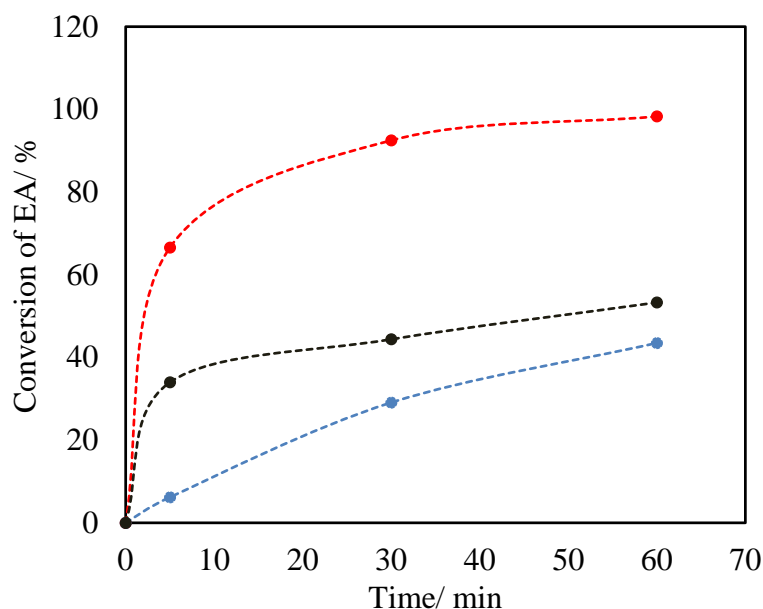


Figure 4-16: Conversion of EA in reactions with CPD in different catalyst amounts in toluene (10 cm³) at 23 °C. —●— 2 mol% AlCl₃, —●— 0.25 mol% [BCl₂(P₈₈₈)][Ga₂Cl₇], —●— 0.25 mol% [BCl₂(mim)][Ga₂Cl₇]. Dotted lines are just a guideline for the eye.

In conclusion, introducing toluene as the solvent impaired the reaction rate, but allowed for a very rudimentary kinetic study, which revealed that initial reaction rates are (at least within the limited scope of this study) related to AN measurements.

Further Diels–Alder reactions were carried out using 2 mol% loading of [BCl₃(mim)][Ga₂Cl₇] as the catalyst, at varying temperatures: -5 and -10 °C, in dichloromethane as a solvent, used at two different amounts (Figure 4-17). In all these experiments, an immediate colour change was observed, from a clear colourless solution to a light/dark brown colour, upon the dropwise addition of the diene.

As expected, lowering the reaction temperature resulted in lower initial reaction rates; also, conversions were halted at relatively low levels. When 30 cm³ of DCM were used, conversion at -10 °C reached *ca.* 20%, which increased to *ca.* 26% at -5 °C. However, when the solvent amount was halved to 15 cm³ of DCM, reaction at -10 °C reached *ca.* 57% of EA conversion.

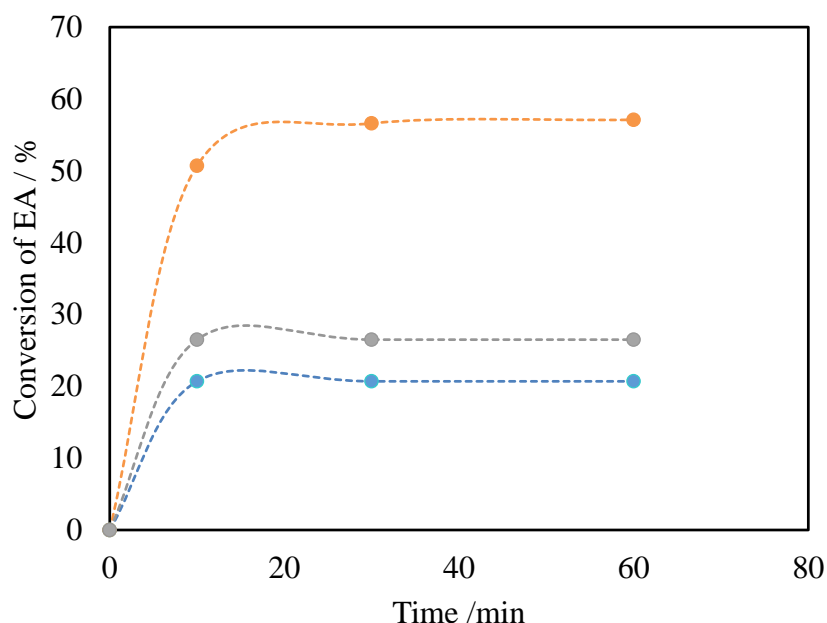


Figure 4-17: Conversion of EA in varying volumes of DCM and temperature with 2 mol% $[\text{BCl}_2(\text{mim})][\text{Ga}_2\text{Cl}_7]$. —●— - 10 °C with 30 ml DCM, —●— -10 °C with 15 ml DCM, —●— -5 °C with 30 ml DCM. Dotted lines are just a guideline for the eye.

From experiments described in this section, it is visible that the use of solvent impaired the reaction rate, but it is unsure whether this was due to altered concentration, or due to solvation of the borenium cation. Elucidating this should be a matter of future work, with the combination of multinuclear NMR studies of borenium ILs in different organic solvents, and normalized concentrations of reactants for comparable kinetic studies. Unfortunately, time constraints did not permit to follow up further with this strand of work (as mentioned previously, this work was carried out during a short term scientific mission placement at Silesian University of Technology, Poland).

4.4.2.6 Substrate scope

Finally, borenium ionic liquids were tested in a Diels-Alder reaction with a range of dienophiles (Table 4-2). Substrate scope was expected to determine their practical applicability and robustness as Lewis acidic catalysts.


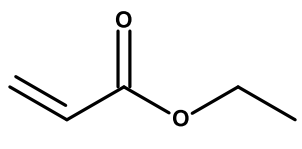
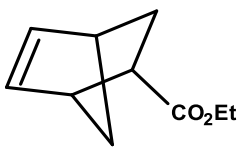
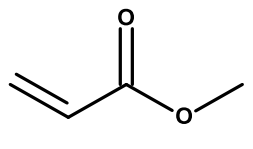
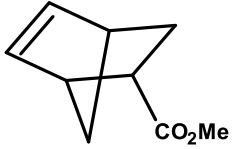
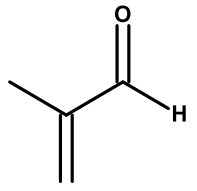
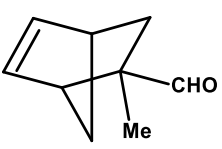
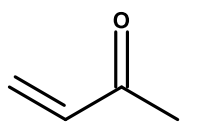
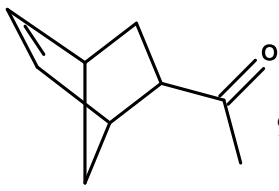
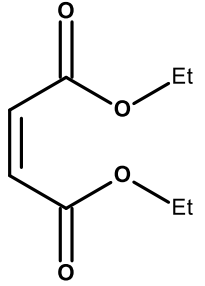
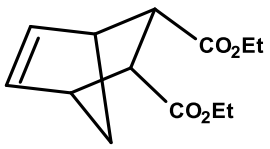
Table 4-2: A list of dienes and dienophiles used in this work and their abbreviations.

Compound	Abbreviation
Cyclopentadiene	CPD
Ethyl acrylate	EA
Methyl acrylate	MA
Diethyl maleate	DEM
Methyl vinyl ketone	MVK
Methyl methacrylate	MMA
Methacrolein	MAC
Isoprene	IPN
Acrylonitrile	ACN
Dichloromethane	DCM

Two borenium ionic liquids with varying Lewis acidities were selected for the study: $[\text{BCl}_2(\text{mim})][\text{Ga}_2\text{Cl}_7]$, with AN = 173, and $[\text{BCl}_2(\text{P}_{888})][\text{Ga}_2\text{Cl}_7]$, with AN = 159, at 0.20 mol% loading per dienophile.

Table 4-3 compares the outcomes of a small substrate scope study that included CPD (diene) and five dienophiles. Cycloadducts were formed with high yields and high stereoselectivities, and within very short reaction times. In most cases, full conversions were achieved after 5-15 min at 0 °C. With the exception of the cycloadducts from cyclopentadiene with methacrolein and cyclopentadiene with diethyl maleate, all the others were isolated with yields ranging from 86 to 93%. This was true also for less reactive substrates. Only in the reaction of cyclopentadiene with dimethyl maleate had slightly lower conversion (60-70%), but endo selectivity was impressively high, with endo: exo ratio of 98:2 and 99:1 for $[\text{BCl}_2(\text{mim})][\text{Ga}_2\text{Cl}_7]$ and $[\text{BCl}_2(\text{P}_{888})][\text{Ga}_2\text{Cl}_7]$, respectively. Furthermore, no other products (e.g. haloborated side products) have been detected by NMR spectroscopy or by GC-MS.

Table 4-3: Conversions and selectivities in Diels-Alder reactions of cyclopentadiene with different dienophiles, catalyzed by borenium chlorogallate ionic liquids.

Diene	Dienophile	Product	Conversion (%)	Selectivity (%) <i>endo: exo</i>
	 EA	 1	100 ^a 99 ^b	96:4 ^a 94:6 ^b
	 MA	 2	97 ^a 97 ^b	95:5 ^a 95:5 ^b
	 MAC	 3	100 ^a 100 ^b	98:2 ^a 97:3 ^b
	 MVK	 4	100 ^a 98 ^b	94:6 ^a 94:6 ^b
	 DEM	 5	70 ^a 60 ^b	98:2 ^a 99:1 ^b

Reaction conditions: No solvent, cyclopentadiene (6mmol), dienophile (4mmol), T =0 °C, time=5mins: ^a with 0.20 mol% [BCl₂(mim)][Ga₂Cl₇]

^b with 0.20 mol% [BCl₂(P₈₈₈)][Ga₂Cl₇].

4.4.3 Triflate boron complexes as catalysts for Diels-Alder reaction

Quite disappointingly, no catalytic activity was recorded for the triflate systems, despite their AN values (AN = 108 to 143) being higher than that of AlCl_3 (AN = 96). It must be assumed, that the dienophile was not basic enough, and therefore was unable to replace triflate in the masked borenium cation. It is suspected that other catalytic reactions may be feasible - but despite several triflate systems screened here, none were catalytically active for Diels-Alder cycloaddition.

4.5 CONCLUSIONS

Work reported in this chapter was the first demonstration of catalytic application of borenium ionic liquids. It was successfully demonstrated, that borenium chlorometallate ionic liquids are extremely active Lewis acidic catalyst for Diels-Alder cycloaddition, and their activity was related to the AN values reported in Chapter 3. These results were reported in a *Cat. Sci. Tech.* paper.²¹⁵

Further multinuclear NMR study revealed - in accord with catalytic results - that the active species is the borenium cation, whereas chlorometallate anions assume the role of chloride acceptors, even if they are considered Lewis acidic in their own right. Attempt was made to study the solvent effect - it was indeed demonstrated that dilution with either toluene or DCM decreases dramatically reaction rates. However, from experiments carried out here, it was impossible to elucidate whether this was the concentration effect, or due to solvation of borenium cation. It can be safely speculated that it is due to combination of both factors; however, to examine which one is dominant, would require more experimental work.

Disappointingly, triflate-containing liquids, which had significant Lewis acidity by AN values - and thus were hoped to have good catalytic activity - were not active in Diels-Alder reaction.



CHAPTER FIVE

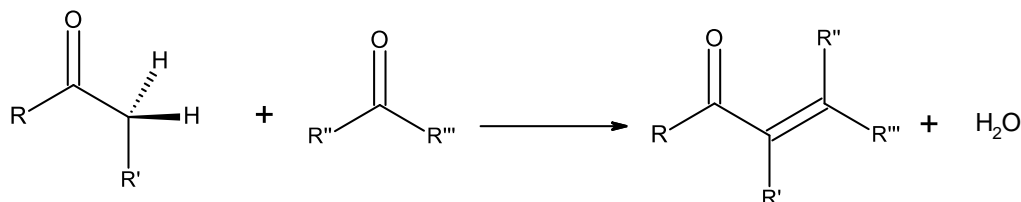
“The race is not to the swift, nor the battle to the strong, neither yet bread to the wise, nor yet riches to men of understanding, nor yet favour to men of skill; but time and chance happens to them all.”

— Ecc 9:11



5 ALDOL CONDENSATION

Aldol reaction brings two relatively simple carbonyl-bearing compounds together, resulting in a more complex molecule (Scheme 5-1).



Scheme 5-1: General Aldol condensation reaction.²²⁷

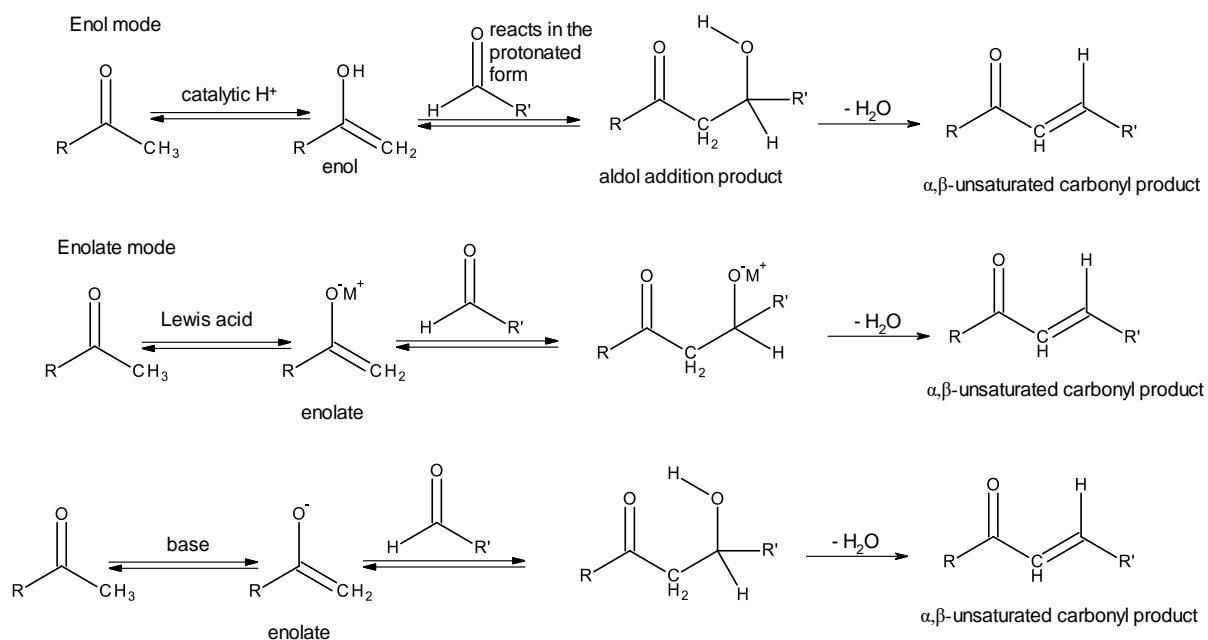
Self-condensation of a simple aromatic ketone, acetophenone, was used as the second test reaction to probe Lewis acidity of borenium ionic liquids.

5.1 INTRODUCTION

5.1.1 Aldol condensation

Aldol condensation was firstly reported by Würtz and Borodin in 1872.²²⁷ Borodin first observed the formation of an aldol (3-hydroxybutanal) from acetaldehyde, in the presence of acidic catalysts, such as hydrochloric acid (Brønsted acid) or zinc chloride (Lewis acid).²²⁷ Currently, aldol condensation is among the most important carbon-carbon bond-forming reactions in organic chemistry.²²⁸ It is of great importance in the synthesis of pharmaceuticals,²²⁹ ligands for catalytic complexes, and functional materials including electrode devices, resistance materials, conducting polymers and organic light-emitting diodes.^{230,231} Aldol condensation products, such as 1,3,5-triarylbenzenes, have been used as starting materials for the synthesis of polycyclic aromatic hydrocarbons (PAHs), dendrimers and fullerene fragments.²³⁰

The mechanism of aldol condensation (Scheme 5-2) involves the reaction of one carbonyl compound, acting as a nucleophile in the form of its enol or enolate derivative, with another carbonyl compound (aldehyde or ketone), acting as an electrophile, to form a β -hydroxyaldehyde or β -hydroxyketone, also known as aldol.^{232,232,233} The formation of the aldol adduct is not the final step of an aldol condensation: the aldol adduct goes further to form an α,β -unsaturated carbonyl compound (a conjugate enone) *via* dehydration.^{234,235}



Scheme 5-2: Enol and enolate pathway for aldol condensation.²³⁶

The two carbonyl compounds partaking in condensation may be the same (self-condensation or symmetrical aldol condensation), with one still acting as a nucleophile and the other as an electrophile, or may be different (mixed or crossed aldol reactions).^{235,237}

Mixed or crossed aldol reactions occur typically between aldehydes and ketones.^{234,235} They are achievable in aprotic solvents and are particularly favourable when the aldehyde has no α -hydrogen, and there is no competition from the ketone for self-condensation. With mixed aldol reaction, one of the carbonyl reactants (ketone) is required to readily form an enolate, and the other (aldehyde) must be reactive enough for nucleophilic addition. In contrast, when the aldehyde has α -hydrogen, the α -carbon of the ketone will add to the carbonyl of the aldehyde.²³⁵ Mixed aldol condensation between ketones and aromatic aldehydes, leading to α,β -unsaturated derivatives, is called the Claisen-Schmidt reaction.²³⁵

Self-aldol condensation can occur between two molecules of the same aldehyde or the same ketone.²³⁴ The aldehyde must have a hydrogen in the α -position with respect to the carbonyl group for the reaction to occur. Ketones, especially aromatic ones, undergo self-condensation less readily.²³¹

Aldol condensation can be catalysed by a Brønsted acid, a Lewis acid, or a base, with the respective mechanisms shown in Scheme 5-2.

Base catalysis occurs through the abstraction of the α -proton to form enolate. This depends on two factors: the strength of the surface basic site and the acidity of the proton (Scheme 5-2).²³⁶ Weaker bases, like hydroxide ion, may not be strong enough to convert all aldehyde or ketone molecules to the corresponding enolate ions, with the reaction equilibrium shifted to the left, and hindering further steps.^{234,235} Self-condensations of ketones were traditionally promoted by hydroxide bases, in protic solvents.²³⁴ Stronger bases, such as alkoxides (RO^-), amides (R_2N^-) or amines, are now also common.^{234,235} The most effective catalysts for self-condensation of aldehydes are basic ion-exchange resins, yielding aldols and/or the products of their dehydration.^{234,231}

Although most aldol condensations are catalysed by bases, acid-catalysed reactions are also reported.²²⁹ The main catalytic action of Brønsted acids is the activation of the electrophile through its protonation, for which a sufficiently strong acid is required (Scheme 5-2).²³⁸ Common Brønsted acids, such as hydrochloric or sulphuric, have been reported to catalyse aldol condensations.^{228,239} In addition, Mukaiyama aldol reaction (addition of silyl enolates to aldehydes) was catalysed with a Brønsted acid derived from squaric acid.²³⁸

Lewis acids are much more popular catalysts than Brønsted acids. Lewis acid catalysis in aldol condensation is still relatively new, although it is gaining popularity, as permitting for milder reaction conditions compared to base catalysis. Lewis acids, like base catalysts, promote aldol condensation *via* enolate formation (Scheme 5-2). The most frequently used solvents are aprotic, polar media, such as tetrahydrofuran, dimethyl sulfoxide and dichloromethane. Some of the commonly utilized enolates were derived from group 1 and 2 elements. However, enolates based on group 14 elements, such as silicon and tin, were found to be relatively stable and isolable.^{228,233,240} They serve as convenient carbonyl equivalent donors through nucleophilic additions to aldehydes and ketones.²²⁹ Enolates are versatile reagents for the formation of α -substituted carbonyl compounds and are therefore important intermediates for the synthesis of complex molecules.^{232,241} In aldol condensation, magnesium, aluminium, or zinc enolates were found to permit milder reaction conditions.²³² Other Lewis acids, such as zinc chloride,

anhydrous copper triflate, anhydrous magnesium chloride, boron trifluoride diethyl etherate ($\text{BF}_3 \cdot \text{OEt}$) and aluminium chloride have also been used.^{232,242}

Strong Lewis acids, such as AlCl_3 , gave higher product yields due to higher degree of activation of the $\text{C}=\text{O}$ group. One of the first uses of Lewis acid-generated enolate was Mukaiyama aldol condensation of silyl enolates with aldehydes.^{242,243,244} The stereo-chemical outcome of an enolate reaction often depends on the geometry of the enolate and therefore the selective formation of enolates is a key step in many bond-forming processes.^{232,241} Asymmetric variants of Mukaiyama reaction have been well explored, since silicon enolates have played a vital role in the development of many useful chiral Lewis acid catalysts.²⁴⁵ Asymmetric formation of β -hydroxycarbonyl compounds can also be achieved using boron enolates.^{232,241} Many publications had reported the usefulness of these boron enolate in aldol condensation from being efficient intermediate to their ability to be highly selective enolate which helps in the control of the reaction.^{246,247,248} Most reported boron enolate formation has been through using α -hydrogens carbonyl compounds together with the triflic salt form of an dialkyl boron compound in the presence of a base mostly amines.^{249,247,248}

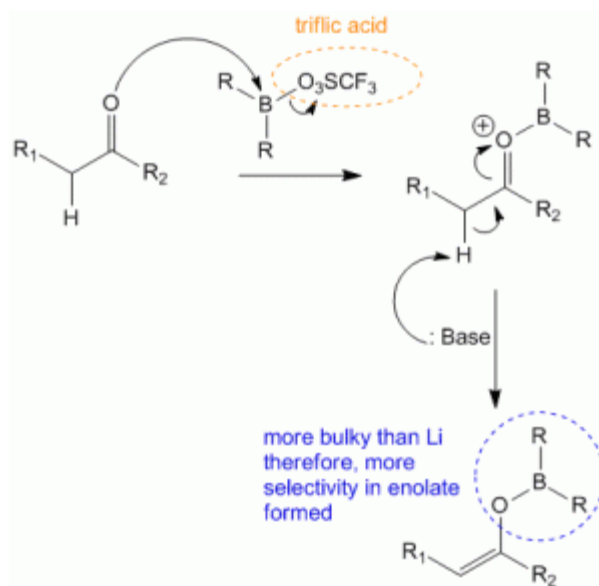


Figure 5-1: Formation of boron enolate in aldol condensation.²⁴⁸

The first published synthesis of this boron enolate compound for aldol condensation was in 1976,²⁵⁰ with regards to the synthesis of di-*n*-butylboron trifluoromethanesulfonate (Bu_2BOTf),

where it was used for the generation of boron enolates as efficient intermediates in aldol condensation.²⁵⁰

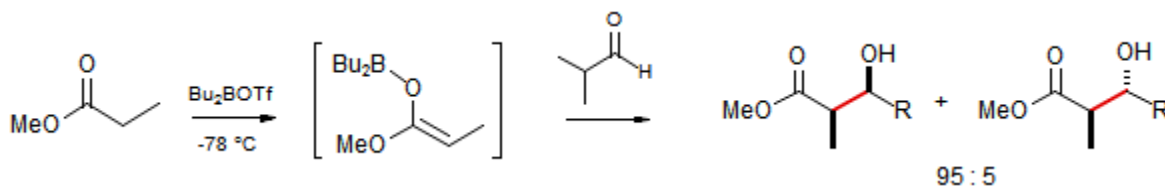


Figure 5-2: Boron enolates in aldol condensation.^{250,248}

The aim of this work was to screen the activity of borenium ionic liquids, rather than pursuing advances in aldol condensation as such. Therefore, a simple but difficult to activate reaction was considered as the ideal model. Utilising a strong boron-based Lewis acid, and thus going through boron enolate, this work was designed as screening towards possible applications in more ambitious, asymmetric synthesis.

5.1.2 Synthesis of dypnone

Dypnone (1,3-diphenyl-2-buten-1-one) is a carbonyl compound produced from the self-condensation of acetophenone (Figure 5-3).²³¹ It is used as an intermediate in the production of a large number of commodity chemicals: softening agents, plasticizers, perfumery bases and sunscreens lotions.²²⁸

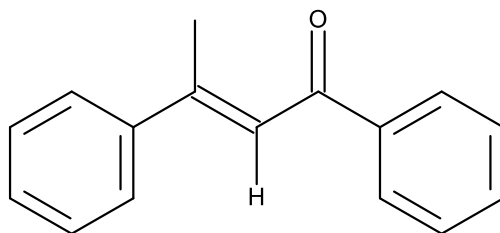


Figure 5-3: Structure of dypnone.²³¹

Dypnone synthesis requires either acid or base catalysis, and the initial product is a β -hydroxycarbonyl compound. Under some conditions, this primary product undergoes dehydration, resulting in α , β -unsaturated carbonyl compound (Figure 5-4).

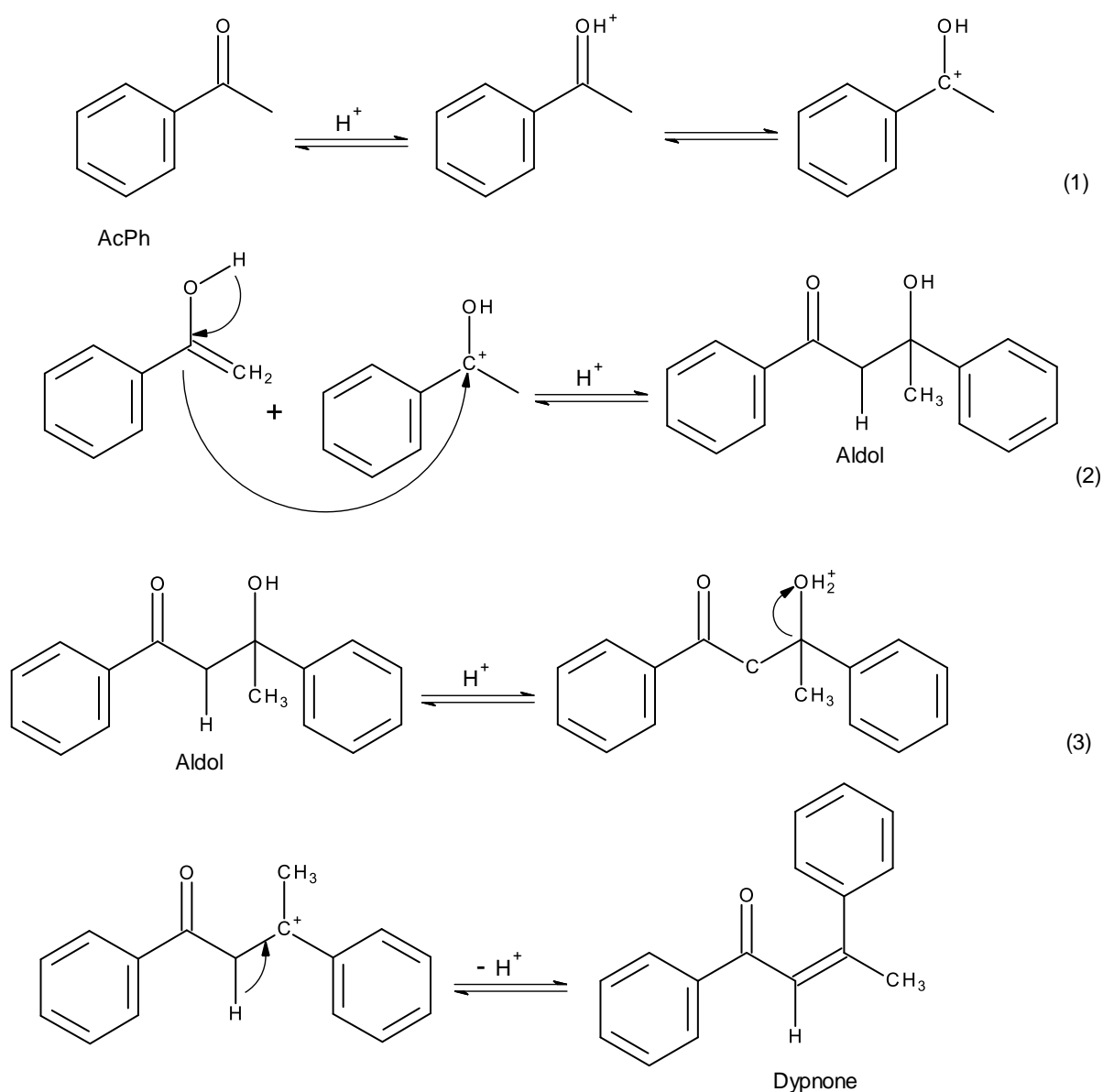


Figure 5-4: Mechanism for the synthesis of dyponone via self-condensation of acetophenone over an acidic catalyst.²²⁸

Dehydration can be affected by the reaction conditions,^{235,251} but typically, once the aldol addition product is formed, it rapidly loses water to form the α,β -unsaturated carbonyl compound. The conjugation of the newly formed double bond with the carbonyl group stabilizes the α,β -unsaturated carbonyl compound.²³⁵ This stabilisation provides the driving force for the dehydration, and controls the regioselectivity.²³⁵ The elimination of a water molecule results in the formation of *trans*-dyponone as the major (desired) product, with *cis*-dyponone as the

secondary product, in addition to the trimer, 1-phenyl-2-(2-vinylphenyl) ethanone, and other ketenes (Figure 5-5).^{228,230,252}

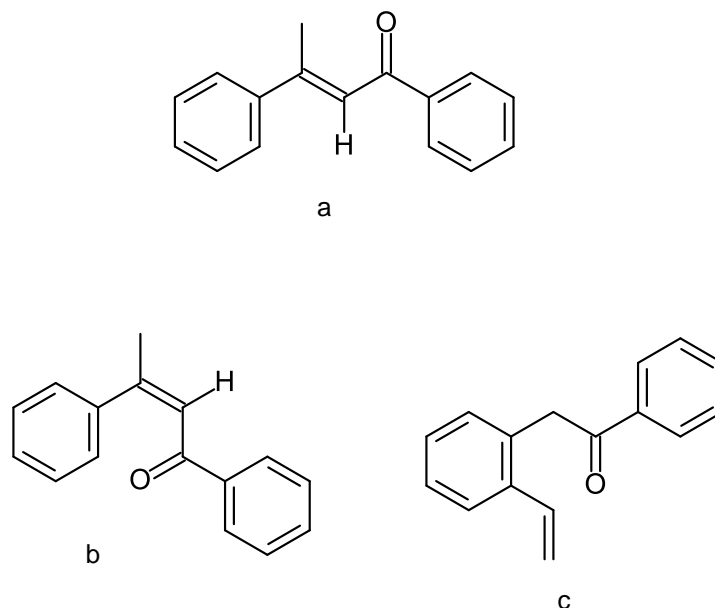


Figure 5-5: Typical products of the self-condensation of acetophenone: a) trans-dyprone, b) cis-dyprone, and c) 1-phenyl-2-(2-vinylphenyl) ethanone

Dyprone was been firstly synthesised by self-condensation of acetophenone in the presence of aluminium *tert*-butoxide by Adkins and Cox in 1938 in their attempt to measure relative oxidation-reduction reactivities of ketones and aldehydes.²⁵³ A year before, Oppenauer reported on a method for preparing complex ketones from simple ketones, such as acetone, in the presence of tertiary aluminium alcohols, to give the complex corresponding ketones.²⁵⁴ This paper was complimentary and a building block to other publications which also reported the synthesis of dyprone by the action of aniline hydrochloride on acetophenone, followed by treatment with hydrochloric acid.^{229,240}

Conventional methods of dyprone synthesis from acetophenone rely on polyphosphoric acid catalysis in benzene,²⁵⁵ or on aluminium *tert*-butoxide catalysis in xylene²⁵³ or dioxane.²⁵⁶ Modern industrial synthesis of dyprone employ AlCl_3 or aluminium *tert*-butoxide.²⁵⁷ However, earlier publications report on a plethora of other catalysts, including sodium ethoxide, aluminium bromide, phosphorous pentachloride, aluminium triphenyl, zinc diethyl, calcium hydroxide, aluminium chloride and hydrogen fluoride on acetophenone (ACP).²⁴⁰

Over the past decade, new catalytic approaches for dyprone synthesis have been investigated, employing catalysts such as polyphosphoric acid, ion-exchange resins, and organometallic compounds (*e.g.* dialkylboron acetate).^{231,240} Amongst these, polyphosphoric acid gave the lowest yield of dyprone (below 27%),²³¹ whereas dialkylboron acetate and gave 72%.²³¹

Many publications described the synthesis of dyprone under extreme conditions: high temperature, long reactions time, enormous catalyst loadings (which makes the term ‘catalyst’ disputable).^{228,240} Venkatesam *et al.*²⁵⁸ reported results of aldol condensation at elevated temperatures (90-160 °C), with reaction time up to 10 h. In 2011, Saravanan *et al.*²⁴⁰ reported the synthesis of dyprone using nano-crystalline sulphated zirconia catalyst to achieve 68.2% acetophenone conversion, with a maximum selectivity of 92%, at 170 °C and 7 h reaction time.

An overview of typical reaction conditions, conversions and selectivities for various catalysts is listed in Tale 5-1.

Table 5-1: Typical literature examples of various dyprone synthesis.

catalyst	Reaction conditions	Conversion of ACP (α , %)	Selectivity to dyprone (%)
SO ₂ /Al-MCM-41	160 °C, 10 h	60.3	93.5
Al-MCM-41	160 °C, 10 h	40.8	80.3
USY	160 °C, 10 h	60.1	89.3
H-b(0.2g)	160 °C, 10 h	60.4	50.7
H-ZSM-5	160 °C, 10 h	7.2	30.7
Silica–alumina	160 °C, 10 h	21.3	35.3
SZ-650(0.5g)	140°C, 7 h	55.0	90.0
SO ₄ ²⁻ /ZrO ₂ (0.5 g)*	160 °C, 5 h	40.1	86.0
SO ₄ ²⁻ /TiO ₂ (0.5 g)*	160 °C, 5 h	28.5	86.0
H-beta(0.5 g)*	160 °C, 5 h	40.8	85.0
H ₂ SO ₄ (0.2 g)	160 °C, 10 h	68.9	88.2
AlCl ₃ (0.5 g)*	160 °C, 10 min	36.0	84.0

Condensation of acetophenone:²²⁸ variation with different catalysts.²²⁸ Catalyst: sulfuric acid impregnated in mesopores of Al-MCM-41, a mesoporous aluminosilicate, zeolite catalyst, aluminosilicate zeolite, amorphous silica–alumina and Nano-crystalline sulfated zirconia catalyst. Reaction conditions: 0.2 g of catalyst; reaction temperature—160 °C; reaction time—10 h; acetophenone—5 ml. Reaction conditions for SZ-650 : ACP = 10 mmol, catalyst = 0.1 g, reaction time = 7 h. Commercial catalysts: Amorphous silica–alumina (Si/Al/45.7, Strem), H-b (Si/Al/425.7, Strem), USY (Si/Al/427.5, PQ) and HZSM-5 (Si/Al/425.5, PQ). Others—cis form of dyprone and ketenes.²²⁸ * Results from Venkatesam *et al* paper.²⁵⁸

The kinetically controlled, boron-mediated aldol reaction is particularly powerful for the efficient synthesis of β -hydroxy carbonyl compounds.²³² One of the earliest publication on the utilization of boron enolates in aldol condensations was by Evans *et al.*,²⁴⁸ who employed boron

enolates in stereoselective aldol condensations of aldehydes.²⁴⁸ Koster²⁴⁸ reported on aldol condensation of ethyl ketones with triethylborane, whilst Mukaiyama published paper in 1976¹⁷ that disclosed the use di-*n*-butylboryl trifluoromethanesulfonate ((Bu₂BOTf) in aldol condensation.^{246,259} However, none of these earlier publications specifically targeted the synthesis of dypnone using boron enolates.

As shown in Table 5-1, the synthesis of dypnone is a challenging one, requiring harsh conditions and long reaction times, even in the presence of a catalyst. Borenium ionic liquids, due to their very high acidity, were hoped to operate under milder conditions. Although there was no possibility of recycling due to release of water in the course of reaction, it was envisaged that low catalyst amounts together with mild conditions and high product yield will deliver a greener alternative to extant synthetic procedures.

5.2 EXPERIMENTAL

Unless otherwise stated, all chemicals were purchased from Sigma-Aldrich. Acetophenone was distilled under reduced pressure (10⁻² bar, 160 °C), dried over molecular sieves (3 Å) and stored under argon prior to use. All glassware, stirring bars, syringes *etc.* were oven-dried (*ca.* 140 °C, min. 24 h) prior to use.

5.2.1 Aldol condensation of acetophenone

The reaction set-up comprised a 50 cm³ three-neck Schlenk flask, equipped with a stirring bar, thermometer and a septum, attached to an argon Schlenk line and purged with argon. Acetophenone (0.50 g, 4.16 mmol) and an internal standard, *n*-decane (0.10 g, 0.57 mmol) was added to the flask using a syringe. The flask was immersed in an oil bath equipped with a thermometer, and the mixture was heated to 30 or 60 °C with vigorous stirring (800 rpm). In the glovebox, an appropriate amount of ionic liquid catalyst (0.10 g, 0.12-0.29 mmol) was weighed into a gas-tight syringe. The tip of the syringe needle was protected from the atmosphere, until it was plunged through the septum of the reaction flask. The catalyst was added slowly, dropwise and the mixture was stirred vigorously (800 rpm). Afterwards, the reaction was allowed to proceed (2 h, 30 or 60 °C, 800 rpm) before placing the flask in an ice bath (0 °C) and quenching the reaction with deionised water (5 cm³). The quenched reaction mixture was washed with 3 × 2 cm³ of chloroform and the combined organic layers were dried over anhydrous magnesium

sulphate (MgSO_4) and filtered. The solvent was subsequently removed using a rotary evaporator (40-50 °C). Five drops of the product were dissolved in chloroform and analysed by GC-MS (Sahimadzu, QP 2000a with SH-RtxTM-5 DB-5 column, 30 m \times 0.25 mm \times 0.25 μm), and GC with FID detector (Sahimadzu GC-2010 with SUPELCOWAXTM 10 column, 30 m \times 0.2 mm \times 0.2 μm).

5.2.2 Large-scale reaction to isolate the product

A 150 cm³ three-neck Schlenk flask, equipped with a stirring bar, thermometer and a septum, was attached to an argon Schlenk line and purged with argon. Acetophenone (2.50 g, 20.8 mmol) and an internal standard, *n*-decane (0.5 g, 0.57 mmol) was added to the flask using a syringe. The flask was immersed in an oil bath equipped with a thermometer and the mixture was heated to 30 °C with vigorous stirring (800 rpm). In the glovebox, an appropriate amount of ionic liquid, $[\text{BCl}_2(\text{mim})][\text{Al}_2\text{Cl}_7]$ (0.1 g, *ca.* 1.07 mmol) was weighed into a gas-tight syringe. The catalyst was then added dropwise to the reaction mixture under vigorously stirring (800 rpm). The reaction mixture was allowed to proceed with vigorously stirring under argon for 2 h at 30 °C before it was stopped. After 2 h, the reaction flask was then placed in an ice bath (0 °C) to cool and quenched with deionised water (5 cm³). The mixture was extracted thrice of chloroform (with 3 \times 5 cm³) and the combined organic extracts were dried over anhydrous magnesium sulphate (MgSO_4) and filtered. The solvent was subsequently removed using a rotary evaporator (40-50 °C) to produce the crude aldol adducts.

Five drops of the crude product was dissolved in chloroform and analysed by GC-MS (Sahimadzu, QP 2000a with SH-RtxTM-5 DB-5 column, 30 m \times 0.25 mm \times 0.25 μm), and GC with FID detector (Sahimadzu GC-2010 with SUPELCOWAXTM 10 column, 30 m \times 0.2 mm \times 0.2 μm). This reaction processes was carried out thrice in order to get sufficient amount which was then ready for use in subsequent product isolation.

To isolate dypnone, the product mixture was separated using silica gel (60-120 mesh) column chromatography (20:80 EtOAc, ethyl acetate/hexanes). All the fractions were analysed by TLC (Merck pre-coated silica gel plates with F254 indicator; R_f $\frac{1}{4}$ 0.48, 30:70 ethyl acetate/hexanes; R_f $\frac{1}{4}$ 0.72, 20:80 diethyl ether/dichloromethane). The dry TLC plate was placed in the TLC jar with a good-sealing lid containing a dry mix of iodine crystals and watched until

the brown spots developing. The use of iodide beads for staining was employed to complement the use of the UV light as some compounds did not appear clearly under UV light. Fractions containing pure dyprnone were combined, and the solvent was removed using a rotary evaporator (40-50 °C), and subsequently under high vacuum (temperature, pressure).

The product, a yellow oil, was dissolved in *d*-chloroform and analysed using ^1H and ^{13}C NMR spectroscopy (400 MHz) and GC-MS (Sahimadzu, QP 2000 a, using SH-RtxTM-5 DB-5 column, 30 m \times 0.25 mm \times 0.25 μm). FT-IR spectra was also recorded for the isolated product using the Perkin Elmer Spectrum 100 Series FT-IR spectrometer with an ATR attachment.

5.3 RESULTS AND DISCUSSION

5.3.1 Reaction conditions

Small-scale condensations of acetophenone were carried out at 30 °C for 2 h, with borenium chlorometallate ionic liquids as a catalyst. The ILs were of a general formula $[\text{BCl}_2\text{L}][\text{M}_n\text{Cl}_{3n+1}]$, where M = Al or Ga and L was 4-pic, mim, dma, P₈₈₈O or P₈₈₈ (Figure 5-6).

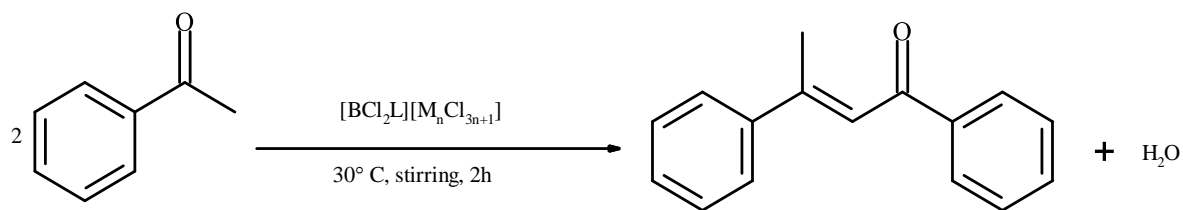


Figure 5-6: Synthesis of dyprnone catalysed with borenium ionic liquids.

Since all borenium ILs react rapidly with water (Chapter 3), great care was taken to avoid contact of these reagents and their solutions with atmospheric moisture. Since it was suggested that the use of molecular solvent decreased Lewis acidity of borenium ionic liquids, all reactions were by default carried out solvent free. Having already tested the reactivity of borenium ionic liquids with Diels-Alder reaction (Chapter 4) it was confirmed that they were highly reactive catalysts. From previous work, it was anticipated that interaction of the borocation with a carbonyl would be very exothermic. Therefore, initial reaction conditions were much milder than those reported in the literature (see Table 5-1).

Reactions were carried out at a small scale, with borenium ionic liquids (0.10 g, 0.12 - 0.29 mmol) added drop-wise to neat acetophenone (0.50 g, 4.16 mmol). Overall catalyst loading was on average ~ 2.8 mol% , at 30 °C. Small scale ensured efficient thermal control, but there was a drawback - it was not feasible to measure exactly the same molar equivalent of each ionic liquid. The reasonably measurable amount (by weight, 0.10 g) - was amounting to about three drops when added using a microsyringe.

In the first reaction, repeated three times, 0.10 g of $[\text{BCl}_2(\text{mim})][\text{Al}_2\text{Cl}_7]$ was used as the catalyst, added neat to acetophenone stirred at 30 °C. The progress of each reaction was followed by GS by taking aliquots of the reaction mixture at $t = 0, 30, 60, 90, 120, 150$ and 240 min. However, the results were completely irreproducible between the three runs, with varying reaction rates and conversions recorded for each run. Despite all precautions, it was concluded that the introduction of adventitious moisture occurred every time a sample was collected. This resulted, presumably, in the decomposition of the borenium ionic liquid, and consequent reaction quenching. However, these imperfect initial data led to concluding that 2 h was a reasonable reaction time, leading to high conversions. Therefore, all reactions were carried out over 2 h at 30 °C, quenched with water and analysed.

5.3.2 Screening of borenium chlorometallate ionic liquids

5.3.2.1 Preliminary observations

Addition of borenium ionic liquid to acetophenone was exothermic. The reaction mixture turned dark yellowish-green immediately upon the addition of the ionic liquid catalyst, with some of the reaction mixtures appearing so deeply coloured as to appear black, but on quenching the reaction with water, a yellow colour consistently reappeared. Furthermore, the reaction mixtures coagulated after a few minutes under stirring. Such colour and physical changes were observed upon the addition of the borenium catalysts. The colour changes were immediate after every addition of the catalyst (listed in Table 5-2) and the intensity differed depending on the donor ligand present. This coagulation occurred with all the borenium ionic liquids, however, no coagulation was observed with the benchmark Lewis and Brønsted acids (entries 1 and 2 in Table 5-2).

This was not unexpected, as both coagulation and colour change was reported in many publications.^{251,230} This was consistent of what we see in the literature about the colour of dypnone and other hydrocarbon products in this specific reaction. Roger *et al*²⁵⁵ for example reported this colour formation in their work on dypnone synthesis with acetophenone using phosphoric acid.²⁵⁵ And having isolated their crude products (dypnone inclusive), they associated some of the yellow coloured products to hydrocarbon compounds or diarylalkenes.²⁵⁵

In all reactions listed in Table 5-2, the catalyst was added dropwise over 30 min intervals (a drop every 30 min). This slow addition of the catalyst was intended to prevent exothermic hot spots occurring and to sustain the catalyst activity during the reaction despite generation of moisture. It was envisaged as a very rudimentary attempt at continuous addition of a catalyst.

5.3.2.2 Comparison of catalysts

All starting materials and products of preliminary reactions, catalysed with $[\text{BCl}_2(\text{mim})][\text{Al}_2\text{Cl}_7]$, were identified by GC-MS. Following this, GC was used to quantify the amounts of acetophenone and dypnone in every sample, using *n*-decane as the internal standard. Calibration curves Figure 5-7 were prepared for both acetophenone and dypnone; dypnone for this purpose was synthesised and purified as a part of this work (see section 5.3.5). The conversion was defined as the amount of acetophenone consumed, divided by the initial amount and multiplied by 100%. The selectivity to the product was expressed as the amount of dypnone formed, divided by amount of acetophenone consumed, and multiplied by 100%.

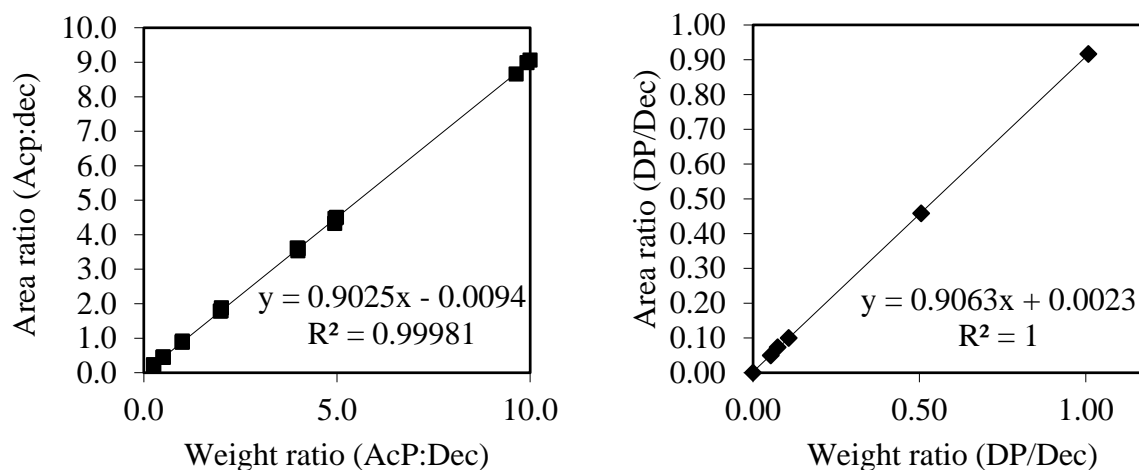


Figure 5-7: Left: GC calibration curve of dypnone with *n*-decane as internal standard (AcP - acetophenone, Dec - *n*-decane); right: GC calibration curve of acetophenone with *n*-decane as internal standard (DP - dypnone, Dec - *n*-decane)

Reactions were repeated in triplicate for most of the borenium ionic liquids, in order of confirm the reproducibility/repeatability - as this was an issue in the initial set of experiments. The results summarised in Table 5-2 demonstrate good reproducibility across all catalysts. In addition to borenium ILs, benchmark Lewis and Brønsted acids (AlCl₃ and H₂SO₄, respectively) were tested. *N.B.*: These two catalysts were used at much higher loading of 0.50 g (3.7 and 5.1 mmol, respectively) rather than 0.10 g because from literature 0.50 g of these benchmark Lewis and Brønsted acids were published to produce comparable high conversion results.²²⁸

Table 5-2: Condensation of acetophenone over borenium halometallate ionic liquids as catalyst and benchmark acids.

Entry	Catalyst	AN	Conversion α_{ACP} , (%)				Selectivity to <i>trans</i> -dypnone (%)
			1	2	3	average	
1	H ₂ SO ₄ ^a		92	86	85	89	88
2	AlCl ₃ ^a	96	91	92	90	91	82
3	[BCl ₂ (4-pic)][Al ₂ Cl ₇]	170	90	91	-	91	79
4	[BCl ₂ (mim)][Al ₂ Cl ₇]	174	91	92	91	91	78
5	[BCl ₂ (dma)][Al ₂ Cl ₇]	163	88	89	-	89	77
6	[BCl ₂ (P ₈₈₈)][Al ₂ Cl ₇]	98	86	86	-	86	30
7	[BCl ₂ (4-pic)][AlCl ₄]	124	90	89	-	90	78
8	[BCl ₂ (P ₈₈₈ O)][AlCl ₄]	136	83	83	77	81	10
9	[BCl ₂ (P ₈₈₈ O)][GaCl ₄]	156	91	89	90	90	35
10	[BCl ₂ (4-pic)][Ga ₂ Cl ₇]	140	99	99	99	99	73
11	[BCl ₂ (mim)][Ga ₂ Cl ₇]	172	89	90	90	90	77
12	[BCl ₂ (dma)][Ga ₂ Cl ₇]	163	89	89	89	89	72
13	[BCl ₂ (P ₈₈₈)][Ga ₂ Cl ₇]	159	98	98	98	98	75
14	[BCl ₂ (mim)][Ga ₃ Cl ₁₀]	174	92	89	91	91	74
15	[BCl ₂ (4-pic)][Ga ₃ Cl ₁₀]	180	97	97	-	97	76
16	[BCl ₂ (dma)][Ga ₃ Cl ₁₀]	163	92	92	92	92	75
17	[BCl ₂ (P ₈₈₈)][Ga ₃ Cl ₁₀]	159	97	97	-	97	73

Reaction conditions: 0.10 g of borenium ionic liquid catalyst was used, reaction was carried out at 30 °C for 2 h. ACP - acetophenone. a - 0.50 g of the catalyst loading.

As a general conclusion, the conversion of acetophenone and selectivity to dypnone were significantly higher compared to the literature reports, where reactions were carried out under higher temperature and longer reactions time, such as 160 °C for 10 h (*viz.* Table 5-1),²²⁸ despite using milder temperature conditions (30 °C for 2 h) and relatively low catalyst loadings. Average conversions were comparable to those obtained with 5-times higher loading of the benchmark catalysts: H₂SO₄ or AlCl₃, although slightly lower selectivities were obtained (*ca.* 75% for ILs, *vs.* 82 and 88% for benchmark catalysts).

The enhanced conversion of acetophenone for the borenium Lewis acidic catalysts is due to the high catalytic activity (high Lewis acidity) of the catalyst. Indeed, Selvaraji *et al.* reported that increasing the reaction temperature increased the catalytic activity sharply, and that the yield of dypnone depended on the rate of self-condensation, which in turn depended the acidity of the catalyst.²²⁸ Selvaraji *et al.* reported conversion of acetophenone and dypnone selectivity at 60.8% and 93.5%, respectively, at 160 °C for 10 h.²²⁸ However, borenium ionic liquids delivered comparable results at near-ambient conditions.

Both the acetophenone conversion and selectivity to dypnone differed for different borenium ionic liquids, depending both on the ligands and the anions. Changing the metal in the anion had marginal impact on conversion, with slightly higher results for chlorogallate systems. However, the borenium chloroaluminate ionic liquid offered higher dypnone selectivity for the same borocation - with the exception of $[\text{BCl}_2(\text{P}_{888})][\text{Al}_2\text{Cl}_7]$. A typical example is the comparison between the reactions catalysed by $[\text{BCl}_2(4\text{-pic})][\text{Al}_2\text{Cl}_7]$ and $[\text{BCl}_2(4\text{-pic})][\text{Ga}_2\text{Cl}_7]$. Where $[\text{BCl}_2(4\text{-pic})][\text{Al}_2\text{Cl}_7]$ had higher selectivity to dypnone (79.0 %) than $[\text{BCl}_2(4\text{-pic})][\text{Ga}_2\text{Cl}_7]$ with 73.0 %, the conversions were 91 % and 99 %, respectively (Table 5-2, entries 3 and 10). Ligands had no clear influence on the conversion and selectivity, except for markedly low selectivity noted for the combination of hydrophobic donors (P_{888} and P_{888}O) with chloroaluminate anions (Table 5-2, entries 6 and 8).

Ionic liquids with neutral chlorometallate anions, *i.e.* $[\text{C}_8\text{min}][\text{AlCl}_4]$ and $[\text{P}_{66614}][\text{GaCl}_4]$, had no catalytic activity due to the absence of a Lewis acid site. The tetrachlorometallate borenium ionic liquids (Table 5-2, entries 7 and 8) on the other hand, also showed comparatively high selectivity to dypnone and significant conversion of acetophenone, which reiterated the notion that it is the borenium cations that has catalytic properties, and suggested the reaction path was proceeding through boron enolate.

Overall, it was observed that the selectivity to dypnone was rather consistent between different borenium catalysts, but the conversion of acetophenone varied slightly with each catalyst reaction. The conversion of acetophenone (Figure 5-7) and selectivity to trans-dypnone (Figure 5-8) were plotted against AN values. Unfortunately, neither Boltzman (plotted) nor linear function could be successfully fitted.

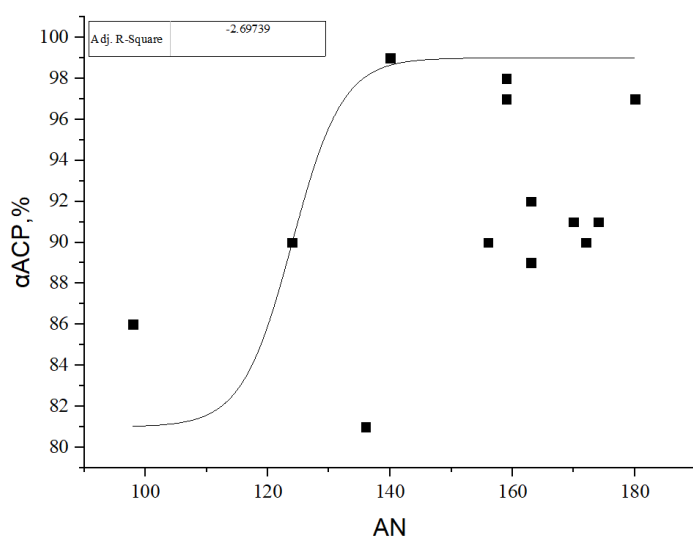


Figure 5-8: Experimental data showing conversions in aldol condensation of acetophenone to dynone catalysed with 2.8 mol% of Lewis acidic ionic liquids vs. AN values of the catalysts. Boltzman fit plotted as an illustration.

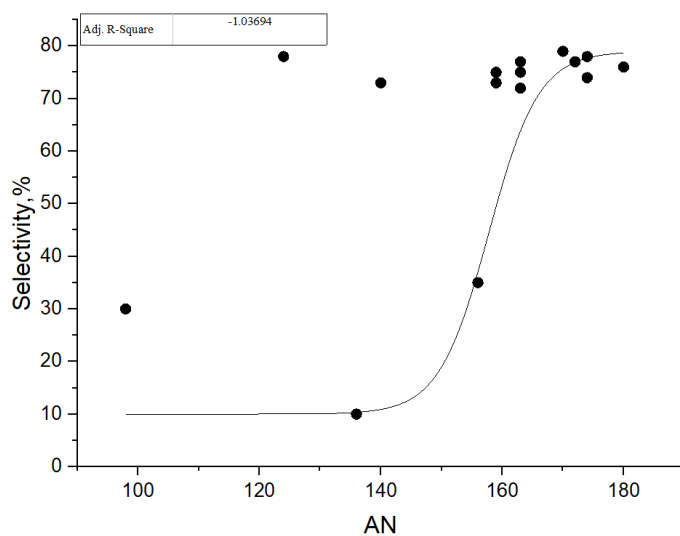


Figure 5-9: Experimental data showing selectivity in Aldol condensation of acetophenone to dynone catalysed with 2.8 mol% of Lewis acidic ionic liquids vs. AN values of the catalysts. Boltzman fit plotted as an illustration.

An important factor that could have influenced the conversion was the already-mentioned coagulation, which occurred every time upon the addition of a borenium ionic liquid. However, extent of this coagulation differed between reactions, which may have hindered mass transfer, thereby affecting the conversion of acetophenone.

5.3.2.3 Effect of solvent, temperature and reaction time

The effect of temperature and solvent on conversion was studied under otherwise similar conditions, at 30 or 60 °C, in 1 cm³ of chloroform (Table 5-3).

Table 5-3: Condensation of acetophenone over borenium halometallate ionic liquids as catalyst, in chloroform.

Entry	Catalyst	Reaction conditions	Conversion of ACP (%)				Selectivity to trans-dypnone (%)
			1	2	3	average	
1	[BCl ₂ (mim)][Al ₂ Cl ₇]	30 °C, 2 h	30	29	31	30	80
2	[BCl ₂ (dma)][Al ₂ Cl ₇]	30 °C, 2 h	15	16	17	16	76
3	[BCl ₂ (P ₈₈₈ O)][Al ₂ Cl ₇]	30 °C, 2 h	11	10	-	11	31
4	[BCl ₂ (P ₈₈₈)][Al ₂ Cl ₇]	30 °C, 2 h	8	7	10	8	26
5	[BCl ₂ (mim)][Ga ₂ Cl ₇]	30 °C, 2 h	18	21	22	21	81
6	[BCl ₂ (P ₈₈₈)][Ga ₂ Cl ₇]	30 °C, 2 h	15	15	15	15	51
7	[BCl ₂ (mim)][Al ₂ Cl ₇] *	60 °C, 2 h	47	-	-	47	78
8	[BCl ₂ (mim)][Ga ₂ Cl ₇]*	60 °C, 2 h	34	-	-	34	80

Reaction conditions: 0.10g (2.8 mol%) of borenium ionic liquid catalyst was used. ACP=acetophenone, Feedstock = 0.50 g.

*single reactions.

Conversion decreased significantly with the introduction of a solvent, compared to the reactions carried out solvent-free. This was paralleled by the lower AN readings when measured in a solvent (section 3.2.5.12 and impaired catalytic performance in Diels-Alder reaction (section 4.4.2.5) - but also resulted from the lower concentration of the reactants. In chloroform, the highest conversion/selectivity (30% and 80%, respectively) were recorded for [BCl₂(mim)][Al₂Cl₇], at 30 °C and 2 h. With increased temperature conversion was enhanced, but dypnone selectivity has not (Table 5-3, entries 7-8). Increased conversion was of course due to kinetically controlled mechanism of the reaction,^{260,258} with the highest conversion of 47% recorded with [BCl₂(mim)][Al₂Cl₇] at 60 °C, 2 h, with selectivity to dypnone at 78%. However, it is important to note that this seemingly unremarkable result was better than most outcomes reported by Selvaraji *et al.*, who worked at 160 °C, with reaction times 5-10 h. Only SO₂/AlMCM-41 catalyst (160 °C, 10 h) gave conversion of acetophenone at 60.3% and selectivity to dypnone at 93.5%, with other values below outcomes reported here.²²⁸

5.3.2.4 Side-products

It was observed that at 60 °C (*i.e.* as the temperature was increased) more side products were generated, especially 1,3,5-triarylbenzenes. The formation of the trimer was thought to be due to further self-condensation of dypnone, which led to the rearrangement of dypnone to 1,3,5-

triarylbenzenes.²³⁰ Deng *et al.* also reported on 1,3,5-triarylbenzenes formation in aldol condensation of acetophenone, and proposed a reaction pathway to be due to aldol self-condensation of dypnone, followed by an intramolecular [2+2] cycloaddition and a retro-[2+2] cycloaddition.²³⁰ Deng *et al.* worked under relatively mild conditions (10 mol % of TsOH, 80 °C), in comparison to 160 °C reaction temperature used by Selvaraj *et al.*, who reported no trimer formation.²²⁸ Hu *et al.* also highlighted dypnone as the intermediate product in tricondensation of acetophenone to triarylbenzenes, under mild conditions (Figure 5-10).^{251,261}

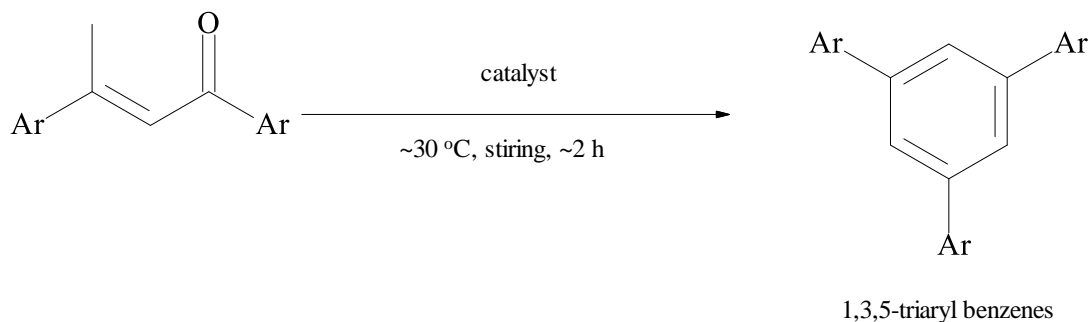


Figure 5-10: Aldol-type self-condensation of dypnone to 1,3,5-triarylbenzene.

5.3.3 Isolated dypnone

Selected reactions were scaled up, followed by the chromatographic separation of dypnone from other aldol adducts. Scale up dypnone synthesis (5x scale-up: acetophenone (2.50 g, 20.8 mmol)) were carried out at 30 °C for 2 h, using $[\text{BCl}_2(\text{mim})][\text{Al}_2\text{Cl}_7]$ (0.5 g, *ca.* 1.07 mmol), in solvent free, to control thermal effects. Interestingly, the issue of coagulation which was observed in the small scale reactions did not occur in these scaled-up reactions, likely due to the presence of a solvent.

There has been several reports on the successful separation of the two dypnone isomers by GLC and TLC.²⁶² Selvaraj *et al.*, in their publication separated the *trans*-dypnone from the *cis*-dypnone and the ketenes.^{228,252} They identified *trans*-dypnone as the primary product and *cis*-dypnone and the ketenes as secondary products (Table 5-1). In this work, dypnone was purified by silica gel flash column chromatography (2.2 cm internal diameter x 12 cm silica height) using 20:80 ethyl acetate/hexanes as eluent, following literature procedure.²⁶³ Separation was only carried out to separate dypnone from its side products, without further separation of the small amount of *cis*-dypnone from *trans*-dypnone.

Isolated dyprnone was analysed by IR (Figure 5-13) and ^1H NMR (Figure 5-14 and Figure 5-15) spectroscopies, which conformed to reference spectra of pure dyprnone found in the literature.

Infrared spectrum (Figure 5-13) of the isolated dyprnone showed absorptions around 3056 cm^{-1} , indicative of a C-H stretching of benzenes, bands around 2918 cm^{-1} from the aliphatic C-H stretching, as well as 690 cm^{-1} bands for aromatic C-H bending and 750 cm^{-1} bands for mono-substituted aromatics. Additionally, strong bands associated with an C-H aromatic stretching was detected at 1212 cm^{-1} , together with C=C stretches at 1596 cm^{-1} and 1448 cm^{-1} . Importantly, the 1654 cm^{-1} band was indicative of a ketone carbonyl.

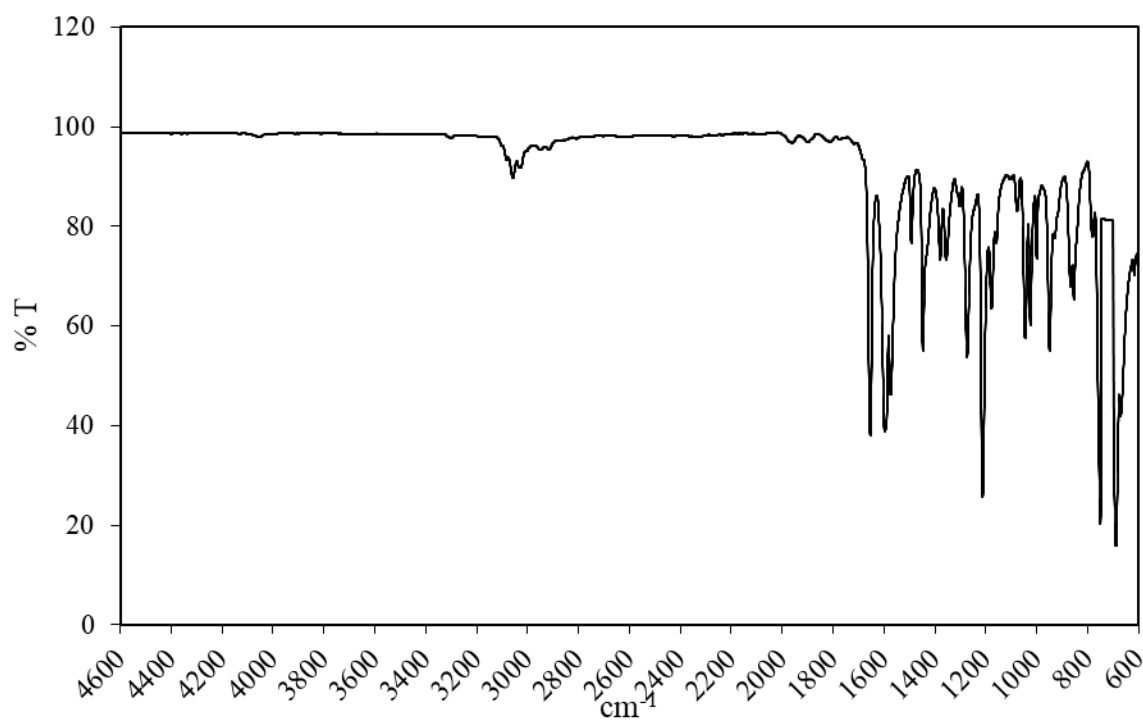


Figure 5-11: IR spectrum of isolated pure dyprnone.

Assignments for the ^1H NMR spectrum (Figure 5-14, and a fragment in Figure 5-15) are shown graphically.

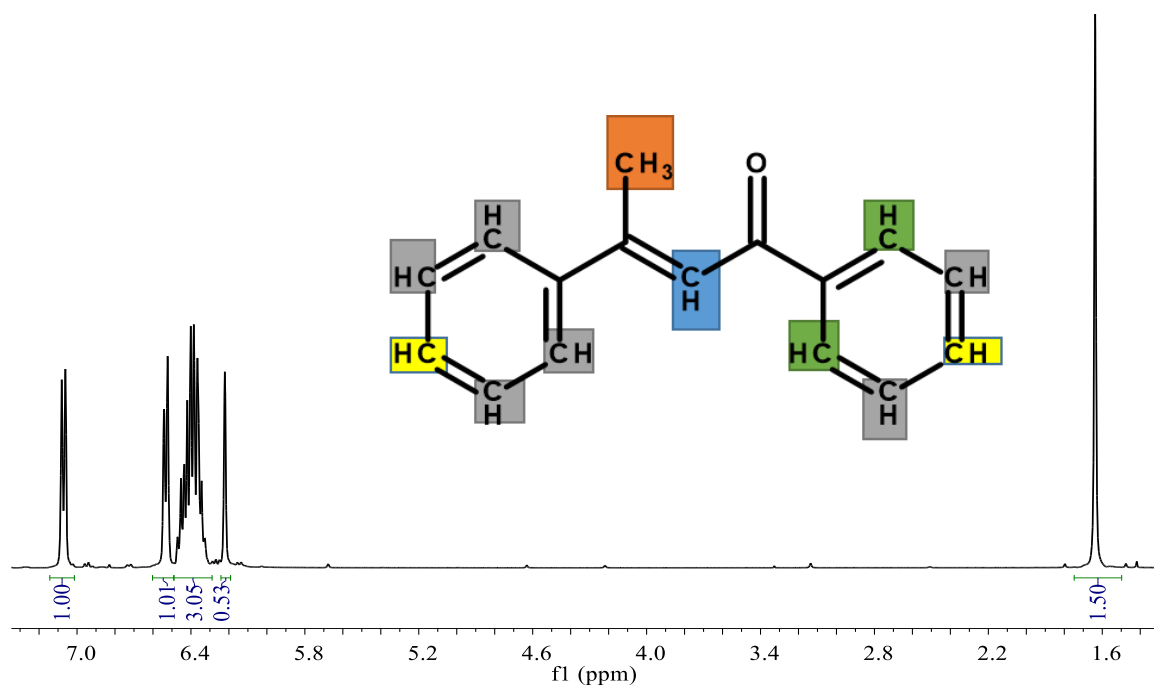


Figure 5-12: ^1H NMR (400 MHz, DMSO) NMR spectrum of reaction product in dynpnone synthesis.

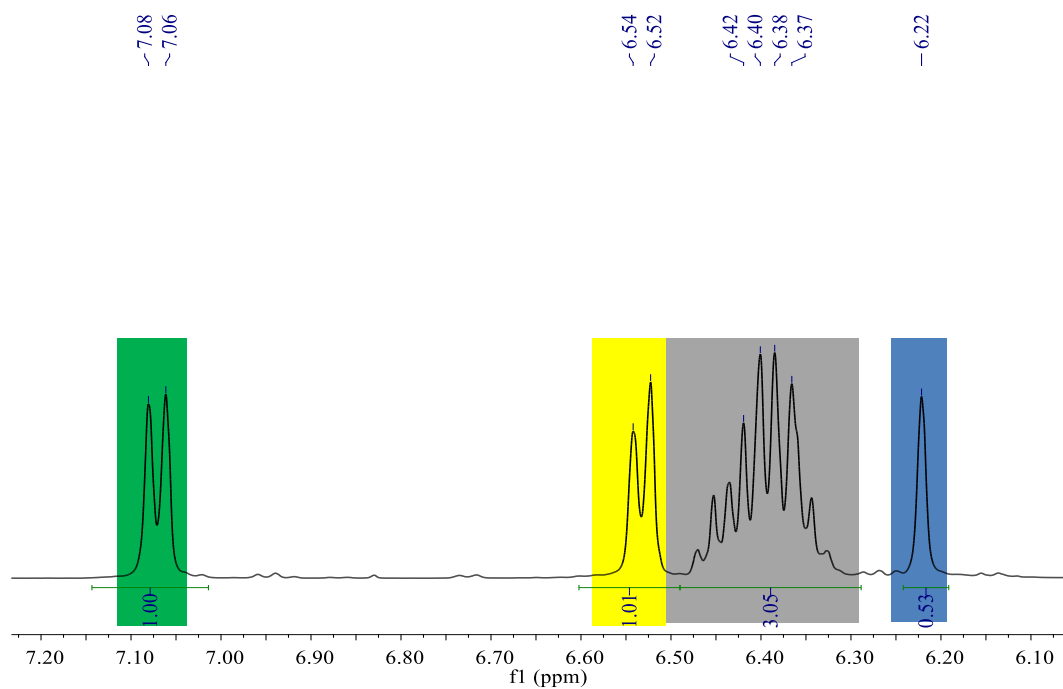


Figure 5-13: Enlarge area of integration of dynpnone between 6 to 7 ppm showing individual peak splitting.

5.4 CONCLUSIONS

Due to harsh conditions used traditionally in dypnone synthesis, along with large catalyst amounts, there has been a need to develop greener technology of its production through a more active catalyst.

This work has demonstrated that self-condensation of acetophenone using borenium ionic liquids as catalyst allows for mild reaction conditions. All borenium ionic liquids were found to be very active and exhibited high conversion and very high selectivity towards *trans*-dypnone. Systems with *N*-donors - the actual borenium ILs - were found to produce the highest conversions and selectivities. However, the precipitation of solid sediment under solvent-free conditions was a major drawback.

6 SUMMARY AND FUTURE WORK

Research covered in this thesis led to the development of a new class of Lewis acidic ionic liquids, based on borenium cations, with Lewis acidity placed uniquely in the cation. The first generation of these ionic liquids comprised chlorometallate anions, and was found to be extremely Lewis acidic (AN up to 181). Drawbacks included chloride-rich liquid (corrosion issues) and another Lewis acidity centre present in the anion, potentially impairing the catalytic process. The second generation was attempted with triflate anions, but these coordinated to the boron centre. Future work should be directed at developing other systems with less coordination anions, such as bistriflimide or tetracyanoborate.

The first generation of these ILs was successfully used for Diels-Alder reaction, delivering exceptional catalytic activity. High activity was also noted in aldol condensation of acetophenone to dypnone, albeit here solvent free reaction contained solid side-products that impaired mass transfer. Most likely, the preferred route forward would be to optimise reaction conditions towards minimum solvent amount that would allow for homogenous reaction mixture, even if reactivity remains compromised. This can be addressed by slightly elevated temperature.

7 REFERENCES

1. H. Olivier-Bourbigou, L. Magna, and D. Morvan, *Appl. Catal. A Gen.*, 2010, **373**, 1–56.
2. R. Sheldon, *Chem. Commun.*, 2001, 2399–2407.
3. J. Estager, J. D. Holbrey, and M. Swadźba-Kwaśny, *Chem. Soc. Rev.*, 2014, **43**, 847–86.
4. S. Coffie, J. M. Hogg, L. Cailler, A. Ferrer-Ugalde, R. W. Murphy, J. D. Holbrey, F. Coleman, and M. Swadźba-Kwaśny, *Angew. Chem. Int. Ed. Engl.*, 2015, **54**, 14970–14973.
5. K. Matuszek, S. Coffie, A. Chrobok, and M. Swadźba-Kwaśny, *Catal. Sci. Technol.*, 2017, **7**, 1045–1049.
6. S. Aldridge, A. J. Downs, and A. . . Aldridge, Anthony:Downs, *The Group 13 Metals Aluminium, Gallium, Indium And Thallium:: Chemical Patterns And Peculiarities*, John Wiley & Sons, Chichester, West Sussex, 2011.
7. M. Freemantle, *An Introduction to Ionic Liquids*, Royal Society of Chemistry, 2010, vol. 2.
8. T. S. De Vries, A. Prokofjevs, and E. Vedejs, *Chem. Rev.*, 2012, **112**, 4246–82.
9. Kirk-Othmer Encyclopedia of Chemical Technology, *Kirk-Othmer Encyclopedia of Chemical Technology*, John Wiley & Sons, Inc., Hoboken, NJ, USA, 2000, vol. 4.
10. Carlos A. Franca and Reinaldo Pis Diez, *J. Argent. Chem. Soc.*, 2009, 119–126.
11. D. R. Booth, Harold Simmons:Martin, *Boron trifluorides and its derivatives*, John Wiley & Sons, London, 1949.
12. D. C. Apperley, C. Hardacre, P. Licence, R. W. Murphy, N. V. Plechkova, K. R. Seddon, G. Srinivasan, M. Swadźba-Kwaśny, and I. J. Villar-Garcia, *Dalton Trans.*, 2010, **39**, 8679–87.
13. A. Fox, J. Hartman, and R. Humphries, *J. Chem. Soc. ...*, 1982, **3**.
14. I. B. Sivaev and V. I. Bregadze, *Coord. Chem. Rev.*, 2014, **270–271**, 75–88.
15. J. Stephen, G. J. Schrobilgen, and U. Brock, 1975.
16. F. J. Sowa, G. F. Hennion, and J. A. Nieuwland, *J. Am. Chem. Soc.*, 1935, **57**, 709–711.
17. J. Matsuo and M. Murakami, *Angew. Chemie Int. Ed.*, 2013, **52**, 9109–9118.
18. B. D. Rowsell, R. J. Gillespie, G. L. Heard, C. Ls, and R. V June, 1999, 4659–4662.
19. P. Koelle and H. Noeth, *Chem. Rev.*, 1985, **85**, 399–418.
20. O. P. Shitov, S. L. Ioffe, V. A. Tartakovskii, and S. S. Novikov, *Russ. Chem. Rev.*, 1970, **39**, 905–922.
21. G. E. Ryschkewitsch and J. W. Wiggins, *J. Am. Chem. Soc.*, 1970, **92**, 1790–1791.
22. P. Kölle and H. Nöth, *Chem. Rev.*, 1985, 399–418.
23. W. E. Piers, S. C. Bourke, and K. D. Conroy, *Angew. Chemie Int. Ed.*, 2005, **44**, 5016–5036.
24. Michael J. Ingleson, *Synthesis and Application of Organoboron Compounds*, Springer

International Publishing, Cham, 2015, vol. 49.

25. A. Prokofjevs, J. W. Kampf, A. Solovyev, D. P. Curran, and E. Vedejs, *J. Am. Chem. Soc.*, 2013, **135**, 15686–9.
26. A. Del Grosso, P. J. Singleton, C. a. Muryn, and M. J. Ingleson, *Angew. Chemie Int. Ed.*, 2011, **50**, 2102–2106.
27. P. Eisenberger, A. M. Bailey, and C. M. Crudden, *J. Am. Chem. Soc.*, 2012, **134**, 17384–17387.
28. D. W. Stephan and G. Erker, *Angew. Chemie Int. Ed.*, 2015, **54**, n/a-n/a.
29. E. R. Clark and M. J. Ingleson, *Organometallics*, 2013, **32**, 6712–6717.
30. A. Del Grosso, E. R. Clark, N. Montoute, and M. J. Ingleson, *Chem. Commun. (Camb.)*, 2012, **48**, 7589–91.
31. 1983, **88b**, 1161–1164.
32. H. Noth, S. Weber, B. Rasthofer, C. Narula, and A. Konstantinov, *Pure Appl. Chem.*, 1983, **55**, 1453–1461.
33. J. G. . V. Voet, Judith G.; Voet, Donald; Voet, *Biochemistry*, 2004, 496–500.
34. W. B. Jensen, *The Lewis acid-base concepts : an overview*, Wiley, 1980.
35. N. F. Hall, *J. Chem. Educ.*, 1930, **7**, 782.
36. I. B. Sivaev and V. I. Bregadze, *Coord. Chem. Rev.*, 2013.
37. A. Lavoisier, A. Lavoisier, S. Lavoisier, T. Lavoisier, and S. H. Davy, 1810, 1–9.
38. R. P. Bell, *Q. Rev. Chem. Soc.*, 1947, **1**, 113–125.
39. P. W. Ayers, *Faraday Discuss.*, 2007, **135**, 161.
40. N. F. Hall and J. B. Conant, *J. Am. Chem. Soc.*, 1927, **49**, 3047–3061.
41. A. F. O. Germann, *J. Am. Chem. Soc.*, 1925, **47**, 2461–2468.
42. G. L. Miessler, P. J. Fischer, D. A. Tarr, C. F. Macrae, I. J. Bruno, J. A. Chisholm, P. R. Edgington, P. McCabe, E. Pidcock, L. Rodriguez-Monge, R. Taylor, J. Van De Streek, and P. A. Wood, *Inorganic Chemistry* , 2008, vol. 41.
43. A. Corma and H. Garcia, *Chem. Rev.*, 2003.
44. J. G. Speight, *Lange's Handbook Of Chemistry, 16th ed.*, 2005.
45. N. F. Hall, *J. Chem. Educ.*, 1940, **17**, 124.
46. R. G. Pearson, *J. Am. Chem. Soc.*, 1963, **85**, 3533–3539.
47. R. G. Parr and R. G. Pearson, *J. Am. Chem. Soc.*, 1983, **105**, 7512–7516.
48. M. Smith, *Organic synthesis*, Academic Press, an imprint of Elsevier, 2011.
49. R. G. Pearson, *J. Chem. Educ.*, 1968, **45**, 581.
50. G. Klopman, *J. Am. Chem. Soc.*, 1968, **90**, 223–234.

51. R. S. Mulliken, *J. Chem. Phys.*, 1934, **2**, 782–793.
52. T. Bressmann, *J. Can. Dent. Assoc.*, 2004, **70**, 156–7.
53. M. A. Beckett, G. C. Strickland, J. R. Holland, and K. Sukumar Varma, *Polymer (Guildf.)*, 1996, **37**, 4629–4631.
54. U. Mayer, V. Gutmann, and W. Gerger, *Monatshefte für Chemie*, 1975, **106**, 1235–1257.
55. V. Gutmann, *Coord. Chem. Rev.*, 1976, **18**, 225–255.
56. V. Gutmann, *Electrochim. Acta*, 1976, **21**, 661–670.
57. T. A. Zawodzinski and R. A. Osteryoung, *Inorg. Chem.*, 1989, **28**, 1710–1715.
58. R. F. Childs, D. L. Mulholland, and A. Nixon, *Can. J. Chem.*, 1982, **60**, 809–812.
59. R. F. Childs, D. L. Mulholland, and A. Nixon, *Can. J. Chem.*, 1982, **60**, 801–808.
60. P. Laszlo and M. Teston, *J. Am. Chem. Soc.*, 1990, **112**, 8750–8754.
61. K. O. Christe, D. A. Dixon, D. McLemore, W. W. Wilson, J. A. Sheehy, and J. A. Boatz, *J. Fluor. Chem.*, 2000, **101**, 151–153.
62. I. Krossing and I. Raabe, *Chemistry*, 2004, **10**, 5017–30.
63. E. R. Clark, A. Del Grosso, and M. J. Ingleson, *Chemistry*, 2013, **19**, 2462–6.
64. S. A. Solomon, A. Del Grosso, E. R. Clark, V. Bagutski, J. J. W. McDouall, and M. J. Ingleson, *Organometallics*, 2012, **31**, 1908–1916.
65. J. Olah, G. A.; Prakash, G. K. S.; Molnar, Á.; Sommar, *Superacid Chemistry*, Wiley, 2009.
66. G. a Olah, G. K. S. Prakash, and J. Sommer, *Science (80-.)*, 1979, **206**, 13–20.
67. F. Scholz, D. Himmel, H. Scherer, and I. Krossing, *Chem. - A Eur. J.*, 2013, **19**, 109–116.
68. S. Gabriel and J. Weiner, *Berichte der Dtsch. Chem. Gesellschaft*, 1888, **21**, 2669–2679.
69. C. Austen Angell, Y. Ansari, and Z. Zhao, *Faraday Discuss.*, 2012, **154**, 9–27.
70. F. Endres and S. Zein El Abedin, *Phys. Chem. Chem. Phys.*, 2006, **8**, 2101–2116.
71. F. H. Hurley and T. P. Wier, *J. Electrochem. Soc.*, 1951, **98**, 207.
72. F. H. Hurley and T. P. Wier, *J. Electrochem. Soc.*, 1951, **98**, 203.
73. H. L. Jones and R. A. Osteryoung, in *Advances in Molten Salt Chemistry*, Springer US, Boston, MA, 1975, pp. 121–176.
74. J. S. Wilkes, J. A. Levisky, R. A. Wilson, and C. L. Hussey, *Inorg. Chem.*, 1982, **21**, 1263–1264.
75. J. S. Wilkes and M. J. Zaworotko, *J. Chem. Soc. Chem. Commun.*, 1992, **213**, 965.
76. A. P. Abbott, G. Capper, D. L. Davies, H. L. Munro, R. K. Rasheed, V. Tambyrajah, T. Welton, M. J. Earle, K. R. Seddon, P. Wassercheid, W. Keim, J. S. Wilkes, J. A. Levisky, R. A. Wilson, C. L. Hussey, J. A. A. Fannin, L. A. King, J. A. Levisky, J. S. Wilkes, T. M. Laher, C. L. Hussey, M. S. Sitze, E. R. Schreiter, E. V. Patterson, R. G. Freeman, R. J. Gale, B. P. Gilbert, R. A. Osteryoung, J. S. Wilkes, J. S. Frye, G. F. Reynolds, S. P. Wicelinski, R. J. Gale, K. M. Pamidimukkala, R. A.

- Laine, R. A. Carpio, L. A. King, R. E. Lindstrom, J. C. Nardi, and C. L. Hussey, *Chem. Commun.*, 2001, **99**, 2010–2011.
77. T. Fischer, A. Sethi, T. Welton, and J. Woolf, *Tetrahedron Lett.*, 1999, **40**, 793–796.
 78. T. Welton, *Coord. Chem. Rev.*, 2004, **248**, 2459–2477.
 79. I. Kimaru and J. Fisher, *Lab. J.*, 2011, 2–5.
 80. H. Tokuda, S. Tsuzuki, M. A. B. H. Susan, K. Hayamizu, and M. Watanabe, *J. Phys. Chem. B*, 2006, **110**, 19593–600.
 81. C. Schröder and O. Steinhauser, *J. Chem. Phys.*, 2008, **128**, 224503.
 82. S. Theivaprakasam, D. R. MacFarlane, and S. Mitra, *Electrochim. Acta*, 2015, **180**, 737–745.
 83. B. Yang, C. Li, J. Zhou, J. Liu, and Q. Zhang, *Electrochim. Acta*, 2014, **148**, 39–45.
 84. O. Zavgorodnya, J. L. Shamshina, M. Mittenthal, P. D. McCrary, G. P. Rachiero, H. M. Titi, and R. D. Rogers, *New J. Chem.*, 2017, **41**, 1499–1508.
 85. J. Stoimenovski and D. R. MacFarlane, *Chem. Commun.*, 2011, **47**, 11429–11431.
 86. K. Fujita, D. R. MacFarlane, and M. Forsyth, *Chem. Commun.*, 2005, 4804.
 87. D. Constatinescu, C. Herrmann, and H. Weingärtner, *Phys. Chem. Chem. Phys.*, 2010, **12**, 1756.
 88. L. C. Brown, J. M. Hogg, and M. Swadźba-Kwaśny, *Top. Curr. Chem.*, 2017, **375**, 1–40.
 89. T. Welton, *Chem. Rev.*, 1999, **99**, 2071–2084.
 90. A. S. Amarasekara, *Chem. Rev.*, 2016, **116**, 6133–6183.
 91. J. R. Harjani, S. J. Nara, and M. M. Salunkhe, *Tetrahedron Lett.*, 2002, **43**, 1127–1130.
 92. D. Keyes, T. Phipps, and W. Klabunde, 1933.
 93. F. H. Hurley, 1948.
 94. M. Earle, K. Seddon, and C. Adams, *Chem. Commun.*, 1998, 2097–2098.
 95. Y. Qin, G. Cheng, A. Sundararaman, and F. Ja, 2002, 12672–12673.
 96. X. Q. Xing, G. Y. Zhao, and J. Z. Cui, *Sci. China Chem.*, 2012, **55**, 1542–1547.
 97. M. P. Atkins, / Kenneth R. Seddon, and / Małgorzata Swadźba-Kwaśny, *Pure Appl. Chem.*, 2011, **83**, 1391–1406.
 98. M. Markiton, A. Chrobok, K. Matuszek, K. R. Seddon, and M. Swadźba-Kwaśny, *RSC Adv.*, 2016, **6**, 30460–30467.
 99. Y. J. Kim and R. S. Varma, *Tetrahedron Lett.*, 2005, **46**, 7447–7449.
 100. Y. F. Lin and I. W. Sun, *Electrochim. Acta*, 1999, **44**, 2771–2777.
 101. P.-Y. Chen, M.-C. Lin, and I.-W. Sun, *J. Electrochem. Soc.*, 2000, **147**, 3350–3355.
 102. P.-Y. Chen and I.-W. Sun, *Electrochim. Acta*, 2001, **46**, 1169–1177.
 103. M. S. Sitze, E. R. Schreiter, E. V. Patterson, and R. G. Freeman, *Inorg. Chem.*, 2001, **40**, 2298–

- 2304.
104. A. P. Abbott, G. Capper, D. L. Davies, and R. Rasheed, *Inorg. Chem.*, 2004, **43**, 3447–3452.
 105. A. P. Abbott, G. Capper, D. L. Davies, R. K. Rasheed, and V. Tambyrajah, *Trans. Inst. Met. Finish.*, 2001, **79**, 204–206.
 106. A. P. Abbott, G. Capper, D. L. Davies, R. K. Rasheed, and V. Tambyrajah, *Green Chem.*, 2002, **4**, 24–26.
 107. R. C. Morales, V. Tambyrajah, P. R. Jenkins, D. L. Davies, and A. P. Abbott, *Chem. Commun.*, 2003, 158–159.
 108. G. W. Parshall, *J. Am. Chem. Soc.*, 1972, **94**, 8716–8719.
 109. T. Tamura, K. Yoshida, T. Hachida, M. Tsuchiya, M. Nakamura, Y. Kazue, N. Tachikawa, K. Dokko, and M. Watanabe, *Chem. Lett.*, 2010, **39**, 753–755.
 110. K. Ueno, R. Tatara, S. Tsuzuki, S. Saito, H. Doi, K. Yoshida, T. Mandai, M. Matsugami, Y. Umabayashi, K. Dokko, and M. Watanabe, *Phys. Chem. Chem. Phys.*, 2015, **17**, 8248–57.
 111. K. Shimizu, A. A. Freitas, R. Atkin, G. G. Warr, P. A. FitzGerald, H. Doi, S. Saito, K. Ueno, Y. Umabayashi, M. Watanabe, and J. N. Canongia Lopes, *Phys. Chem. Chem. Phys.*, 2015, **17**, 22321–22335.
 112. D. J. Eyckens, M. E. Champion, B. L. Fox, P. Yoganantharajah, Y. Gibert, T. Welton, and L. C. Henderson, *European J. Org. Chem.*, 2016, **2016**, 913–917.
 113. M. A. Forman and W. P. Dailey, *J. Am. Chem. Soc.*, 1991, **113**, 2761–2762.
 114. M. J. Earle, P. B. McCormac, and K. R. Seddon, *Green Chem.*, 1999, **1**, 23–25.
 115. F. Mutelet, J.-N. Jaubert, M. Rogalski, M. Boukherissa, and A. Dicko, *J. Chem. Eng. Data*, 2006, **51**, 1274–1279.
 116. V. Gutmann, *Pure Appl. Chem.*, 1971, **27**, 73–88.
 117. R. A. Mantz, P. C. Trulove, R. T. Carlin, T. L. Theim, and R. A. Osteryoung, *Inorg. Chem.*, 1997, **36**, 1227–1232.
 118. J. Estager, A. a Oliferenko, K. R. Seddon, and M. Swadźba-Kwaśny, *Dalt. Trans.*, 2010, **39**, 11375.
 119. J. Estager, P. Nockemann, K. R. Seddon, M. Swadźba-Kwaśny, and S. Tyrrell, *Inorg. Chem.*, 2011, **50**, 5258–5271.
 120. J. Estager, P. Nockemann, K. R. Seddon, M. Swadźba-Kwaśny, and S. Tyrrell, *Inorg. Chem.*, 2011, **50**, 5258–5271.
 121. M. Currie, J. Estager, P. Licence, S. Men, P. Nockemann, K. R. Seddon, M. Swadźba-Kwaśny, and C. Terrade, *Inorg. Chem.*, 2013, **52**, 1710–1721.
 122. J. A. Lercher, C. Gründling, and G. Eder-Mirth, *Catal. Today*, 1996, **27**, 353–376.
 123. Y. Yang and Y. Kou, *Chem. Commun.*, 2004, 226.
 124. S. E. Denmark and G. L. Beutner, *Angew. Chem. Int. Ed. Engl.*, 2008, **47**, 1560–638.

125. W. F. Schneider, C. K. Narula, H. Noeth, and B. E. Bursten, *Inorg. Chem.*, 1991, **30**, 3919–3927.
126. T. Brinck, J. S. Murray, and P. Politzer, 1993, **32**, 2622–2625.
127. T. Ruman, K. Długopolska, A. Jurkiewicz, K. Rydel, A. Leś, and W. Rode, *Bioorg. Chem.*, 2010, **38**, 87–91.
128. J. M. Rivera, S. Rincón, N. Farfán, and R. Santillan, *J. Organomet. Chem.*, 2011, **696**, 2420–2428.
129. A. Fratiello, G. A. Vidulich, and R. E. Schuster, *J. Inorg. Nucl. Chem.*, 1974, **36**, 93–95.
130. J. R. Durig, S. Riethmiller, V. F. Kalasinsky, and J. D. Odom, *Inorg. Chem.*, 1974, **13**, 2729–2735.
131. S. Dagorne and D. A. Atwood, *Chem. Rev. (Washington, DC, United States)*, 2008, **108**, 4037–4071.
132. Boundless, *Trihalides: Boron-Halogen Compounds*, Boundless, 2016.
133. H. Höpfl, *J. Organomet. Chem.*, 1999, **581**, 129–149.
134. J. Slattery and S. Hussein, *Dalt. Trans.*, 2012, 1808–1815.
135. I. López-Martin, E. Burello, P. N. Davey, K. R. Seddon, and G. Rothenberg, *ChemPhysChem*, 2007, **8**, 690–695.
136. J. Burt, W. Levason, and G. Reid, *Coord. Chem. Rev.*, 2014, **260**, 65–115.
137. S. Saha, R. K. Kottalanka, T. K. Panda, K. Harms, S. Dehnen, and H. P. Nayek, *J. Organomet. Chem.*, 2013, **745–746**, 329–334.
138. P. N. Gates, E. J. McLaughlan, and E. F. Mooney, *Spectrochim. Acta*, 1965, **21**, 1445–8, and references cited therein.
139. E. Chénard, A. Sutrisno, L. Zhu, R. S. Assary, J. A. Kowalski, J. L. Barton, J. A. Bertke, D. L. Gray, F. R. Brushett, L. A. Curtiss, and J. S. Moore, *J. Phys. Chem. C*, 2016, **120**, 8461–8471.
140. D. E. Young, G. E. McAchran, and S. G. Shore, *J. Am. Chem. Soc.*, 1966, **88**, 4390–4396.
141. E. Tsurumaki, S. Hayashi, F. S. Tham, C. A. Reed, and A. Osuka, *J. Am. Chem. Soc.*, 2011, **133**, 11956–9.
142. E. J. McLaughlan and E. F. Mooney, *Spectrochim. Acta Part A Mol. Spectrosc.*, 1967, **23**, 1227–1230.
143. W. L. Smith, *J. Chem. Educ.*, 1977, **54**, 469.
144. F. A. Perras and D. L. Bryce, *Chem. Sci.*, 2014, **5**, 2428.
145. W. D. Phillips, H. C. Miller, and E. L. Muetterties, *J. Am. Chem. Soc.*, 1959, **81**, 4496–4500.
146. P. P. Power, *Angew. Chemie Int. Ed. English*, 1990, **29**, 449–460.
147. D. . Walsh and B. . Doyle, *Nucl. Instruments Methods Phys. Res. Sect. B Beam Interact. with Mater. Atoms*, 2000, **161–163**, 629–634.
148. C. K. Narula and H. Nöth, *Zeitschrift für Naturforsch. B*, 1983, **38**, 1161–1164.
149. A. Zheng, S. J. Huang, W. H. Chen, P. H. Wu, H. Zhang, H. K. Lee, L. C. De Ménorval, F. Deng,

- and S. Bin Liu, *J. Phys. Chem. A*, 2008, **112**, 7349–7356.
150. A. Zheng, H. Zhang, X. Lu, S. Bin Liu, and F. Deng, *J. Phys. Chem. B*, 2008, **112**, 4496–4505.
 151. A. Zheng, S.-J. Huang, S.-B. Liu, and F. Deng, *Phys. Chem. Chem. Phys.*, 2011, **13**, 14889.
 152. I. O. Sutherland, in *Annual Reports on NMR Spectroscopy vol.4*, Academic Press, 1972, pp. 71–235.
 153. R. A. Oliveira, R. O. Silva, G. A. Molander, and P. H. Menezes, *Magn. Reson. Chem.*, 2009, **47**, 873–878.
 154. F. B. Mallory and C. W. Mallory, *J. Am. Chem. Soc.*, 1985, **107**, 4816–4819.
 155. J. H. Miller and L. Andrews, *J. Am. Chem. Soc.*, 1980, **102**, 4900–4906.
 156. P. A. Z. Suarez, S. Einloft, J. E. L. Dullius, R. F. de Souza, and J. Dupont, *J. Chim. Phys. Physico-Chimie Biol.*, 1998, **95**, 1626–1639.
 157. M. M. Kappes, J. S. Uppal, and R. H. Staley, *Organometallics*, 1982, **1**, 1303–1307.
 158. J. A. Dean, *Lange's Handbook of Chemistry*, McGraw-Hill INC: New york, New York, 15th edn., 2005.
 159. M. Blesic, M. Swadźba-Kwaśny, T. Belhocine, H. Q. N. Gunaratne, J. N. C. Lopes, M. F. C. Gomes, A. A. H. Pádua, K. R. Seddon, and L. P. N. Rebelo, *Phys. Chem. Chem. Phys.*, 2009, **11**, 8939–48.
 160. X. Paredes, O. Fandiño, A. S. Pensado, M. J. P. Comuñas, and J. Fernández, *J. Chem. Thermodyn.*, 2012, **44**, 38–43.
 161. T. Bui, W. Korth, S. Aschauer, and A. Jess, *Green Chem.*, 2009, **11**, 1961.
 162. DR. ANTHONY MELVIN CRASTO., .
 163. S. Zhang, N. Sun, X. He, X. Lu, and X. Zhang, *J. Phys. Chem. Ref. Data*, 2006, **35**, 1475–1517.
 164. C. R. Martinez and B. L. Iverson, *Chem. Sci.*, 2012, **3**, 2191.
 165. K. Matuszek, A. Chrobok, F. Coleman, K. R. Seddon, and M. Swadźba-Kwaśny, *Green Chem.*, 2014, **16**, 3463.
 166. T. L. Greaves and C. J. Drummond, *Chem. Rev.*, 2015, **115**, 11379–11448.
 167. K. M. Johansson, E. I. Izgorodina, M. Forsyth, D. R. MacFarlane, and K. R. Seddon, *Phys. Chem. Chem. Phys.*, 2008, **10**, 2972.
 168. C. . Hussey, *Elsevier New York*, 1983, **5**, 185.
 169. I.-W. Sun and C. L. Hussey, *J. Electroanal. Chem. Interfacial Electrochem.*, 1989, **274**, 325–331.
 170. H. A. Øye, M. Jagtoyen, T. Oksefjell, and J. S. Wilkes, *Mater. Sci. Forum*, 1991, **73–75**, 183–190.
 171. C. Hardacre, R. W. Murphy, K. R. Seddon, G. Srinivasan, and M. Swadźba-Kwaśny, in *Australian Journal of Chemistry*, 2010, vol. 63, pp. 845–848.
 172. Y.-R. Luo, *Comprehensive handbook of chemical bond energies /*, CRC Press, Boca Raton, FL :, 2007.

173. F. Coleman, G. Srinivasan, and M. Swadźba-Kwaśny, *Angew. Chemie - Int. Ed.*, 2013, **52**, 12582–12586.
174. V. Bagutski, A. Del Grosso, J. A. Carrillo, I. A. Cade, M. D. Helm, J. R. Lawson, P. J. Singleton, S. A. Solomon, T. Marcelli, and M. J. Ingleson, *J. Am. Chem. Soc.*, 2013, **135**, 474–487.
175. *Ionic Liquids in Chemical Analysis*, CRC Press, 2008.
176. J. S. Wilkes, J. S. Frye, and G. F. Reynolds, *Inorg. Chem.*, 1983, **22**, 3870–3872.
177. J. S. Wilkes, C. L. Hussey, and J. R. Sanders, *Polyhedron*, 1986, **5**, 1567–1571.
178. J. Mason, in *Multinuclear NMR*, Springer US, Boston, MA, 1987, pp. 1–2.
179. H. W. Bae, J.-S. Han, S. Jung, M. Cheong, H. S. Kim, and J. S. Lee, *Appl. Catal. A Gen.*, 2007, **331**, 34–38.
180. K. Nakamoto, *Infrared and Raman spectra of inorganic and coordination compounds. Part A, Theory and applications in inorganic chemistry*, Wiley, 2009.
181. J. Coates, in *Encyclopedia of Analytical Chemistry*, 2006.
182. L. W. Daasch and D. C. Smith, *Anal. Chem.*, 1951, **23**, 853–868.
183. J. Jacquemin, P. Husson, A. A. H. Padua, and V. Majer, *Green Chem.*, 2006, **8**, 172–180.
184. N. V. Plechkova, R. D. Rogers, and K. R. Seddon, Eds., *Ionic Liquids: From Knowledge to Application*, American Chemical Society, Washington DC, 2010, vol. 1030.
185. H. Tokuda, S. Tsuzuki, M. A. B. H. Susan, K. Hayamizu, and M. Watanabe, *J. Phys. Chem. B*, 2006, **110**, 19593–600.
186. S. Mahluddin and K. Ismail, *J. Phys. Chem.*, 1983, **3244**, 5241–5244.
187. A. E. Andreatta, A. Arce, E. Rodil, and A. Soto, *J. Solution Chem.*, 2010, **39**, 371–383.
188. L. Vinet and A. Zhedanov, *J. Phys. A Math. Theor.*, 2011, **44**, 85201.
189. L. S. Garca-Coln, L. F. del Castillo, and P. Goldstein, *Phys. Rev. B*, 1989, **40**, 7040–7044.
190. E.-J. Donth, *The Glass Transition*, Springer Berlin Heidelberg, Berlin, Heidelberg, 2001, vol. 48.
191. J. R. Lawson, E. R. Clark, I. A. Cade, S. A. Solomon, and M. J. Ingleson, *Angew. Chemie Int. Ed.*, 2013, **52**, 7518–7522.
192. E. L. Myers, C. P. Butts, and V. K. Aggarwal, *Chem. Commun. (Camb.)*, 2006, 4434–6.
193. J. M. Farrell and D. W. Stephan, *Angew. Chemie Int. Ed.*, 2015, **54**, 5214–5217.
194. G. R. Eaton, *J. Chem. Educ.*, 1969, **46**, 547.
195. M. A. Beckett, D. S. Brassington, P. Owen, M. B. Hursthouse, M. E. Light, K. M. A. Malik, and K. S. Varma, *J. Organomet. Chem.*, 1999, **585**, 7–11.
196. A. Del Grosso and R. Pritchard, ..., 2009, 241–249.
197. T. S. De Vries and E. Vedejs, *Organometallics*, 2007, **26**, 3079–3081.
198. A. H. Cowley and M. C. Damasco, *J. Am. Chem. Soc.*, 1971, **93**, 6815–6821.

199. I. Krossing, J. M. Slattery, C. Daguenet, P. J. Dyson, A. Oleinikova, and H. Weingärtner, *J. Am. Chem. Soc.*, 2006, **128**, 13427–13434.
200. M. S.-K. and G. F. F. Coleman, S. Coffie, M.P. Atkins, J. Hogg, A. Ugalde, *United Kingdom Pat. Appl.*, 1974, 1–10.
201. M. J. Earle, P. B. McCormac, and K. R. Seddon, *Green Chem.*, 1999, **1**, 23–25.
202. E. Janus, I. Goc-Maciejewska, M. Łożyński, and J. Pernak, *Tetrahedron Lett.*, 2006, **47**, 4079–4083.
203. C. Chiappe, M. Malvaldi, and C. S. Pomelli, *Green Chem.*, 2010, **12**, 1330.
204. O. Diels and K. Alder, *Berichte der Dtsch. Chem. Gesellschaft (A B Ser.)*, 1929, **62**, 2081–2087.
205. O. Diels and K. Alder, *Justus Liebig's Ann. der Chemie*, 1928, **460**, 98–122.
206. S. Kobayashi and K. Manabe, *Acc. Chem. Res.*, 2002, **35**, 209–217.
207. F. A. Carey and R. J. Sundberg, *Advanced Organic Chemistry Part A: Structure and Mechanisms*, 2007.
208. F. A. Carey and R. J. Sundberg, *Advanced Organic Chemistry Part B: Reactions and Synthesis*, 2007.
209. J. Bah and J. Franzén, *Chem. - A Eur. J.*, 2014, **20**, 1066–1072.
210. E. J. Corey, T. Shibata, and T. W. Lee, *J. Am. Chem. Soc.*, 2002, **124**, 3808–3809.
211. Y. Hayashi, J. J. Rohde, and E. J. Corey, *J. Am. Chem. Soc.*, 1996, **118**, 5502–5503.
212. B. M. Mikhailov and K. L. Cherkasova, *Bull. Acad. Sci. USSR Div. Chem. Sci.*, 1976, **25**, 1927–1932.
213. S. R. Waldvogel, *Tietze, L. F.; Beifuss, U*, 1991, **2**, 341–392.
214. L. Eberlin, F. Tripoteau, F. Carreaux, A. Whiting, and B. Carboni, *Beilstein J. Org. Chem.*, 2014, **10**, 237–250.
215. I. Meracz and T. Oh, *Tetrahedron Lett.*, 2003, **44**, 6465–6468.
216. D. A. Jaeger and C. E. Tucker, *Tetrahedron Lett.*, 1989, **30**, 1785–1788.
217. C. W. Lee, *Tetrahedron Lett.*, 1999, **40**, 2461–2464.
218. Y. Xiao and S. V. Malhotra, *Tetrahedron Lett.*, 2004, **45**, 8339–8342.
219. A. Schnurr, M. Bolte, H.-W. Lerner, and M. Wagner, *Eur. J. Inorg. Chem.*, 2012, **2012**, 112–120.
220. B. B. Snider, *Acc. Chem. Res.*, 1980, **13**, 426–432.
221. K. Matuszek, A. Chrobok, P. Latos, M. Markiton, K. Szymańska, A. Jarzębski, and M. Swadźba-Kwaśny, *Catal. Sci. Technol.*, 2016, **6**, 8129–8137.
222. P. Wasserscheid, *Catal. Letters*, 2015, **145**, 380–397.
223. C. W. Lee, *Tetrahedron Lett.*, 1999, **40**, 2461–2464.
224. J. M. Hogg, L. C. Brown, K. Matuszek, P. Latos, A. Chrobok, and M. Swadźba-Kwaśny, *Dalt.*

- Trans.*, 2017, **46**, 11561–11574.
225. K. Erfurt, I. Wandzik, K. Walczak, K. Matuszek, and A. Chrobok, *Green Chem.*, 2014, **16**, 3508.
 226. M. J. S. Dewar, S. Olivella, and J. J. P. Stewart, *J. Am. Chem. Soc.*, 1986, **108**, 5771–5779.
 227. Trost B. M., I. Fleming, C. H. Heathcock, *C. H. Heathcock, In Comprehensive Organic Synthesis, No Title*, Pergamon Press, Oxford, oxford, 1991.
 228. M. Selvaraj, P. . Sinha, and A. Pandurangan, *Microporous Mesoporous Mater.*, 2004, **70**, 81–91.
 229. K. Tanaka, S. Motomatsu, K. Koyama, and K. Fukase, *Tetrahedron Lett.*, 2008, **49**, 2010–2012.
 230. K. Deng, Q.-Y. Huai, Z.-L. Shen, H.-J. Li, C. Liu, and Y.-C. Wu, *Org. Lett.*, 2015, **17**, 1473–6.
 231. and S. A. L. S. Yatluk Yu. G. , Sosnovskikh V. Ya., *Russ. J. Org. Chem.*, 763–765.
 232. T. Mukaiyama, *Organic Reactions*, John Wiley & Sons, Inc., Hoboken, NJ, USA, 2004.
 233. D. Tichit, M. Naciri Bennani, F. Figueras, R. Tessier, and J. Kervennal, *Appl. Clay Sci.*, 1998, **13**, 401–415.
 234. smith B. Micheal, *March's Advanced Organic Chemistry: Reactions, Mechanisms, and Structure, 7th Edition - Michael B. Smith, 2013*, 2013.
 235. Carey A. Francis, *Organic chemistry*, 5th ed. Ed., 2003.
 236. J. I. Di Cosimo, V. K. Díez, and C. R. Apesteguía, *Appl. Catal. A Gen.*, 1996, **137**, 149–166.
 237. C. H. Heathcock, *Comprehensive Organic Synthesis*, Elsevier, 1991.
 238. C. H. Cheon and H. Yamamoto, *Tetrahedron Lett.*, 2009, **50**, 3555–3558.
 239. S. Kobayashi, Y. Mori, S. Nagayama, and K. Manabe, *Green Chem.*, 1999, **1**, 175–177.
 240. K. Saravanan, B. Tyagi, and H. C. Bajaj, *J. Sol-Gel Sci. Technol.*, 2011, **61**, 275–280.
 241. S. Kobayashi, Y. Yamashita, W.-J. Yoo, T. Kitanosono, and J.-F. Soulé, in *Comprehensive Organic Synthesis II*, Elsevier, 2014, pp. 396–450.
 242. J. B. F. N. Engberts, B. L. Feringa, E. Keller, and S. Otto, *Recl. des Trav. Chim. des Pays-Bas*, 2010, **115**, 457–464.
 243. A. Scettri, V. De Sio, R. Villano, P. Manzo, and M. R. Acocella, *Tetrahedron Lett.*, 2010, **51**, 3658–3661.
 244. C. Palomo, M. Oiarbide, and J. M. García, *Chem. Soc. Rev.*, 2004, **33**, 65–75.
 245. N. Mase and Y. Hayashi, in *Comprehensive Organic Synthesis II*, Elsevier, 2014, pp. 273–339.
 246. A. Abiko, in *ACS Symposium Series*, 2016, vol. 1236, pp. 123–171.
 247. A. Coca, *Boron Reagents in Synthesis*, American Chemical Society, Washington, DC, 2016, vol. 1236.
 248. D. A. Evans, J. V. Nelson, E. Vogel, and T. R. Taber, *J. Am. Chem. Soc.*, 1981, **103**, 3099–3111.
 249. H. Defrancesco, J. Dudley, and A. Coca, in *ACS Symposium Series*, 2016, vol. 1236, pp. 1–25.

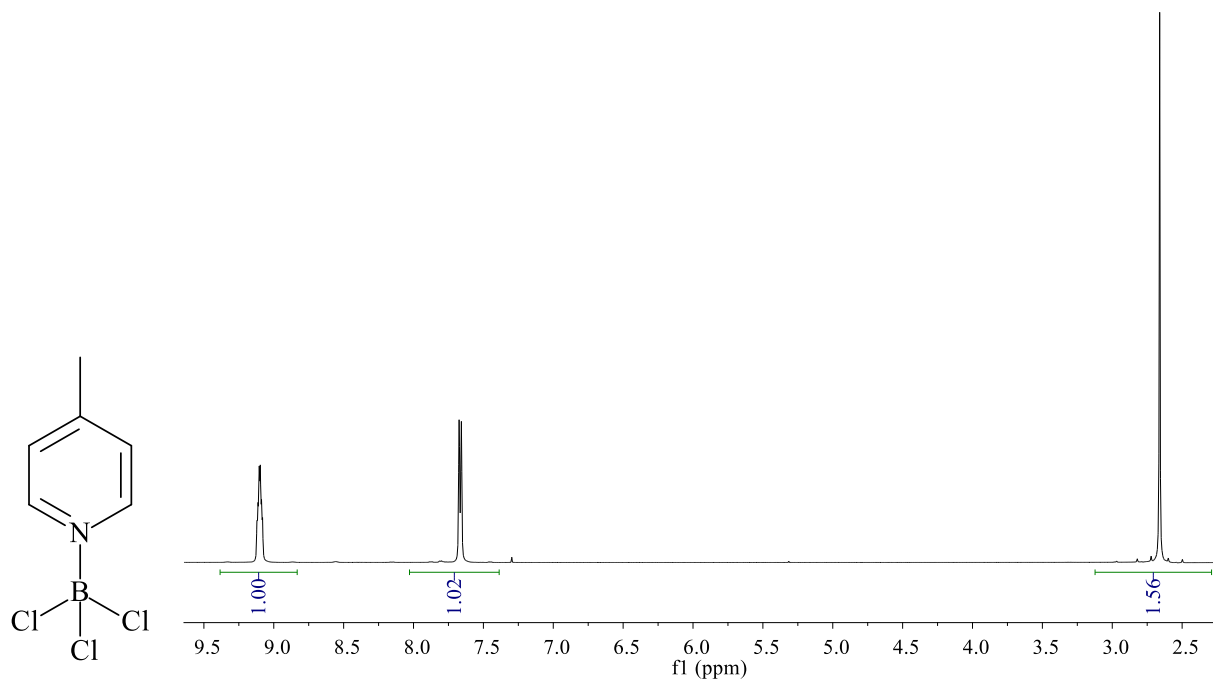
250. T. . I. Mukaiyama, *T. Chem. Lett*, 1976, 559—562.
251. Z. Hu, J. Liu, G. Li, Z. Dong, and W. Li, *J. Chinese Chem. Soc.*, 2004, **51**, 581–583.
252. A. B. Northrup and D. W. C. MacMillan, *J. Am. Chem. Soc.*, 2002, **124**, 6798–6799.
253. H. Adkins and F. W. Cox, *J. Am. Chem. Soc.*, 1938, **60**, 1151–1159.
254. R. V. Oppenauer, *Recl. des Trav. Chim. des Pays???Bas*, 1937, **56**, 137–144.
255. R. W. Roeske, D. B. Bright, R. L. Johnson, W. J. DeJarlais, R. W. Bush, and H. R. Snyder, *J. Am. Chem. Soc.*, 1960, **82**, 3128–3133.
256. R. Aumann, B. Jasper, and R. Frohlich, 1995, 3167–3172.
257. NIIR Board, *Modern Technology of Industrial Chemicals*, 2003.
258. C. Venkatesan, *J. Mol. Catal. A Chem.*, 2002, **181**, 179–187.
259. M. Braun, *Modern Enolate Chemistry: From Preparation to Applications in Asymmetric . Manfred Braun*, 2016.
260. Ganapati D. Yadav* and Ginish George, in *Green engineering and sustainability in the pharmaceutical engineering*, Philadelphia, PA, 2009, pp. 4–10.
261. Z. Hu, J. Liu, Z. Dong, L. Guo, D. Wang, and P. Zeng, *J. Chem. Res.*, 2004, 158–159.
262. N. Gelsomini, L. J. Mazza, and A. Guarna, *J. Chromatogr. A*, 1974, **101**, 182–184.
263. K. M. Cergol and M. J. Coster, *Nat. Protoc.*, 2007, **2**, 2568–73.

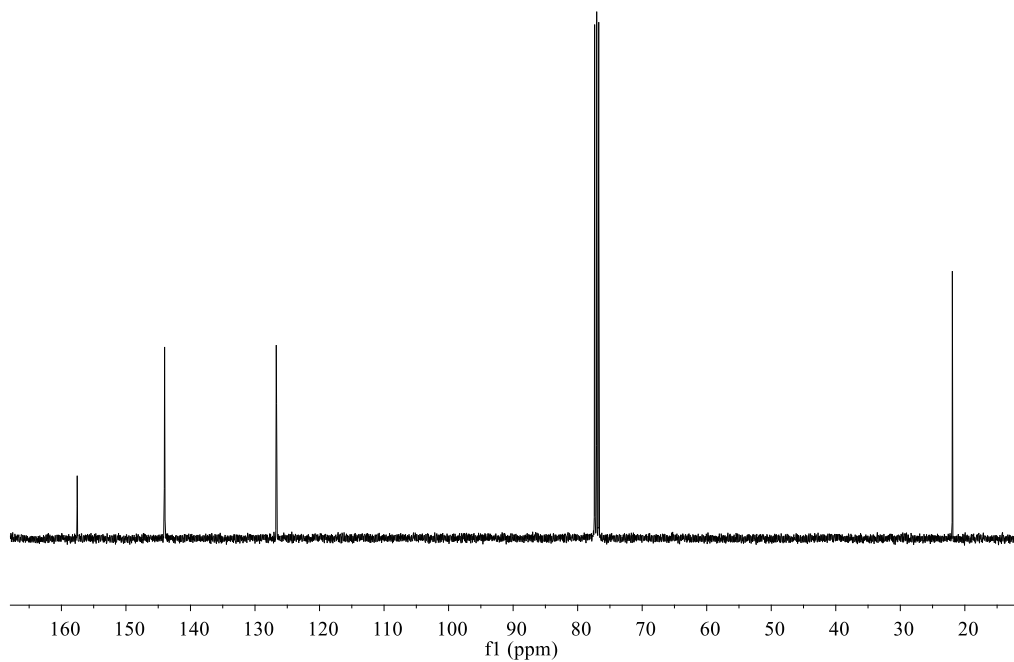
APPENDIX A - NMR Spectroscopy Data

Boron trichloride 4-methylpyridine

BCl₃C₆H₇N. ¹H NMR (400 MHz, CDCl₃) δ 9.15 (d, 2H), 7.61 (d, 2H), 2.65 (s, 3H) ppm.

¹³C NMR (101 MHz, CDCl₃) δ 157.55, 144.01, 126.73, 126.71, 126.68, 126.66, 21.93, ppm.

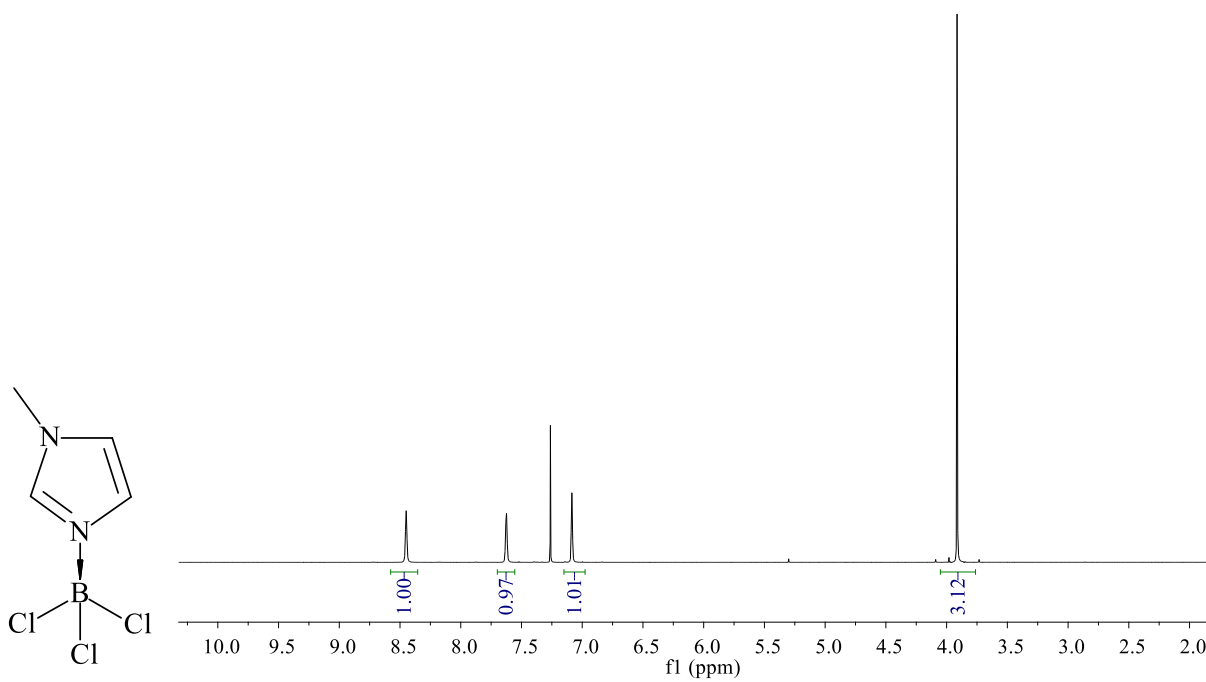


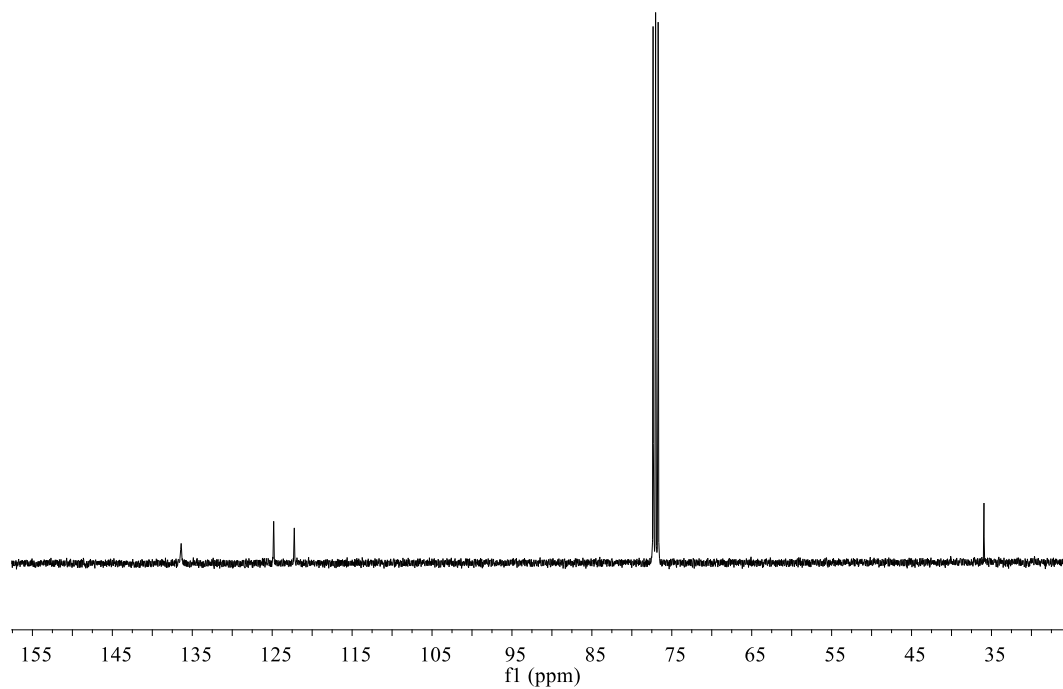


Boron trichloride 1-methylimidazole

$\text{BCl}_3\text{C}_4\text{H}_6\text{N}_2$. ^1H NMR (400 MHz, CDCl_3) δ 8.46 (s, 1H), 7.62 (s, 1H), 7.09 (s, 1H), 3.92 (s, 3H), ppm.

^{13}C NMR (101 MHz, CDCl_3) δ 136.39, 124.82, 122.24, 35.94 ppm.

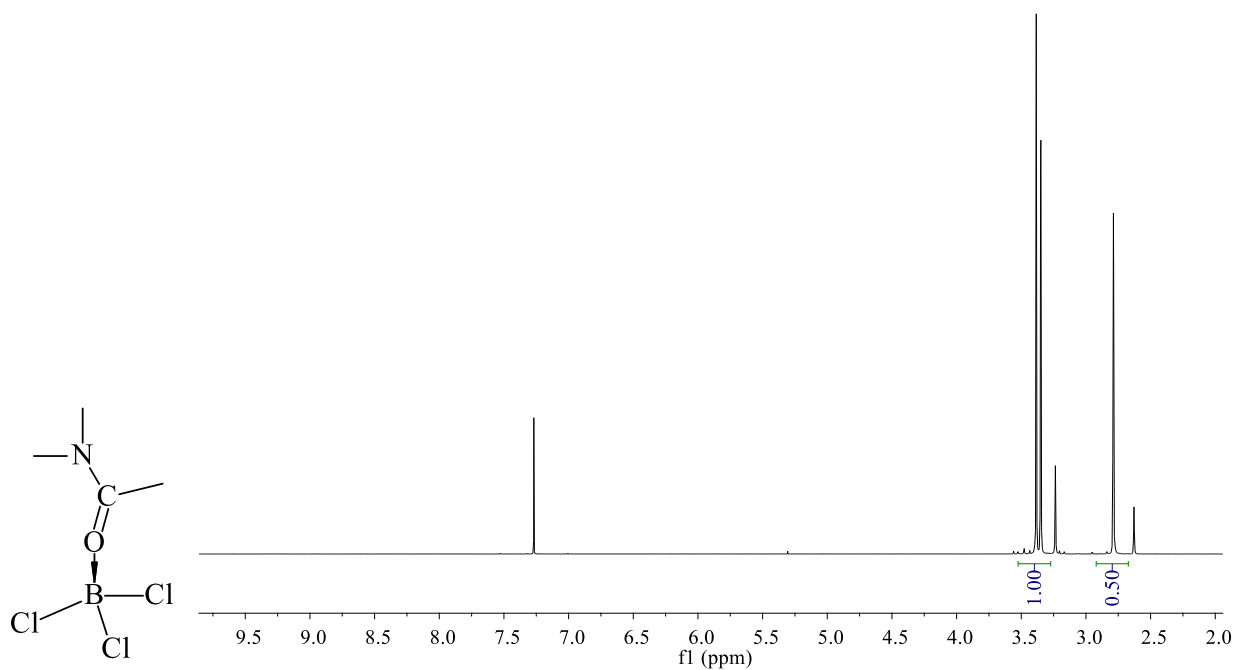


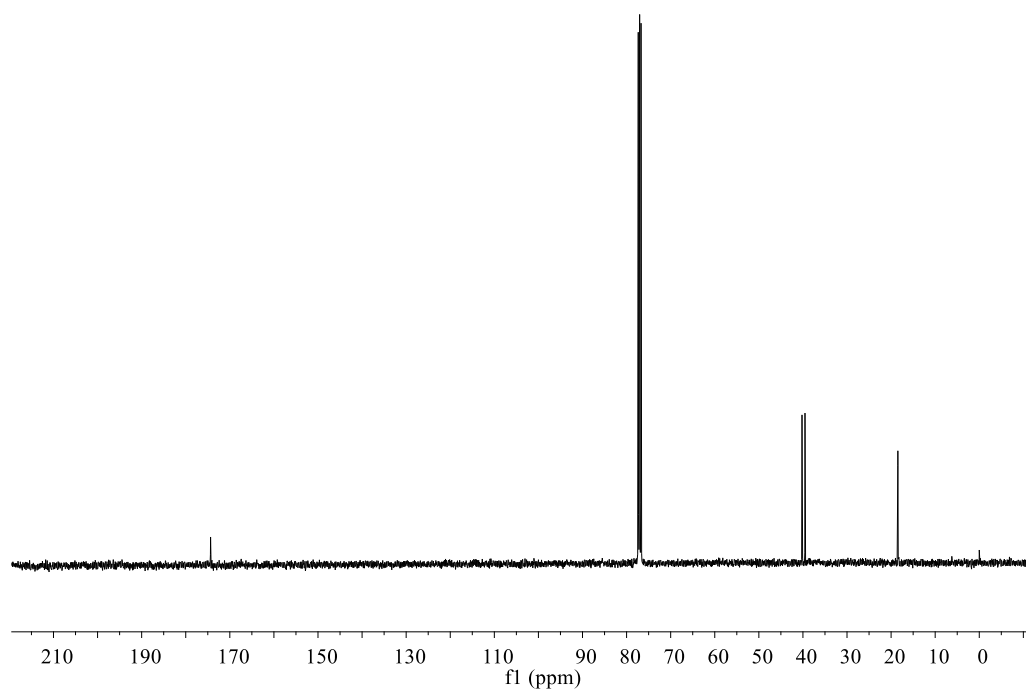


Boron trichloride dimethylacetamide

BCl₃C₄H₉NO. ¹H NMR (400 MHz, CDCl₃) δ 3.41 – 3.32 (m, 2H), 2.79 (s, 1H).

¹³C NMR (101 MHz, CDCl₃) δ 174.37 (s), 40.21 (s), 39.53 (s), 18.47 (s), ppm.

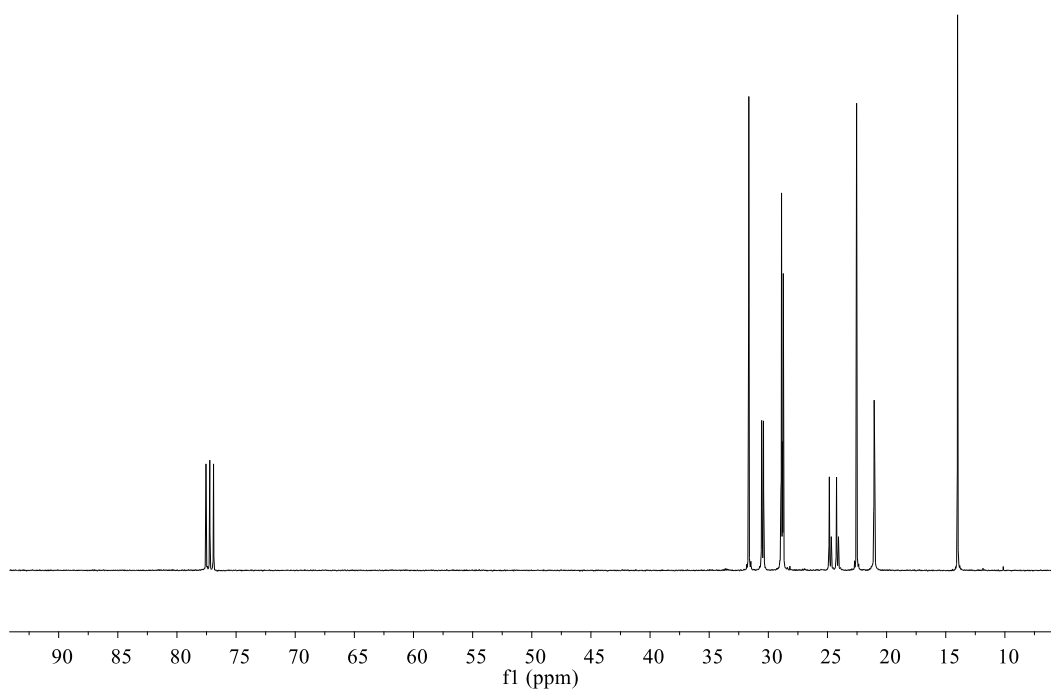
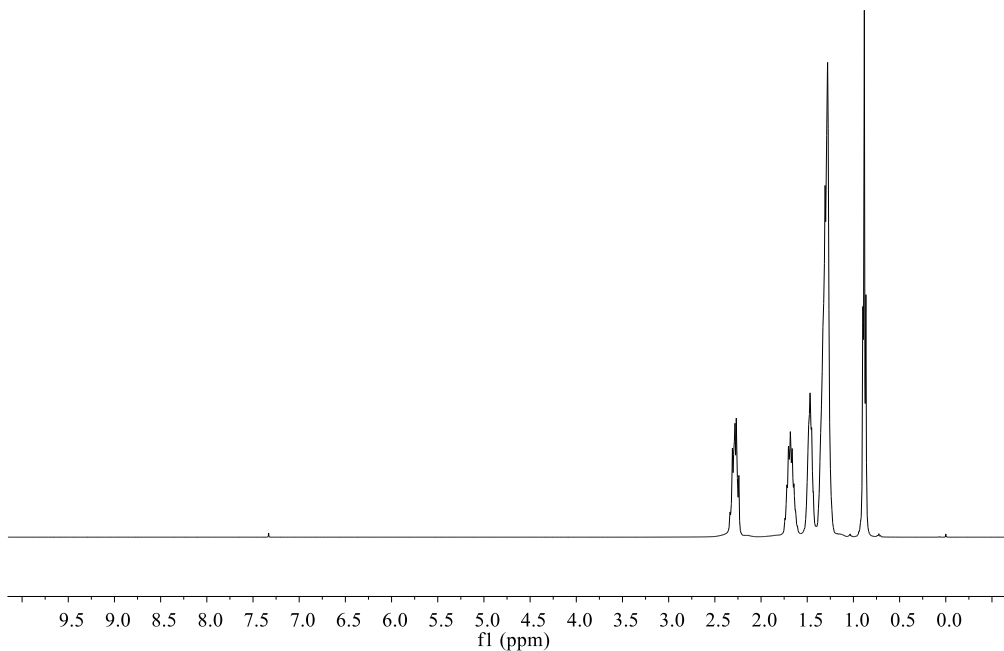
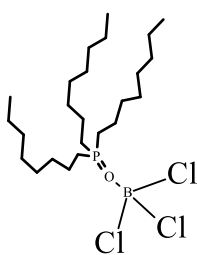




Boron trichloride trioctylphosphine oxide

$\text{BCl}_3\text{OP}(\text{C}_8\text{H}_{17})_3$. ^1H NMR (400 MHz, CDCl_3) δ 2.58 – 2.17 (m, 2H), 1.95 – 1.59 (m, 2H), 1.59 – 0.06 (m, 13H), 1.14 – 0.06 (m, 3H), 1.14 – 0.81 (m, 3H).

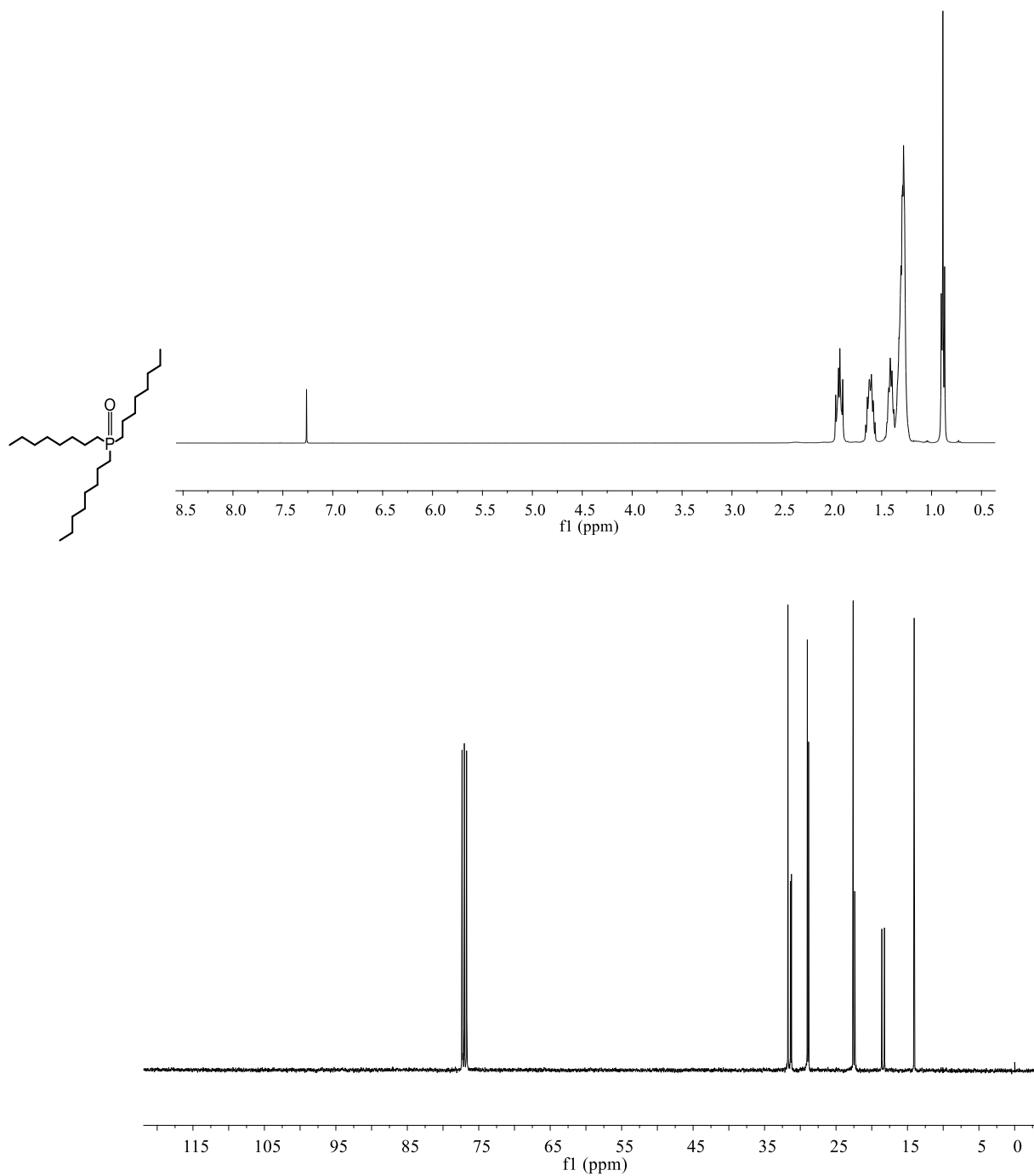
^{13}C NMR (101 MHz, CDCl_3) δ 31.65 (s), 30.47 (dd, $J = 15.5, 3.5$ Hz), 28.84 (dd, $J = 13.3, 5.8$ Hz), 24.76 (d, $J = 16.7$ Hz), 24.15 (d, $J = 16.3$ Hz), 22.54 (s), 21.05 (t, $J = 3.9$ Hz), 14.00 (s).



Boron trichloride trioctylphosphine

$\text{BCl}_3\text{P}(\text{C}_8\text{H}_{17})_3$. ^1H NMR (400 MHz, CDCl_3) δ 1.92 (td, $J = 11.5, 7.1$ Hz, 2H), 1.61 (td, $J = 14.6, 7.3$ Hz, 2H), 1.42 (dd, $J = 10.2, 4.1$ Hz, 2H), 1.38 – 1.15 (m, 8H), 0.89 (t, $J = 6.8$ Hz, 3H).

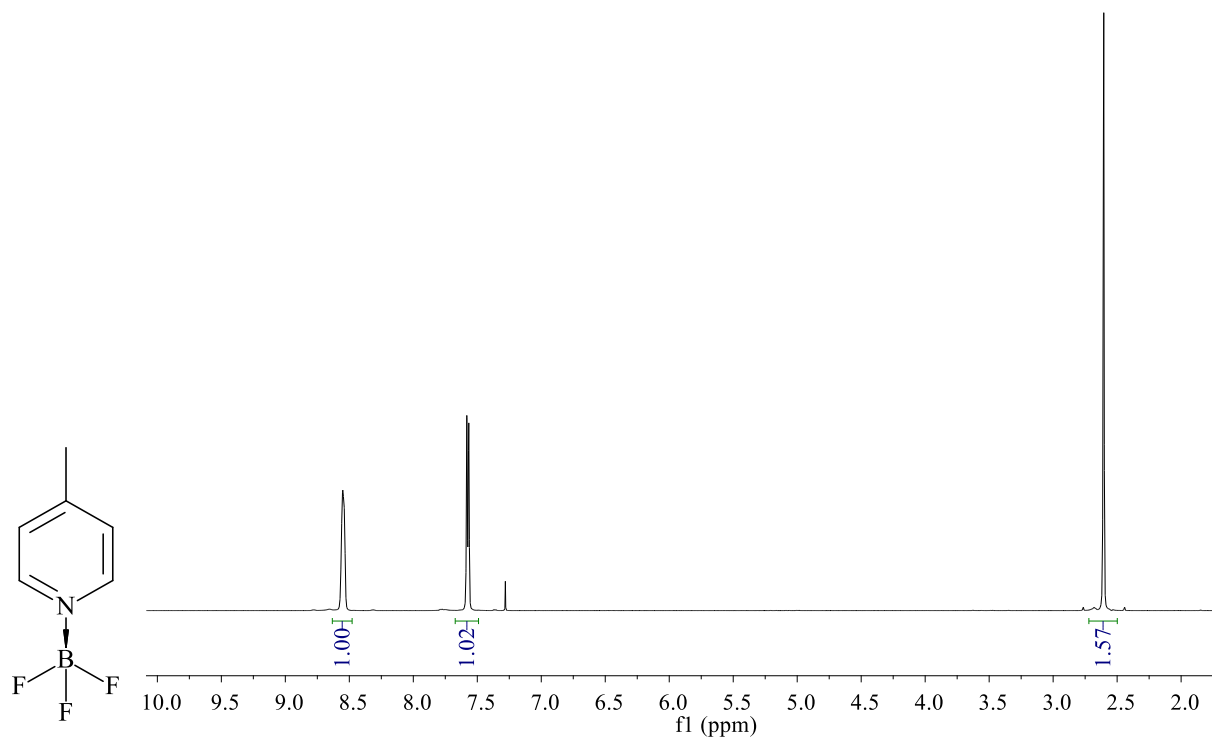
^{13}C NMR (101 MHz, CDCl_3) δ 31.73 (s), 31.30 (d, $J = 12.6$ Hz), 28.92 (d, $J = 18.0$ Hz), 22.60 (s), 22.36 (d, $J = 4.6$ Hz), 18.59 (s), 18.22 (s), 14.06 (s).

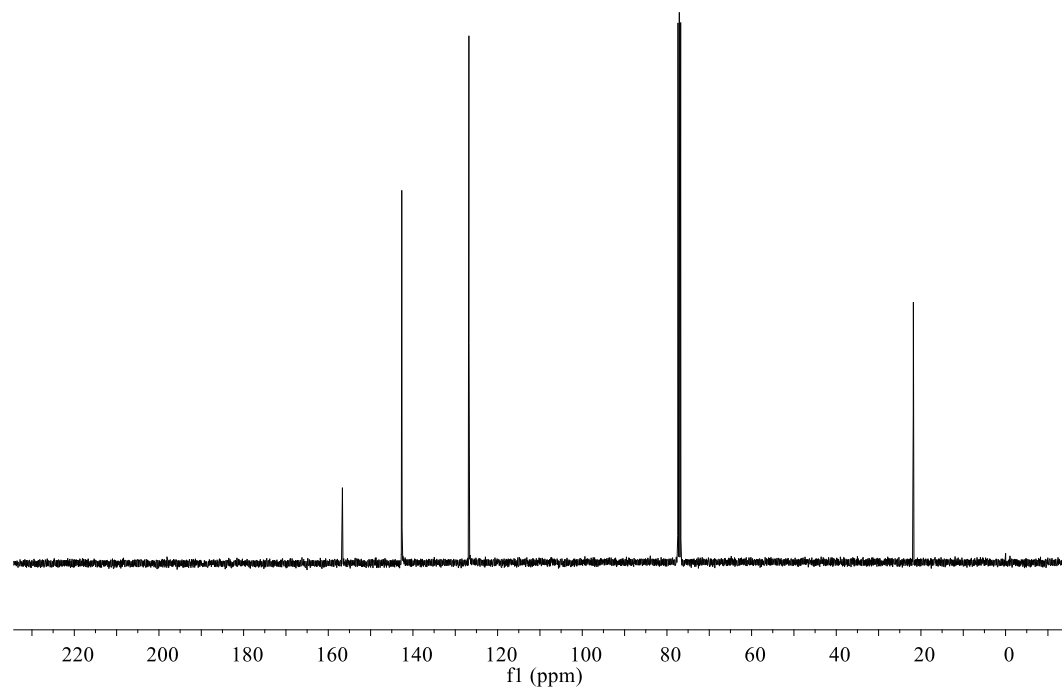


Boron trifluoride 4-methyl pyridine

$\text{BCl}_3\text{C}_6\text{H}_7\text{N}$. ^1H NMR (400 MHz, CDCl_3) δ 8.55 (s, 2H), 7.57 (d, $J = 6.2$ Hz, 2H), 2.60 (s, 3H) ppm.

^{13}C NMR (101 MHz, CDCl_3) δ 156.66, 142.64, 126.78, 21.78 ppm.

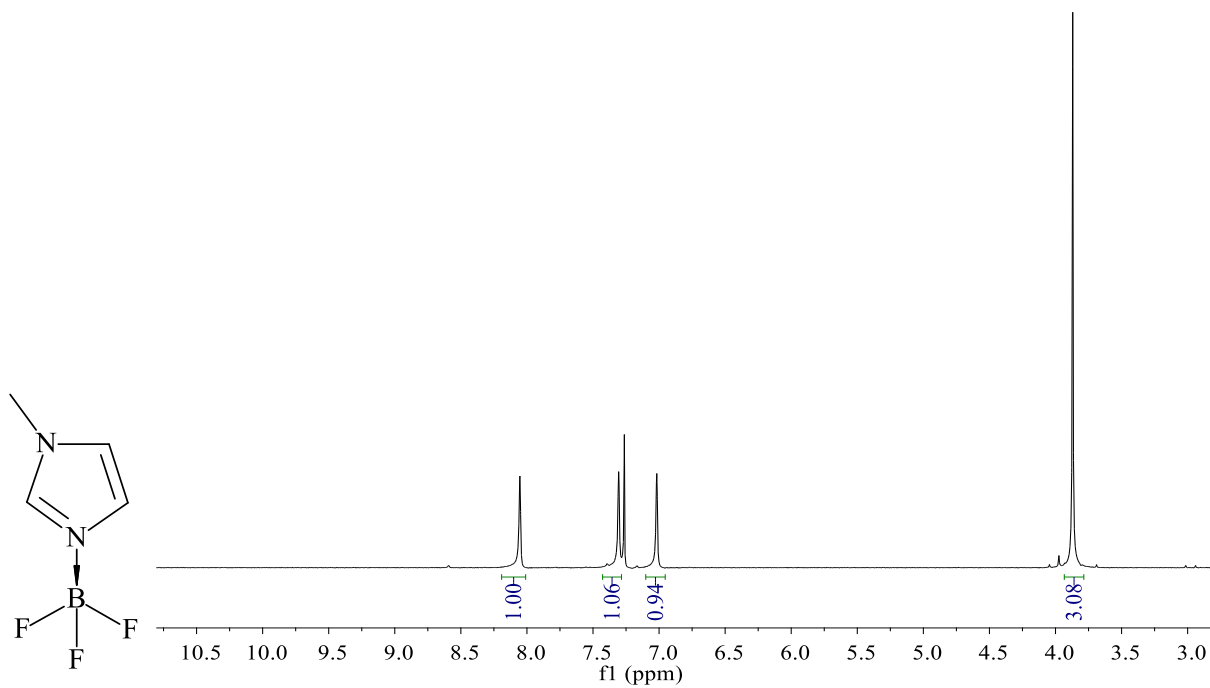


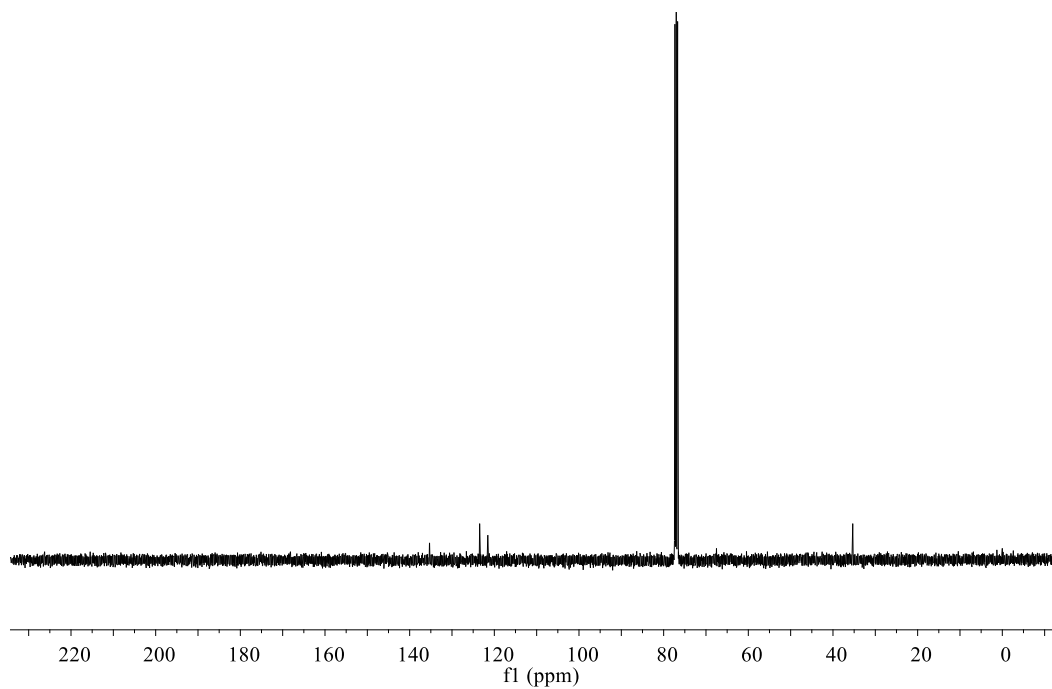


Boron trifluoride 1-methylimidazole

$\text{BCl}_3\text{C}_4\text{H}_6\text{N}_2$. ^1H NMR (400 MHz, CDCl_3) δ 8.05 (s, 2H), 7.31 (s, 3H), 7.02 (s, 2H), 3.87 (s, 6H) ppm.

^{13}C NMR (101 MHz, CDCl_3) δ 135.30, 123.47, 121.53, 35.33.

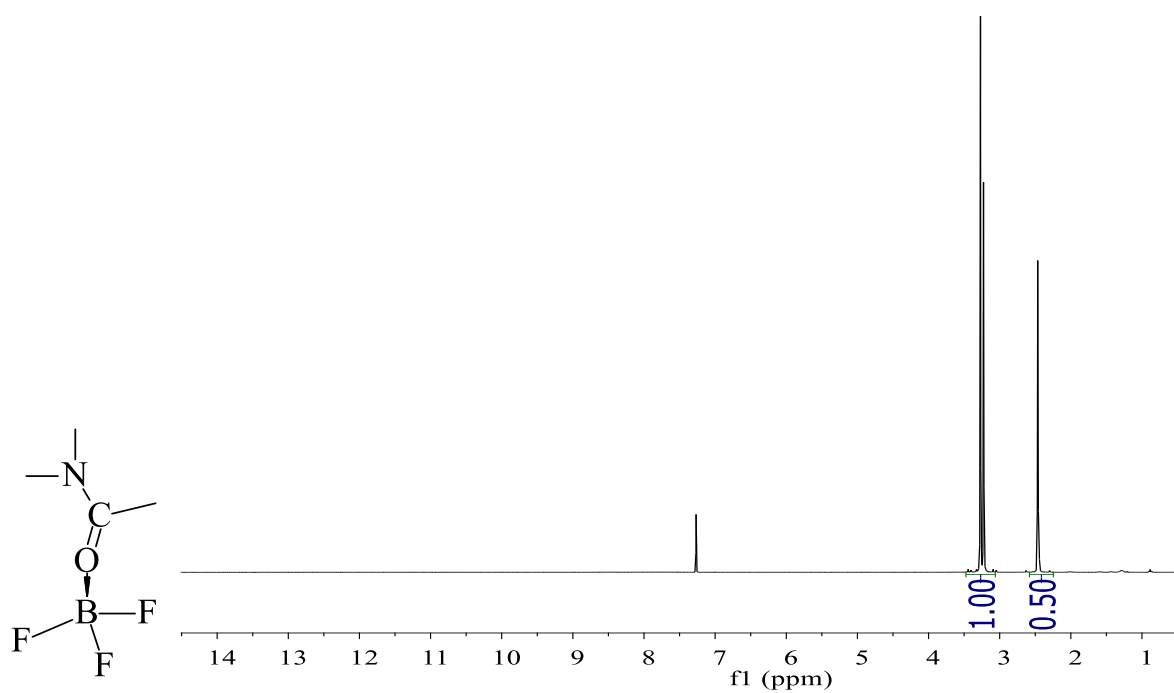


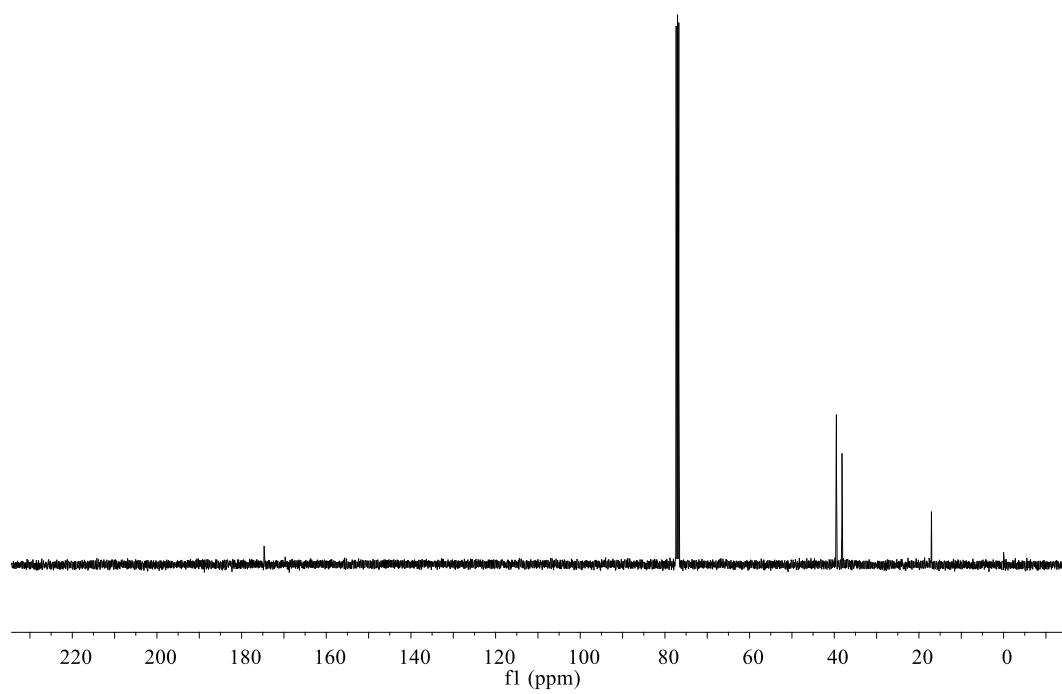


Boron trifluoride dimethylacetamide

$\text{BCl}_3\text{C}_4\text{H}_9\text{NO}$. ^1H NMR (400 MHz, CDCl_3) δ 3.25 (d, 2H), 2.47 (s, 1H) ppm.

^{13}C NMR (101 MHz, CDCl_3) δ 174.68, 39.49 (s), 38.17, 17.06 ppm.

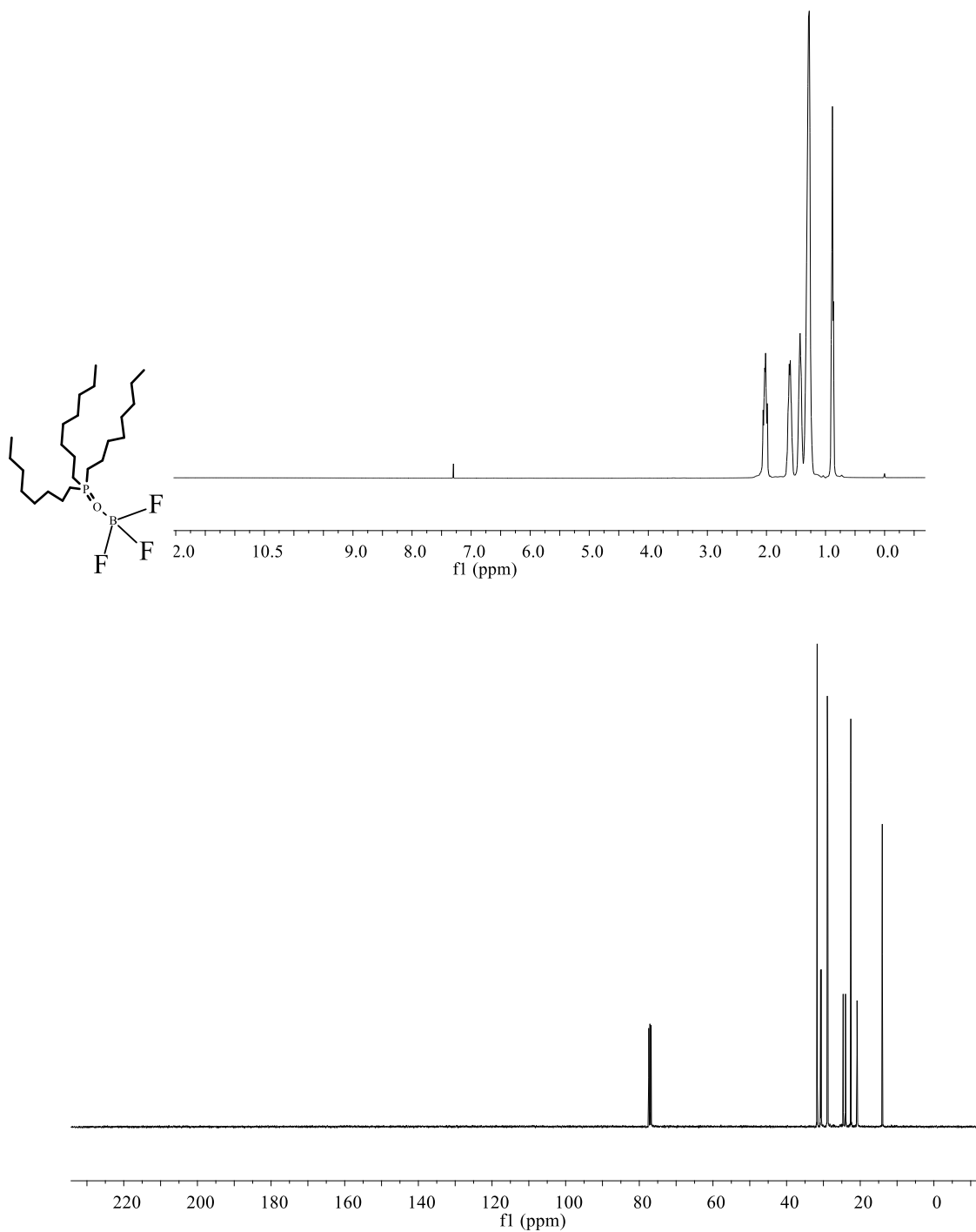




Boron trifluoride trioctylphosphine oxide

$\text{BCl}_3\text{OP}(\text{C}_8\text{H}_{17})_3$. ^1H NMR (400 MHz, CDCl_3) δ 2.02 (dd, 2H), 1.56 (dd, 3H), 1.30 (s, 4H), 1.28 (s, 5H), 0.88 (dd, 3H) ppm.

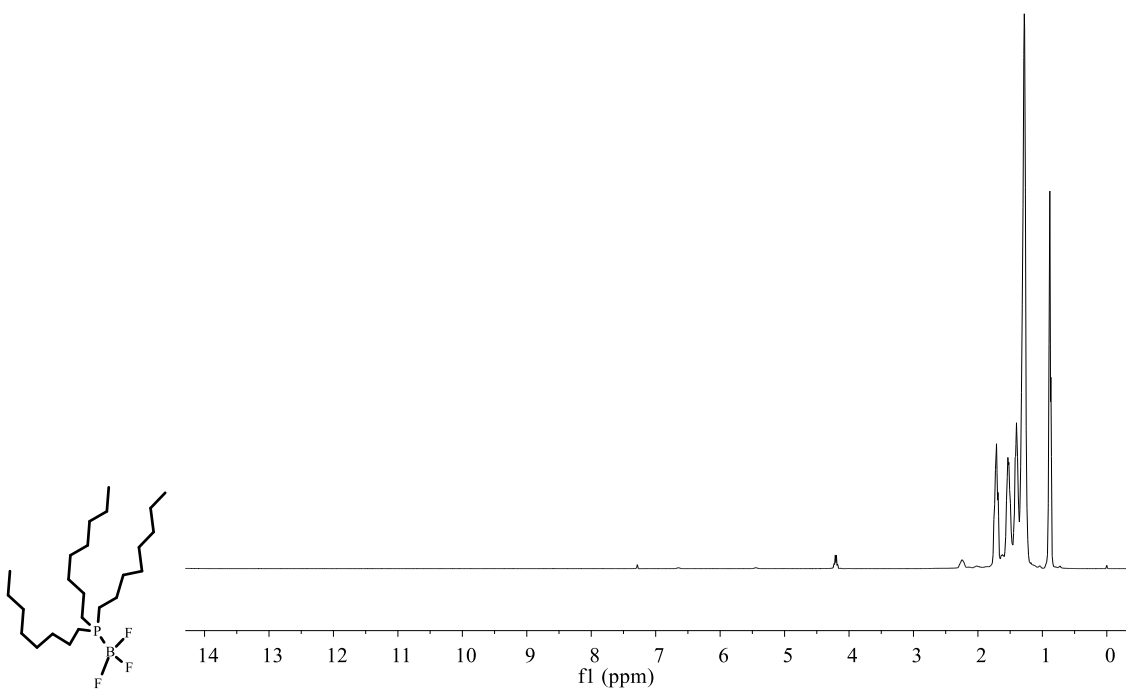
^{13}C NMR (101 MHz, CDCl_3) δ 31.70, 30.68, 28.88, 24.64, 24.01, 22.56, 20.84, 14.01 ppm.

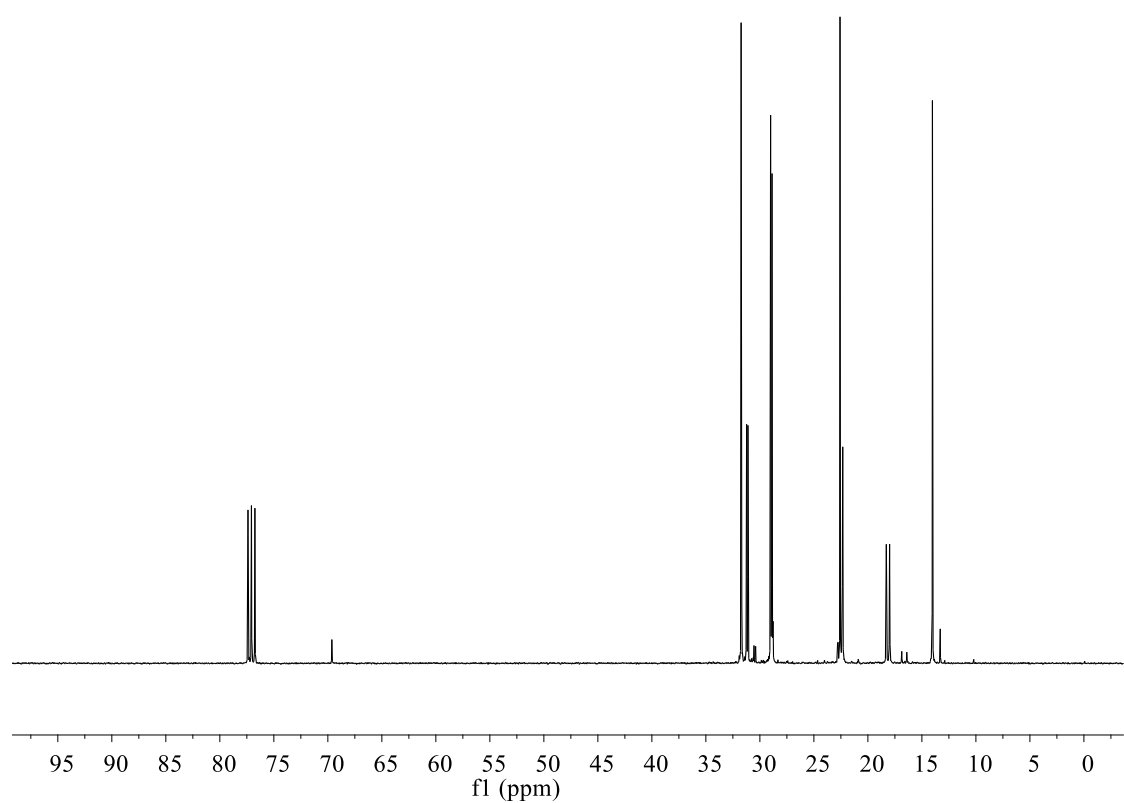


Boron trifluoride trioctylphosphine

$\text{BCl}_3\text{P}(\text{C}_8\text{H}_{17})_3$. ^1H NMR (400 MHz, CDCl_3) δ 1.70 (d, 2H), 1.53 (d, 2H), 1.49 – 1.13 (m, 11H), 0.88 (t, 3H) ppm.

^{13}C NMR (101 MHz, CDCl_3) δ 31.71, 31.17, 29.15 – 28.54, 22.58, 22.34, 18.29, 17.99, 14.02 ppm



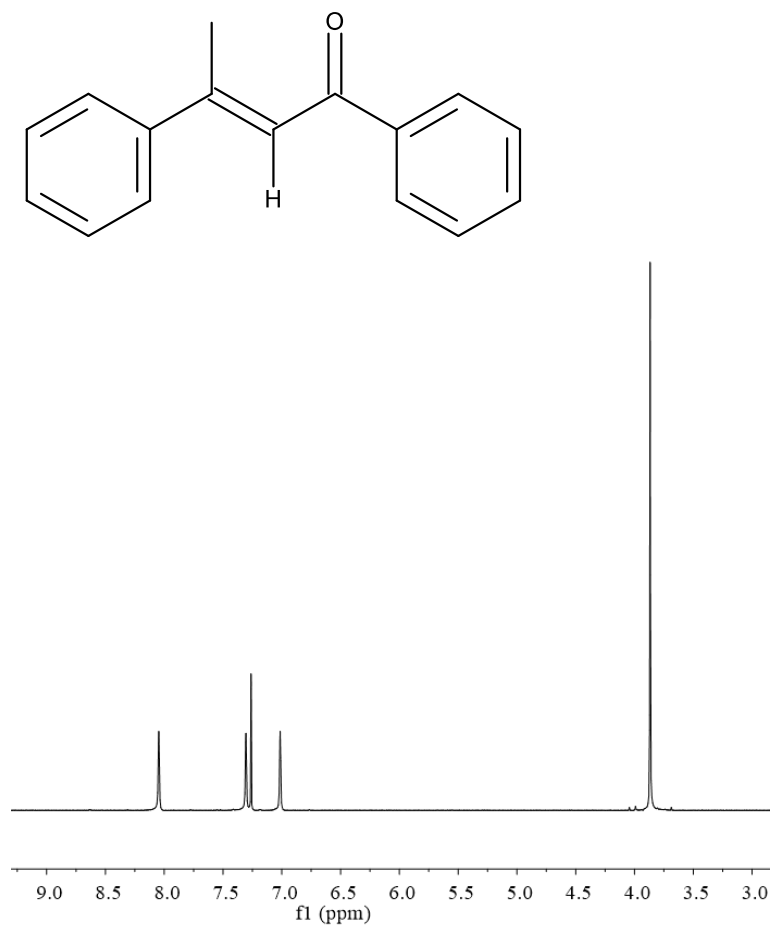


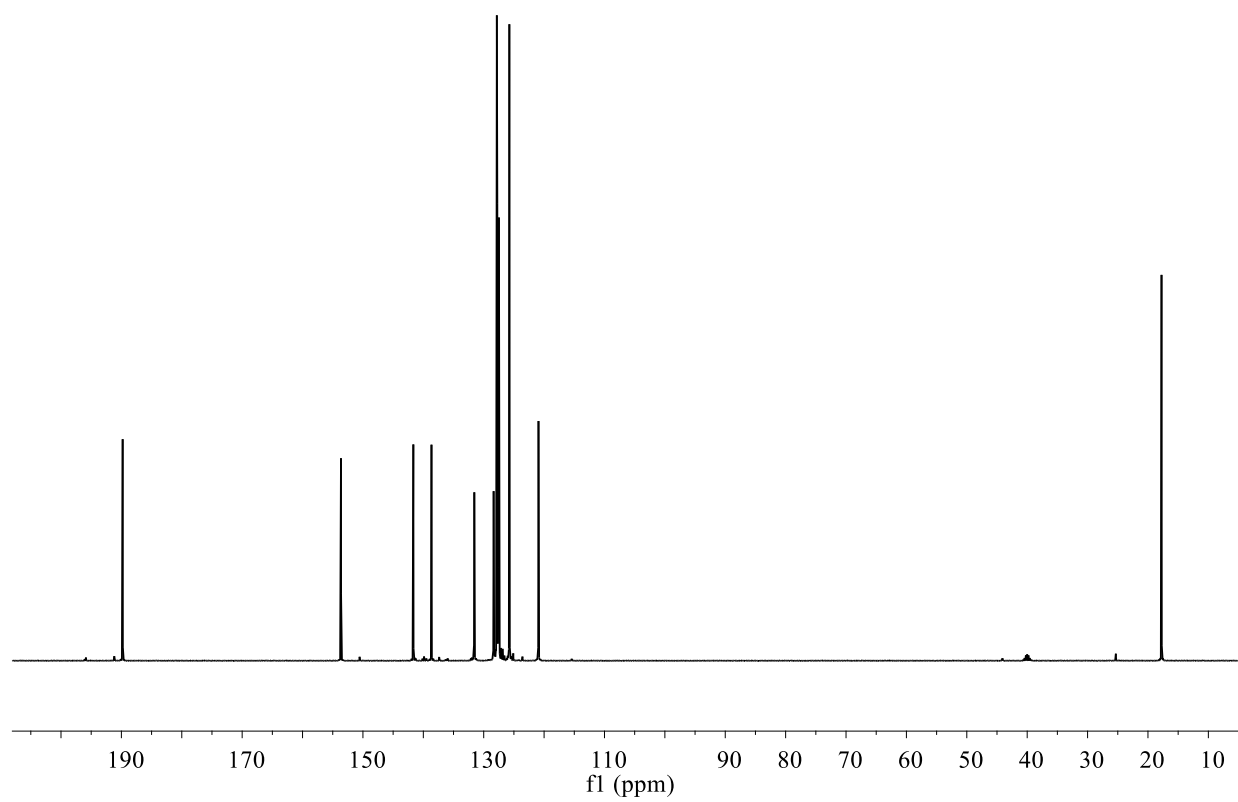
APPENDIX B - NMR Spectroscopy Data

Dypnone

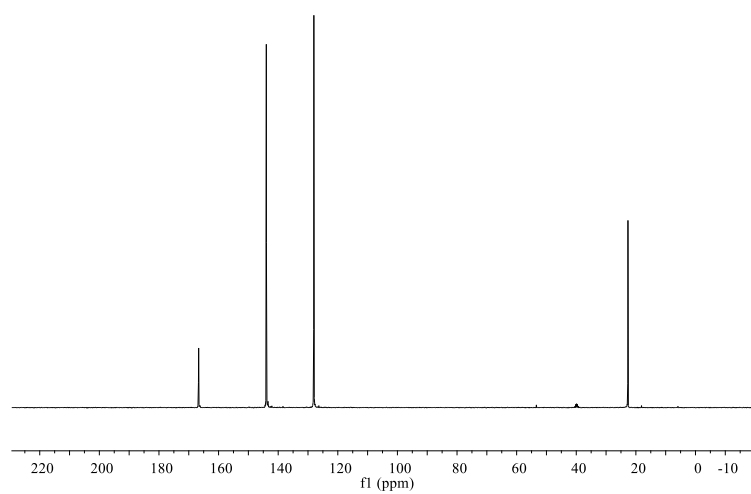
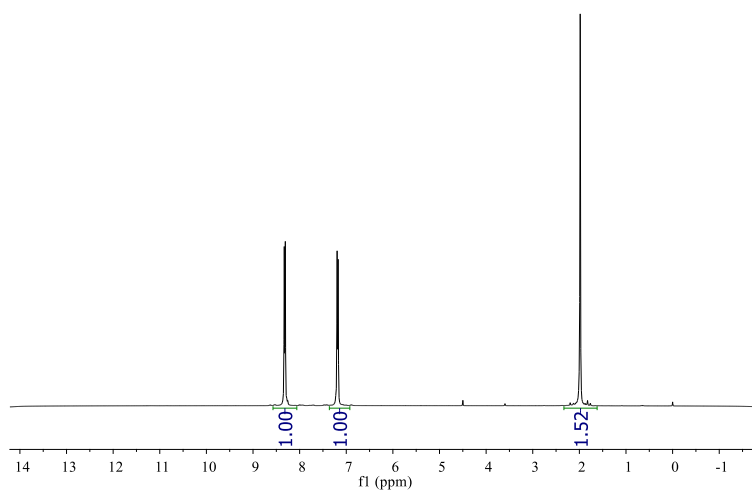
C₁₆H₁₄O: ¹H NMR (400 MHz, DMSO) δ 7.07 (d, 2H), 6.54 (d, 2H), 6.40 (m, 6H), 6.22 (s, 1H), 1.65 (s, 3H).

¹³C NMR (101 MHz, DMSO) δ 189.79, 153.63, 141.65, 138.65, 131.56, 128.36, 127.83, 127.75, 127.48, 125.75, 120.93, 17.75. ppm

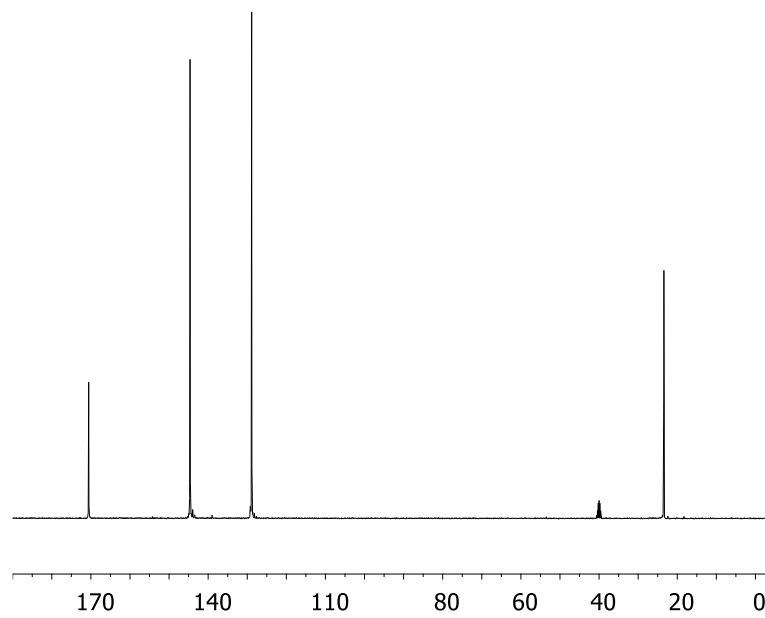
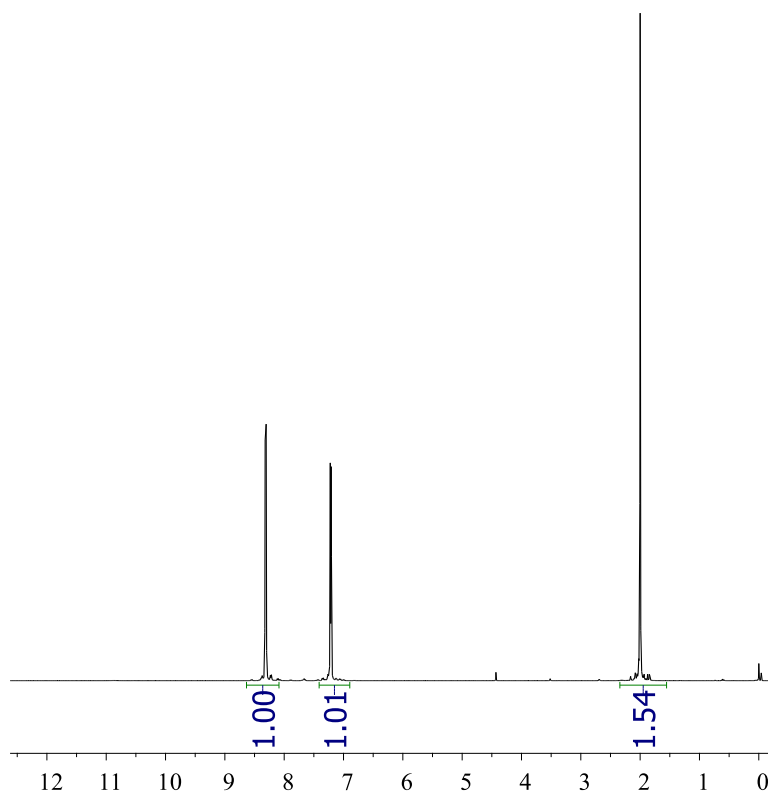




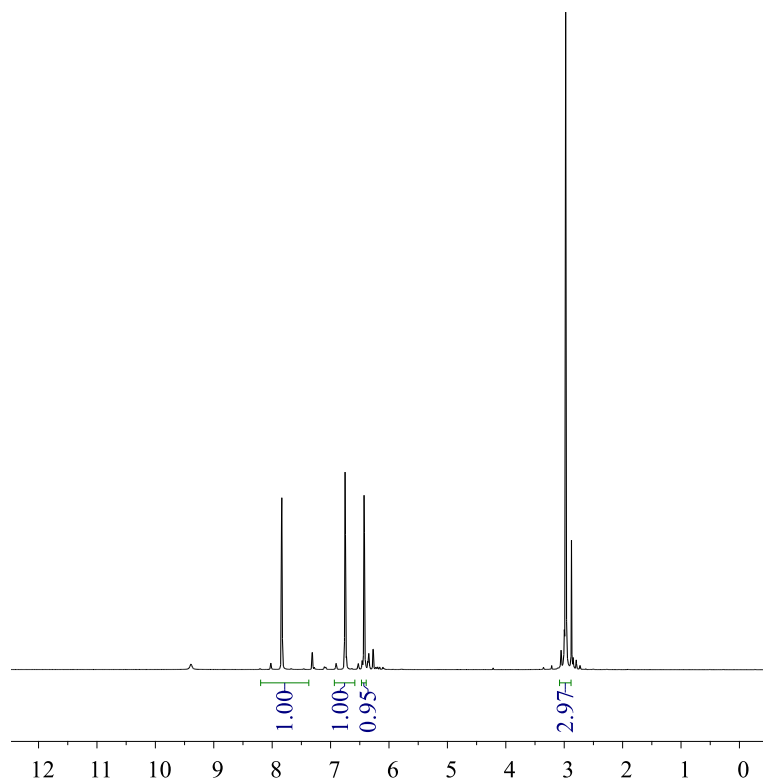
4-pic-BCl₃-AlCl₃

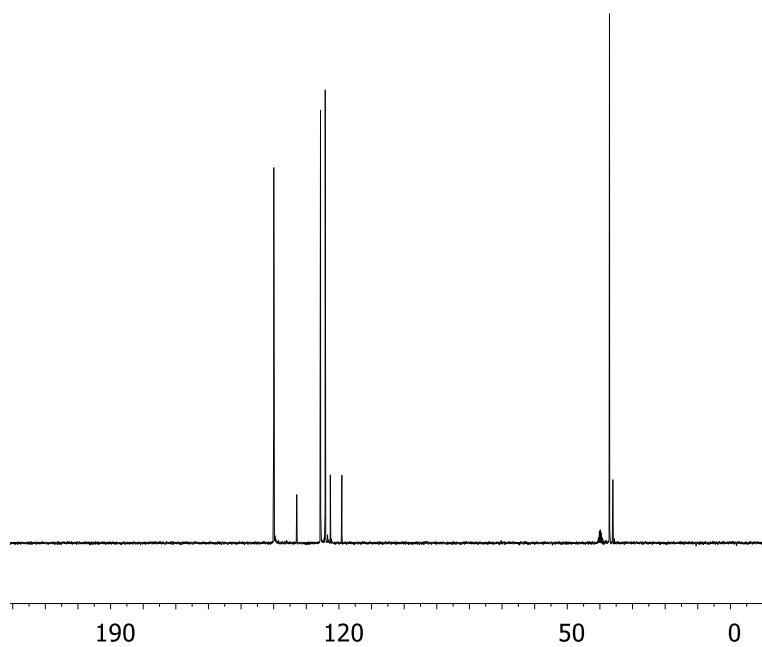


4-pic-BCl₃-2AlCl₃

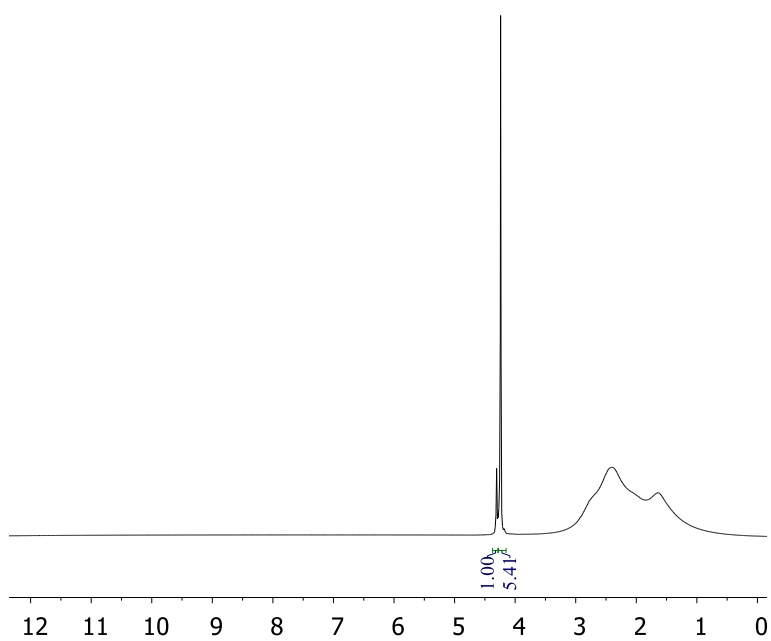


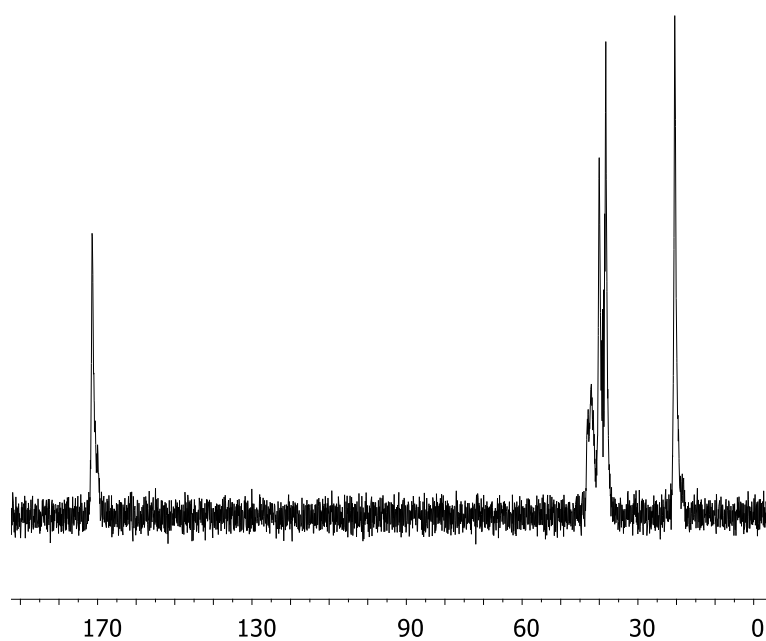
mim-BCl₃-2AlCl₃



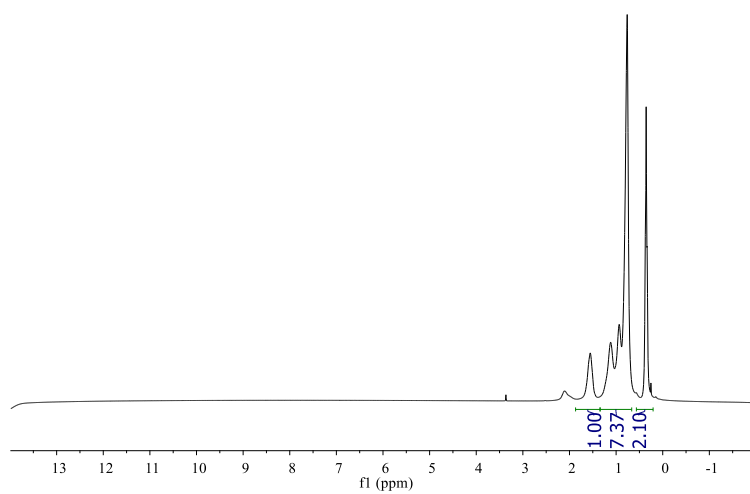


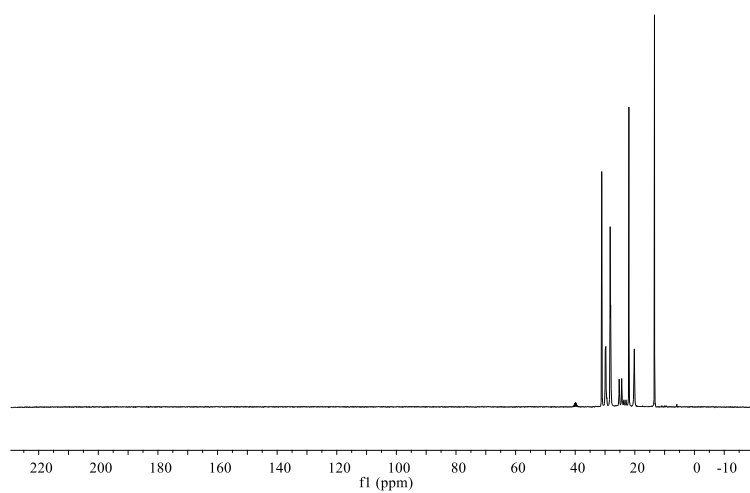
$\text{dma-BCl}_3\cdot 2\text{AlCl}_3$



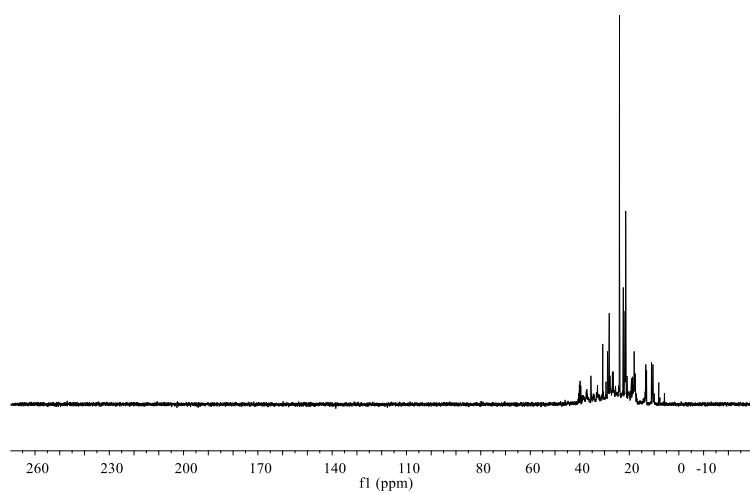
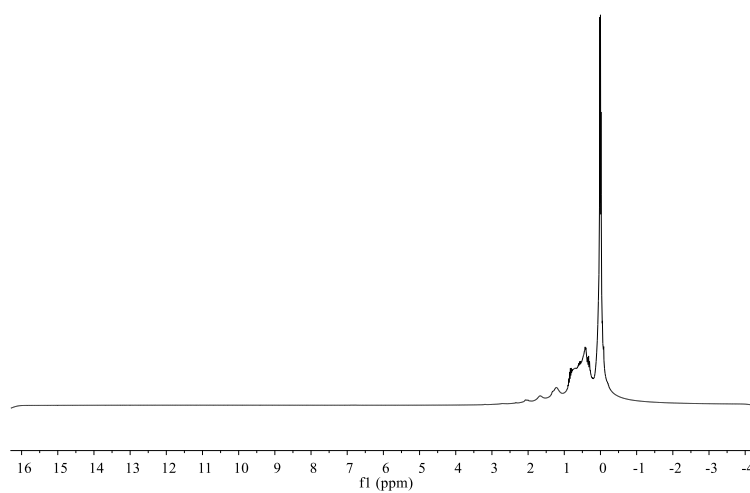


P₈₈₈O-BCl₃-AlCl₃

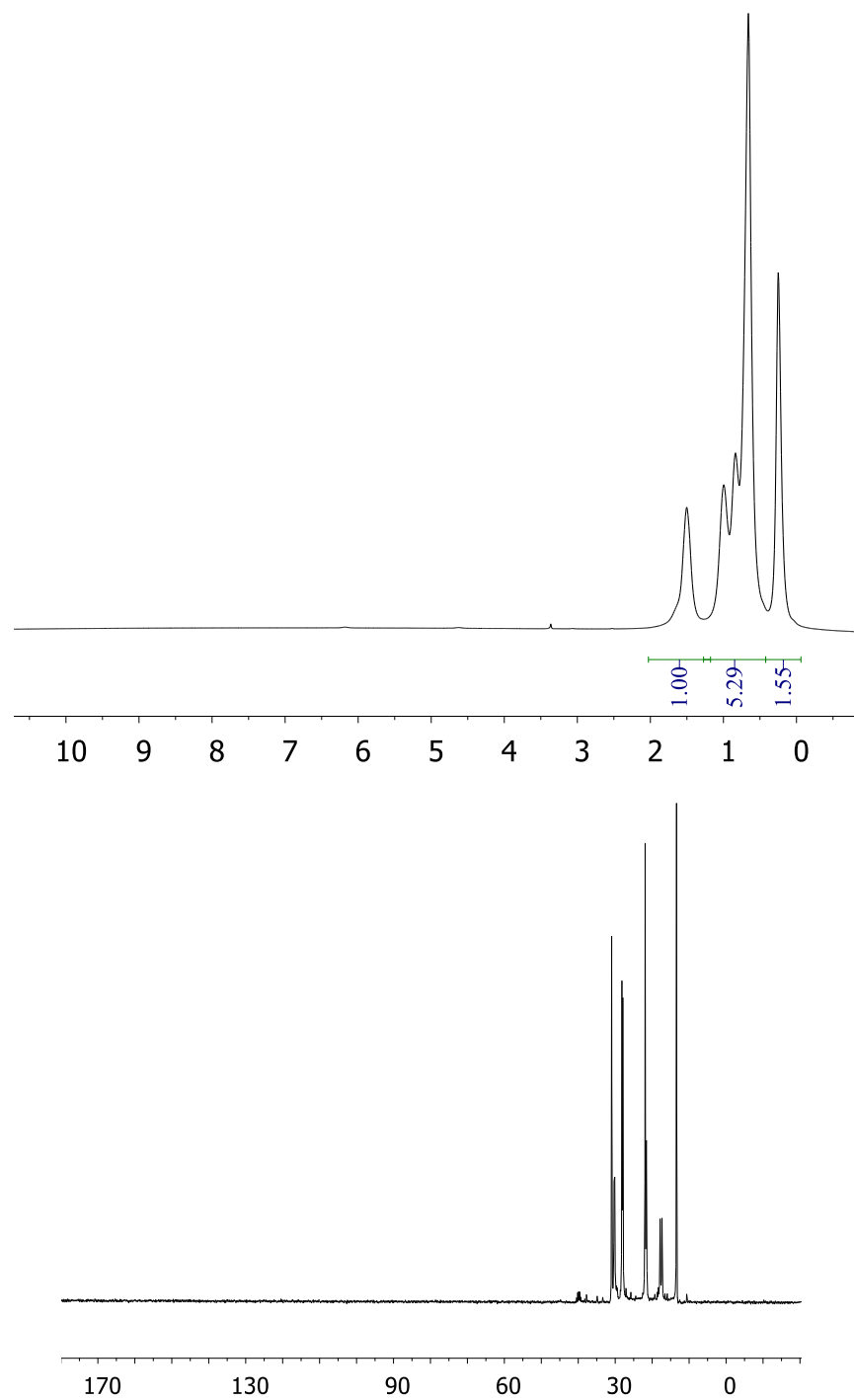




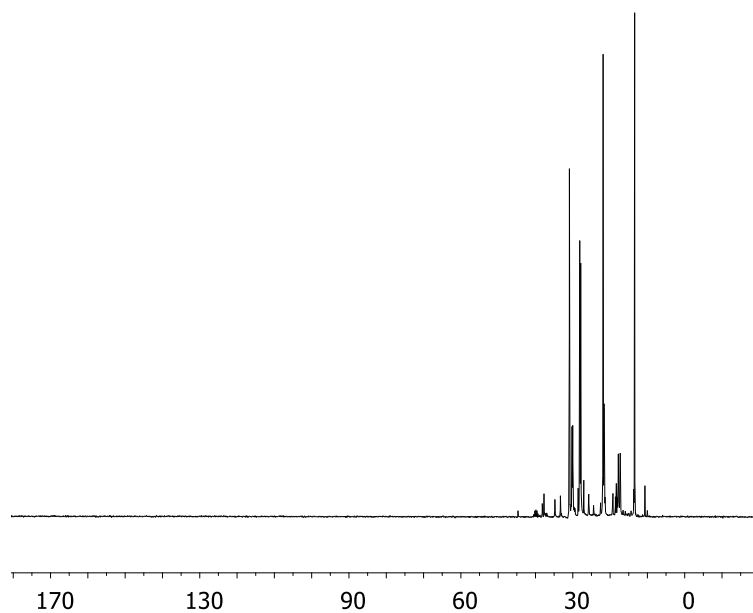
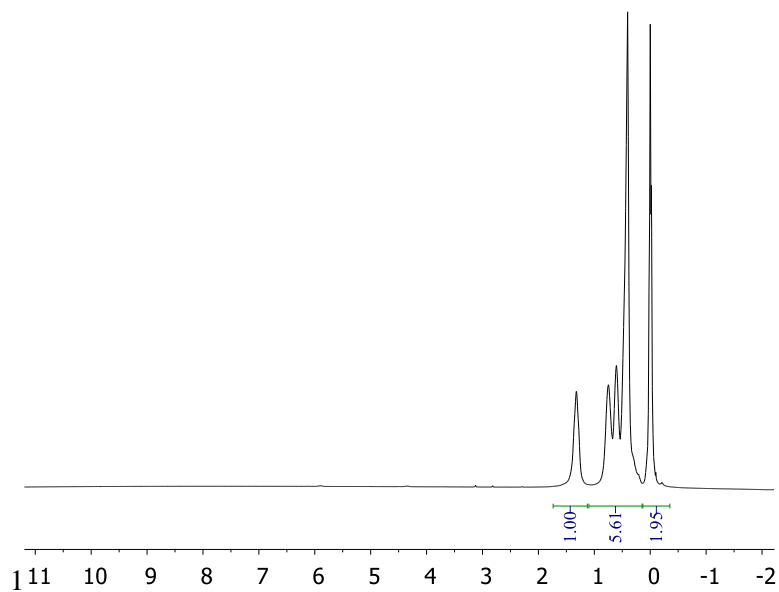
$\text{P}_{888}\text{0-BCl}_3\text{-2AlCl}_3$



P₈₈₈-BCl₃-AlCl₃



P₈₈₈-BCl₃-2AlCl₃



APPENDIX C - *Infrared spectroscopy*

